

The only official copy of this document is the one online in the SharePoint Document Center. Before using a printed copy, verify that it is current by checking the printed document's Revision History log with that of the online version.

Electron-Ion Collider, Brookhaven National Laboratory and Thomas Jefferson National Accelerator Facility			
Doc No. EIC-SHC-TN-24-005	Author: Sandesh Gopinath	Effective Date: 12/05/2024	Review Frequency: NA
Process Description: EIC Design Report MARCO Magnet			Revision: 00

EIC Design Report: MARCO Magnet

December 5, 2024

Prepared by:

gopinath

Digitally signed by gopinath
Date: 2024.12.10 10:01:53
-05'00'

S. Gopinath, Engineer

12/05/2024

Date: _____

Reviewed by:

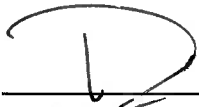
Renuka Rajput-Ghoshal

Digitally signed by Renuka Rajput-Ghoshal
Date: 2024.12.10 10:14:06 -05'00'

R. Rajput-Ghoshal, CAM and SME


Date: _____

Approved by:



R. Ent, L2

Date: 12/10/24



E Aschenauer, L2

Date: 12/10/2024

The only official copy of this document is the one online in the SharePoint Document Center. Before using a printed copy, verify that it is current by checking the printed document's Revision History log with that of the online version.

Electron-Ion Collider, Brookhaven National Laboratory and Thomas Jefferson National Accelerator Facility			
Doc No. EIC-SHC-TN-24-005	Author: Sandesh Gopinath	Effective Date: 12/05/2024	Review Frequency: NA
Process Description: EIC Design Report MARCO Magnet			Revision: 00

REVISION HISTORY

Revision #	Effective Date	List of Reviewers	Summary of Change
00	12/05/2024		Initial release.

The only official copy of this document is the one online in the SharePoint Document Center. Before using a printed copy, verify that it is current by checking the printed document's Revision History log with that of the online version.

Electron-Ion Collider, Brookhaven National Laboratory and Thomas Jefferson National Accelerator Facility			
Doc No. EIC-SHC-TN-24-005	Author: Sandesh Gopinath	Effective Date: 12/05/2024	Review Frequency: NA
Process Description: EIC Design Report MARCO Magnet			Revision: 00

MARCO Magnet Design Team

- **JLab**
 - Team Lead: Renuka Rajput-Ghoshal
 - Design Team Members: Probir Ghoshal, Sandesh Gopinath, Eric Sun, and Dan Young
- **CEA, Saclay**
 - Team Lead: Valerio Calvelli
 - Design Team Members: Christophe Berriaud, Jean-Pierre Lottin, Hugo Reymond, Michel Segreti, Damien Simon, and Francesco Stacchi
- **BNL**
 - Team Members: Rahul Sharma, Roland Wimmer and Roberto Than

The only official copy of this document is the one online in the SharePoint Document Center. Before using a printed copy, verify that it is current by checking the printed document's Revision History log with that of the online version.

Electron-Ion Collider, Brookhaven National Laboratory and Thomas Jefferson National Accelerator Facility			
Doc No. EIC-SHC-TN-24-005	Author: Sandesh Gopinath	Effective Date: 12/05/2024	Review Frequency: NA
Process Description: EIC Design Report MARCO Magnet			Revision: 00

Contents

1	Introduction to EIC	17
1.1	Interaction region and the detector area	18
2	Magnet Specification	19
2.1	Magnet Specification Parameters.....	19
2.2	Flat Field Area	20
2.3	RICH detector area.....	21
2.4	Stray field limitations at IR magnets and on RCS.....	22
2.5	Description of Key Interfaces	22
3	Magnetic Design - Electromagnetic	24
3.1	Return Flux	25
3.2	Yoke Material Properties	28
3.3	The Superconducting coils and the Mandrel	30
3.4	The Electromagnetic model and the magnet performance	36
3.5	Fault scenario studies	40
3.5.1	Impact of axial misalignment and tolerances	42
3.5.2	Impact of radial misalignments.....	44
3.5.3	Impact of one missing layer	46
3.5.4	Impact of Permeability of Yoke Material	46
3.5.5	Impact of Misalignments of Yoke	47
4	Conductor Design and Stability.....	49
4.1	Strand	49
4.2	Cable	50
4.3	Copper Channel.....	51
4.4	Conductor	51
4.5	Conductor Stability.....	54
5	Mechanical Design	55
5.1	Material properties and Acceptance criteria.....	57
5.1.1	Cooper.....	57
5.1.2	Niobium-titanium alloy	58

The only official copy of this document is the one online in the SharePoint Document Center. Before using a printed copy, verify that it is current by checking the printed document's Revision History log with that of the online version.

Electron-Ion Collider, Brookhaven National Laboratory and Thomas Jefferson National Accelerator Facility			
Doc No. EIC-SHC-TN-24-005	Author: Sandesh Gopinath	Effective Date: 12/05/2024	Review Frequency: NA
Process Description: EIC Design Report MARCO Magnet			Revision: 00

5.1.3	G10	59
5.1.4	Glass fiber epoxy	62
5.1.5	Brass	63
5.1.6	AgSn 3.5/96.5 Soft Solder	63
5.1.7	Ti6Al4V	64
5.1.8	Acceptance Criteria	64
5.2	Coil Pack Homogenization	65
5.2.1	Homogenization of the Cable	65
5.2.2	Homogenization of the Insulated Conductor.....	66
5.2.3	Homogenization of the Coil	67
5.3	Models and Assumptions.....	68
5.3.1	2D Modeling.....	68
5.3.2	3D Modeling.....	72
5.4	Results and Discussions	75
5.4.1	Self-weight, seismic and transportation loads.....	75
5.4.2	Cool-down	78
5.4.3	Energization	83
6	Magnet Structure and Materials.....	91
6.1	Materials Used	91
6.2	Magnet Structure.....	95
6.3	Code Requirements	95
6.3.1	Specifications	96
6.4	Helium Phase Separator.....	96
6.4.1	Inner Vessel.....	96
6.4.2	Outer Vessel.....	97
6.5	Vacuum Vessel	98
6.5.1	Overview	98
6.5.2	Design-by-Rules.....	98
6.5.3	Design-by-Analysis	98
6.5.4	Protection Against Plastic Collapse.....	99

The only official copy of this document is the one online in the SharePoint Document Center. Before using a printed copy, verify that it is current by checking the printed document's Revision History log with that of the online version.

Electron-Ion Collider, Brookhaven National Laboratory and Thomas Jefferson National Accelerator Facility			
Doc No. EIC-SHC-TN-24-005	Author: Sandesh Gopinath	Effective Date: 12/05/2024	Review Frequency: NA
Process Description: EIC Design Report MARCO Magnet			Revision: 00

6.5.5	Protection against Local Failure	101
6.5.6	Protection against Collapse from Buckling	102
6.5.7	Protection against Failure from cyclic loading.....	104
6.6	Cryogenic Chimney	104
6.7	Pressure Piping.....	105
6.8	Manufacturing Requirements.....	105
6.9	Summary	105
7	Cooling Scheme and Heat Loads.....	106
7.1	Cryogenic processes.....	108
7.1.1	Cool-down Process.....	108
7.1.2	Thermosiphon	109
7.1.3	Long Shut-down	110
7.1.4	Refrigerator Shut-down	112
7.1.5	Quench.....	113
7.1.6	Vacuum Loss	114
7.2	Heat Loads.....	115
7.2.1	Conduction Heat Loads	115
7.2.2	Heat Load from Thermal Radiation.....	118
7.2.3	Heat Load from Electrical Junctions.....	118
7.2.4	Heat Load from Eddy Current and Hysteresis of Conductor.....	119
7.2.5	Heat load from Eddy Current in the Mandrel	119
7.2.6	Heat Load from Current Leads	120
7.2.7	Total Heat Load Budget.....	120
7.3	Thermosiphon	120
7.3.1	Thermosiphon Piping Overview	125
7.4	Thermal shield.....	130
7.4.1	Pressure Drops and Temperature along the Circuit	132
7.4.2	Temperature Difference in the Panels.....	134
7.5	Helium Phase Separator.....	134
7.6	Safety Analysis	138

The only official copy of this document is the one online in the SharePoint Document Center. Before using a printed copy, verify that it is current by checking the printed document's Revision History log with that of the online version.

Electron-Ion Collider, Brookhaven National Laboratory and Thomas Jefferson National Accelerator Facility			
Doc No. EIC-SHC-TN-24-005	Author: Sandesh Gopinath	Effective Date: 12/05/2024	Review Frequency: NA
Process Description: EIC Design Report MARCO Magnet			Revision: 00

7.6.1	Helium Circuits	138
7.7	Vacuum Vessel	140
8	Thermal Analysis	142
8.1	Thermosiphon Overview.....	142
8.2	Geometry Overview	144
8.3	FEA	146
8.3.1	Workflow.....	146
8.3.2	Geometry	146
8.4	FLUENT FEA.....	147
8.4.1	Fluid Geometry	147
8.4.2	Fluid Mesh.....	148
8.4.3	Fluid Properties.....	148
8.4.4	Fluent Boundary Conditions	149
8.4.5	Results and Discussion	151
8.5	Steady State Thermal Analysis	153
8.5.1	Mesh	154
8.5.2	Material Properties	154
8.5.3	Boundary Condition	157
8.5.4	Results and Discussion	157
8.6	Cool-down Transient.....	159
8.6.1	Geometry	159
8.6.2	Mesh	159
8.6.3	Material Properties	160
8.6.4	Boundary Conditions.....	160
8.6.5	Results and Discussion	162
8.7	Summary	164
9	Quench Protection and Analysis	165
9.1	Transient Analysis	165
9.1.1	Ramp-up and Ramp-down	165
9.1.2	Fast Discharge	166

The only official copy of this document is the one online in the SharePoint Document Center. Before using a printed copy, verify that it is current by checking the printed document's Revision History log with that of the online version.

Electron-Ion Collider, Brookhaven National Laboratory and Thomas Jefferson National Accelerator Facility			
Doc No. EIC-SHC-TN-24-005	Author: Sandesh Gopinath	Effective Date: 12/05/2024	Review Frequency: NA
Process Description: EIC Design Report MARCO Magnet			Revision: 00

9.2	Quench Analysis.....	168
9.2.1	Single coil quench analysis.....	168
9.2.2	Quench analysis in COMSOL.....	172
9.3	Quench Protection circuit.....	186
10	Instrumentations	188
10.1	Voltage Taps.....	188
10.2	Cryogenic Instrumentation Plan	191
10.3	Mechanical sensors.....	193
11	Shipping.....	194
12	Quality Assurance Plan	196
12.1	Requirements Traceability	196
12.2	In-Process Inspection and Test	198
12.3	Vendor/Partner In-Process Monitoring and Measurement Activities.....	198
12.4	Incoming Inspection and Acceptance Tests.....	199
12.5	Travelers, Procedures, and Checklists	199
12.6	Verification Plans: Methods and Activities	199
12.7	Deliverable Documentation and Records	200
12.8	Associated Equipment	201
12.9	Calibration Plans	201
12.10	Serialization and Material Traceability Requirements.....	201
12.11	Planned Partner and Vendor Communication & Visits.....	202
12.12	Control of Nonconformances.....	202
13	References	203
14	Appendix	205

Electron-Ion Collider, Brookhaven National Laboratory and Thomas Jefferson National Accelerator Facility			
Doc No. EIC-SHC-TN-24-005	Author: Sandesh Gopinath	Effective Date: 12/05/2024	Review Frequency: NA
Process Description: EIC Design Report MARCO Magnet			Revision: 00

List of Figures

Figure 1.1 EIC Layout	17
Figure 1.2 Interaction region layout.....	18
Figure 1.3 The Detector Layout.....	18
Figure 2.1 Flat Field Area.....	20
Figure 2.2 RICH Area.....	21
Figure 2.3 RCS Location.....	22
Figure 3.1 The yoke surrounding the coils.....	24
Figure 3.2 Simplified geometry that captures the soft magnetic steel – including steel in the detectors and steel used for shielding a. TOSCA model of the baseline geometry with the coils shown in red b. detailed dimensions with a cross section view of the implemented geometry ...	25
Figure 3.3 Electromagnetic nomenclature showing the Barrel Hadron calorimeter and the Barrel steel that is added for magnetic shielding.....	26
Figure 3.4 Electromagnetic nomenclature showing the Lepton/Backward Endcap assembly. All components were added for magnetic shielding.....	27
Figure 3.5 Electromagnetic nomenclature showing the Hadron/Forward Endcap assembly. The hadronic calorimetry were approximated as the Hadron plate, all components were added for magnetic shielding	27
Figure 3.6 BH curve of 1020 steel.....	29
Figure 3.7 MARCO cold-mass layout inside the cryostat.....	30
Figure 3.8 Schematic cross-section of the coil pack and mandrel, with materials and thickness of the different item	31
Figure 3.9 detailed dimensions of the conductors on the left.....	31
Figure 3.10 Warm (in black) and cold (in blue) dimensions of the cold mass	32
Figure 3.11 Electrical Schematic of MARCO Solenoid	33
Figure 3.12 Conductor entrance and exit schematic for each module	33
Figure 3.13 Design of the splices exits from the mandrel	34
Figure 3.14 Cross-section of the splices	35
Figure 3.15 Schematics of the geometry at the interface between each coil.	35
Figure 3.16 Three modules connected with their flanges.	36
Figure 3.17 Section of the 2D axisymmetric geometry of the MARCO magnet.....	37
Figure 3.18 Coil of MOD1, which shows the magnetic field distribution and peak field on cable	37
Figure 3.19 3D geometry of the MARCO magnet.....	38
Figure 3.20 Projectivity calculation for the RICH region in the 3D FE model	39
Figure 3.21 Field uniformity in the central region calculated in the 3D FE model.....	40
Figure 3.22 Amplitude of the possible misalignments for the cold mass and modules with respect to the nominal position.....	42
Figure 3.23 Example of misalignments distribution for MOD1, MOD2 and MOD3	43
Figure 3.24 The maximum variation of the fringe field at B5300, B7200, B3400.....	48
Figure 4.1 SEM image of a single strand with 468 NbTi filaments shown.....	50
Figure 4.2 Cross-section of the RICC conductor designed for MARCO solenoidal magnet.....	52

Electron-Ion Collider, Brookhaven National Laboratory and Thomas Jefferson National Accelerator Facility			
Doc No. EIC-SHC-TN-24-005	Author: Sandesh Gopinath	Effective Date: 12/05/2024	Review Frequency: NA
Process Description: EIC Design Report MARCO Magnet			Revision: 00

Figure 4.3 Jc curve @4.7 K, load line and load line margin for the reference case study $B_0 = 2T$. The working point (green rectangle) is shown, corresponding to a current sharing temperature of 7.15 K.	53
Figure 5.1 Cold mass of MARCO, consisting of 3 modules	55
Figure 5.2 Inter-module fixation.....	55
Figure 5.3 Cross sections of coil and conductor	56
Figure 5.4 Axial and radial tie rods on the cold mass	57
Figure 5.5 Homogenization of cable.....	65
Figure 5.6 Model to homogenize the insulated conductor	66
Figure 5.7 homogenization of the coil.....	67
Figure 5.8 2D axisymmetric magnetic model (left); representation of the Lorentz forces acting on each of the 3 coils at nominal field (right)	68
Figure 5.9 2D axisymmetric mechanical model (left), which includes the coils in gray and the mechanical structure (in blue); zoom-in view (right) of one of the two areas where the 3 modules are assembled	69
Figure 5.10 Coil wedges settings optimization. A: No wedges; B: Bonded contact, R θ fibers; C: Bonded contact, θZ fibers; D: Sliding contacts, R θ fibers; E: Sliding contact θZ fibers; F: Sliding contact except between the wedges and the mandrels (bonded contact), θZ fibers. The configuration is the one kept in 2D calculations.....	70
Figure 5.11 Zoom-in view on a portion of the coil, 6 layers and 2 turns	71
Figure 5.12 3D model.....	72
Figure 5.13 Contact configuration in the 3D model. On the left, the 2D optimized contacts. On the right, the cold mass fully impregnated contacts. The differences between both cases are marked by black dotted circles.	74
Figure 5.14 Thermal boundary conditions	75
Figure 5.15 – Von Mises equivalent stress distribution in the tie-rods and cold mass due to the self-weight.....	76
Figure 5.16 - Von Mises equivalent stress distribution in the tie-rods and cold mass due to a 3g acceleration along the X axis. This is the worst case in terms of stress for the tie-rods.....	76
Figure 5.17 - Von Mises equivalent stress distribution in the tie-rods and cold mass due to a 3g acceleration along the Y axis.	77
Figure 5.18 - Von Mises equivalent stress distribution in the tie-rods and cold mass due to a 3g acceleration along the Z axis.....	77
Figure 5.19 2D cool down results. On the left, the deflection; at the middle, the Von-Mises equivalent stresses; on the right, the distribution of von-Mises equivalent stress in the coils	78
Figure 5.20 Zoom-in view of the coil area where the peak Von Mises stress occurs. On the left, with properties of the detailed insulated conductor (left); on the right, with properties of the homogenized conductor. (right).....	78
Figure 5.21 2D cool-down shear results. On the left, the deflection; at the middle, the Von-Mises equivalent stresses; on the right, the Von-Mises equivalent stress distribution in the coils.	79
Figure 5.22 Zoom-in view of the conductor insulation area where the peak RZ shear stress occurs. On the top, with properties of the detailed insulated conductor; on the left, with properties of the homogenized conductor on the right.	79

Electron-Ion Collider, Brookhaven National Laboratory and Thomas Jefferson National Accelerator Facility			
Doc No. EIC-SHC-TN-24-005	Author: Sandesh Gopinath	Effective Date: 12/05/2024	Review Frequency: NA
Process Description: EIC Design Report MARCO Magnet			Revision: 00

Figure 5.23 Cold mass displacements in the three directions of the Cartesian frame after cool-down	80
Figure 5.24 Von-Mises equivalent stress in the mandrel (left) and in the tie rods (right), after cool-down	81
Figure 5.25 Von-Mises equivalent stress (left) and hoop stress (right) in the coils, after cool-down	81
Figure 5.26 Coil shear stress in R θ (left), θ Z (center), and RZ (left), after cool-down	82
Figure 5.27 Results from 2D energization model. On the left, the deflection; in the middle, the peak von-Mises equivalent stresses; on the right, the distribution of von-Mises equivalent stress in the coils.....	83
Figure 5.28 Zoom-I view of the conductor insulation area where the Von-Mises equivalent peak stress occurs, using the properties of the detailed insulated conductor (left), and of the homogenized conductor (right)	84
Figure 5.29 2Shear stress results from the 2D energization model. On the left, the deflection; in the middle, the von-Mises equivalent stresses; on the right, the distribution of von-Mises equivalent stress in the coils.....	84
Figure 5.30 Zoom-in view of the conductor insulation area where the peak RZ shear stress occurs, using the properties of the detailed insulated conductor (left), and of the homogenized conductor (right).....	85
Figure 5.31 displacements of cold mass in cylindrical coordinates and Cartesian frame, during energization	86
Figure 5.32 Von-Mises equivalent stress in the mandrel (left) and the tie rods (right), during energization	87
Figure 5.33 Von-Mises equivalent stress (left) and hoop stress (right) in the coils, during energization	87
Figure 5.34 Coil shear stress in R θ (left) θ Z (center) and RZ (left), during energization	88
Figure 5.35 Summary of von-Mises equivalent stress for each load case with the acceptance criteria shown in dotted lines	90
Figure 6.1 Magnet Assembly.....	94
Figure 6.2 Tie rods.....	95
Figure 6.3 Overview of EIC detector magnet.....	96
Figure 6.4 Inner vessel of helium phase separator.....	97
Figure 6.5 Outer vessel of helium phase separator	97
Figure 6.6 Design-by-Rules of vacuum vessel	98
Figure 6.7 Boundary conditions for load case 2.....	99
Figure 6.8 Convergence history for combination 2 load case	100
Figure 6.9 Converged solution of load case combination 2	100
Figure 6.10 Boundary condition for the local failure analysis	101
Figure 6.11 FEA local failure analysis of vacuum vessel	102
Figure 6.12 Eigenvalue buckling analysis with Load Case (5) $[0.88(P + D) + 0.71Ex + 0.71L]$. The earthquake occurs in the X direction. A factor of 0.0118 is applied to ensure the maximum imperfection is 11 mm.....	103
Figure 6.13 Boundary condition for Step 3.5x	103

Electron-Ion Collider, Brookhaven National Laboratory and Thomas Jefferson National Accelerator Facility			
Doc No. EIC-SHC-TN-24-005	Author: Sandesh Gopinath	Effective Date: 12/05/2024	Review Frequency: NA
Process Description: EIC Design Report MARCO Magnet			Revision: 00

Figure 6.14 Radius (X) of the model in the converged solution in the cylindrical coordinate system. The radius of the outer shell is 1.78 m. Without any loads, the radius should be within 1.759 m to 1.781 m. Since loads were applied, the deformed radius is slightly away from 1.759 m and 1.781 m.	104
Figure 6.15 Cryogenic Chimney of EIC detector magnet	105
Figure 7.1 Cryogenic flowchart	106
Figure 7.2 Cool-down process flowchart	109
Figure 7.3 Thermosiphon process flowchart	110
Figure 7.4 Summer (Long) shut-down process flowchart	111
Figure 7.5 Refrigerator shut-down process flowchart	112
Figure 7.6 Quench process flowchart	113
Figure 7.7 Vacuum loss process flowchart	114
Figure 7.8 Bellow for the pressure relief valve and the burst disc	117
Figure 7.9 Eddy current power in the mandrel	119
Figure 7.10 Piping for thermosiphon	121
Figure 7.11 Primary and spare supply lines	126
Figure 7.12 Soldering and brazing of the tubes	127
Figure 7.13 Primary and spare tubes of the heat exchanger	128
Figure 7.14 Primary and spare piping on top of the mandrel	129
Figure 7.15 Piping in the phase separator vacuum vessel	130
Figure 7.16 Overview of thermal shield	131
Figure 7.17 Surface areas of thermal shield	132
Figure 7.18 Helium phase separator and cryogenic chimney overview	135
Figure 7.19 Phase separator	136
Figure 7.20 Dimensional symbols for the phase separator and its vacuum vessel	137
Figure 8.1 Magnet system layout	142
Figure 8.2 Thermosiphon Schematic, a) detailed layout , b) basic layout	143
Figure 8.3 Magnet detailed model with outer cryostat cylinder hidden	144
Figure 8.4 Thermosiphon piping distribution layout detail	145
Figure 8.5 (a) FEA half module geometry with (b) cross-section view	146
Figure 8.6 FLUENT flow volume with mesh view in the inset	147
Figure 8.7 Sample mesh through pipe	148
Figure 8.8 FLUENT boundary conditions	149
Figure 8.9 Eddy current load during 1.0 A/s ramp up as imported in ANSYS	150
Figure 8.10 Thermosiphon pipe wall temperature distribution	151
Figure 8.11 Fluid mixture density distribution along the pipe wall. The mixture is single phase at the supply header and gets lighter as it heats up	152
Figure 8.12 Pressure drop across flow path	153
Figure 8.13 Mesh Overview	154
Figure 8.14 Steady State FEA boundary conditions	157
Figure 8.15 Steady state FEA temperature distribution with 1 A/s ramp up eddy current in the (a) cold mass and (b) coil	158

Electron-Ion Collider, Brookhaven National Laboratory and Thomas Jefferson National Accelerator Facility			
Doc No. EIC-SHC-TN-24-005	Author: Sandesh Gopinath	Effective Date: 12/05/2024	Review Frequency: NA
Process Description: EIC Design Report MARCO Magnet			Revision: 00

Figure 8.16 Steady state FEA temperature distribution within the cold mass thickness section	159
Figure 8.17 1D fluid mesh element 116.....	160
Figure 8.18 Transient FEA - boundary conditions after 2 days	161
Figure 8.19 Transient FEA results showing duration needed to cool down cold mass from 300 K-50 K.....	162
Figure 8.20 Transient FEA temperature distribution in the a. cold mass and b. coil after 5 days of cool down.....	163
Figure 9.1 Current density distribution in the mandrel during ramp-up	166
Figure 9.2 Current decay of the mandrel and the magnet during a fast discharge	167
Figure 9.3 A zoom-in view on the first seconds of the fast discharge. Current decays of the mandrel and of the magnet are shown.	168
Figure 9.4 MARCO Conductor cross section showing copper stabilizer and superconducting strands.....	169
Figure 9.5 MIITs plots for the magnet evaluation - (a) Plot showing the Coil Hot spot temperature vs MIITs (b) The plot showing the magnet/coil survival time wrt to MIITs, and (c) The Coil hot spot temperature with time evaluated based on MIITs, (d) the coil hot spot temperature in first few seconds (MIITs estimate)	171
Figure 9.6 Logic structure of the COMSOL quench model	172
Figure 9.7 Model used in COMSOL. The overall geometry includes the yoke. A zoom-in view on the area marked with the yellow circle is shown, which illustrates the turns, interlayer insulation, ground insulation, and mandrel.	173
Figure 9.8 Conductor thermal conductivity.	174
Figure 9.9 Conductor electrical resistivity	175
Figure 9.10 MARCO electrical circuit	176
Figure 9.11 Magnetic field computed by COMSOL	177
Figure 9.12 Conductor resistivity for MOD.....	178
Figure 9.13 Current redistribution model.....	178
Figure 9.14 Current decay in the coils (blue and in the mandrel.....	179
Figure 9.15 Quenched turns as a function of the time	180
Figure 9.16 Coil voltage for each module and total resistive voltage at the extremities of the magnet.....	181
Figure 9.17 Coils resistance as a function of time	182
Figure 9.18 Power dissipated in the circuit. The primary circuit consists in the magnet plus the dump resistance.....	183
Figure 9.19 Maximum temperature of each module during quench.	184
Figure 9.20 Temperature profile on the three modules after 65 s. The hotspot is localized in MOD1, where the quench started.....	184
Figure 9.21 Hotspot temperature for the fault case scenario	185
Figure 9.22 Resistive voltage in case of fault scenario	186
Figure 9.23 Magnet protection schematic with dump resistor and two breakers	186
Figure 9.24 Schematic arrangement of magnet protection and I&C layout for interlocks identified	187

The only official copy of this document is the one online in the SharePoint Document Center. Before using a printed copy, verify that it is current by checking the printed document's Revision History log with that of the online version.

Electron-Ion Collider, Brookhaven National Laboratory and Thomas Jefferson National Accelerator Facility			
Doc No. EIC-SHC-TN-24-005	Author: Sandesh Gopinath	Effective Date: 12/05/2024	Review Frequency: NA
Process Description: EIC Design Report MARCO Magnet			Revision: 00

Figure 10.1 MARCO Solenoids layout.....	188
Figure 10.2 Distribution of voltage taps for the MARCO solenoid and its current leads and busbars. The redundant voltage taps are in dashed line.	189
Figure 10.3 Voltage taps distribution on one module. The redundant voltage taps are in dashed line.	190
Figure 10.4 Redundant voltage taps distribution for the full Marco coil	190
Figure 10.5 Distribution of voltage taps on one module for the current leads	191
Figure 10.6 DCCTs positions in the MARCO solenoid lay out	191
Figure 10.7 Thermal sensors distribution	192
Figure 10.8 Cryogenic scheme with the vacuum gauges and the helium level and flow meters localization	193
Figure 10.9 Load cells localization on the tie-rods.....	193
Figure 11.1 MARCO Magnet Overview a. 3D view, b. Overall dimensions, c. Assembly cross-section	194
Figure 12.1 requirements to product specifications and acceptance criteria.....	197

Electron-Ion Collider, Brookhaven National Laboratory and Thomas Jefferson National Accelerator Facility			
Doc No. EIC-SHC-TN-24-005	Author: Sandesh Gopinath	Effective Date: 12/05/2024	Review Frequency: NA
Process Description: EIC Design Report MARCO Magnet			Revision: 00

List of Tables

Table 1.1 EIC High-Level Parameters of the BNL-sited EIC.....	17
Table 2.1 Magnet Specification	19
Table 2.2 The Magnet interface	23
Table 3.1 Iron fraction of the different components in the yoke	29
Table 3.2 Geometric specifications of MARCO solenoid	32
Table 3.3 Number of turns per layer at the extremities of each coil	34
Table 3.4 Nominal magnetic performances of the MARCO magnet	38
Table 3.5 Performances of the MARCO magnet versus requirements needed for the ePIC physics.....	39
Table 3.6 Results for axial displacements and fabrication tolerances.....	44
Table 3.7 Results for a maximum displacement of the cold mass	45
Table 3.8 Results for a maximum displacement of MOD1	45
Table 3.9 Results for a maximum displacement of MOD2	45
Table 3.10 Results for a maximum displacement of MOD3	45
Table 3.11 Impact of one layer missing in a module.....	46
Table 3.12 Impact of permeability variation	46
Table 4.1 Bottura fit parameters from [3] including a 15% degradation factor due to cooling and soldering process.....	49
Table 4.2 Main characteristics of the MARCO RICC Conductor	52
Table 4.3 MARCO conductor margins.....	53
Table 4.4 Conductor stability – Summary of the evaluation criteria for MARCO magnet	54
Table 5.1 Copper Properties	57
Table 5.2 Copper properties as a function of the temperature[8].....	58
Table 5.3 Niobium – Titanium Properties	58
Table 5.4 G10 Properties	59
Table 5.5 G10 Young's modulus, poisson's ratio and tensile strength [13]	60
Table 5.6 G10 young's modulus “ Normal to cloth layers” as a function of the temperature values obtained by curve fitting from [14]	60
Table 5.7 G10 poisson's ratio [16].....	61
Table 5.8 fiber glass epoxy properties.....	62
Table 5.9 Fiber glass epoxy young's modulus and poisson's ratio at 4.2k, adapted from [17] ...	62
Table 5.10 Brass 70/30 Properties	63
Table 5.11 Ag3.5/Sn96.5 Soft solder properties	63
Table 5.12 Ti6AL4V Properties	64
Table 5.13Acceptance criteria for stress	64
Table 5.14 Homogenized properties of the cable	66
Table 5.15 Homogenized properties of the insulated conductor	66
Table 5.16 Homogenized properties of the coil	67
Table 5.17 Wedge configuration for optimization.....	70
Table 5.18 Specifications of Tie Rods	73
Table 5.19.....	76

The only official copy of this document is the one online in the SharePoint Document Center. Before using a printed copy, verify that it is current by checking the printed document's Revision History log with that of the online version.

Electron-Ion Collider, Brookhaven National Laboratory and Thomas Jefferson National Accelerator Facility			
Doc No. EIC-SHC-TN-24-005	Author: Sandesh Gopinath	Effective Date: 12/05/2024	Review Frequency: NA
Process Description: EIC Design Report MARCO Magnet			Revision: 00

Table 6.1 Materials in the magnet	93
Table 6.2 Material thickness and interaction length	94
Table 7.1 List of valves	107
Table 7.2 Cold mass tie rod conduction	115
Table 7.3 Phase separator tie rod conduction	115
Table 7.4 Cold valve heat conduction	116
Table 7.5 Heat load from the bellows	117
Table 7.6 Heat load from the thermal shield supports	118
Table 7.7 Radiation heat loads at 4.5 K	118
Table 7.8 Radiation heat load on the thermal shield between 45 K and 65 K	118
Table 7.9 Thermosiphon calculation results at zero current.....	124
Table 7.10 Thermosiphon calculation results for ramping up current.....	124
Table 7.11 Thermosiphon calculation results for low level heat load with no heaters	124
Table 7.12 Thermosiphon calculation results for low level heat load with 20 W heaters	125
Table 7.13 Thermosiphon calculation results for high level heat load 60 W.....	125
Table 7.14 Pressure drop in the piping of the thermal shield	133
Table 7.15 Diameters of valves	136
Table 7.16 Dimensions of inner helium vessel (helium phase separator) and outer vessel (vacuum vessel).....	137
Table 8.1 Helium Properties considered for simulations.....	148
Table 8.2 Heat loads considered in FEA	150
Table 8.3 Material Properties	155
Table 8.4 Homogenized conductor properties	155
Table 8.5 Summary of boundary conditions	157
Table 8.6 Transient FEA cool-down parameters, highlighted in red are FEA inputs	160
Table 9.1 – Ramp-up / ramp-down results and main magnetic parameters of the mandrel	165
Table 9.2 : Conductor design parameters	168
Table 9.3 Magnet design parameters.....	169
Table 12.1 The traceability of the EIC Project requirements.....	197
Table 12.2 Manufacturing tests, inspections, and acceptance parameters.....	198

Electron-Ion Collider, Brookhaven National Laboratory and Thomas Jefferson National Accelerator Facility			
Doc No. EIC-SHC-TN-24-005	Author: Sandesh Gopinath	Effective Date: 12/05/2024	Review Frequency: NA
Process Description: EIC Design Report MARCO Magnet			Revision: 00

1 Introduction to EIC

The Electron Ion Collider (EIC) at Brookhaven National Laboratory (BNL) is being designed and constructed in close partnership between BNL and the Thomas Jefferson National Accelerator Facility (JLab). The physics requirements that drive the EIC design are specified in the 2015 and 2023 Nuclear Science Advisory Committee Long-Range Plan documents and in the 2018 National Academies of Sciences, Engineering and Medicine reports. The high-level parameters of the BNL-sited EIC are given below in table 1.1:

Table 1.1 EIC High-Level Parameters of the BNL-sited EIC

Parameter	Value/Range
Center of Mass Energies	29 GeV -140 GeV
High Luminosity	$10^{33} - 10^{34} \text{cm}^{-2} \text{sec}^{-1}$
Hadron Beam Polarization	70 %
Electron Beam Polarization	70 %
Ion Species Range	P to Uranium
Number of Interaction regions	Up to 2

The EIC design is based on the existing Relativistic Heavy Ion Collider (RHIC) at BNL. The EIC will use the existing hadron storage ring at 40 GeV and in the range 100-275 GeV, a new electron ring 5-18 GeV, a new electron rapid cycling synchrotron (RCS) and a new high luminosity interaction region (IR). The basic layout of the EIC rings is shown in Figure 1.1. The layout indicates the possible locations of the detectors. The magnet described in this design report is for the first detector-1 (ePIC detector) [1]. The ePIC detector will be installed at the IR6 location at 6 o'clock. A possible future second detector can be installed at the IR8 location at 8 o'clock.

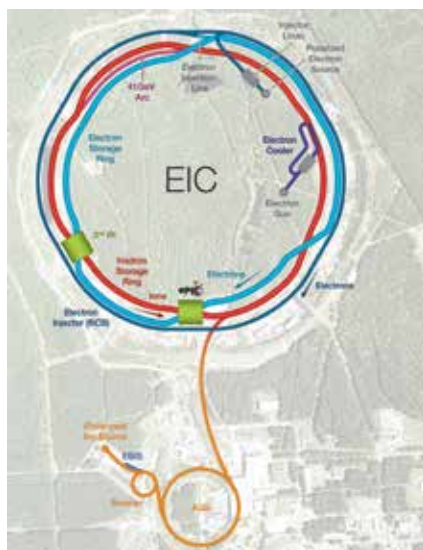


Figure 1.1 EIC Layout

The only official copy of this document is the one online in the SharePoint Document Center. Before using a printed copy, verify that it is current by checking the printed document's Revision History log with that of the online version.

Electron-Ion Collider, Brookhaven National Laboratory and Thomas Jefferson National Accelerator Facility			
Doc No. EIC-SHC-TN-24-005	Author: Sandesh Gopinath	Effective Date: 12/05/2024	Review Frequency: NA
Process Description: EIC Design Report MARCO Magnet			Revision: 00

1.1 Interaction region and the detector area

The EIC project baseline configuration includes one interaction region (IR) and therefore one detector. The IR layout is shown in Figure 1.2. The overall length of the interaction region where the detector elements are integrated is approximately 75 m.

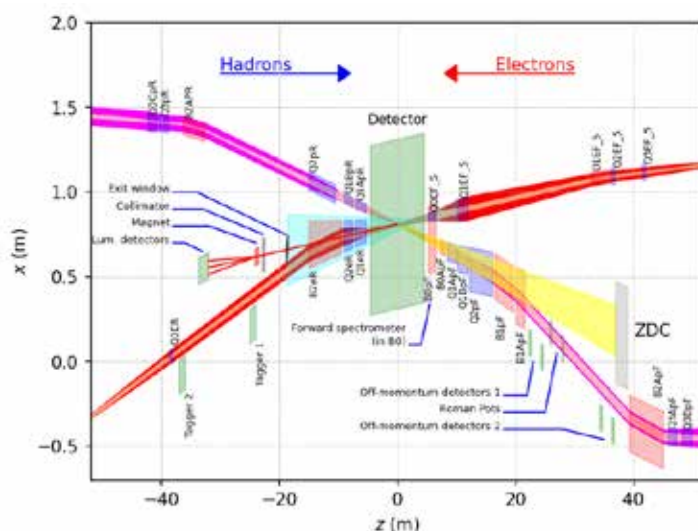


Figure 1.2 Interaction region layout

The detector solenoid will be centered in this area and located in the experimental wide-angle Hall. The magnet will be aligned to the electron beam axis. Figure 1.3 shows the layout of the ePIC detector.

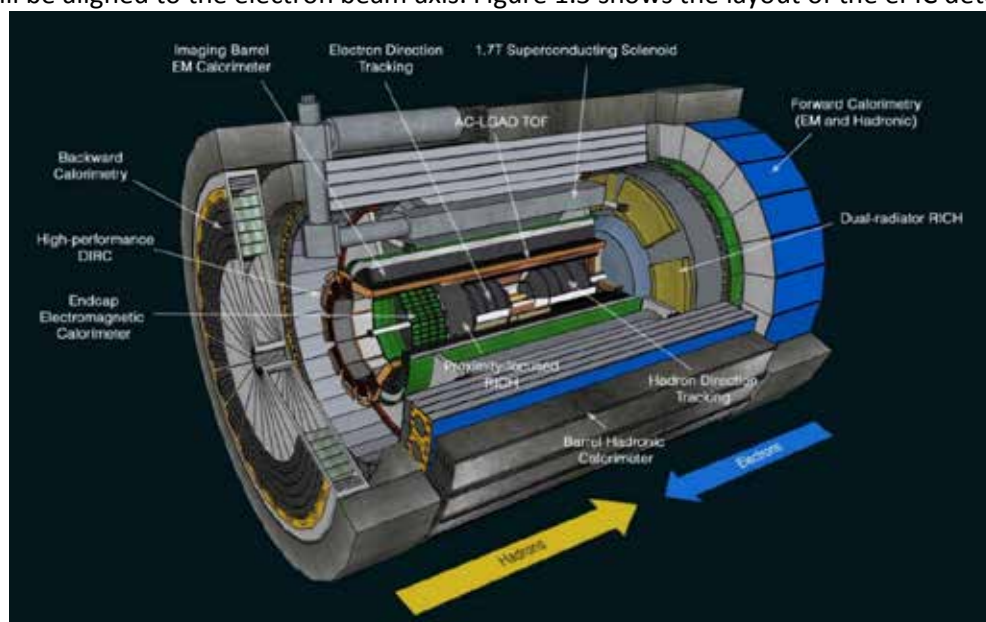


Figure 1.3 The Detector Layout

Electron-Ion Collider, Brookhaven National Laboratory and Thomas Jefferson National Accelerator Facility			
Doc No. EIC-SHC-TN-24-005	Author: Sandesh Gopinath	Effective Date: 12/05/2024	Review Frequency: NA
Process Description: EIC Design Report MARCO Magnet			Revision: 00

2 Magnet Specification

2.1 Magnet Specification Parameters

A 2T solenoid will be used for the ePIC detector. This document outlines the specification of the new solenoid for the EIC. These specifications are with the return flux around the magnet. The details of the return flux is given in 3.1. The magnetic return flux is not part of the magnet vendor contract. The magnet specifications are given in Table 2.1

Table 2.1 Magnet Specification

Parameter	Detector 1-Solenoid
Nominal Central Field at IP (T)	2
Operating Field Range (T)	0.5-2.0
Magnetic Field Polarity	Bipolar
Coil length (mm)	3492
Warm bore diameter (m)	2.84
Cryostat length (m)	<3.85
Cryostat outer diameter (m)	<3.54
Flat Field area	± 100 cm around center 80 cm radius
Field uniformity in Flat field Area (%)	12.5
RICH area	From z=+180 cm to 280 cm
Projectivity in RICH Area (mrad@30GeV/c)	0.1
Projectivity in RICH Area (T/Amm ²)	10
Charging voltage (V)	10
Fast discharge voltage maximum (V)	500
Quench hot spot temperature (K)	<150
Temperature margin (K)	>1.5
Current margin (%)	<30
Charging time (hr)	2-3
Cooldown time (weeks)	3-4
Cooling scheme	Thermosiphon
Conductor	Cu Stabilized NbTi Rutherford cable
Operating Temperature	4.5

There are three areas of importance from the magnetic field point of view, these are:

Electron-Ion Collider, Brookhaven National Laboratory and Thomas Jefferson National Accelerator Facility			
Doc No. EIC-SHC-TN-24-005	Author: Sandesh Gopinath	Effective Date: 12/05/2024	Review Frequency: NA
Process Description: EIC Design Report MARCO Magnet			Revision: 00

1. Flat Field Area
2. RICH detector Area
3. Stray field limitation at IR magnets and on RCS

The details of these areas are given below. The steel around the magnet governs the magnetic field quality and stray field. These specifications are for the reference purpose only and will be met as long as coils are built to the design.

2.2 Flat Field Area

This is 200 cm long and 80 cm in radius around the IP, the field uniformity required in this area is 12.5%. The field uniformity definition, used in this document, is:

$$\text{Field Uniformity (\%)} = \frac{dB * 100}{B_{\text{center}}}$$

Where,

$dB = B_{\text{max}} - B_{\text{min}}$ (in the area of interest), and

$B_{\text{center}} = B$ at the magnet center

The flat field area with respect to the magnet and cryostat is shown in Figure 2.1

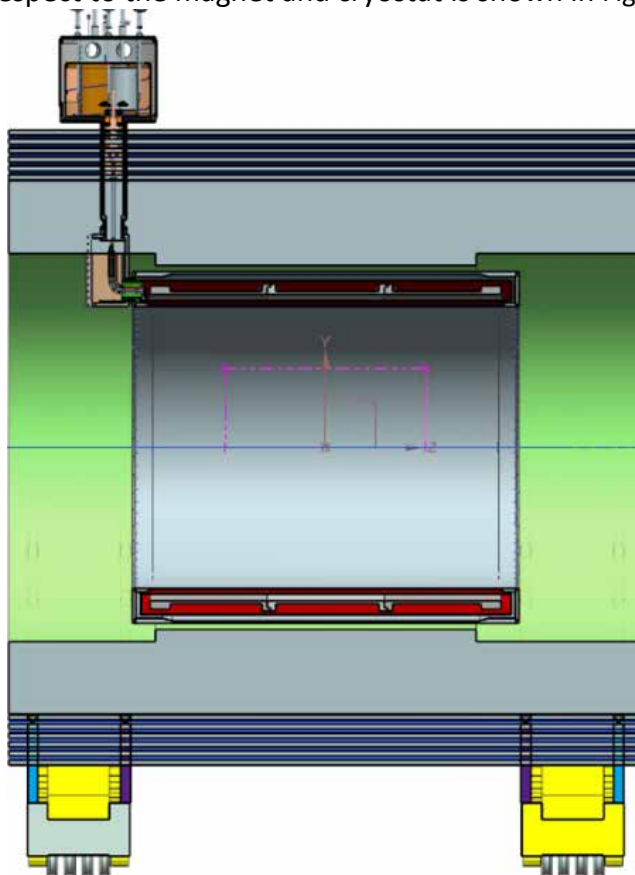


Figure 2.1 Flat Field Area

Electron-Ion Collider, Brookhaven National Laboratory and Thomas Jefferson National Accelerator Facility			
Doc No. EIC-SHC-TN-24-005	Author: Sandesh Gopinath	Effective Date: 12/05/2024	Review Frequency: NA
Process Description: EIC Design Report MARCO Magnet			Revision: 00

2.3 RICH detector area

In order to maximize the RICH performance based on the gas radiator it is critical to minimize the bending of the tracks in the volume of the gas radiator, for this one needs to shape the field such that it is parallel to the different scattering angles of particles covered by the RICH. The RICH area extends from $z=+180$ cm to $+280$ cm. The projectivity in this region should be less than 10 T/Amm² or less than 0.1 mrad @30GeV/c. The projectivity can be calculated as below:

$$Proj = \frac{1}{\Omega} \int_{\Omega} \frac{|B_r| - \left| \frac{r}{z} B_z \right|}{J_e} d\Omega \leq 10 \frac{T}{Amm^2}$$

Where Ω is the gas volume of the detector, B_r and B_z are respectively the radial and the axial component of the magnetic, J_e the engineering current density of the magnet.

The RICH area with respect to the magnet and cryostat is shown in Figure 2.2.

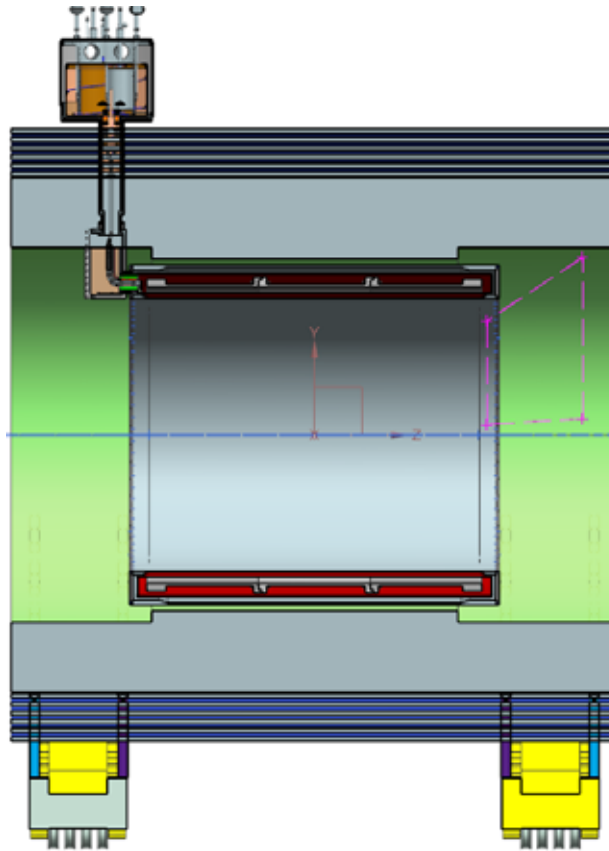


Figure 2.2 RICH Area

Electron-Ion Collider, Brookhaven National Laboratory and Thomas Jefferson National Accelerator Facility			
Doc No. EIC-SHC-TN-24-005	Author: Sandesh Gopinath	Effective Date: 12/05/2024	Review Frequency: NA
Process Description: EIC Design Report MARCO Magnet			Revision: 00

2.4 Stray field limitations at IR magnets and on RCS

The detector solenoid has neighboring IR magnets. In order to reduce the effect of solenoid magnet on IR magnets, there is a requirement of stray field less than 10 G at the B0ApF and Q1ApR magnets (Figure 1.2), these magnets extends from $z = 7.4$ m to 8 m and $z = -5.3$ m to -7.1 m respectively. The RCS is radially 335.2 cm from the magnet central axis and stray field requirement there is <0.007 Tm. The central line of RCS is shown in Figure 2.3. As mentioned earlier that the steel around the magnet governs the stray field. These specifications will be met as long as coils are built to the design.

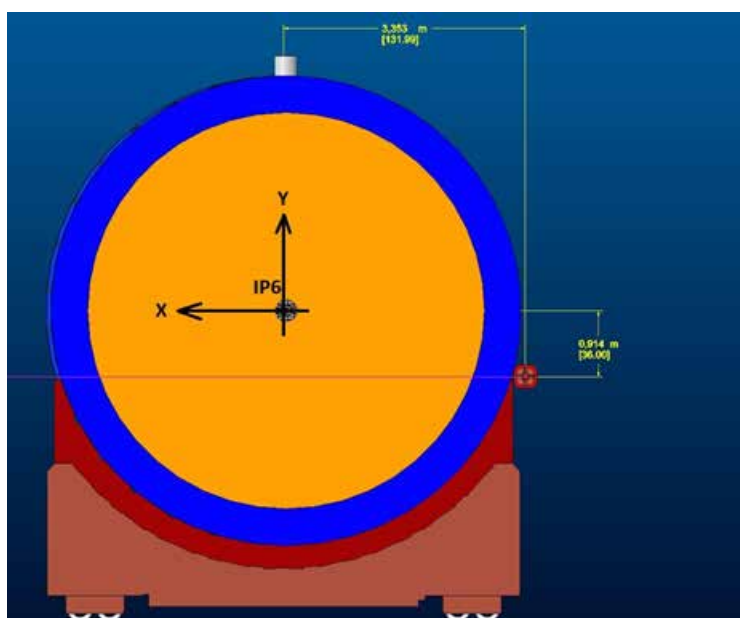


Figure 2.3 RCS Location

2.5 Description of Key Interfaces

Other detectors and detector components surround the detector magnet. In order to install all the sub-components of the detector system various interfaces are defined. These are given in Table 2.2. There is an interface document developed for all these interconnections, this is given as Appendix 1. The experimental hall has required electrical power, low conductivity water (LCW) connection and 4.5 K liquid helium supply. The magnet power supply specifications are given in Appendix 2, the power supply details are not included in this design report. The magnet is protected using a dump resistor, the details of the dump resistor and the location of the

The only official copy of this document is the one online in the SharePoint Document Center. Before using a printed copy, verify that it is current by checking the printed document's Revision History log with that of the online version.

Electron-Ion Collider, Brookhaven National Laboratory and Thomas Jefferson National Accelerator Facility			
Doc No. EIC-SHC-TN-24-005	Author: Sandesh Gopinath	Effective Date: 12/05/2024	Review Frequency: NA
Process Description: EIC Design Report MARCO Magnet			Revision: 00

power supply and dump resistor is also given in Appendix 2. The minimum instrumentation required for this magnet installation and operation is given in section 10. The instrumentation and instrumentation rack is not part of this design report and will be included in the magnet vendor scope. The instrumentations racks will be placed on the north platform shown in the hall infrastructure. The 4.5 K liquid helium will be supplied to the magnet using the cryo flex lines. The cryo flex line design is not included in this design report.

Table 2.2 The Magnet interface

InterfaceID	Type	RelatedSystemID	InterfaceName	Description
I-DET-MAG.1	MECH	DET-INF-MECH	External Support Structure	Total weight of the solenoid and all embedded components must be supported.
I-DET-MAG.2	SPACE	DET-INF-SPACE	LCW Connection	The LCW water cooled leads will need to be fully supported along their path between the electrical room and the magnet.
I-DET-MAG.3	SPACE	DET-INF-SPACE	Cryogenic Connection Point	Cryogenic connection must be as close as possible to the source, and have a flexible line allowing the magnet to be moved between the Hall and the maintenance area while still connected.
I-DET-MAG.4	SPACE	DET-HCAL-BAR	External Space Constraint	The maximum size of the solenoid is limited to the interior bore of the barrel hadron calorimeter and necessary support structures.
I-DET-MAG.5	SPACE	DET-HCAL-BCK	Backward Space Constraint	The maximum backward location for the solenoid is limited by the position of the Lepton Direction Hadron Calorimeter and the associated cabling plenum between them.
I-DET-MAG.6	SPACE	DET-PID-FWD	Forward Space Constraint	The maximum forward location for the solenoid is limited by the position of the Dual RICH detector and the associated cabling plenum between them.
I-DET-MAG.7	SPACE	DET-ECAL-BAR	Interior Space Constraint	The interior radius of the solenoid is limited by the size of the barrel Electromagnetic Calorimeter and its support system.
I-DET-MAG.8	ENV		Ice Management	An ice management system will be required to melt accumulated ice on the chimney. (Water should evaporate and will not require drainage)
I-DET-MAG.9	ENV	INF-SPACE	Fringe Field	A boundary must be established to identify the extent of the magnet's stray field during operations.
I-DET-MAG.10	ENV	DET	Magnetic Material	No detectors or components constructed with magnetic material may be added to the detector without prior consultation with the magnet group.
I-DET-MAG.11	COOL	DET-INF-COOL-LCW	Power Supply Cooling	The power supply, located in an adjacent electrical room, will need to be cooled with low conductivity water.
I-DET-MAG.12	CRYO	DET-INF-CRYO	Magnet Cooling	The solenoid will require a continuous flow of cryogens to maintain temperature in both the experimental hall and the maintenance area. Interface includes cryogenic source and warm return.
I-DET-MAG.13	ELEC	DET-INF-ELEC	Electrical Power	Solenoid will be provided power via the power supply located in an adjacent room.
I-DET-MAG.14	ELEC	DET-INF-ELEC	Instrumentation Backup Power	The instrumentation rack for the solenoid will require backup/UPS power adequate to safely shutdown the system in the event of a power failure.
I-DET-MAG.15	CONTROL	DET-COMP-ONLINE	Controls and Instrumentation	Control cabling for the magnet instrumentation will be run from the solenoid to the instrumentation rack on the carriage.
I-DET-MAG.16	DATA	DET-COMP-ONLINE	Monitoring Data	Live monitoring data from the solenoid's operation must be recorded and maintained for diagnostic purposes.
I-DET-MAG.17	PARAM	DET	Magnetic Field Requirement	All subordinate detectors are dependent on the continuous operation of the solenoid and on the delivery of a consistent, stable magnetic field.

Electron-Ion Collider, Brookhaven National Laboratory and Thomas Jefferson National Accelerator Facility			
Doc No. EIC-SHC-TN-24-005	Author: Sandesh Gopinath	Effective Date: 12/05/2024	Review Frequency: NA
Process Description: EIC Design Report MARCO Magnet			Revision: 00

3 Magnetic Design - Electromagnetic

The main parameters of the MARCO magnet which are related to the physics requirements are the following:

- Field at center: 2 Tesla,
- Field homogeneity: 12.5%
- Projectivity: $<10 \text{ T mm}^2/\text{A}$
- Yoke diameter: 6.5 m on the HCal Barrel Calorimeter,
- Axial yoke length including endcaps: 9.5 m

Only the magnetically active elements are considered for the magnetic design. The magnetic flux generated by the superconducting coils is returned via three distinct sections of yoke described hereafter in this section and shown in Figure 3.1.

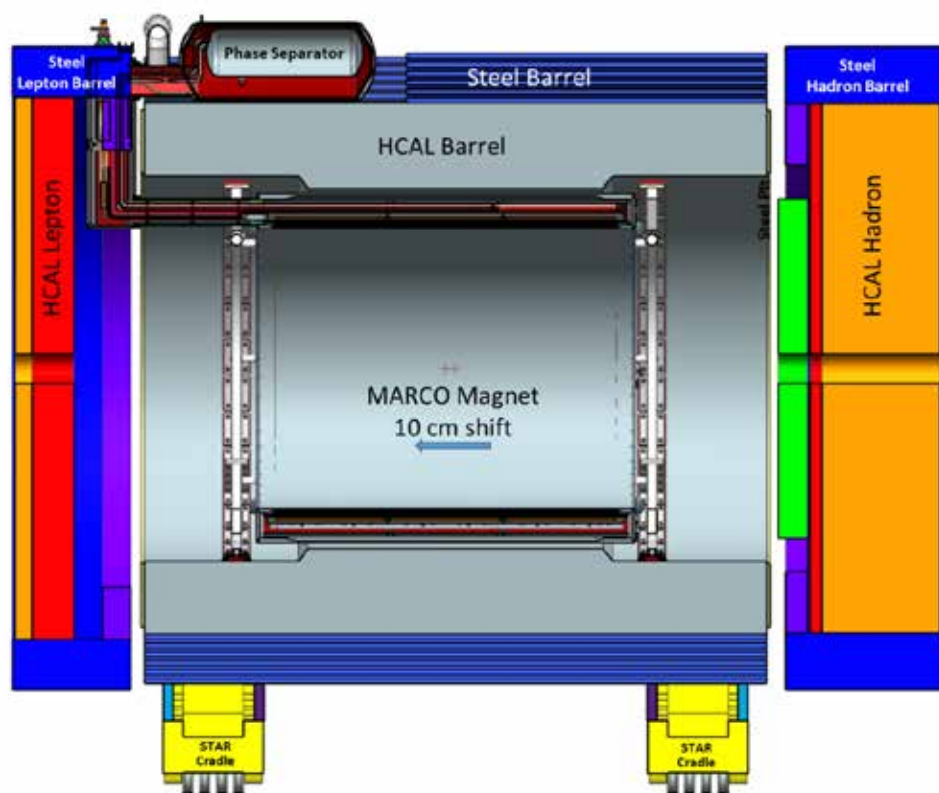


Figure 3.1 The yoke surrounding the coils

Electron-Ion Collider, Brookhaven National Laboratory and Thomas Jefferson National Accelerator Facility			
Doc No. EIC-SHC-TN-24-005	Author: Sandesh Gopinath	Effective Date: 12/05/2024	Review Frequency: NA
Process Description: EIC Design Report MARCO Magnet			Revision: 00

3.1 Return Flux

The magnet is surrounded by steel, which includes the steel in the HCals (Hadronic Calorimeters), and the additional steel was added to further reduce the stray field. This steel works as the flux return. The magnetic field is captured within the flux return steel with minimum leakage. Nevertheless, there are stray field requirements at IP6 that the electromagnetic design is required to adhere to. Various electromagnet studies are completed in order to minimize the stray field at the Rapid Cycling Synchrotron beamline passing through IP6. OPERA/TOSCA [2] was used to perform electromagnetic field analysis with the complex flux return geometry simplified as primitive solid bodies. Figure 3.2 shows the cross section view of the simplified flux return steel as modeled in TOSCA.

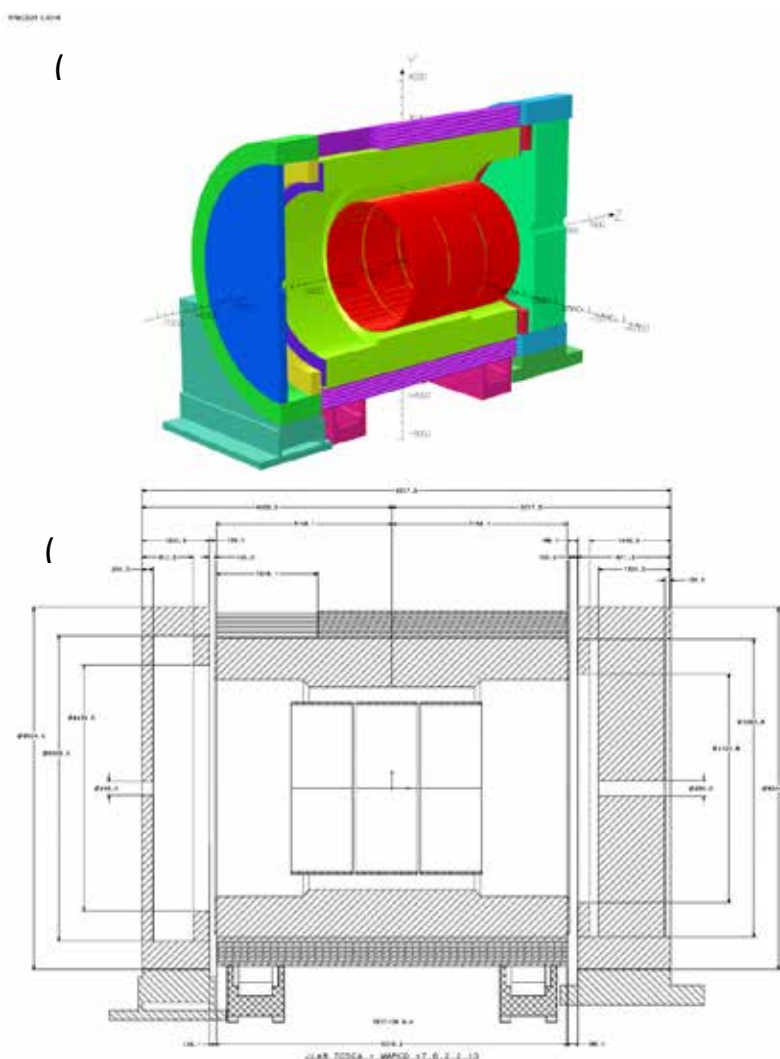


Figure 3.2 Simplified geometry that captures the soft magnetic steel – including steel in the detectors and steel used for shielding a. TOSCA model of the baseline geometry with the coils shown in red b. detailed dimensions with a cross section view of the implemented geometry

Electron-Ion Collider, Brookhaven National Laboratory and Thomas Jefferson National Accelerator Facility			
Doc No. EIC-SHC-TN-24-005	Author: Sandesh Gopinath	Effective Date: 12/05/2024	Review Frequency: NA
Process Description: EIC Design Report MARCO Magnet			Revision: 00

The baseline geometry includes the flux return that is part of the HCals, magnetic shielding steel and the simplified endcap support structures that are made of steel as well. Further details of the simplified geometry are shown in Figure 3.3, Figure 3.4, and Figure 3.5. The number in percentage indicates the quantity of ferromagnetic material in the volume considered (100% means the volume is completely filled with ferromagnetic material).

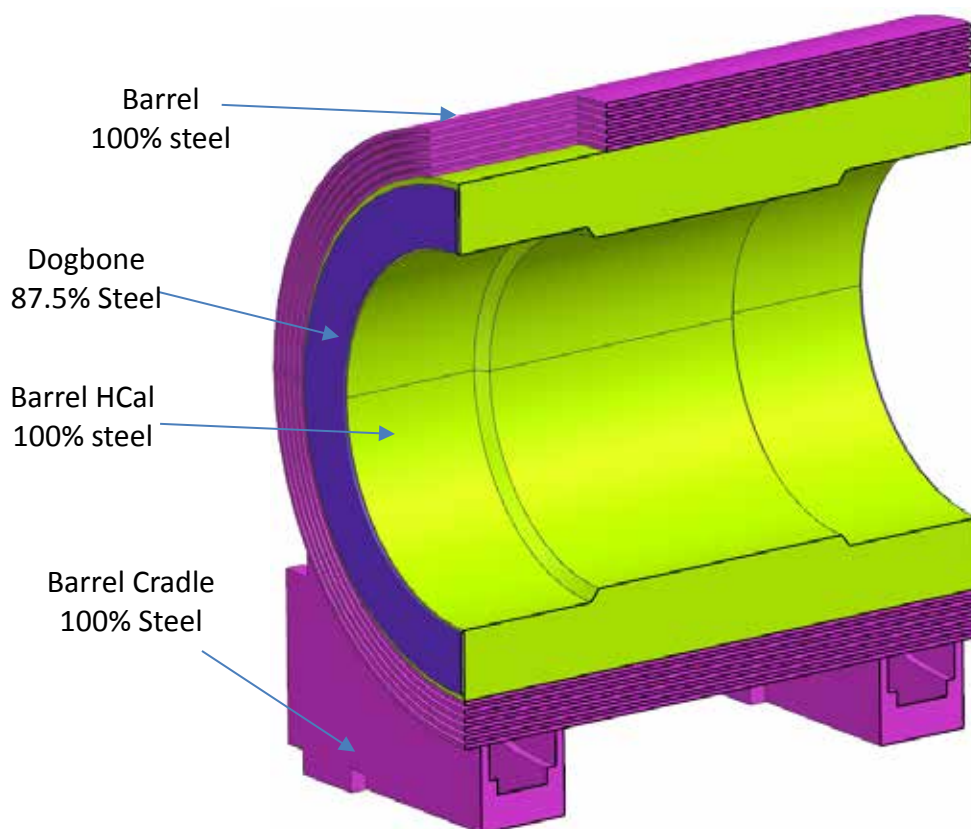


Figure 3.3 Electromagnetic nomenclature showing the Barrel Hadron calorimeter and the Barrel steel that is added for magnetic shielding

Electron-Ion Collider, Brookhaven National Laboratory and Thomas Jefferson National Accelerator Facility			
Doc No. EIC-SHC-TN-24-005	Author: Sandesh Gopinath	Effective Date: 12/05/2024	Review Frequency: NA
Process Description: EIC Design Report MARCO Magnet			Revision: 00

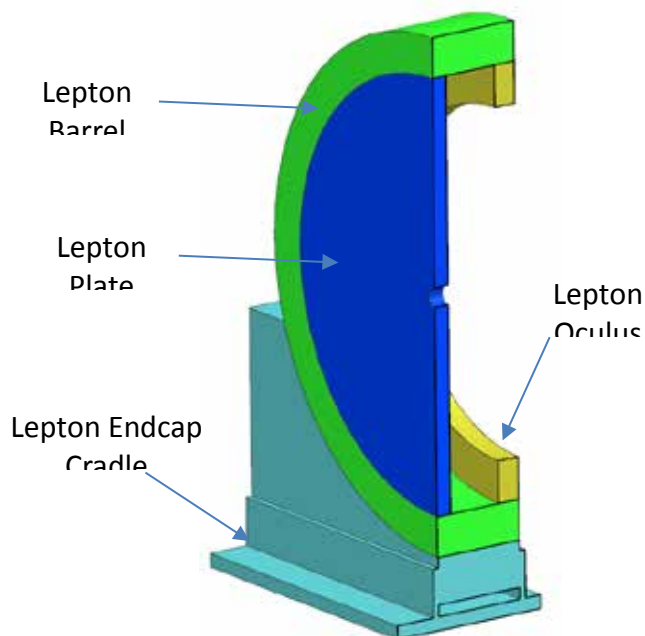


Figure 3.4 Electromagnetic nomenclature showing the Lepton/Backward Endcap assembly. All components were added for magnetic shielding.

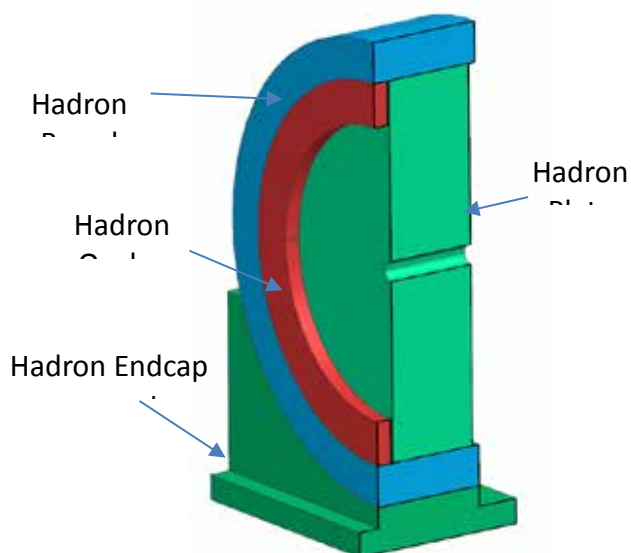


Figure 3.5 Electromagnetic nomenclature showing the Hadron/Forward Endcap assembly. The hadronic calorimetry were approximated as the Hadron plate, all components were added for magnetic shielding

Electron-Ion Collider, Brookhaven National Laboratory and Thomas Jefferson National Accelerator Facility			
Doc No. EIC-SHC-TN-24-005	Author: Sandesh Gopinath	Effective Date: 12/05/2024	Review Frequency: NA
Process Description: EIC Design Report MARCO Magnet			Revision: 00

Barrel Yoke

The Barrel Yoke consists of the HCal Barrel Calorimeter and the Steel Barrel Yoke. The HCal Barrel Calorimeter is made with 32 assembled sectors composed by 10 rows of 8 mm scintillator tiles (24 tiles per row), tilted with an angle of 12°. In each sector, 26.1 mm x 42.4 mm x 6300 mm tapered 1020 steel plates are piled up and used to separate each scintillator tile. The total fraction of steel in the volume is 70%. Dogbones made by the same steel enclose the calorimeter. Their fraction of steel in the volume is 66%. The Steel Barrel Yoke is made by 6 concentric rings of steel 1020, 50 mm thick, 6300 mm long, surrounding the HCal Barrel Calorimeter. Each ring is separated from the other by 40 mm. A specific volume is dedicated to the installation of the He phase separator, from which all the cryogenics circuits inside the cold mass are supplied. Its main purpose is to reduce the stray field. .

Hadron Yoke

The Hadron Yoke is consists of the HCal Hadron Calorimeter, the Steel Barrel Hadron Yoke and the HCal Hadron Oculus. Its name is given by the convention on the direction of the beams. In this case, the hadron beam is the one exiting the detector. The HCal Hadron Calorimeter is made by 70 pieces of 4 mm thick scintillator tiles, 10 pieces of 16 mm thick tungsten plates and 60 pieces of 16 mm thick steel 1020 plates. The average fraction of steel 1020 in the total volume is 75%. The Steel Barrel Hadron Yoke as well as the HCal Hadron Oculus are two structures in steel 1020 surrounding the calorimeter and returning the magnetic flux.

Lepton Yoke

The Lepton Yoke is composed by the HCal Lepton Calorimeter, the Steel Barrel Lepton Yoke and the HCal Lepton Oculus. Its name is given by the convention on the direction of the beams. In this case, the electrons beam is the one exiting the detector. The HCal Lepton Calorimeter is made by 50 pieces of 4 mm thick scintillator tiles, 10 pieces of 16 mm thick tungsten plates and 60 pieces of 16 mm thick steel 1020 plates. The average fraction of steel 1020 in the total volume is 75%. The Steel Barrel Lepton Yoke as well as the HCal Lepton Oculus are two structures in steel 1020 surrounding the calorimeter and returning the magnetic flux.

3.2 Yoke Material Properties

All steel is considered to be 1020 steel. The geometries of detectors that have steel in them are simplified into larger primitive shapes by including the geometric voids and material voids left by presence of nonmagnetic materials. A dilution percentage is assigned to the components according to the average fraction of the ferromagnetic material in the total volume of the HCal steel (see Table 3.1). The revised naming convention for electromagnetic simulation purposes are shown in Figure 3.3, Figure 3.4, and Figure 3.5; geometries with 100% iron are the steel added in addition to the existing steel in

The only official copy of this document is the one online in the SharePoint Document Center. Before using a printed copy, verify that it is current by checking the printed document's Revision History log with that of the online version.

Electron-Ion Collider, Brookhaven National Laboratory and Thomas Jefferson National Accelerator Facility			
Doc No. EIC-SHC-TN-24-005	Author: Sandesh Gopinath	Effective Date: 12/05/2024	Review Frequency: NA
Process Description: EIC Design Report MARCO Magnet			Revision: 00

the detectors. Dogbones are 38.1 mm thick structural plates that are part of the Barrel Hcal. In the electromagnetic model, only the envelope of each element has been modeled.



Figure 3.6 BH curve of 1020 steel

Table 3.1 Iron fraction of the different components in the yoke

Item	Iron fraction
Barrel Calorimeter	70%
Hadron Calorimeter	75%
Lepton Calorimeter	87.5%
Dogbones	66%
Steel Barrel	100%
Steel Hadron Barrel	100%
Steel Lepton Barrel	100%
Cradles	100%
Steel Hadron Oculus	100%
Steel Lepton Oculus	100%

Electron-Ion Collider, Brookhaven National Laboratory and Thomas Jefferson National Accelerator Facility			
Doc No. EIC-SHC-TN-24-005	Author: Sandesh Gopinath	Effective Date: 12/05/2024	Review Frequency: NA
Process Description: EIC Design Report MARCO Magnet			Revision: 00

3.3 The Superconducting coils and the Mandrel

The MARCO solenoid is made of three modules with three identical superconducting coils wound internally on a mandrel in brass 70-30 (Figure 3.7). The coils are indirectly cooled using a thermosiphon.

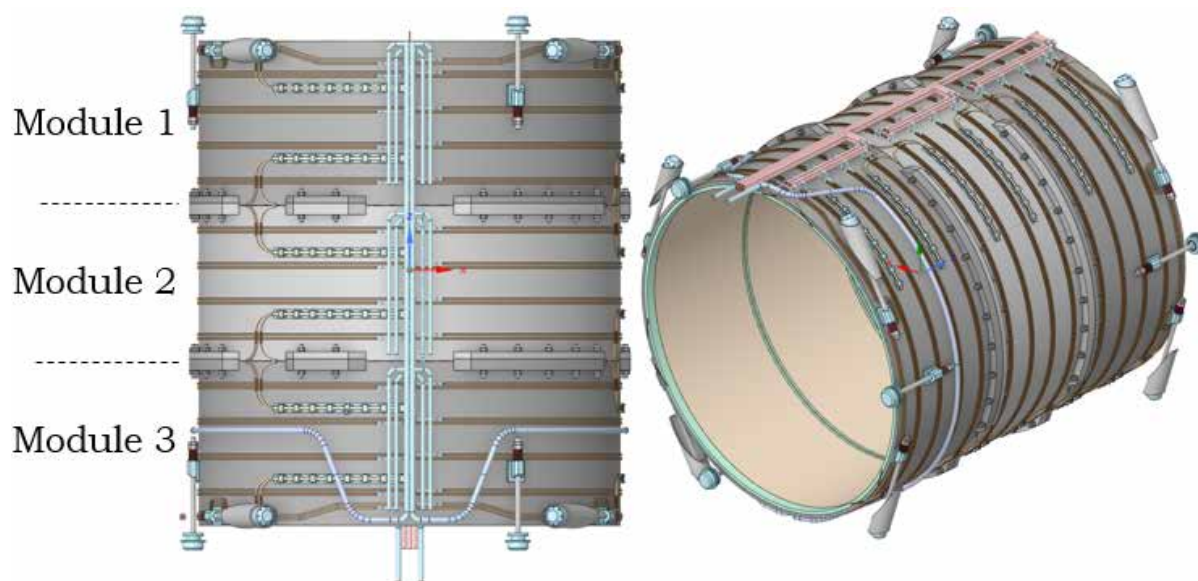


Figure 3.7 MARCO cold-mass layout inside the cryostat

As the Interaction Point (IP) is the center of the detector, the cold mass center is shifted along the axis at $Z = +100$ mm. The three modules are named, from Z- to Z+, MOD1, MOD2, and MOD3. For each module, 6 single layers of superconductor are wound internally to a mandrel, for a total number of turns per layer varying between 92 and 93, according to the conductor exits. The total number of turns per module is 556. Layers are named L1, L2, L3, L4, L5, L6 with L1 being the innermost and L6 the outermost. Each layer is separated by an inter-layer fiber glass insulation of 2 layers of 0.2 mm to achieve a good electrical insulation after winding and to prevent the conductor damages. A schematic drawing of the coil pack and the mandrel is shown in Figure 3.8 and conductor dimensions shown in Figure 3.9.

Electron-Ion Collider, Brookhaven National Laboratory and Thomas Jefferson National Accelerator Facility			
Doc No. EIC-SHC-TN-24-005	Author: Sandesh Gopinath	Effective Date: 12/05/2024	Review Frequency: NA
Process Description: EIC Design Report MARCO Magnet			Revision: 00

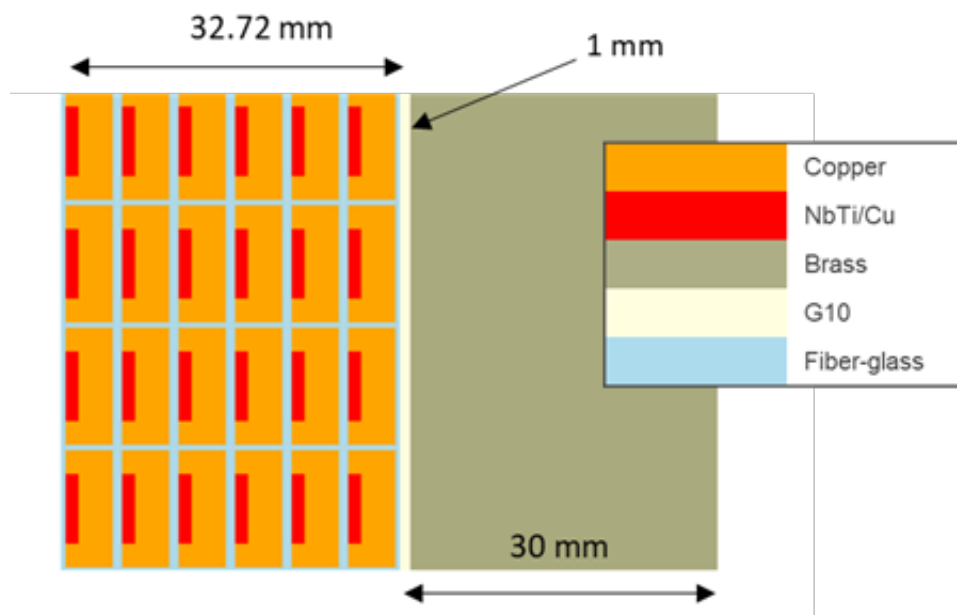
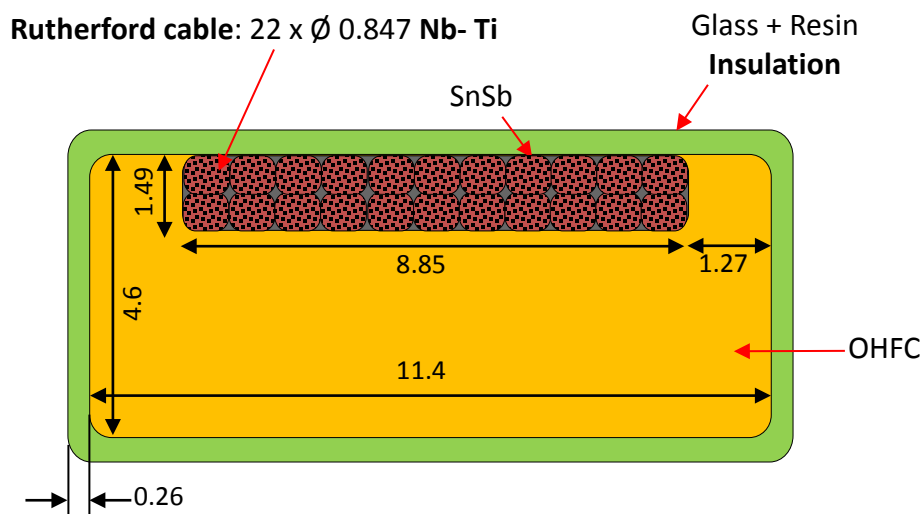


Figure 3.8 Schematic cross-section of the coil pack and mandrel, with materials and thickness of the different item



Dimensions in mm

Figure 3.9 detailed dimensions of the conductors on the left

The coil pack is separated from the mandrel by 1 mm of ground insulation, the same value as CMS solenoid, to prevent electrical short-circuits, to protect the conductor insulation during winding, and to facilitate the impregnation keeping a good thermal coupling for cool-down and quench-back.

The only official copy of this document is the one online in the SharePoint Document Center. Before using a printed copy, verify that it is current by checking the printed document's Revision History log with that of the online version.

Electron-Ion Collider, Brookhaven National Laboratory and Thomas Jefferson National Accelerator Facility			
Doc No. EIC-SHC-TN-24-005	Author: Sandesh Gopinath	Effective Date: 12/05/2024	Review Frequency: NA
Process Description: EIC Design Report MARCO Magnet			Revision: 00

The dimensions of the module is shown in Figure 3.10 and in Table 3.2

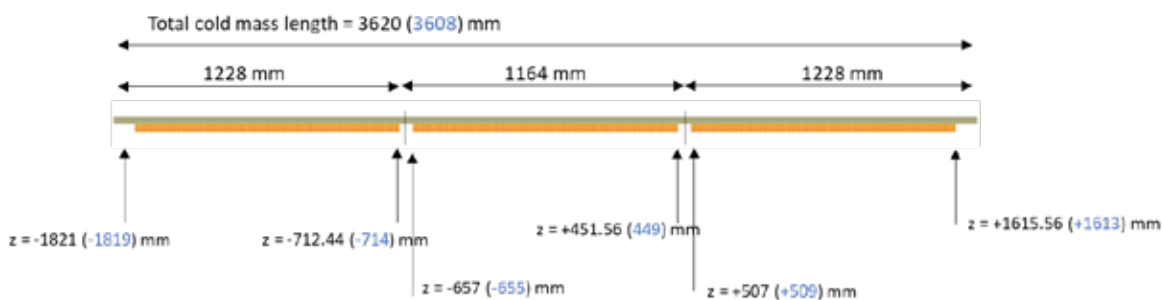


Figure 3.10 Warm (in black) and cold (in blue) dimensions of the cold mass

Table 3.2 Geometric specifications of MARCO solenoid

Parameter	Value	Dimension
Bore radius	1420	mm
Mandrel Length (300K)	3620	mm
Mandrel Length (4K)	3608	mm
Number of Modules	3	
Z- (MOD1) / Z+ (MOD3) Modules Length (300K)	1228	mm
Central Module (MOD 2) Length (300K)	1164	mm
Coils Inner Radius (300K)	1509.5	mm
Coil Inner Radius (4K)	1502.5	mm
Coils Thickness	32.7	mm
Coils Outer Radius (300K)	1542.2	mm
Ground Insulation Thickness	1	mm
Mandrel Inner Radius	1543.2	mm
Mandrel Thickness	30	mm
Mandrel Outer Radius (300K) without Flanges	1573.2	mm
Mandrel Outer Radius (4K) without Flanges	1566.2	mm
Mandrel Outer Radius (300K) including Flanges	1646.1	mm
Mandrel Outer Radius (4K) including Flanges	1639.1	mm
Number of Layers per Module	6	
Number of Turns per Module	556	

The only official copy of this document is the one online in the SharePoint Document Center. Before using a printed copy, verify that it is current by checking the printed document's Revision History log with that of the online version.

Electron-Ion Collider, Brookhaven National Laboratory and Thomas Jefferson National Accelerator Facility			
Doc No. EIC-SHC-TN-24-005	Author: Sandesh Gopinath	Effective Date: 12/05/2024	Review Frequency: NA
Process Description: EIC Design Report MARCO Magnet			Revision: 00

The electrical scheme for the solenoid is shown in Figure 3.11

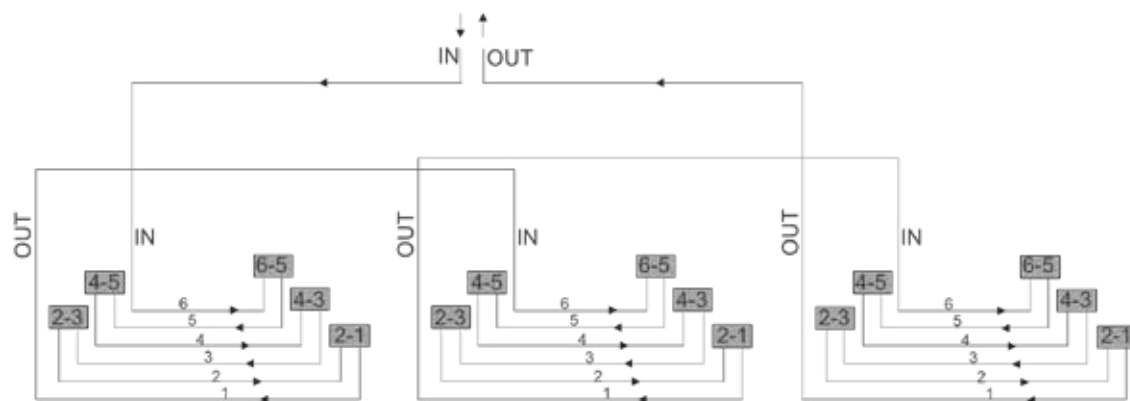


Figure 3.11 Electrical Schematic of MARCO Solenoid

Based on this electrical scheme, the connection between the layers is configured accordingly for each module. Conductor exits are positioned at approximately 120° on the mandrel as shown in Figure 3.12.

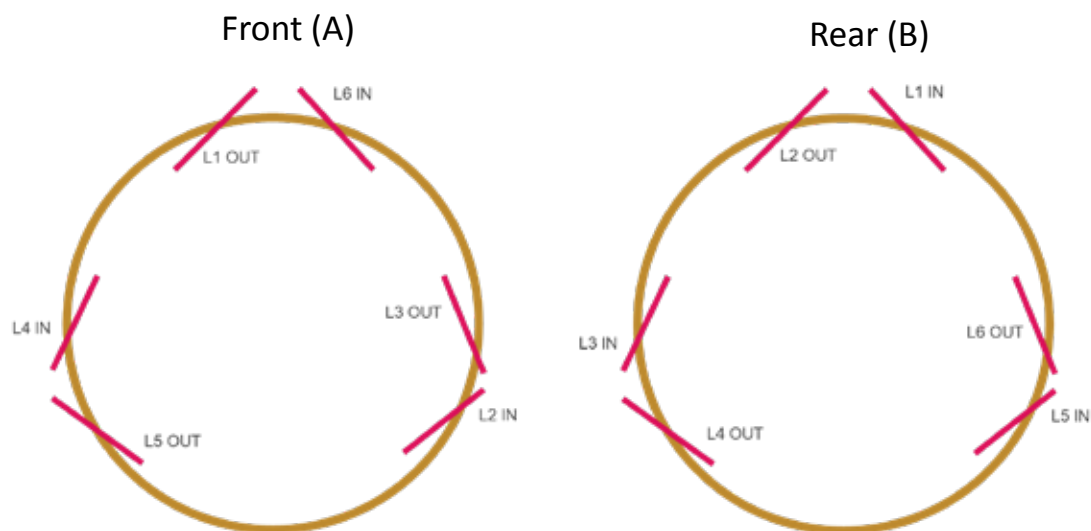


Figure 3.12 Conductor entrance and exit schematic for each module

This arrangement preserves the number of turns. The extremities (front/rear of each coils) have in total 5 turns over 6 (Table 3.3).

Electron-Ion Collider, Brookhaven National Laboratory and Thomas Jefferson National Accelerator Facility			
Doc No. EIC-SHC-TN-24-005	Author: Sandesh Gopinath	Effective Date: 12/05/2024	Review Frequency: NA
Process Description: EIC Design Report MARCO Magnet			Revision: 00

Table 3.3 Number of turns per layer at the extremities of each coil

Layer	Turns FRONT (A)	Turns REAR (B)
L1	1	1
L2	1	2/3
L3	2/3	1
L4	1	1
L5	1/3	1
L6	1	1/3
TOT Turns	5	5

The exits will be made with grooves cut in the mandrel (Figure 3.13). Figure 3.14 shows a cross section of the splice. Each groove must be:

- Thick enough to allow the positioning of a splice (Figure 3.14), where the main conductor of the layer is wrapped with another conductor in order to increase the stability and insulated by G10 fillers and fiberglass insulation;
- Tangent to the outer diameter of each terminal with a 1 mm G10 plate between the splice and the mandrel;
- Separated with a distance larger than two times of the hard-way radius of the conductor (120 mm).

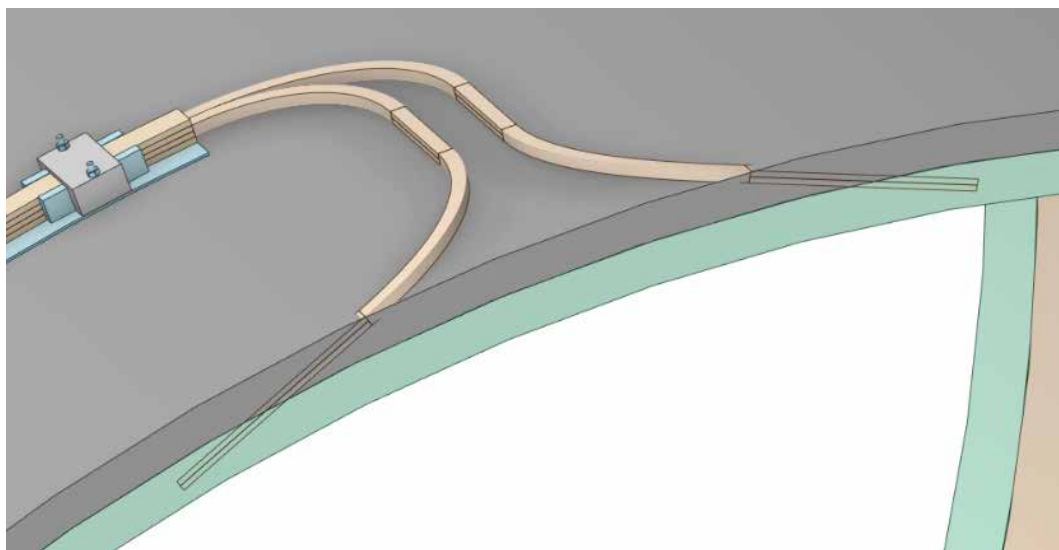


Figure 3.13 Design of the splices exits from the mandrel

Electron-Ion Collider, Brookhaven National Laboratory and Thomas Jefferson National Accelerator Facility			
Doc No. EIC-SHC-TN-24-005	Author: Sandesh Gopinath	Effective Date: 12/05/2024	Review Frequency: NA
Process Description: EIC Design Report MARCO Magnet			Revision: 00

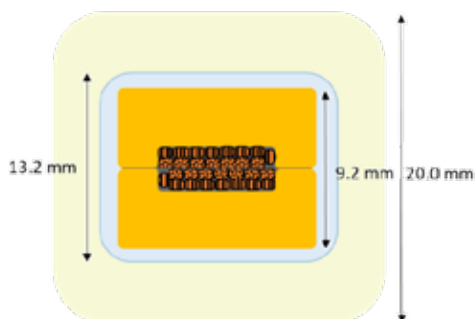


Figure 3.14 Cross-section of the splices

To fulfill the requirements above, the mandrel is longer than the coil for each module. The extra length is equal to 24.84 mm ($2 \cdot 11.92 \text{ mm}$ [2 turns] plus 1 mm for tolerances), which gives a separation of 55.5 mm between each coil, this gap will be filled with G10 wedges, which will be glue to the mandrel, plus a 3 mm insulation between each module (see Figure 3.15) to take care of the tolerances of manufacturing, positioning and tolerance stack up.

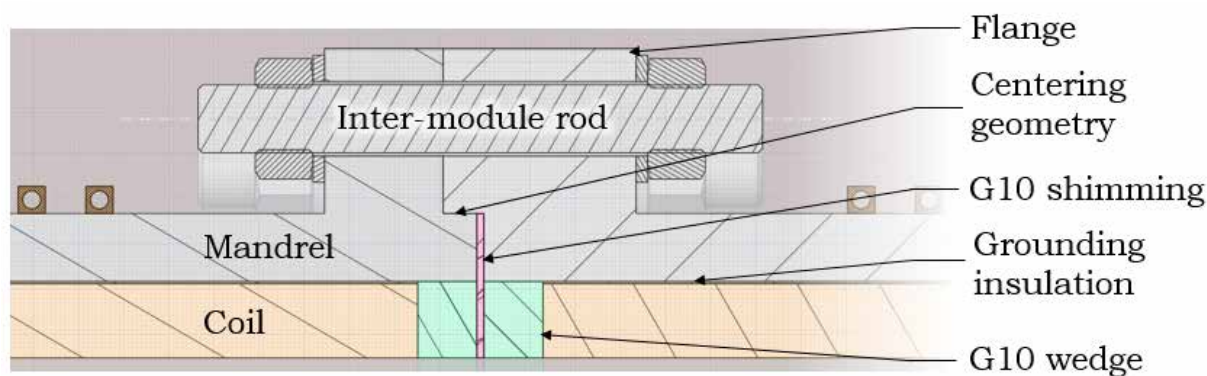


Figure 3.15 Schematics of the geometry at the interface between each coil.

Each module is bolted together through flanges (Figure 3.16). Flanges are not continuous on the entire circumference of the mandrel in order to let the thermosiphon pipes, the conductor joints and wire sensors all the space required.

Electron-Ion Collider, Brookhaven National Laboratory and Thomas Jefferson National Accelerator Facility			
Doc No. EIC-SHC-TN-24-005	Author: Sandesh Gopinath	Effective Date: 12/05/2024	Review Frequency: NA
Process Description: EIC Design Report MARCO Magnet			Revision: 00

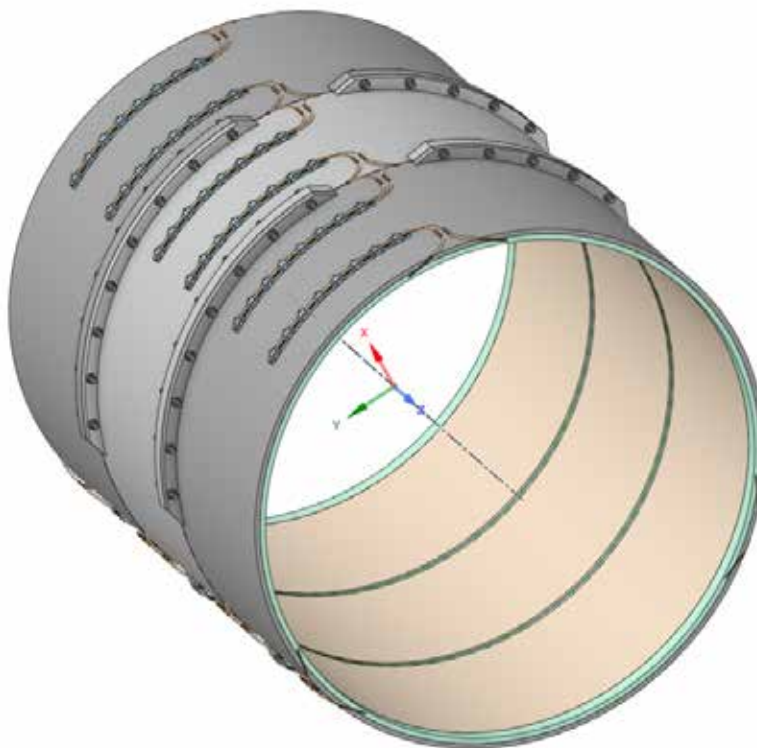


Figure 3.16 Three modules connected with their flanges.

3.4 The Electromagnetic model and the magnet performance

The magnetic field produced by the MARCO solenoid has been calculated using OPERA, 2D and 3D finite elements models. Given the high level of symmetry in the magnet, both models give the same results in terms of magnetic field and magnetic performances.

The 2D axisymmetric model (Figure 3.17) has been used to compute the magnetic field turn-by-turn and determine the magnetic field peak on the cable (Figure 3.18), while the 3D model has been used to take into account the limited effect of the cradles—the only non-symmetric elements present in the yoke (Figure 3.19).

The only official copy of this document is the one online in the SharePoint Document Center. Before using a printed copy, verify that it is current by checking the printed document's Revision History log with that of the online version.

Electron-Ion Collider, Brookhaven National Laboratory and Thomas Jefferson National Accelerator Facility			
Doc No. EIC-SHC-TN-24-005	Author: Sandesh Gopinath	Effective Date: 12/05/2024	Review Frequency: NA
Process Description: EIC Design Report MARCO Magnet			Revision: 00

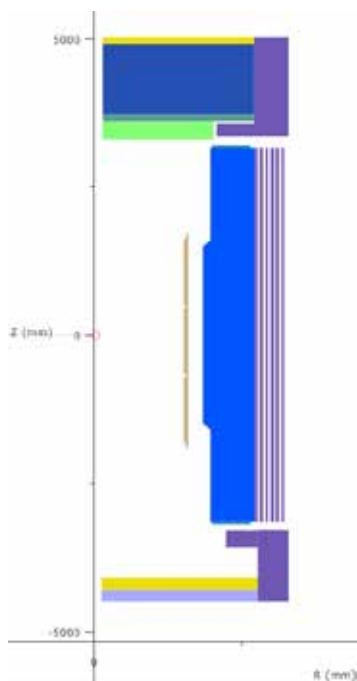


Figure 3.17 Section of the 2D axisymmetric geometry of the MARCO magnet

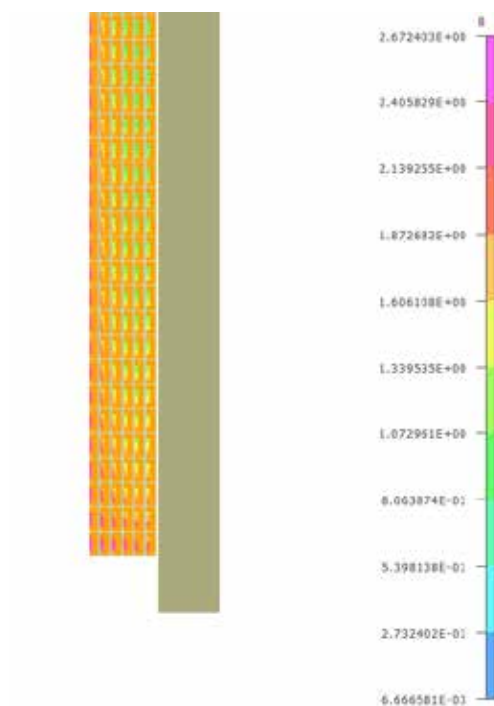


Figure 3.18 Coil of MOD1, which shows the magnetic field distribution and peak field on cable

Electron-Ion Collider, Brookhaven National Laboratory and Thomas Jefferson National Accelerator Facility			
Doc No. EIC-SHC-TN-24-005	Author: Sandesh Gopinath	Effective Date: 12/05/2024	Review Frequency: NA
Process Description: EIC Design Report MARCO Magnet			Revision: 00

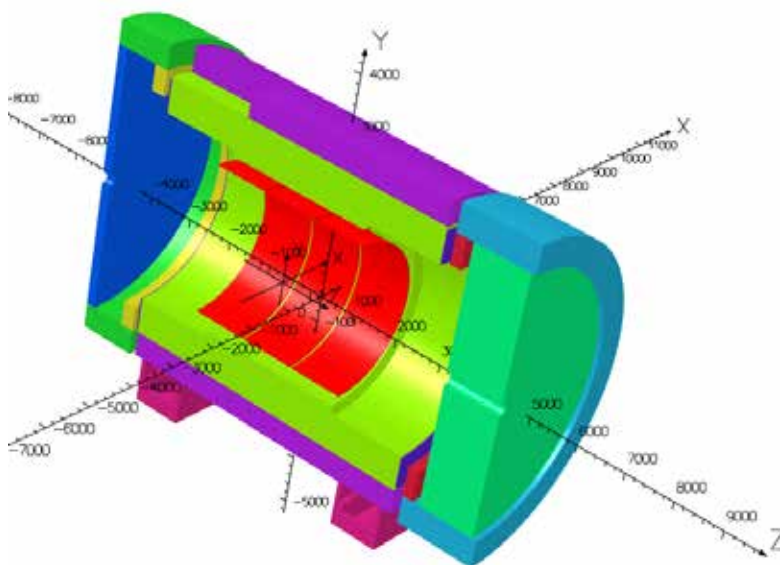


Figure 3.19 3D geometry of the MARCO magnet

The magnetic performance at various central field is summarized in Table 3.4.

Table 3.4 Nominal magnetic performances of the MARCO magnet

Parameter	1.5 T	1.7 T	2.0 T	Unit
Current	2942	3335	3924	A
B_0	1.505	1.706	2.000	T
B_{peak} MOD 1	1.998	2.254	2.672	T
B_{peak} MOD 2	1.859	1.107	2.478	T
B_{peak} MOD 3	2.003	2.271	2.660	T
Energy	25.440	32.689	45.008	MJ
Inductance	5.847	5.847	5.846	H
F_z MOD 1	6.71	8.63	11.88	MN
F_z MOD 2	58.4	41.0	31.9	kN
F_z MOD 3	-6.77	-8.69	-12.00	MN
F_z tot	-23.8	-29.2	-32.2	kN

Electron-Ion Collider, Brookhaven National Laboratory and Thomas Jefferson National Accelerator Facility			
Doc No. EIC-SHC-TN-24-005	Author: Sandesh Gopinath	Effective Date: 12/05/2024	Review Frequency: NA
Process Description: EIC Design Report MARCO Magnet			Revision: 00

At the ultimate working field (B_0) of 2.0 T, the magnet has a stored magnetic energy of 45 MJ and an inductance of 5.847 H. The inductance is constant at every current value up to the nominal current of 3924 A. At nominal position, the magnet is well balanced within the yoke. The maximum axial force (F_z) along the axis of the magnet is 32.2 kN pointing towards the lepton calorimeter.

The magnet satisfies the requirements for magnetic field at center, the projectivity and the field uniformity. Local solutions for the stray field are summarized in Appendix 3. The field uniformity and projectivity is governed by the coil placement, but the stray field is controlled by the return flux. The details of the return flux is shown in Figure 3.19. The projectivity and field uniformity is shown in Figure 3.20 and Figure 3.21 respectively

Table 3.5 Performances of the MARCO magnet versus requirements needed for the ePIC physics

Parameter	2.0 T	Requirement	Unit	Validation
B_0	2.000	2.0	T	OK
Field uniformity	12.5	12.5	%	OK
Projectivity	3.28	< 10	T/(A mm ²)	OK
Transparency	0.468	< 0.5	-	OK
B5300	15.4	< 10	G	Local solution given in Appendix 3
B7200	10.9	< 10	G	
B3400	2.4	< 10	G	

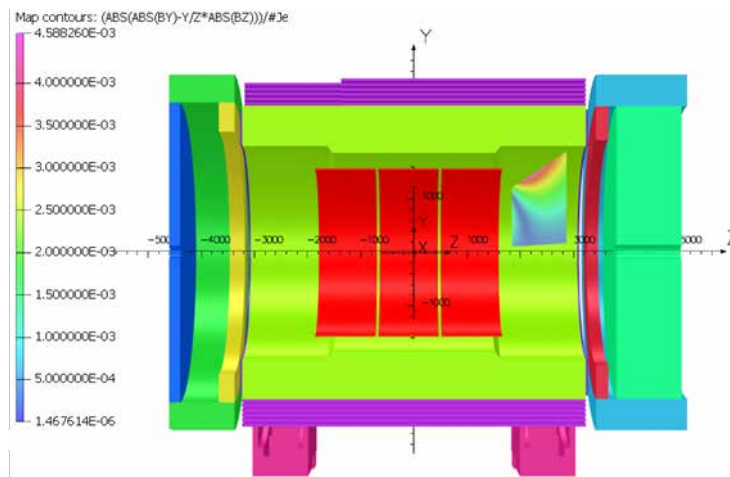


Figure 3.20 Projectivity calculation for the RICH region in the 3D FE model

Electron-Ion Collider, Brookhaven National Laboratory and Thomas Jefferson National Accelerator Facility			
Doc No. EIC-SHC-TN-24-005	Author: Sandesh Gopinath	Effective Date: 12/05/2024	Review Frequency: NA
Process Description: EIC Design Report MARCO Magnet			Revision: 00

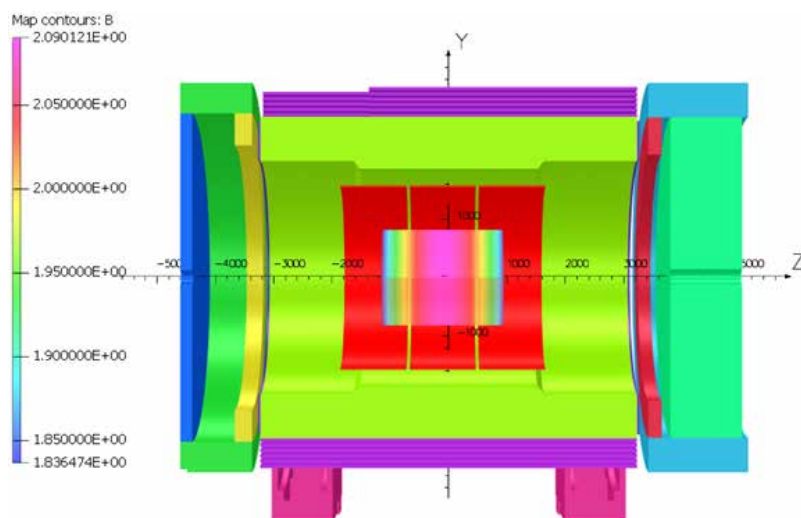


Figure 3.21 Field uniformity in the central region calculated in the 3D FE model

3.5 Fault scenario studies

As part of the risk management procedure, Failure Modes and Effects Analysis, was carried out for both design and system. This exercise allowed us to identify the key risks at each of the critical phases of design and define actions to mitigate each risk moving ahead as team. As part of the exercise, we calculate a Risk Priority Number (RPN) to certain activities and proposed mitigation activities, which in turn results in a revised RPN. This is applied to magnet design required to reduce the likelihood of the occurrence of events that could adversely affect physics experiments. FMEA applied to *magnet design*, and identify the mitigation processes could be used to modify the design or the manufacturing process and guide as appropriate towards magnet and system protection. The primary categories identified for the FMEA are-

1. **Design FMEA** – This is performed on the magnet and the system at the design level (e.g. – conductor design, magnet design – electro-magnetic, electro-mechanical, and cryogenic, etc.)
2. **Manufacturing FMEA** – This is primarily performed on the various manufacturing processes. The output from the FMEA at this stage is usually captured via a structured and well-defined quality plan.
3. **System FMEA (primarily, parts and equipment)** – Here the FMEA would typically focus on the individual parts or sub-systems that make up the whole system.
4. **Functional FMEA** – This type of FMEA focuses on the performance of the intended part or device rather than on the specific characteristic of the individual parts.
5. **User FMEA** – This could be a subset of the Design FMEA that focuses specifically on the user and how the customer/user is intending to use the system.

Electron-Ion Collider, Brookhaven National Laboratory and Thomas Jefferson National Accelerator Facility			
Doc No. EIC-SHC-TN-24-005	Author: Sandesh Gopinath	Effective Date: 12/05/2024	Review Frequency: NA
Process Description: EIC Design Report MARCO Magnet			Revision: 00

6. **Software FMEA** - All of the above FMEA methods (Design, Process, System, Functional, and User) can also be applied to software development.

Beyond the categories as mentioned above, the type of fault is also identified for analysis. The faults identified are-

1. **Primary fault:** This type of fault poses a serious risk to the system. For example, if there is a resistive voltage seen in a superconducting magnet that is not expected, or an excessive leakage current flow to ground, this could pose a safety risk to the magnet itself. These faults and/or the causes must allow the protection system to shut off the magnet system (*either by fast dumping when the magnet is at field or by not allowing the magnet to be energized*).
2. **Secondary fault:** If this fault happens, the magnet starts ramping down from operating current to zero current in a controlled manner. For example, in a superconducting magnet system, say the helium flow or pressure drifted outside of the safe controlled thresholds. This would be considered as a *secondary fault* because the available cooling power could be limited and as a consequence the magnet could have a reduced temperature margin.
3. **Subsystem fault:** System control or monitor function is not executed correctly when faults happen to any subsystem software and/or hardware device.

Based on the categories and type of fault, the magnet design FMEA (d-FMEA) at this stage is grouped into 4 sub-categories as that includes sub-system addressed with-

- I. **Magnet design** - electro-magnetic, electro-mechanical, magnet protection, magnetic field mapping
- II. **Mechanical design** – coil manufacturing, tooling, magnet or coil assembly, alignment, coil support and magnet support structure, vacuum, pressure, cryo-thermal design and safety
- III. **Electrical design** – electrical insulation, power requirements, electrical faults and safety
- IV. **Controls** - instrumentation, interface with other sub-systems, firmware, software, hardware, and electronics

Total number of risks identified for analysis are- Magnet design – 41, Mechanical design – 51, Electrical design – 44, Controls – 28

In summary - total of 164 identified risks (high level) divided in 4 categories, detailed analysis of the tasks indicated that total high risk activities decreased from a c-RPN (cumulative-RPN) of 4310 to 518 after mitigation. There are a few potential failure modes that persisted even after mitigation within magnet design till the commissioning phase, most of the HIGH risk are in conductor and splices (*e.g.*

Electron-Ion Collider, Brookhaven National Laboratory and Thomas Jefferson National Accelerator Facility			
Doc No. EIC-SHC-TN-24-005	Author: Sandesh Gopinath	Effective Date: 12/05/2024	Review Frequency: NA
Process Description: EIC Design Report MARCO Magnet			Revision: 00

damage to superconducting strands, splice – transition from wet to dry (vacuum) at 4.5K, and poor quality of fabricated splice). The detail of FMEA is given in Appendix 4.

3.5.1 Impact of axial misalignment and tolerances

The impact of axial misalignments and fabrication tolerances with respect to the nominal position and dimensions of the magnet has been studied in the 2D model using Monte Carlo simulations. The following hypotheses have been considered (Figure 3.22):

- every module can be displaced along Z with a Gaussian distribution $G(\mu, \sigma) = G(0.0, 5.0 \text{ mm})$ with respect to the nominal position;
- every module can have a different inner radius modeled with a Gaussian distribution $G(\mu, \sigma) = G(1502.5 \text{ mm}, 5.0 \text{ mm})$ with respect to the nominal position;
- every module can have a different angle (as if the mandrel has a conical shape and not cylindrical) modeled with a Gaussian distribution $G(\mu, \sigma) = G(0.0, 0.03 \text{ deg})$ with respect to the nominal position;
- the cold mass can be displaced along Z with a Gaussian distribution $G(\mu, \sigma) = G(0.0, 10.0 \text{ mm})$ with respect to the nominal position;
- 1000 simulations are considered for this study.

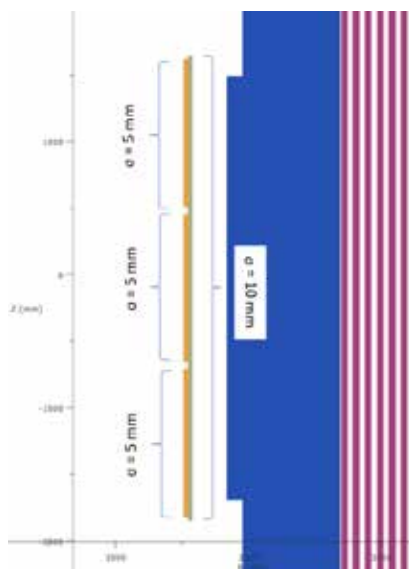


Figure 3.22 Amplitude of the possible misalignments for the cold mass and modules with respect to the nominal position

As a result, 99.7% of modules misalignments with respect to the nominal position are less than 33 mm (1% of the length of the cold mass), with a maximum of 40 mm (Figure 3.23).

The only official copy of this document is the one online in the SharePoint Document Center. Before using a printed copy, verify that it is current by checking the printed document's Revision History log with that of the online version.

Electron-Ion Collider, Brookhaven National Laboratory and Thomas Jefferson National Accelerator Facility			
Doc No. EIC-SHC-TN-24-005	Author: Sandesh Gopinath	Effective Date: 12/05/2024	Review Frequency: NA
Process Description: EIC Design Report MARCO Magnet			Revision: 00

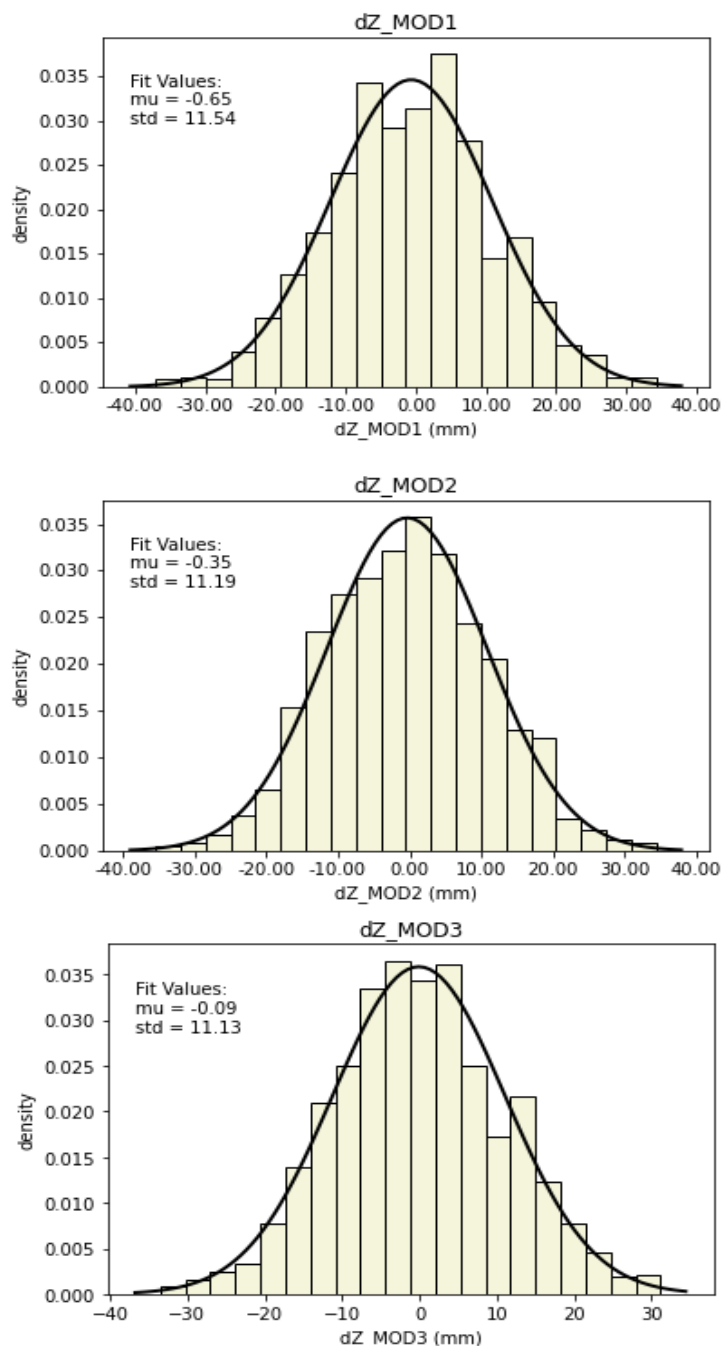


Figure 3.23 Example of misalignments distribution for MOD1, MOD2 and MOD3

Electron-Ion Collider, Brookhaven National Laboratory and Thomas Jefferson National Accelerator Facility			
Doc No. EIC-SHC-TN-24-005	Author: Sandesh Gopinath	Effective Date: 12/05/2024	Review Frequency: NA
Process Description: EIC Design Report MARCO Magnet			Revision: 00

If one assumes that the mandrel may have a conical shape due to the fabrication process, the maximum admissible angle of the cone is 0.1 rad (5.73°), corresponding to a tolerance of 0.3% on the inner radius.

Table 3.6 Results for axial displacements and fabrication tolerances

Parameter	Value	Unit
ΔB_0	± 10	mT
ΔEnergy	± 0.231	MJ
ΔF_z	+14.4 / -50.4	kN
$\Delta \text{Homogeneity}$	± 1	%
ΔB_{5300}	± 0.2	G
ΔB_{7200}	± 0.15	G
ΔB_{3400}	± 0.2	G

The results summarized in Table 3.6 show a negligible impact on the operation of the magnet.

3.5.2 Impact of radial misalignments

The impact of radial misalignments with respect to the nominal position of the magnet has been studied in the 3D model due to the breakdown of symmetry these misalignments create. Due to the complexity of the simulations and especially their computation time, a maximum misplacement has been studied, with the following hypotheses:

- every module can be displaced along Y with a maximum displacement of 5.0 mm;
- the cold mass can be displaced along Y with a maximum displacement of 5.0 mm.

These results are given in Table 3.7, Table 3.8, Table 3.9, and Table 3.10.

The only official copy of this document is the one online in the SharePoint Document Center. Before using a printed copy, verify that it is current by checking the printed document's Revision History log with that of the online version.

Electron-Ion Collider, Brookhaven National Laboratory and Thomas Jefferson National Accelerator Facility			
Doc No. EIC-SHC-TN-24-005	Author: Sandesh Gopinath	Effective Date: 12/05/2024	Review Frequency: NA
Process Description: EIC Design Report MARCO Magnet			Revision: 00

Table 3.7 Results for a maximum displacement of the cold mass

Parameter	MOD1	MOD2	MOD3	MAGNET	Unit
dy				- 5 / +5	mm
B ₀				2.000	T
F _y	-12.3 / 12.3	-14.5 / 14.5	-15.3 / 15.3	-42.2 / 42.2	kN
F _z				-32.5	kN

Table 3.8 Results for a maximum displacement of MOD1

Parameter	MOD1	MOD2	MOD3	MAGNET	Unit
dy	- 5 / +5				mm
B ₀				2.000	T
F _y	-0.5 / 0.7	-39.2 / 39.4	25.3 / -24.9	-14.5 / 15.1	kN
F _z				-32.2	kN

Table 3.9 Results for a maximum displacement of MOD2

Parameter	MOD1	MOD2	MOD3	MAGNET	Unit
dy		- 5 / +5			mm
B ₀				2.000	T
F _y	64.4 / -64.3	-39.7 / 39.6	-14.6 / 14.6	-14.7 / 14.7	kN
F _z				-32.5	kN

Table 3.10 Results for a maximum displacement of MOD3

Parameter	MOD1	MOD2	MOD3	MAGNET	Unit
dy			- 5 / +5		mm
B ₀				2.000	T
F _y	27.8 / -27.6	-39.4 / 39.3	-0.9 / 0.9	-12.3 / 12.4	kN
F _z				-32.4	kN

Electron-Ion Collider, Brookhaven National Laboratory and Thomas Jefferson National Accelerator Facility			
Doc No. EIC-SHC-TN-24-005	Author: Sandesh Gopinath	Effective Date: 12/05/2024	Review Frequency: NA
Process Description: EIC Design Report MARCO Magnet			Revision: 00

Results summarized in the above tables indicate that a misalignment of 5 mm has negligible impact on the correct operation of the magnet; therefore, a tolerance in the position of the coils of 5 mm is acceptable.

3.5.3 Impact of one missing layer

In order to complete the fault case studies the impact of one missing layer in a module is studied, the impact can be different depending on which module is concerned. The results of missing layer in all modules is given in Table 3.11.

Table 3.11 Impact of one layer missing in a module

Parameter	NOM	MOD1	MOD2	MOD3	Unit
B ₀	2.000	1.923	1.838	1.906	T
Energy	45.010	40.610	39.679	40.590	MJ
Homogeneity	12.7	19.3	8.5	19.3	%
Projectivity	3.28	3.26	3.17	2.88	T mm ² /A
F _z	-23.3	-90.8	-39.4	+42.3	kN
B5300	15.3	13.7	14.6	14.6	G
B7200	10.9	10.5	10.5	9.7	G
B3400	2.3	3.0	2.3	1.5	G

In case that one layer is missing in MOD1 or MOD3, the operation of the magnet is compromised due to the high non-homogeneity of the magnetic field. Otherwise, the magnet can still function if only MOD2 has one missing layer. The detail operating margins need to be calculated in the event of a missing layer based on which the operating limits will be set accordingly for all materials. This situation should be avoided during magnet manufacturing.

3.5.4 Impact of Permeability of Yoke Material

A variation of $\pm 10\%$ of the BH curve shows that the variation of the main parameters is negligible (Table 3.12). This study helps in defining the tolerances on steel properties.

Table 3.12 Impact of permeability variation

	Iron85 $\Delta BH = \pm 10\%$	Iron75 $\Delta BH = \pm 10\%$	Iron70 $\Delta BH = \pm 10\%$	Iron100 $\Delta BH = \pm 10\%$	Unit
B ₀	2.000	2.000	2.000	2.000	T
ΔB_{5300}	+0.23 / -0.05	+0.00 / +0.00	+0.96 / -0.43	0.07 / -0.06	G
ΔB_{7200}	-0.00 / -0.00	+0.03 / +0.02	+0.62 / -0.27	+0.01 / -0.04	G
ΔB_{3400}	+ 0.01 / -0.01	+0.00 / +0.00	+0.05 / -0.02	+0.01 / -0.01	G
ΔF_z	+0.04 / -0.01	-0.04 / -0.03	0.74 / -0.37	-0.00 / +0.00	kN

The only official copy of this document is the one online in the SharePoint Document Center. Before using a printed copy, verify that it is current by checking the printed document's Revision History log with that of the online version.

Electron-Ion Collider, Brookhaven National Laboratory and Thomas Jefferson National Accelerator Facility			
Doc No. EIC-SHC-TN-24-005	Author: Sandesh Gopinath	Effective Date: 12/05/2024	Review Frequency: NA
Process Description: EIC Design Report MARCO Magnet			Revision: 00

3.5.5 Impact of Misalignments of Yoke

The impact of axial misalignments and fabrication tolerances with respect to the nominal position and dimensions of the yoke has been studied in the 2D model using Monte Carlo simulations. The following hypotheses have been considered:

- Every yoke element can be displaced along Z with a Gaussian distribution $G(\mu, \sigma) = G(0.0, 5.0 \text{ mm})$ with respect to the nominal position;
- Every yoke can have a different inner/outer radius modeled with a Gaussian distribution $G(\mu, \sigma) = G(0.0, 5.0 \text{ mm})$ with respect to the nominal position;
- 1000 simulations are considered for this study.

Only the fringe field is analyzed for this study.

The impact of yoke misalignments is negligible with respect to the fringe field. Even with misalignments/ tolerances of 15 mm, the maximum variation of the fringe field is shown below with further details captured in Figure 3.24:

- B5300 = ± 1.5 G
- B7200 = ± 1.2 G
- B3400 = ± 0.3 G

Electron-Ion Collider, Brookhaven National Laboratory and Thomas Jefferson National Accelerator Facility			
Doc No. EIC-SHC-TN-24-005	Author: Sandesh Gopinath	Effective Date: 12/05/2024	Review Frequency: NA
Process Description: EIC Design Report MARCO Magnet			Revision: 00

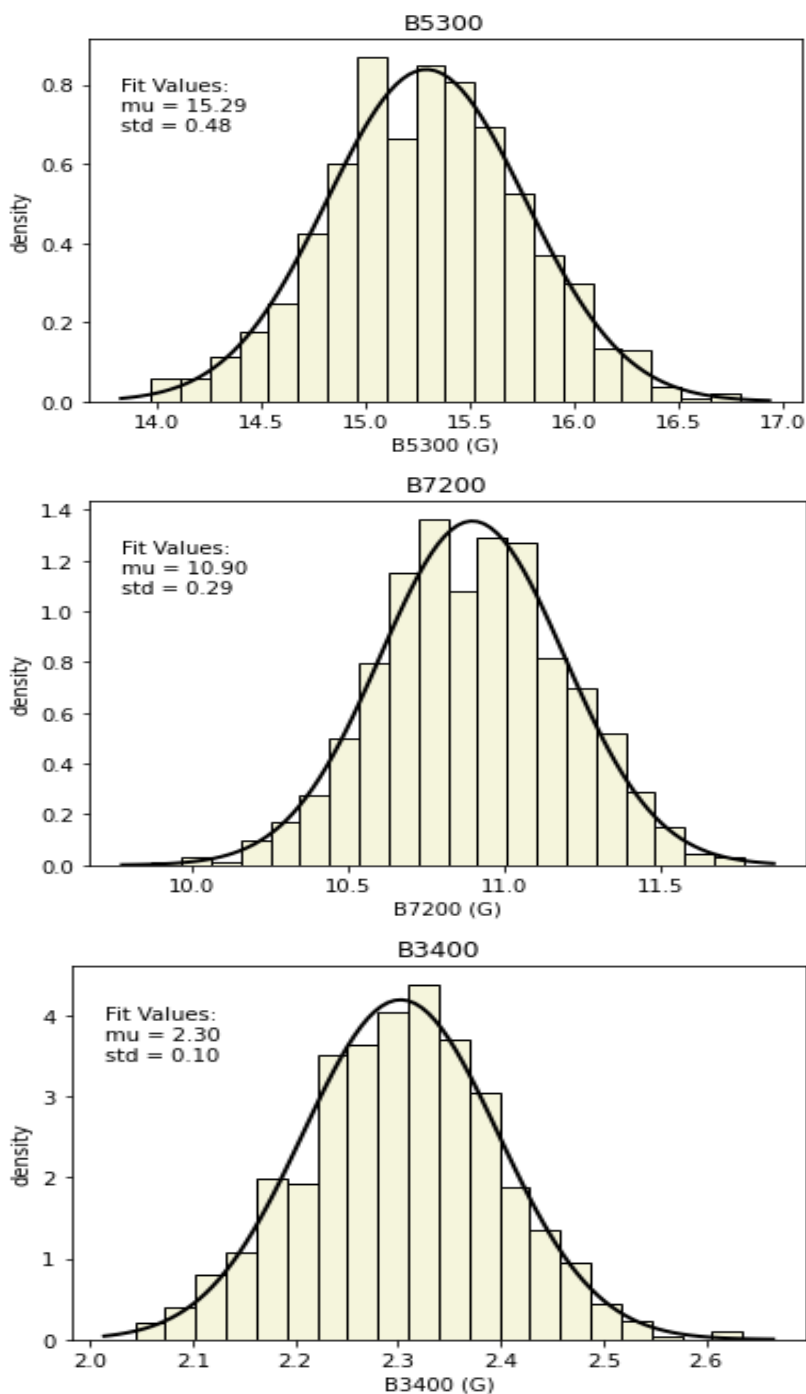


Figure 3.24 The maximum variation of the fringe field at B5300, B7200, B3400

Electron-Ion Collider, Brookhaven National Laboratory and Thomas Jefferson National Accelerator Facility			
Doc No. EIC-SHC-TN-24-005	Author: Sandesh Gopinath	Effective Date: 12/05/2024	Review Frequency: NA
Process Description: EIC Design Report MARCO Magnet			Revision: 00

4 Conductor Design and Stability

The conductor selection is based on the magnet operating parameters and margins required to safely operate the magnet in the collider. The collider magnets normally have a high stored energy and high mass. The collider magnets are one off and therefore, not prototyped. The safe operating margin for this magnet is taken (i) as at least 1.5 K temperature margin between operating temperature and current sharing temperature, (ii) operating current is not more than 30% of critical current at operating temperature and field. The magnetic design gives the maximum magnetic field $B_{peak} = 2.67$ T (including the self-field), and the operating temperature $T_{op} = 4.7$ K. Bottura scaling law [3] is used with the parameter listed in Table 4.1 for the curve J_c versus B. The parameter $C0$ in Table 4.1 (originally equal to 73000 T-A/mm² in [4]) includes “critical current degradation” due to the conductor manufacturing process (cabling + cable soldering into the copper channel). The degradation assumed is based on the experience with similar conductor used in high field MRI (Iseult) at CEA, Saclay. Overall, a 15% degradation is assumed in cabling and soldering the conductor.

Table 4.1 Bottura fit parameters from [3] including a 15% degradation factor due to cooling and soldering process

Parameter	Value	Unit
Bc20	14.5	T
Tc0	9.2	K
n	1.7	
C0	62050	T·A/mm ²
α	0.57	
β	0.9	
γ	1.9	

Figure 4.2 show the dimensions of the final designed conductor.

4.1 Strand

A strand diameter (dst) of 0.847 mm and a number of strands of 22 is selected. This choice, instead of larger strand diameter and lower number of strands, comes from the following considerations:

- smaller strand diameter increases slightly the critical current density;
- the self-field is slightly lower with a wider rectangular cable;
- the surface of contact with the copper channel (stabilizer) is larger with a wider rectangular cable.

To define the diameter of the filaments d_{fil} , the following formula Invalid source specified:

Electron-Ion Collider, Brookhaven National Laboratory and Thomas Jefferson National Accelerator Facility			
Doc No. EIC-SHC-TN-24-005	Author: Sandesh Gopinath	Effective Date: 12/05/2024	Review Frequency: NA
Process Description: EIC Design Report MARCO Magnet			Revision: 00

$$d_{fil} = 2 \sqrt{\frac{8k(T_c - T_{op})(1 - \lambda)}{\lambda J_c^2 \rho}}$$

where k is the conductivity of Nb-Ti; λ is the filling factor $1/(1+\text{Cu/Sc})$; T_c is the critical temperature; J_c is the critical current density; and ρ is the resistivity of the copper. With $T_{op} = 4.7$ K, $B_{self} = 0.4$ T and RRR = 50, a d_{fil} of 30.5 μm is found (parameters k and ρ taken from *CryoComp*[5]).

In order to avoid filament breakage, the twist pitch should be more than 15-20 times the strand diameter. On the other hand, the intra-strand coupling currents loss increases with the twist pitch. Since MARCO is a steady state magnet, AC losses are not critical; thus, we set a twist pitch of 30 mm. The strand specification is given in Table 4.2. A cross section SEM view of the currently procured sample strand is shown in Figure 4.1.

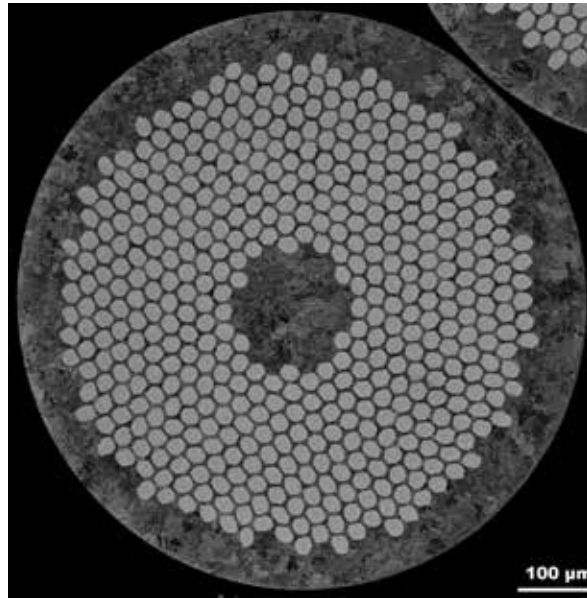


Figure 4.1 SEM image of a single strand with 468 NbTi filaments shown

4.2 Cable

The number of strands in the cable is chosen to be 22.

The final dimensions of the cable are estimated by taking into consideration a packing factor of 90% and an angle of 15°, resulting in a cable of 8.85 mm x 1.49 mm (width x thickness). The exact dimensions of the cable will depend on the cable fabrication process itself. What is important is that the cable holds

Electron-Ion Collider, Brookhaven National Laboratory and Thomas Jefferson National Accelerator Facility			
Doc No. EIC-SHC-TN-24-005	Author: Sandesh Gopinath	Effective Date: 12/05/2024	Review Frequency: NA
Process Description: EIC Design Report MARCO Magnet			Revision: 00

mechanically, i.e. no spring out/pop out effect; to do this, the right tensions to be applied during the cabling must be set, as well as the dimensions of the die where the cable will pass through.

With an angle of 15°, the transposition length of the cable is determined to be 50 mm.

With these parameters, the calculated void cross-section that will be filled with solder normally is approximately 0.79 mm². The cable specifications are given in Table 4.2

4.3 Copper Channel

The exact amount of copper is defined according to the magnetic design of the coil, in particular, with the engineering current density J_e that has been fixed to 56.5 A/mm². It must be noted that the amount of copper also defines the conductor enthalpy margin. This aspect is addressed in 4.5.

For indirect cooled magnets (thermosiphon technique), the volumetric enthalpy difference ΔH [J m⁻³] between the operating and the current sharing temperature must be considered:

$$\Delta H = \int_{T_{op}}^{T_{cs}} \bar{C}(T) dT$$

where $\bar{C}(T)$ [J K⁻¹ m⁻³] is the conductor average volumetric heat capacity. For MARCO, the enthalpy margin results in 6.7 kJ m⁻³. It is useful to compare this value with an existing running coil of the same kind, e.g. BaBar ($B_0 = 1.5$ T, Energy = 27 MJ, $I_n = 4.6$ kA, aluminum stabilized conductor). BaBar has an enthalpy margin of about 3.6 kJ m⁻³ [6]. In terms of energy per unit length of conductor, we have 0.4 J m⁻¹ for MARCO and 0.36 J m⁻¹ and 0.65 J m⁻¹ for BaBar's thin and thick conductors respectively [6].

Residual Resistance Ratio (RRR) of commercial oxygen free copper can be 50 to 500 depending on the purity of the copper, while the yield strength ($\sigma_{0.2\%}$) at room temperature is lower than 100 MPa [6]. The copper channel can be cold-worked to improve its mechanical properties, but, consequently, the RRR will decrease. In addition, due to the heating of the process of soldering the cable onto the copper channel, the copper recovers a bit (increase of RRR and decrease of $\sigma_{0.2\%}$). With all these considerations a final RRR = 80 and $\sigma_{0.2\%} = 165$ MPa

4.4 Conductor

The conductor is defined as Rutherford cable soldered in copper channel. This is the final product used in magnet winding. The dimension tolerance of the conductor is critical for the coil buildup. The conductor specifications are given in Table 4.2. The overall size of the conductor is shown in Figure 4.2.

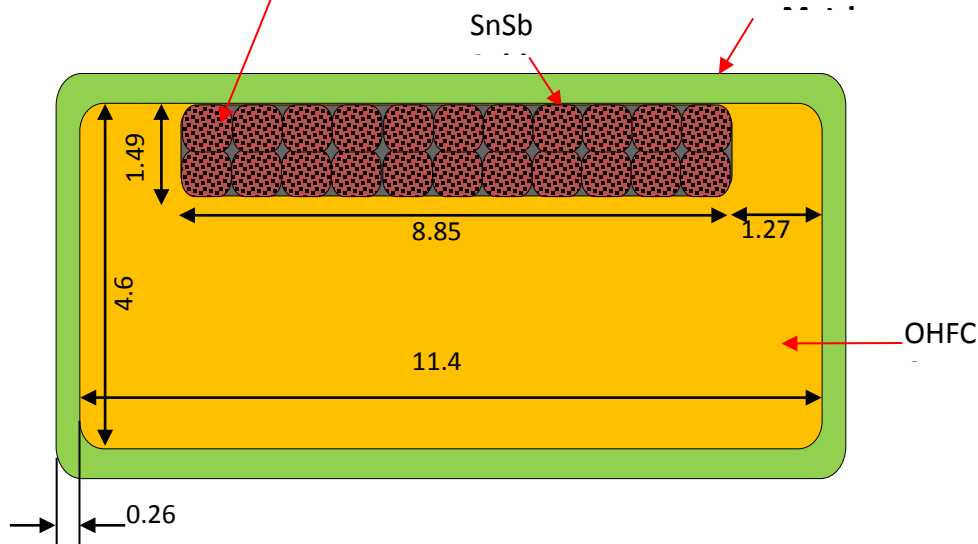
Electron-Ion Collider, Brookhaven National Laboratory and Thomas Jefferson National Accelerator Facility			
Doc No. EIC-SHC-TN-24-005	Author: Sandesh Gopinath	Effective Date: 12/05/2024	Review Frequency: NA
Process Description: EIC Design Report MARCO Magnet			Revision: 00

Table 4.2 Main characteristics of the MARCO RICC Conductor

	Parameter	Value	Unit
Strand	Strand diameter	0.847	mm
	Cu/NbTi	1.31	
	I_c @ 3T & 4.7K	> 735	A
	Filament diameter	< 30	μm
	Filament twist pitch	30	mm
Cable	NbTi strands	22	
	Transposition pitch	50	mm
	Width	8.85	mm
	Thickness	1.49	mm
Conductor	Copper channel section	43.7	mm^2
	Nominal current @ 2 T	3924	A
	RRR conductor	≥ 80	
	Yield strength $\sigma_{0.2\%}$ @ 293 K	≥ 165	MPa
	Unit length	1.05	km
	Total length	18.9	km

Rutherford cable: 22 x \varnothing 0.847 Nb- Ti

Glass + Resin
Insulation



Dimensions in mm

Figure 4.2 Cross-section of the RICC conductor designed for MARCO solenoidal magnet

Electron-Ion Collider, Brookhaven National Laboratory and Thomas Jefferson National Accelerator Facility			
Doc No. EIC-SHC-TN-24-005	Author: Sandesh Gopinath	Effective Date: 12/05/2024	Review Frequency: NA
Process Description: EIC Design Report MARCO Magnet			Revision: 00

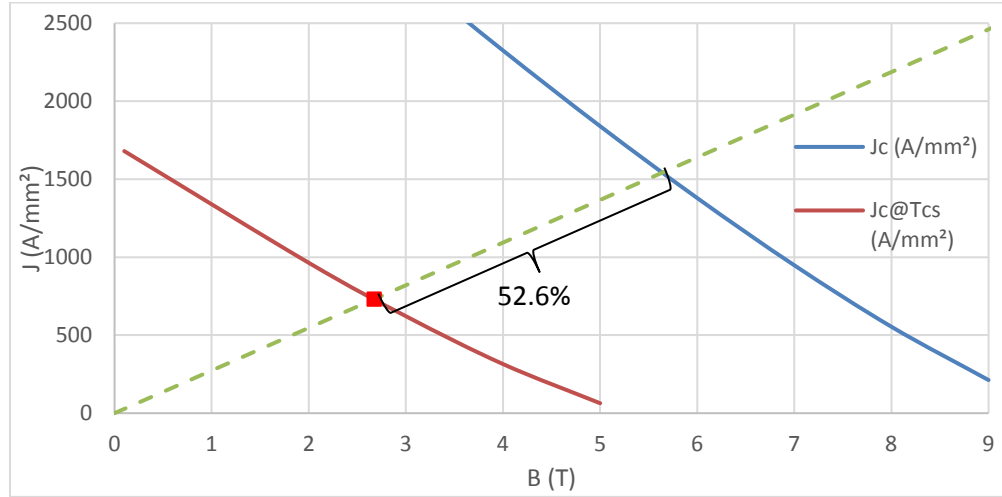


Figure 4.3 J_c curve @4.7 K, load line and load line margin for the reference case study $B_0 = 2T$. The working point (green rectangle) is shown, corresponding to a current sharing temperature of 7.15 K.

Table 4.3 MARCO conductor margins

B_0	1.5 T	1.7 T	2.0 T	Unit
Current (I_n)	2942	3335	3924	A
T_{op}	4.7	4.7	4.7	K
B_{peak}	2.00	2.27	2.67	T
Temp. margin	2.78	2.59	2.3	K
Load line margin	64.4	59.7	52.6	%
$I / I_c(T, B_{peak})$	16.4	19.3	24.3	%

The amount of NbTi, copper, and solder in the conductor has been defined. In addition, a layer of 0.26 mm thick (0.13 mm 50% overlap tape) fiberglass insulation must be considered also. Therefore, the total section of the conductor is about 61.1 mm². To determine the overall dimensions of the conductor, i.e. width and thickness, we started by setting the thickness because it is directly related to the thickness of the coil (33.6 mm) and the number of layers. For MARCO, we found that a number of six layers is optimal, resulting in a rectangular conductor of 5.12 x 11.92 mm (aspect ratio of 2.3). The main reasons behind this choice are:

- windability—the conductor will be wound on its wide side, making the winding process easier;

Electron-Ion Collider, Brookhaven National Laboratory and Thomas Jefferson National Accelerator Facility			
Doc No. EIC-SHC-TN-24-005	Author: Sandesh Gopinath	Effective Date: 12/05/2024	Review Frequency: NA
Process Description: EIC Design Report MARCO Magnet			Revision: 00

- conductor unit length—the manufacturing process of the conductor defines its maximum unit length. For MARCO conductor it mostly depends on the speed of the cable soldering process onto the copper channel for a continuous length of conductor. This speed is about 3 m/min, which means about 1 km of conductor per work day. With such unit length and number of layers, the conductor length is decided to be 1.05 km per spool and one spool will be used for each layer.

4.5 Conductor Stability

Based on the magnet specifications and requirements from the magnet team, the conductor design realized using NbTi-Rutherford type cable with copper stabilizer for quench and thermal stability.

The following criteria is used to evaluate the conductor stability at the worst-case operating scenario –

1. Temperature margin from the current sharing temperature
2. Short sample performance (SSP) of the conductor at operating current (typical for detector magnet)
3. Adiabatic stability
4. Dynamic stability
5. Adiabatic self-field stability
6. Twist pitch length and finite element diameter

The criteria set for the temperature margin ($>1.5K$) and SSP ($<40\%$) are based on other magnets of similar size detector magnets and more recently with 12 GeV CLAS magnets at JLAB for conduction-cooled magnet.

The assumptions made for stability calculations are –

1. Superconducting (SC) strands of NbTi in copper matrix with Cu:Sc ratio ~ 1.3
2. Copper stabilized SC strands with overall Cu:Sc ratio ~ 8.57
3. Operating temperature 4.7K
4. Operating Current 3950A
5. Peak field in the conductor 2.6T
6. Residual Resistivity Ratio (RRR) minimum 80

Table 4.4 Conductor stability – Summary of the evaluation criteria for MARCO magnet

Summary	Remarks
Stable for SSP value (Defined earlier)	Yes
Stable for T_{cs} (Current sharing temp) value (Margin)	Yes
Stable for Beta - Adiabatic stability	Yes
Adiabatic flux jump stability	Yes
Dynamic stability	Yes
Adiabatic self-field stability	Yes
Stable in term of twist pitch	Yes
Stable for finite element size	Yes

Electron-Ion Collider, Brookhaven National Laboratory and Thomas Jefferson National Accelerator Facility			
Doc No. EIC-SHC-TN-24-005	Author: Sandesh Gopinath	Effective Date: 12/05/2024	Review Frequency: NA
Process Description: EIC Design Report MARCO Magnet			Revision: 00

5 Mechanical Design

Contrary to the usual detector magnets made with an aluminum stabilizer conductor, MARCO is made with a copper stabilized NbTi Rutherford in channel, making it one of its kind. Due to the limit placed by the fabrication process on the maximum unit length of the conductor, this solenoid comprises three modules (Figure 5.1), drawing significant design inspiration from the CMS magnet[7].

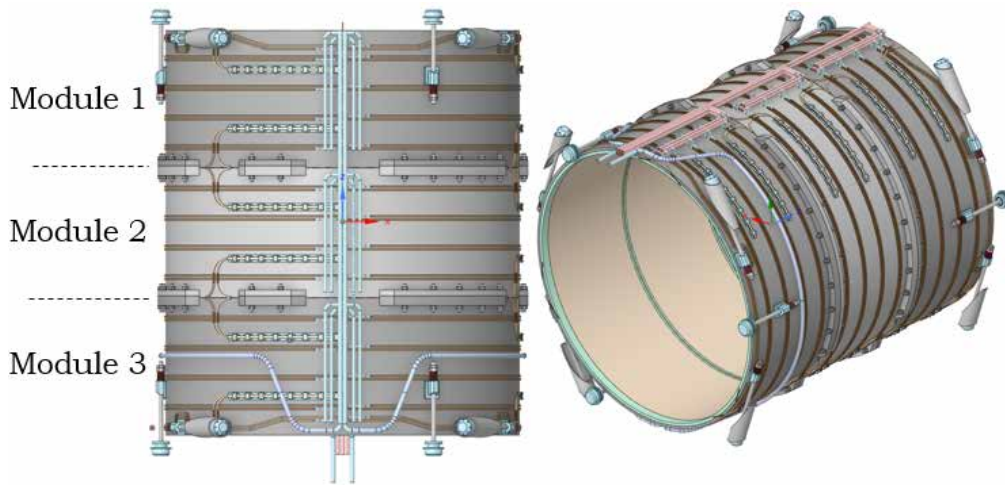


Figure 5.1 Cold mass of MARCO, consisting of 3 modules

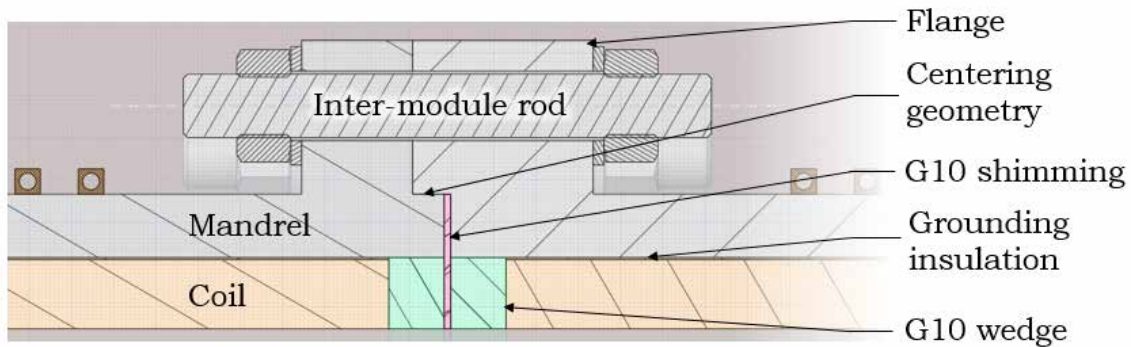


Figure 5.2 Inter-module fixation

The modules are impregnated independently, joined altogether with the brass rods and nuts, and aligned with the centering geometry in the mandrel. The mandrel is made of brass 70/30 due to its slightly higher coefficient of expansion than that of the coil. The resulting slight constraint created on the coil during cool-down maintains continuous contact between the two components over the magnet's lifetime. To compensate the fabrication imperfections, customized G10 shims are placed between two adjacent

Electron-Ion Collider, Brookhaven National Laboratory and Thomas Jefferson National Accelerator Facility			
Doc No. EIC-SHC-TN-24-005	Author: Sandesh Gopinath	Effective Date: 12/05/2024	Review Frequency: NA
Process Description: EIC Design Report MARCO Magnet			Revision: 00

mandrels (Figure 5.2). At the extremities of each coil module, a G10 wedge allows the conductor terminals to exit and serves as a shear stop. The flanges are designed to be discontinuous (Figure 5.1) to provide space for the thermosiphon pipes (essentially the distributor and collector manifolds) and also for the exiting conductor. The inter-module M30 rods in Figure 5.2 are made with the same brass of the mandrel to avoid any shrinkage difference during cool-down. The use of Belleville washers for stress relieving are avoided this way. The M30 rods are positioned at every 10° except in the cuts; there are a total of 25 rods per flange.

The cold mass assembly is suspended and adjusted with respect to the vacuum vessel with 8 radial and 6 axial tie rods (Figure 5.4). The cold interfaces are made by brass brackets attached to the mandrel. The tie rods are captured by the brackets and have Belleville washers and nuts to reduce thermal stress due to differential contraction. The warm sides of the tie rods are fixed on the vacuum vessel with nuts. A O-ring-sealed cap is bolted around the warm interface to maintain the vacuum inside. At both interfaces, female/male ball joints are installed to allow movements during the calibration phase and the cool down phase. These two-ball joint assemblies are designed in a manner to have the largest center-to-center distance. The length of the tie rods has been chosen by considering the available footprint, the heat load conducted to the magnet and the initial length versus shrinkage displacements. The longer the tie rod, the smaller the thermal budget, but the greater the shrinkage displacements. The compromise is shown in Table 5.18.

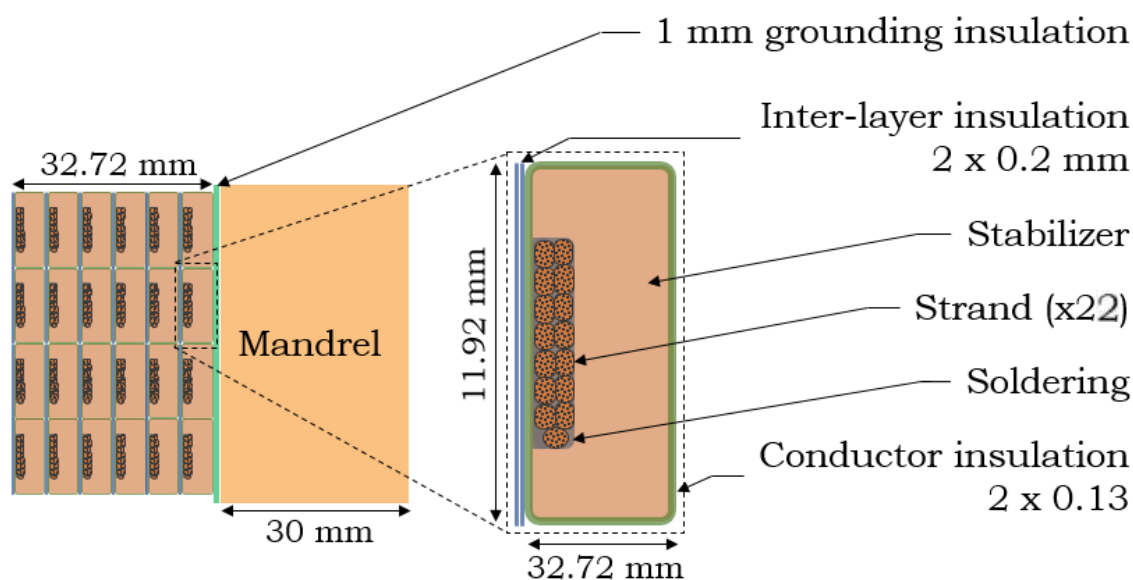


Figure 5.3 Cross sections of coil and conductor

The only official copy of this document is the one online in the SharePoint Document Center. Before using a printed copy, verify that it is current by checking the printed document's Revision History log with that of the online version.

Electron-Ion Collider, Brookhaven National Laboratory and Thomas Jefferson National Accelerator Facility			
Doc No. EIC-SHC-TN-24-005	Author: Sandesh Gopinath	Effective Date: 12/05/2024	Review Frequency: NA
Process Description: EIC Design Report MARCO Magnet			Revision: 00

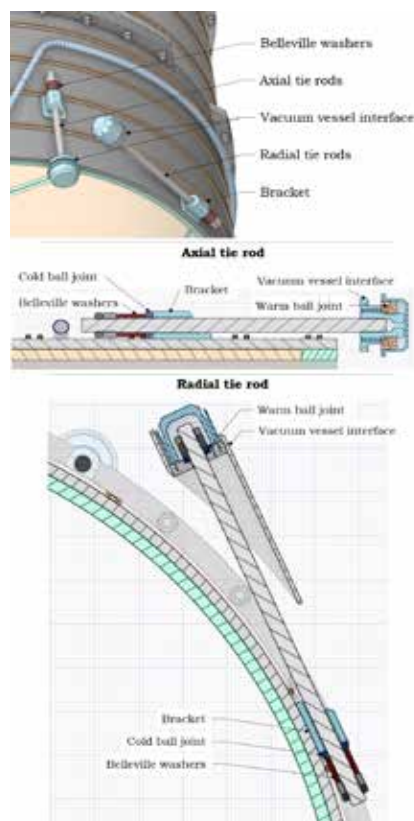


Figure 5.4 Axial and radial tie rods on the cold mass

5.1 Material properties and Acceptance criteria

A complete and detailed description of the chosen material properties values is proposed in this chapter.

5.1.1 Cooper

Table 5.1 Copper Properties

Property	Unit	293 K	4 K
Density	kg/m ³	8960 ⁽¹⁾	
Young's modulus	GPa	128.2 ⁽²⁾	138.6 ⁽²⁾
Shear modulus	GPa	47.7 ⁽²⁾	51.9 ⁽²⁾
Poisson's ratio		0.344 ⁽²⁾	0.338 ⁽²⁾
Thermal expansion (293 K to 4 K)		0.32% ^(*1)	
Thermal Conductivity	W/(m K)	398 ⁽¹⁾	628 ⁽¹⁾
Yield strength	MPa	69 ^(3,4)	86 ^(3,4)
Tensile strength	MPa	200	455

The only official copy of this document is the one online in the SharePoint Document Center. Before using a printed copy, verify that it is current by checking the printed document's Revision History log with that of the online version.

Electron-Ion Collider, Brookhaven National Laboratory and Thomas Jefferson National Accelerator Facility			
Doc No. EIC-SHC-TN-24-005	Author: Sandesh Gopinath	Effective Date: 12/05/2024	Review Frequency: NA
Process Description: EIC Design Report MARCO Magnet			Revision: 00

(1) Cryocomp, RRR100, 1.6 T

(2) The tables in the reference [8] have been redesign in a single one (see table II)

(3) Reference [9]

(4) Reference [10]

For the yield strength, the most conservative values between (3) and (4) have been chosen. In any case, it will depend on the fabrication process.

Table 5.2 Copper properties as a function of the temperature[8]

Temperature (K)	Young modulus (GPa)	Shear modulus (GPa)	Poisson's ratio
0	138.6	51.9	0.338
20	138.6	51.8	0.338
40	138.4	51.8	0.338
60	138	51.6	0.338
80	137.5	51.4	0.338
100	136.9	51.2	0.338
120	136.2	50.9	0.339
140	135.4	50.5	0.339
160	134.6	50.2	0.34
180	133.7	49.9	0.341
200	132.9	49.6	0.341
220	132	49.2	0.342
240	131.1	48.8	0.342
260	130.1	48.5	0.343
280	129.2	48.1	0.343
300	128.2	47.7	0.344

Table 5.1 and Table 5.2 list the copper properties for the conductor stabilizer and the strand matrix.

5.1.2 Niobium-titanium alloy

Table 5.3 Niobium – Titanium Properties

Property	Unit	293 K	4 K
Density	kg/m ³	6550 ⁽¹⁾	
Young's modulus	GPa	84 ⁽²⁾	120 ⁽³⁾
Shear modulus	GPa	31.5 ⁽²⁾	53.6 ⁽⁴⁾
Poisson's ratio		0.33 ⁽³⁾	0.326 ⁽⁵⁾
Thermal expansion (293 K to 4 K)		0.15%	
Thermal Conductivity	W/(m K)	9.44 ⁽¹⁾	0.176 ⁽¹⁾

(1) CryoComp

(2) Reference [11]

(3) Reference [12], figure 6, graphic interpretation and extrapolation

Electron-Ion Collider, Brookhaven National Laboratory and Thomas Jefferson National Accelerator Facility			
Doc No. EIC-SHC-TN-24-005	Author: Sandesh Gopinath	Effective Date: 12/05/2024	Review Frequency: NA
Process Description: EIC Design Report MARCO Magnet			Revision: 00

(4) The ratio between Young modulus and shear stress at 293 K has been applied to find the shear stress at 4 K from the Young modulus at 4 K

(5) Law of mixture from values taken in MPDB V9.39

(6) MPDB V9.39

Table 5.3 gathers the niobium titanium properties used for the conductor filaments modeling of the coil homogenization

5.1.3 G10

Table 5.4 G10 Properties

Property	Unit	293 K	4 K
Density	kg/m ³	1948 ⁽¹⁾	
Young's modulus (X)	GPa	28 ⁽²⁾	35.9 ⁽²⁾
Young's modulus (Y)	GPa	22.4 ⁽²⁾	29.1 ⁽²⁾
Young's modulus (Z)	GPa	14.5 ⁽³⁾	21.8 ⁽³⁾
Shear modulus G _{XY}	GPa	12.2 ⁽⁴⁾	14.8 ⁽⁴⁾
Shear modulus G _{YZ}	GPa	8.7 ⁽⁴⁾	10.2 ⁽⁴⁾
Shear modulus G _{XZ}	GPa	10.8 ⁽⁴⁾	12.6 ⁽⁴⁾
Poisson's ratio v _{XY}		0.15 ⁽²⁾	0.21 ⁽²⁾
Poisson's ratio v _{YZ}		0.29 ⁽⁵⁾	0.42 ⁽⁵⁾
Poisson's ratio v _{XZ}		0.3 ⁽⁵⁾	0.42 ⁽⁵⁾
Thermal expansion (293 K to 4 K) (X)		0.246%	
Thermal expansion (293 K to 4 K) (Y)		0.246%	
Thermal expansion (293 K to 4 K) (Z)		0.717%	
Thermal Conductivity (X)	W/(m K)	0.81 ⁽⁶⁾	0.06 ⁽¹⁾
Thermal Conductivity (Y)	W/(m K)	0.81 ⁽⁶⁾	0.03 ⁽¹⁾
Thermal Conductivity (Z)	W/(m K)	0.63 ⁽⁶⁾	0.05 ⁽¹⁾
Tensile strength TS _x	MPa	415 ⁽²⁾	862 ⁽²⁾
Tensile strength TS _y	MPa	257 ⁽²⁾	496 ⁽²⁾

(1) Cryocomp

(2) Reference [13],

(3) Reference [14], gives the data to built the Table 5.6. Values at 274 K and 75 K has been used respectively from the 295 K and 4 K Young's modulus in this table

(4) Has been calculated from the formula 1

$$G_i = \frac{E_i}{2(1+v_i)} \quad (1)$$

Where G is the Shear modulus, E is the Young modulus and v is the Poisson's ratio.

The only official copy of this document is the one online in the SharePoint Document Center. Before using a printed copy, verify that it is current by checking the printed document's Revision History log with that of the online version.

Electron-Ion Collider, Brookhaven National Laboratory and Thomas Jefferson National Accelerator Facility			
Doc No. EIC-SHC-TN-24-005	Author: Sandesh Gopinath	Effective Date: 12/05/2024	Review Frequency: NA
Process Description: EIC Design Report MARCO Magnet			Revision: 00

(5) Reference [13], adapted in the

Table 5.7. For the "VPI epoxy with glass fiber", the elastic and mechanical properties are taken as the same as

pregreg. According to the

Table 5.7, the ratio can be estimated in the formula 2:

$$\frac{\nu_{12}}{\nu_{23}} = 0.515 \quad (2)$$

Since fill and warp have been detailed separately in the MARCO project, these ratios have been applied (see formula 3):

$$\frac{\nu_{12}}{\nu_{23}} = \frac{\nu_{21}}{\nu_{23}} = 0.5 \quad (3)$$

(6) NIST[15]

Table 5.4 gathers the G10 properties used for the grounding insulation and the wedges modelling

Table 5.5 G10 Young's modulus, poisson's ratio and tensile strength [13]

Temp.	Young's modulus		Poisson's ratio		Tensile strength	
(K)	(GPa)				(MPa)	
	Warp	Fill	Warp	Fill	Warp	Fill
295	28	22.4	0.15	0.114	415	257
76	33.7	27	0.19	0.183	825	459
4	35.9	29.1	0.211	0.21	862	496

Table 5.6 G10 young's modulus "Normal to cloth layers" as a function of the temperature values obtained by curve fitting from [14]

Temp (K)	Youngs modulus (Gpa)
273.98	14.5
251.7	15.5
233.42	16.6
216.46	17.7
197.02	18.8

The only official copy of this document is the one online in the SharePoint Document Center. Before using a printed copy, verify that it is current by checking the printed document's Revision History log with that of the online version.

Electron-Ion Collider, Brookhaven National Laboratory and Thomas Jefferson National Accelerator Facility			
Doc No. EIC-SHC-TN-24-005	Author: Sandesh Gopinath	Effective Date: 12/05/2024	Review Frequency: NA
Process Description: EIC Design Report MARCO Magnet			Revision: 00

176.03	19.7
154.38	20.1
132.89	20.5
115.46	20.9
99.39	21.3
86.369	21.6
75.04	21.8

Table 5.7 G10 poisson's ratio [16]

Components	Material	Poisson's ratio
TF, CS,	VPI epoxy glass	$\nu_{12} = 0.17$
PF Turn insulation	with kapton barrier	$\nu_{13} = \nu_{23} = 0.33$
Filler for radial plate grooves CS,PF winding pack filler	VPI epoxy glass	$\nu_{12} = 0.17$
		$\nu_{13} = \nu_{23} = 0.33$
Radial plate insulation	VPI epoxy glass With kapton barrier	$\nu_{12} = 0.17$
		$\nu_{13} = \nu_{23} = 0.33$
TF, CS, PF ground insulation	VPI epoxy glass with kapton barrier	$\nu_{12} = 0.17$
		$\nu_{13} = \nu_{23} = 0.33$
TF winding - Case filler	VPI epoxy with glass filler	$\nu_{12} = 0.17$
		$\nu_{13} = \nu_{23} = 0.33$

Electron-Ion Collider, Brookhaven National Laboratory and Thomas Jefferson National Accelerator Facility			
Doc No. EIC-SHC-TN-24-005	Author: Sandesh Gopinath	Effective Date: 12/05/2024	Review Frequency: NA
Process Description: EIC Design Report MARCO Magnet			Revision: 00

5.1.4 Glass fiber epoxy

Table 5.8 fiber glass epoxy properties

Property	Unit	293 K	4 K
Density	kg/m ³	1948	
Young's modulus (X)	GPa	15.51	
Young's modulus (Y)	GPa	15.51 ⁽²⁾	20
Young's modulus (Z)	GPa	8.29 ⁽²⁾	12.5
Shear modulus G _{XY}	GPa	6.76 ⁽³⁾	8
Shear modulus G _{YZ}	GPa	4.4 ⁽³⁾	5 ⁽⁶⁾
Shear modulus G _{XZ}	GPa	4.4 ⁽³⁾	5 ⁽⁶⁾
Poisson's ratio ν_{XY}		0.14 ⁽⁴⁾	0.21 ⁽⁵⁾
Poisson's ratio ν_{YZ}		0.30 ⁽⁴⁾	0.21 ⁽⁵⁾
Poisson's ratio ν_{XZ}		0.30 ⁽⁴⁾	0.21 ⁽⁵⁾
Thermal expansion (293 K to 4 K) (X)		0.246%	
Thermal expansion (293 K to 4 K) (Y)		0.246%	
Thermal expansion (293 K to 4 K) (Z)		0.717%	
Thermal Conductivity (X)	W/(m K)	0.81 ⁽¹⁾	0.06 ⁽¹⁾
Thermal Conductivity (Y)	W/(m K)	0.81 ⁽¹⁾	0.06 ⁽¹⁾
Thermal Conductivity (Z)	W/(m K)	0.63 ⁽¹⁾	0.05 ⁽¹⁾
Tensile strength TS _X	MPa	415 ⁽⁵⁾	862 ⁽⁷⁾
Tensile strength TS _Y	MPa	257 ⁽⁵⁾	496 ⁽⁷⁾

(1) Cryocomp

(2) Being the magnet impregnated, the fiber glass epoxy properties has been calculated the following way: the G10 average Young's modulus "fill" and "warp" direction at 293 K is 25.2 GPa. At 4 K, the average is 32.5 GPa. The ratio between both is about 1.29. This ratio has been applied to the Young's modulus at 4 K of the fiberglass epoxy to estimate the Young's modulus at 293 K. The same method has been used to estimate the Young's modulus in the "normal" direction at 293 K.

(3) The same method than (2) has been used to estimate the Shear modulus in the "fill" and "warp" and "normal" direction at 293 K, from the calculated values at 4 K.

(4) The same method than (2) has been used to estimate the Poisson's ratio in the "fill" and "warp" and "normal" direction at 293 K.

(5) Reference [17], adapted in the Table 5.9

(6) See equation 1 page 54

(7) Reference [13]

Table 5.9 Fiber glass epoxy young's modulus and poisson's ratio at 4.2k, adapted from [17]

Orientation	Temp. (K)	Young's modulus (Gpa)	Poisson ratio
-------------	-----------	-----------------------	---------------

The only official copy of this document is the one online in the SharePoint Document Center. Before using a printed copy, verify that it is current by checking the printed document's Revision History log with that of the online version.

Electron-Ion Collider, Brookhaven National Laboratory and Thomas Jefferson National Accelerator Facility			
Doc No. EIC-SHC-TN-24-005	Author: Sandesh Gopinath	Effective Date: 12/05/2024	Review Frequency: NA
Process Description: EIC Design Report MARCO Magnet			Revision: 00

// to fiber direction	4.2	20	0.21
⊥ to fiber direction		12.5	0.21

Table 5.8 gathers the glass fiber epoxy properties used for the conductor insulation and the inter-layer insulation.

5.1.5 Brass

Table 5.10 Brass 70/30 Properties

Property	Unit	293 K	4 K
Density	kg/m ³	8525 ⁽¹⁾	
Young's modulus	GPa	101 ⁽²⁾	110 ⁽²⁾
Shear modulus	GPa	41 ⁽³⁾	45 ⁽³⁾
Poisson's ratio		0.310 ⁽⁴⁾	0.309 ⁽⁴⁾
Thermal expansion (293 K to 4 K)		0.38% ⁽²⁾	
Thermal Conductivity	W/(m K)	115 ⁽¹⁾	3.59 ⁽¹⁾
Yield strength	MPa	413 ⁽⁵⁾	517 ⁽⁵⁾

(1) Cryocomp

(2) MPDB V9.39

(3) Copper.org

(4) Law of mixture from MPDB V9.39 values

(5) <https://wpw.bnl.gov/rgupta/material-properties-sc-magnets/>

Table 5.10 gathers the brass properties used for the mandrel and the inter module flange screws

5.1.6 AgSn 3.5/96.5 Soft Solder

Table 5.11 Ag3.5/Sn96.5 Soft solder properties

Property	Unit	293 K	4 K
Density	kg/m ³	8403 ⁽¹⁾	
Young's modulus	GPa	50 ⁽²⁾	58.8 ⁽³⁾
Shear modulus	GPa	18.8 ⁽²⁾	18.8 ⁽⁴⁾
Poisson's ratio		0.33 ⁽²⁾	0.338 ⁽³⁾
Thermal expansion (293 K to 4 K)		0.44%	
Thermal Conductivity	W/(m K)	189.3 ⁽¹⁾	1781.7 ⁽¹⁾

(1) Cryocomp

(2) <https://www.azom.com/article.aspx?ArticleID=9120>

(3) Law of mixture from data MPDB V9.39

(4) Same value as 293 K

(5) MPDB V9.39

Table 5.11 gathers the properties used for the soldering filling the voids between the cable strands and between the cable and the copper stabilizer. Here the soldering is supposed to be

Electron-Ion Collider, Brookhaven National Laboratory and Thomas Jefferson National Accelerator Facility			
Doc No. EIC-SHC-TN-24-005	Author: Sandesh Gopinath	Effective Date: 12/05/2024	Review Frequency: NA
Process Description: EIC Design Report MARCO Magnet			Revision: 00

AgSn. The conductor manufacturer may change the soldering during the fabrication. However, due to the small amount of soldering present in conductor (around 1% of the conductor cross-section), this change will not impact the mechanical design.

5.1.7 Ti6Al4V

Table 5.12 Ti6Al4V Properties

Property	Unit	293 K	4 K
Density	kg/m ³	4540 ⁽¹⁾	
Young's modulus	GPa	112 ⁽²⁾	126 ⁽²⁾
Shear modulus	GPa	42 ⁽²⁾	46 ⁽³⁾
Poisson's ratio		0.333 ⁽²⁾	0.368 ⁽²⁾
Thermal expansion (293 K to 4 K)		0.18% ⁽¹⁾	
Thermal Conductivity	W/(m K)	7.7 ⁽¹⁾	0.403 ⁽¹⁾

(1) Cryocomp

(2) Reference [18]

(3) See formula 1 page 54

Table 5.12 gathers the titanium alloy properties used for the tie rods.

5.1.8 Acceptance Criteria

Table 5.13 Acceptance criteria for stress

Material	Property	Unit	293 K	4 K
Coil	Yield strength	MPa	165 ⁽¹⁾	200 ⁽¹⁾
	Shear strength	MPa	15 ⁽³⁾	72 ⁽⁹⁾
G10	Tensile strength	MPa	257 ⁽⁴⁾	496 ⁽⁴⁾
	Shear strength	MPa	42 ⁽⁴⁾	72.6 ⁽⁴⁾
Brass	Yield strength	MPa	413 ⁽⁶⁾	517 ⁽⁶⁾
	Shear strength	MPa	220 ⁽⁷⁾	264 ⁽⁷⁾
Ti6Al4V	Yield strength	MPa	1030 ⁽⁸⁾	1693 ⁽⁸⁾

Material	Allowable	Unit	293 K	4 K
Coil	Stress	MPa	110 ⁽²⁾	133 ⁽²⁾
	Shear stress	MPa	10 ⁽²⁾	24 ⁽⁹⁾
G10	Stress	MPa	103 ⁽⁵⁾	198 ⁽⁵⁾
	Shear stress	MPa	17 ⁽⁵⁾	29 ⁽⁵⁾
Brass	Stress	MPa	275 ⁽²⁾	345 ⁽⁶⁾
	Shear stress	MPa	88 ⁽⁵⁾	106 ⁽⁵⁾
Ti6Al4V	Stress	MPa	687 ⁽²⁾	1129 ⁽²⁾

(1) Specification to the manufacturer

Electron-Ion Collider, Brookhaven National Laboratory and Thomas Jefferson National Accelerator Facility			
Doc No. EIC-SHC-TN-24-005	Author: Sandesh Gopinath	Effective Date: 12/05/2024	Review Frequency: NA
Process Description: EIC Design Report MARCO Magnet			Revision: 00

- (2) 2/3rd of the initial value
- (3) JLab internal communication
- (4) Reference [13]
- (5) Design factor = 2.5
- (6) <https://wpw.bnl.gov/rgupta/material-properties-sc-magnets/>
- (7) https://www.matweb.com/search/SearchProperty.asp?gad_source=1&gclid=Cj0KCQjwz7C2BhDkARIsAA_SZKb1dwNH0vMCv2knQagxUmRyja0DdALhAVg6iqdtVSK7LF2Jgsob0P8aAghkEALw_wcB
- (8) Reference [18]
- (9) Reference [17]

The acceptance criteria to validate the mechanical design are showed in Table 5.13

5.2 Coil Pack Homogenization

To effectively integrate the multi-scale structure of the conductor into the 3D mechanical model of the magnet for finite element analysis (FEA), the coil must undergo homogenization. The homogenization has been done in 3 steps: the cable, the insulated conductor, and the coil. For each step, the density (ρ), the Young's modulus (E), the shear modulus (G), the Poisson's ratio (ν), the thermal conductivity, and the thermal expansion coefficient are computed in all orientations at 293 K and at 4 K as the materials are orthotropic. The Material Designer module of ANSYS Workbench version 2023 R2 is used to compute the homogenized properties.

5.2.1 Homogenization of the Cable

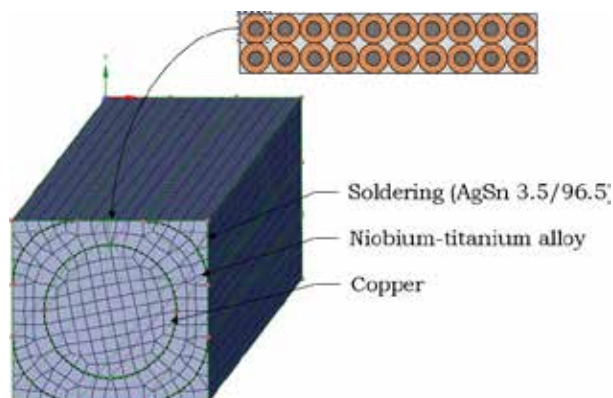


Figure 5.5 Homogenization of cable

The cable is composed of 20 strands with soldering in between (Figure 5.5). It is modelled with 20 repetitive squares of copper, NbTi (with Cu/SC = 1.3), and solder at the angles. Table 5.14 lists the homogenized properties of the cable at 293 K and 4 K. The conductor was later modified to 22 strands of 0.847 mm diameter. It is assumed that the homogenization of the cable will not be too different with this change, therefore, mechanical analysis still assumes the older version of cable and conductor.

The only official copy of this document is the one online in the SharePoint Document Center. Before using a printed copy, verify that it is current by checking the printed document's Revision History log with that of the online version.

Electron-Ion Collider, Brookhaven National Laboratory and Thomas Jefferson National Accelerator Facility			
Doc No. EIC-SHC-TN-24-005	Author: Sandesh Gopinath	Effective Date: 12/05/2024	Review Frequency: NA
Process Description: EIC Design Report MARCO Magnet			Revision: 00

Table 5.14 Homogenized properties of the cable

Property	Symbol	Unit	293 K	4 K
Density	ρ	kg/m ³	7965.8	7965.8
Young's modulus	E1	GPa	97	119
Young's modulus	E2	GPa	97	119
Young's modulus	E3	GPa	103	123
Shear modulus	G12	GPa	37	45
Shear modulus	G23	GPa	37	45
Shear modulus	G31	GPa	37	45
Poisson's ratio	ν_{12}		0.348	0.337
Poisson's ratio	ν_{13}		0.318	0.322
Poisson's ratio	ν_{23}		0.318	0.322
Thermal expansion 1 (293 K to 4 K)	a1		0.267%	
Thermal expansion 2 (293 K to 4 K)	a2		0.266%	
Thermal expansion 3 (293 K to 4 K)	a3		0.104%	
Thermal Conductivity 1	K1	W/(m K)	155.6	296.0
Thermal Conductivity 2	K2	W/(m K)	164.2	324.9
Thermal Conductivity 3	K3	W/(m K)	221.9	501.0

5.2.2 Homogenization of the Insulated Conductor

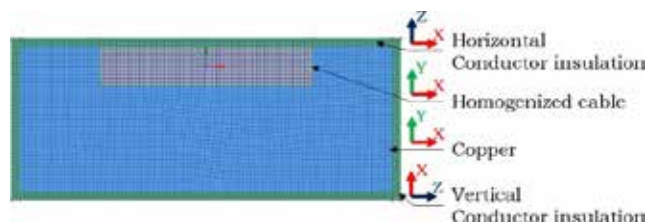


Figure 5.6 Model to homogenize the insulated conductor

The conductor model consists of a homogenized cable, a copper stabilizer, and an insulation layer of glass fiber epoxy. The insulation is split into two horizontal sections and two vertical sections. Figure 5.6 shows their orientation. Table 5.15 lists the homogenized properties of the insulated cable at 293 K and 4 K.

Table 5.15 Homogenized properties of the insulated conductor

Property	Symbol	Unit	293 K	4 K
Density	ρ	kg/m ³	7965.8	7965.8
Young's modulus	E1	GPa	97	119
Young's modulus	E2	GPa	97	119
Young's modulus	E3	GPa	103	123
Shear modulus	G12	GPa	37	45

The only official copy of this document is the one online in the SharePoint Document Center. Before using a printed copy, verify that it is current by checking the printed document's Revision History log with that of the online version.

Electron-Ion Collider, Brookhaven National Laboratory and Thomas Jefferson National Accelerator Facility			
Doc No. EIC-SHC-TN-24-005	Author: Sandesh Gopinath	Effective Date: 12/05/2024	Review Frequency: NA
Process Description: EIC Design Report MARCO Magnet			Revision: 00

Shear modulus	G23	GPa	37	45
Shear modulus	G31	GPa	37	45
Poisson's ratio	v12		0.348	0.337
Poisson's ratio	v13		0.318	0.322
Poisson's ratio	v23		0.318	0.322
Thermal expansion 1 (293 K to 4 K)	a1		0.267%	
Thermal expansion 2 (293 K to 4 K)	a2		0.266%	
Thermal expansion 3 (293 K to 4 K)	a3		0.104%	
Thermal Conductivity 1	K1	W/(m K)	155.6	296.0
Thermal Conductivity 2	K2	W/(m K)	164.2	324.9
Thermal Conductivity 3	K3	W/(m K)	221.9	501.0

5.2.3 Homogenization of the Coil

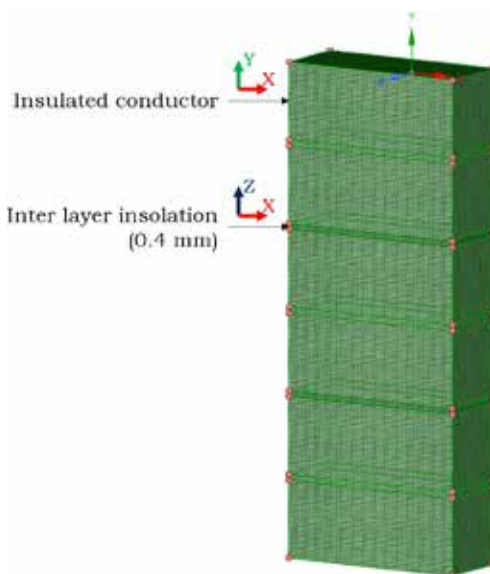


Figure 5.7 homogenization of the coil

The coil model is a stack of homogenized conductors separated by a layer of insulation fiber-glass epoxy. Figure 5.7 shows the orientation of different materials. Table 5.16 lists the homogenized properties of the coil at 293 K and 4 K.

Table 5.16 Homogenized properties of the coil

Property	Symbol	Unit	293 K	4 K
Density	ρ	kg/m ³	7489.8	7489.8
Young's modulus	E1	GPa	71	86
Young's modulus	E2	GPa	41	54
Young's modulus	E3	GPa	104	114

The only official copy of this document is the one online in the SharePoint Document Center. Before using a printed copy, verify that it is current by checking the printed document's Revision History log with that of the online version.

Electron-Ion Collider, Brookhaven National Laboratory and Thomas Jefferson National Accelerator Facility			
Doc No. EIC-SHC-TN-24-005	Author: Sandesh Gopinath	Effective Date: 12/05/2024	Review Frequency: NA
Process Description: EIC Design Report MARCO Magnet			Revision: 00

Shear modulus	G12	GPa	22	25
Shear modulus	G23	GPa	23	27
Shear modulus	G31	GPa	32	36
Poisson's ratio	v12		0.246	0.245
Poisson's ratio	v13		0.230	0.247
Poisson's ratio	v23		0.128	0.148
Thermal expansion 1 (293 K to 4 K)	a1		0.14%	
Thermal expansion 2 (293 K to 4 K)	a2		0.29%	
Thermal expansion 3 (293 K to 4 K)	a3		0.09%	
Thermal Conductivity 1	K1	W/(m K)	13	1.0
Thermal Conductivity 2	K2	W/(m K)	4.0	0
Thermal Conductivity 3	K3	W/(m K)	300	492

5.3 Models and Assumptions

5.3.1 2D Modeling

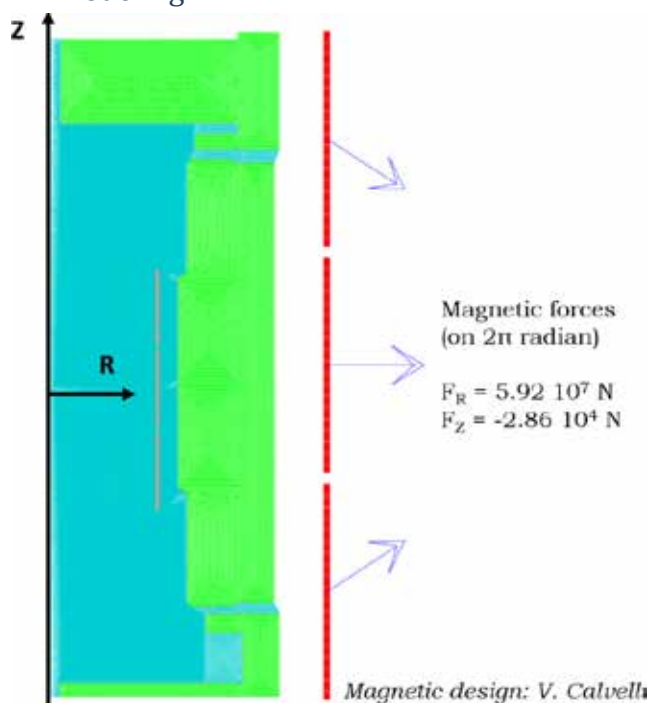


Figure 5.8 2D axisymmetric magnetic model (left); representation of the Lorentz forces acting on each of the 3 coils at nominal field (right)

The 2D mechanical calculation was conducted with CAST3M [19], using its magneto-static solver to calculate the Lorentz forces and its mechanical solver to analyze their impact on the magnet

Electron-Ion Collider, Brookhaven National Laboratory and Thomas Jefferson National Accelerator Facility			
Doc No. EIC-SHC-TN-24-005	Author: Sandesh Gopinath	Effective Date: 12/05/2024	Review Frequency: NA
Process Description: EIC Design Report MARCO Magnet			Revision: 00

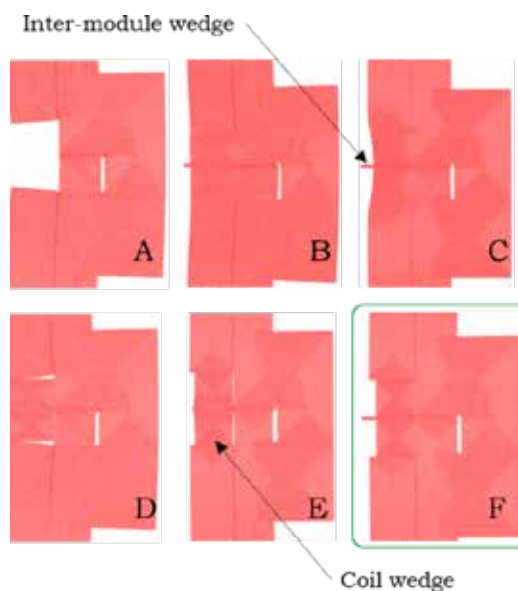


Figure 5.10 Coil wedges settings optimization. A: No wedges; B: Bonded contact, $R\theta$ fibers; C: Bonded contact, θZ fibers; D: Sliding contacts, $R\theta$ fibers; E: Sliding contact θZ fibers; F: Sliding contact except between the wedges and the mandrels (bonded contact), θZ fibers. The configuration is the one kept in 2D calculations.

Table 5.17 Wedge configuration for optimization

Case	Scenario	Peak von-Mises Stress in Coil (MPa)	Peak Shear Stress RZ in Coil (MPa)
A	No wedge	100	54
B	Full bonded contact, $R\theta$ fibers	95	49
C	Full bonded contact, θZ fibers	125	38
D	Full sliding contact, $R\theta$ fibers	100	54
E	Full sliding contact, θZ fibers	69	24
F	Full sliding contact except wedge-mandrel bonded contact θZ fibers	69	24

The 2D axisymmetric mechanical model was also created using the same (R, θ, Z) cylindrical coordinate system, with the vertical revolution axis in the Z longitudinal direction. The three coil modules in gray, as in Figure 5.9 (left), are wound and impregnated internal to the 3 external 30 mm thick brass mandrels, which are colored in blue in Figure 5.9.. A zoom-in view on one of the two areas where the 3 modules are assembled via the mechanical structure is presented in Figure 5.9 (right). The detailed modeling illustrates each coil, composed of six layers with 93 turns of insulated conductors per module. The 1 mm thick G10 orthotropic ground insulation, in yellow, is positioned between the coils and the mechanical structure. Additionally, the G10 orthotropic wedges, also in yellow, and the 3 mm thick inter-module wedge in pink are depicted

Electron-Ion Collider, Brookhaven National Laboratory and Thomas Jefferson National Accelerator Facility			
Doc No. EIC-SHC-TN-24-005	Author: Sandesh Gopinath	Effective Date: 12/05/2024	Review Frequency: NA
Process Description: EIC Design Report MARCO Magnet			Revision: 00

for structural support and insulation. These two types of wedges allow the large longitudinal Lorentz forces to be transmitted from the outer modules to the middle one (around 1430 tons acting on both sides toward the center). For the boundary conditions, the center of the mechanical structure is fixed in the longitudinal direction. The 29 kN of imbalanced longitudinal Lorentz forces is handled mainly by the longitudinal tie rods. In each module, the coil, the ground insulation and the mechanical structure are bonded together to simulate the impregnation. The coil wedges are bonded to mechanical structure and have a sliding contact with possible separation with the coils and with the inter-module wedges. There is also a sliding contact between the inter-module wedges and the mechanical structure. In this configuration, the peak shear stress is minimized. The detail of this optimization study is shown in Figure 5.10 and Table 5.17. To determine the best settings to optimize the interaction between the coil wedges, inter-module wedges, coil, grounding insulation, two variables have been considered: the fibers orientation and the contact type.

Table 5.17 lists the Von-Mises and shear stress results in the coil after energization for each configuration.

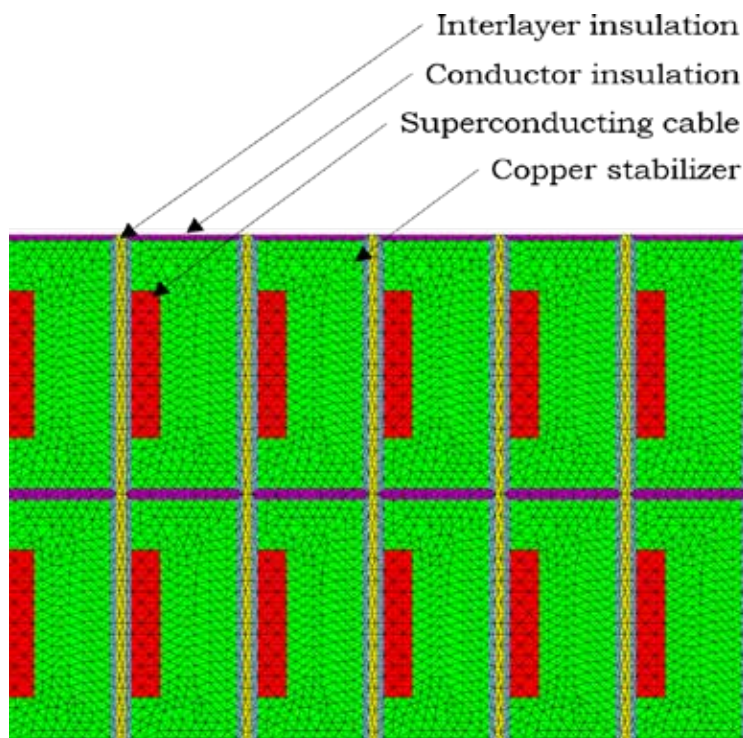


Figure 5.11 Zoom-in view on a portion of the coil, 6 layers and 2 turns

The fibers of the ground insulation and of the coil wedges are oriented in the θ and Z directions. The inter-module wedges are oriented in the R and θ directions. Other configurations have been analyzed, but the results showed high stresses during the cool down and energizing phase.

Electron-Ion Collider, Brookhaven National Laboratory and Thomas Jefferson National Accelerator Facility			
Doc No. EIC-SHC-TN-24-005	Author: Sandesh Gopinath	Effective Date: 12/05/2024	Review Frequency: NA
Process Description: EIC Design Report MARCO Magnet			Revision: 00

Figure 5.11 shows a zoom-in view on a portion of the coil (on 6 layers of only 2 turns). Each insulated conductor consists of a superconducting cable (in red), a copper stabilizer (in green), an insulation layer of 0.26 mm thickness (in pink and cyan). The 6 layers are separated by a layer of 0.4 mm thick glass fiber inter-layer insulation (in yellow), which is modeled with the same glass fiber epoxy material as the conductor insulation.

5.3.2 3D Modeling

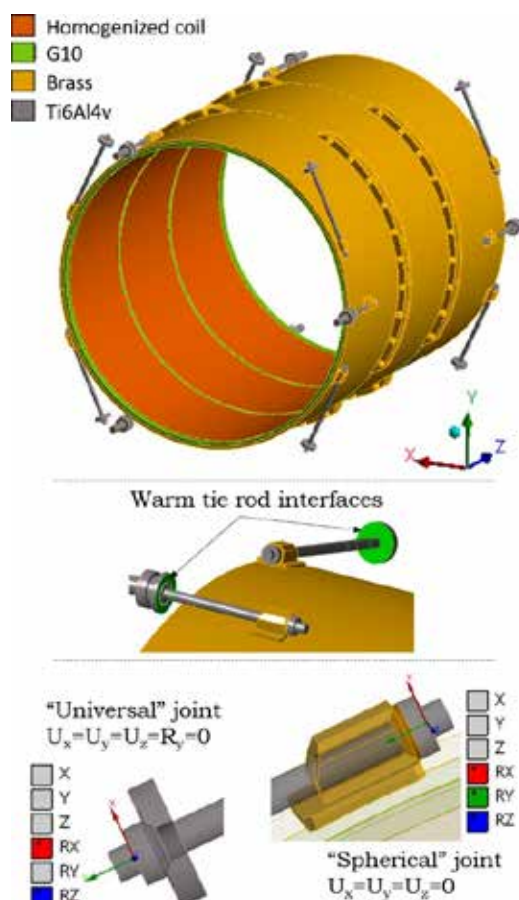


Figure 5.12 3D model

Figure 5.12 illustrates the geometry of the model and the various materials: homogenized coil, G10, brass and titanium alloy. The boundary conditions are imposed on the warm end of the tie rods. They are fixed for room temperature load cases and have an axial displacement corresponding to the calculated squeezing distance that the Belleville washers can allow (4.2 mm for the axial tie rods and 2 mm for the radial ones).

The only official copy of this document is the one online in the SharePoint Document Center. Before using a printed copy, verify that it is current by checking the printed document's Revision History log with that of the online version.

Electron-Ion Collider, Brookhaven National Laboratory and Thomas Jefferson National Accelerator Facility			
Doc No. EIC-SHC-TN-24-005	Author: Sandesh Gopinath	Effective Date: 12/05/2024	Review Frequency: NA
Process Description: EIC Design Report MARCO Magnet			Revision: 00

The model has been tested with different frictional coefficients of ball joints. For frictional coefficients values from 0 to 0.9, the global displacements does not change significantly since the moving angles of the tie rods are very small. The results showed in 5.4.2.2 and 5.4.3.2 are given with a frictional coefficient of 0.2. In the tie-rods sub-model one ball joint is set as a spherical joint (with all the rotations free) and the other one is set as a universal joint with a fixed axial rotation. This avoids the problem of non-convergent solver output due to the free rotation of the middle part of each tie rods.

Table 5.18 Specifications of Tie Rods

Specification	Radial tie rod	Axial tie rod	Total
Number	8	6	14
Calculated diameter (mm) (Transportation load = 3g + Safety factor = 3)	36	37	NA
Chosen diameter			NA
Length - center distance between cold and warm ball joints (mm)	657	880	NA
Heat load to the cold mass at 4.5 K (W)	0.24 per rod	0.34 per rod	3.95
Heat load to the thermal shield at 60 K (W)	4.67 per rod	7.44 per rod	82
Shrinkage between 293 K and 4 K (mm)	1.29	0.85	NA

Electron-Ion Collider, Brookhaven National Laboratory and Thomas Jefferson National Accelerator Facility			
Doc No. EIC-SHC-TN-24-005	Author: Sandesh Gopinath	Effective Date: 12/05/2024	Review Frequency: NA
Process Description: EIC Design Report MARCO Magnet			Revision: 00

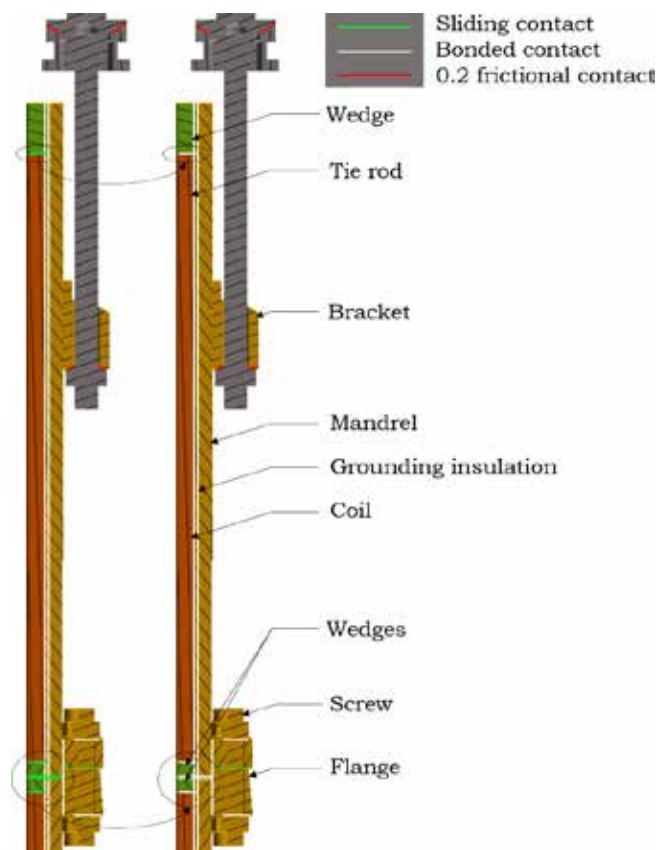


Figure 5.13 Contact configuration in the 3D model. On the left, the 2D optimized contacts. On the right, the cold mass fully impregnated contacts. The differences between both cases are marked by black dotted circles.

The contacts between the wedges, coils, grounding insulation, mandrel has been studied in two different configurations: the 2D optimized contacts (see Figure 5.10 (case F) and Figure 5.13 (left)) and the cold mass fully impregnated contacts (Figure 5.13 (right)). In the 3D model, both configurations yield the same acceptable results, giving the manufacturer more freedom in terms of fabrication. To be consistent with the 2D model, only the results from the model with 2D optimized contacts (Figure 5.13, on the right) will be showed in 5.4.2.1 and 5.4.3.1.

Electron-Ion Collider, Brookhaven National Laboratory and Thomas Jefferson National Accelerator Facility			
Doc No. EIC-SHC-TN-24-005	Author: Sandesh Gopinath	Effective Date: 12/05/2024	Review Frequency: NA
Process Description: EIC Design Report MARCO Magnet			Revision: 00

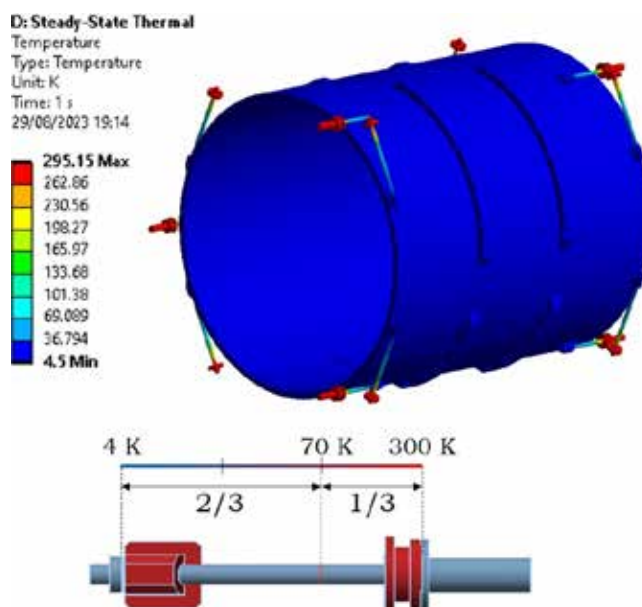


Figure 5.14 Thermal boundary conditions

The thermal boundary conditions (Figure 5.14) simulate a simplified final state of the cool-down. The cold mass assembly and the cold interfaces are at 4.5 K; the warm interfaces are at 293 K; the thermalization is imposed at 70 K. Figure 5.14 Thermal boundary conditions illustrates these thermal boundary conditions, with a detailed view of thermal interception at the tie rod. In the model, the rod is divided in two parts connected together with a contact. This allows to create and select the surface of thermal interception. Table 5.18 lists the specifications of the tie rods.

5.4 Results and Discussions

5.4.1 Self-weight, seismic and transportation loads

Self weight, seismic and transportation loads are fundamental cases in order to dimension the tie-rods diameter as well as to assess the main criticalities the magnet can stand before the installation. Due to the asymmetry of gravity and tie-rods positions, these cases have been modeled only in 3D at ambient temperature. For transportation loads, an acceleration of 3g along every axis has been considered, plus a safety factor of 3. For seismic loads, an acceleration of 1.25g along every axis has been considered. Since the transportation loads are more conservatives than the seismic ones (3g versus 1.25g), the analysis has been focused on the transportation loads. Results in terms of stress are showed in for the self-weight and in for transportation loads in the X, Y, Z direction, the worst one for the tie-rods. In each case, stress is well mastered by the cold mass as well as the tie-rods. For self-weight and transportation loads, each component of the magnet is well below the 2/3 of the elastic limit.

Electron-Ion Collider, Brookhaven National Laboratory and Thomas Jefferson National Accelerator Facility			
Doc No. EIC-SHC-TN-24-005	Author: Sandesh Gopinath	Effective Date: 12/05/2024	Review Frequency: NA
Process Description: EIC Design Report MARCO Magnet			Revision: 00

Table 5.19

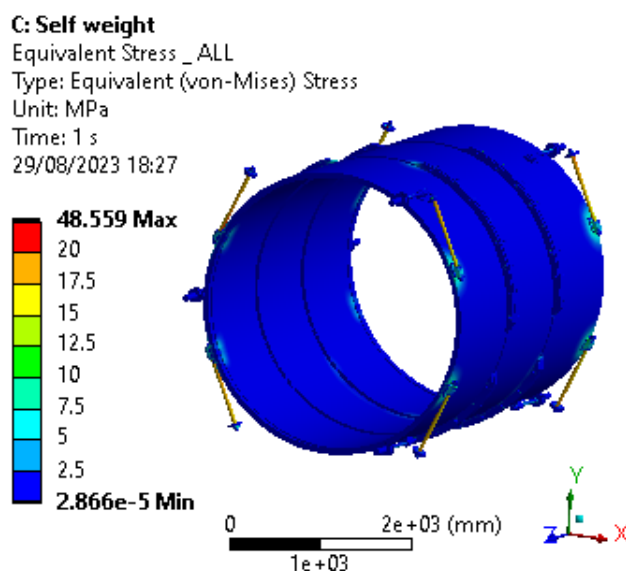


Figure 5.15 – Von Mises equivalent stress distribution in the tie-rods and cold mass due to the self-weight.

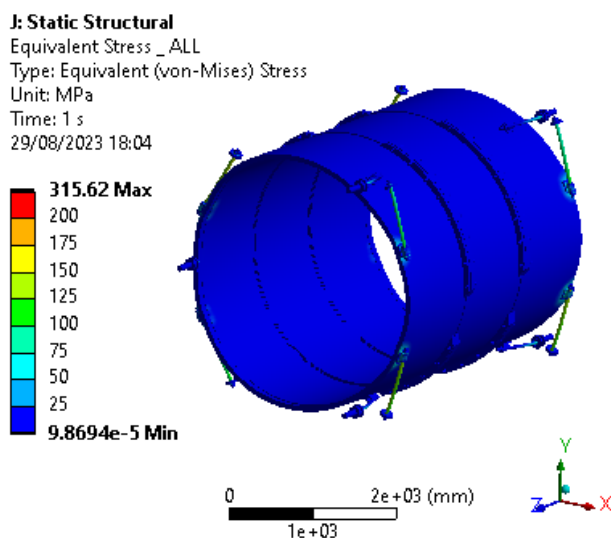


Figure 5.16 - Von Mises equivalent stress distribution in the tie-rods and cold mass due to a 3g acceleration along the X axis. This is the worst case in terms of stress for the tie-rods.

Electron-Ion Collider, Brookhaven National Laboratory and Thomas Jefferson National Accelerator Facility			
Doc No. EIC-SHC-TN-24-005	Author: Sandesh Gopinath	Effective Date: 12/05/2024	Review Frequency: NA
Process Description: EIC Design Report MARCO Magnet			Revision: 00

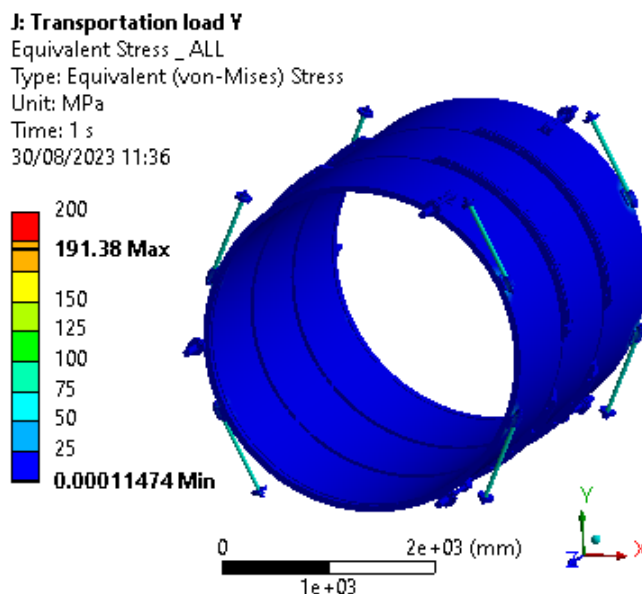


Figure 5.17 - Von Mises equivalent stress distribution in the tie-rods and cold mass due to a 3g acceleration along the Y axis.

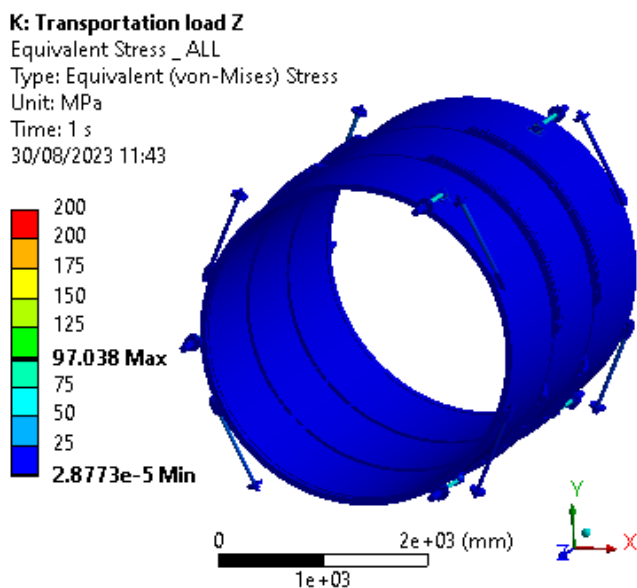


Figure 5.18 - Von Mises equivalent stress distribution in the tie-rods and cold mass due to a 3g acceleration along the Z axis

Electron-Ion Collider, Brookhaven National Laboratory and Thomas Jefferson National Accelerator Facility			
Doc No. EIC-SHC-TN-24-005	Author: Sandesh Gopinath	Effective Date: 12/05/2024	Review Frequency: NA
Process Description: EIC Design Report MARCO Magnet			Revision: 00

5.4.2 Cool-down

5.4.2.1 2D Cooldown Models

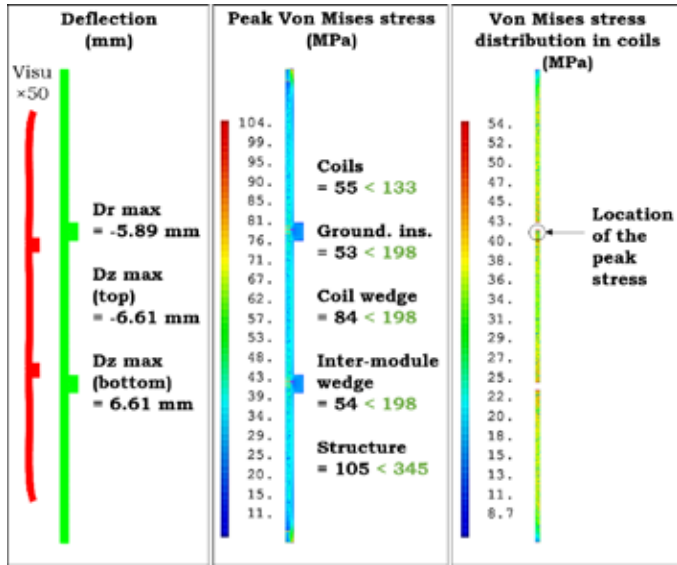


Figure 5.19 2D cool down results. On the left, the deflection; at the middle, the Von-Mises equivalent stresses; on the right, the distribution of von-Mises equivalent stress in the coils

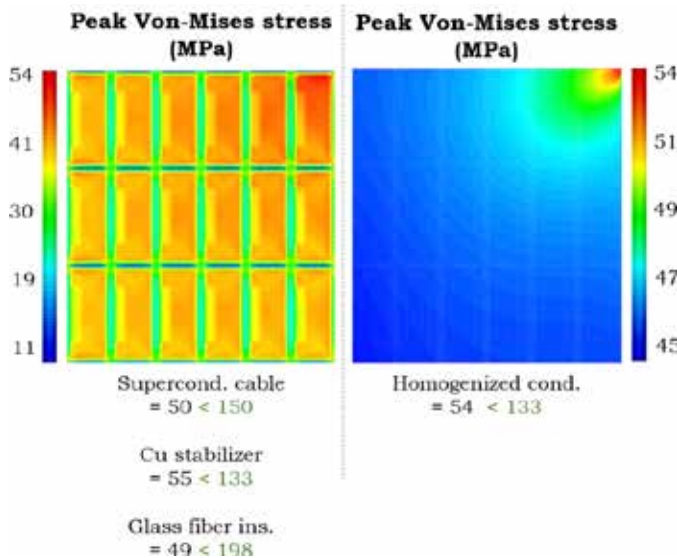


Figure 5.20 Zoom-in view of the coil area where the peak Von Mises stress occurs. On the left, with properties of the detailed insulated conductor (left); on the right, with properties of the homogenized conductor. (right)

Electron-Ion Collider, Brookhaven National Laboratory and Thomas Jefferson National Accelerator Facility			
Doc No. EIC-SHC-TN-24-005	Author: Sandesh Gopinath	Effective Date: 12/05/2024	Review Frequency: NA
Process Description: EIC Design Report MARCO Magnet			Revision: 00

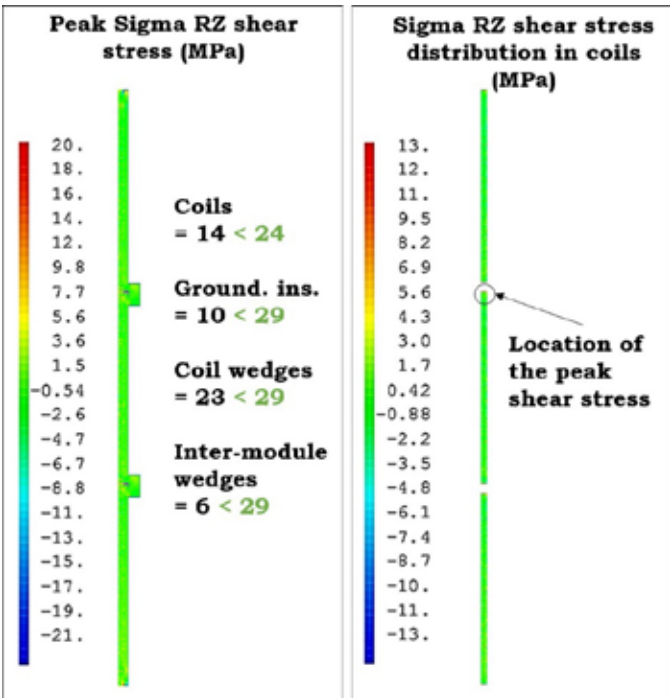


Figure 5.21 2D cool-down shear results. On the left, the deflection; at the middle, the Von-Mises equivalent stresses; on the right, the Von-Mises equivalent stress distribution in the coils.

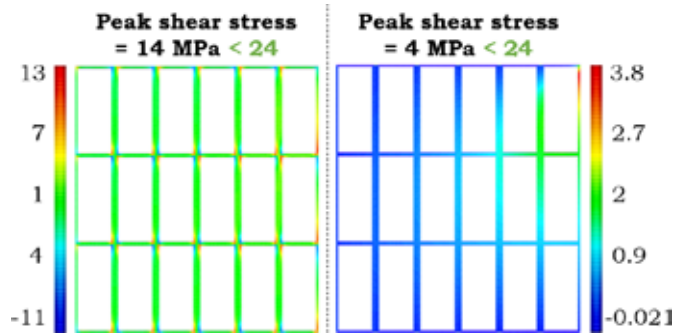


Figure 5.22 Zoom-in view of the conductor insulation area where the peak RZ shear stress occurs. On the top, with properties of the detailed insulated conductor; on the left, with properties of the homogenized conductor on the right.

At 4 K, the radial and longitudinal deflection of MARCO is shown in Figure 5.19 (left). The peak von-Mises equivalent stress remains below the corresponding acceptance criteria in the coils (133 MPa max), see Figure 5.19 (center). The stresses in the G10 components such as ground insulation, in the coil wedges and inter-module wedges are also below the criterion; the same is true for the mechanical structure made of brass. Figure 5.19 (right) shows the von Mises stress distribution in the coils and the location of the peak stress at the top of the center

Electron-Ion Collider, Brookhaven National Laboratory and Thomas Jefferson National Accelerator Facility			
Doc No. EIC-SHC-TN-24-005	Author: Sandesh Gopinath	Effective Date: 12/05/2024	Review Frequency: NA
Process Description: EIC Design Report MARCO Magnet			Revision: 00

coil. Figure 5.20 illustrates zoom-in views of the coil areas where the peak von Mises stresses occur, using the properties of the detailed insulated conductor and of the homogenized conductor.

The peak RZ shear stress is below the acceptance in the coils for all components as shown in Figure 5.21. The distribution of RZ shear stress in the coils is shown in the Figure 5.21 (right). The peak shear stress occurs at the extremity of the center coil. Figure 5.18 provides a zoom-in view of the conductor insulation area where the peak shear stress occurs, using the properties of the detailed insulated conductor and of the homogenized conductor. All the values are below the 24 MPa criterion. The peak stress is higher in the case of detailed properties as the differential thermal shrinkage between the conductor components is not taken into account in the homogenized configuration.

5.4.2.2 3D Cool-down Models:

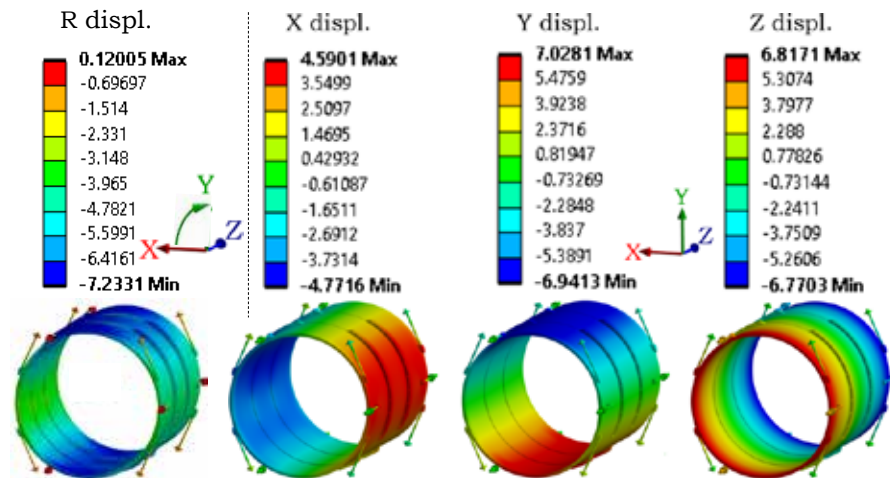


Figure 5.23 Cold mass displacements in the three directions of the Cartesian frame after cool-down

Electron-Ion Collider, Brookhaven National Laboratory and Thomas Jefferson National Accelerator Facility			
Doc No. EIC-SHC-TN-24-005	Author: Sandesh Gopinath	Effective Date: 12/05/2024	Review Frequency: NA
Process Description: EIC Design Report MARCO Magnet			Revision: 00

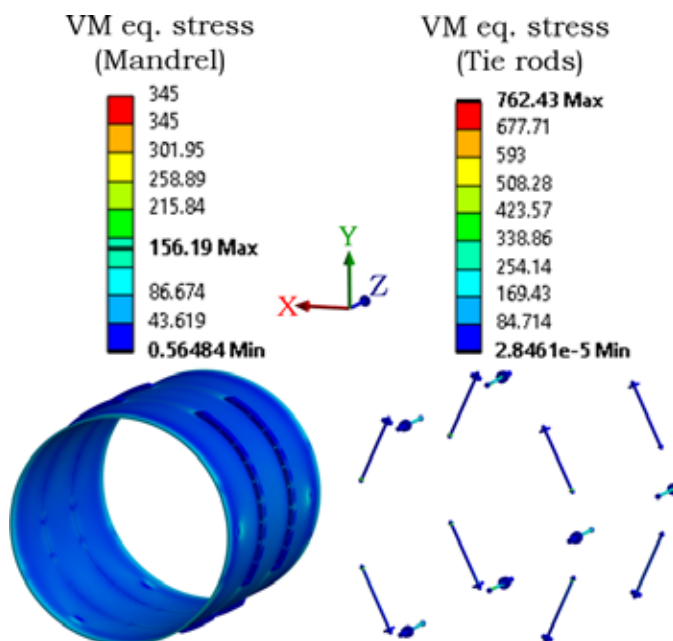


Figure 5.24 Von-Mises equivalent stress in the mandrel (left) and in the tie rods (right), after cool-down

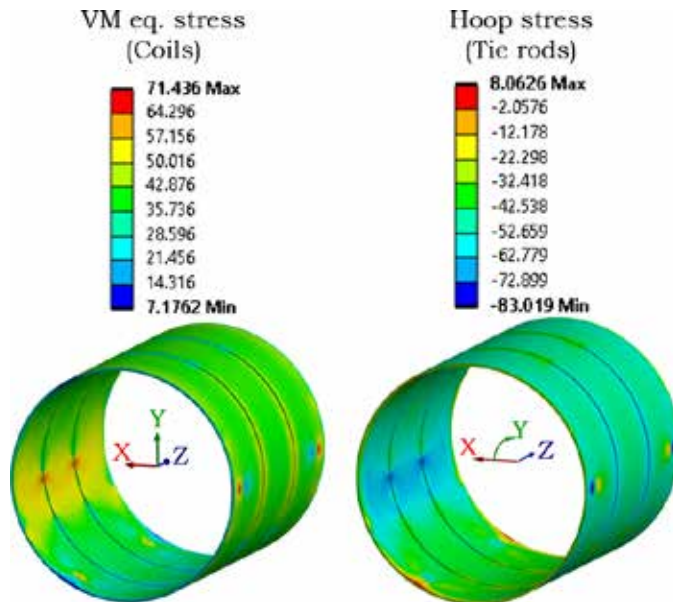


Figure 5.25 Von-Mises equivalent stress (left) and hoop stress (right) in the coils, after cool-down

Electron-Ion Collider, Brookhaven National Laboratory and Thomas Jefferson National Accelerator Facility			
Doc No. EIC-SHC-TN-24-005	Author: Sandesh Gopinath	Effective Date: 12/05/2024	Review Frequency: NA
Process Description: EIC Design Report MARCO Magnet			Revision: 00

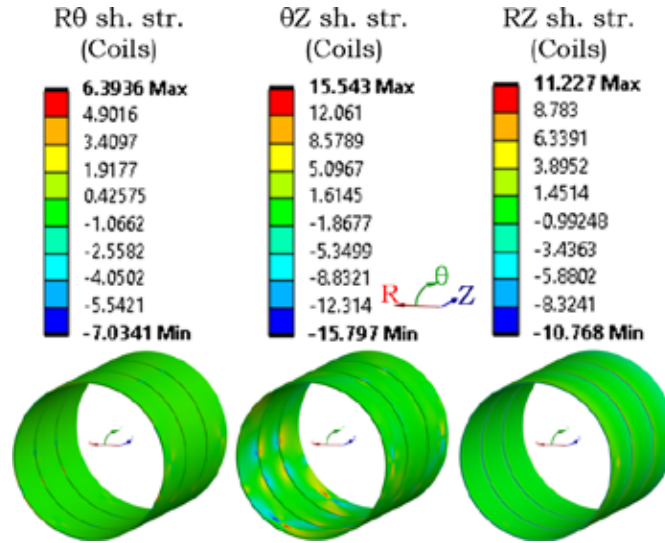


Figure 5.26 Coil shear stress in $R\theta$ (left), θZ (center), and RZ (left), after cool-down

As explained in 5.3.2, the boundary conditions are different in 2D and in 3D. Then, the results are not expected to be the same. As an example, even before analysis, a quite evenly-spread stresses in the mandrel were expected in 2D; however, on the other hand, stress concentrations in the mandrel where the tie rods are attached were expected in 3D. Also, in terms of displacements, the structural behavior should not be comparable because the 2D model is axisymmetric and designed from a section with flanges. This implies a magnet with continuous flange in the 2D model. As explained in the introduction, and as visible in Figure 5.4 and Figure 5.9, the magnet doesn't have continuous flanges. This creates non-axisymmetric behaviors.

Figure 5.23 shows the displacements in the three directions (cartesian frame) of the complete cold mass. It is interesting to notice how far the simplified model is from the more detailed one at each step of the calculation. The radial displacements in Figure 5.19 is 5.89 mm. In Figure 5.23, the average of the maximum displacements in X and Y is 5.98 mm. In the Z direction, the results are not perfectly symmetrical (within 0.05 mm) because the boundary conditions are not symmetrical. In this case the average of the two absolute maximum z-displacements in the 3D analysis differs by only 0.2 mm from the 2D results, which is very reasonable.

Figure 5.24 demonstrates the von-Mises equivalent stresses of the mandrel and the tie rods in the complete cold mass model.

As shown in the Table 5.13, the acceptable stresses are 354 MPa for brass and 1129 MPa for Ti6Al4V. Therefore, the safety margin is high for these components. The

Electron-Ion Collider, Brookhaven National Laboratory and Thomas Jefferson National Accelerator Facility			
Doc No. EIC-SHC-TN-24-005	Author: Sandesh Gopinath	Effective Date: 12/05/2024	Review Frequency: NA
Process Description: EIC Design Report MARCO Magnet			Revision: 00

brass inter-modules screws - has a peak von Mises stress of 52 MPa (< 354 MPa); the grounding insulation and the wedges maximum stress, 47 MPa and 94 MPa respectively (< 198 MPa). Figure 5.25 illustrates two different results on the coils, the von-mises equivalent stresses in the XYZ cartesian frame and the hoop stress in the R θ Z cylindrical frame. It is important to notice that the shrinkage of the coil is considered from 295 K to 4.5 K. The temperature change during the resin impregnation process have not been considered.

Also, the shear stress in all the directions have been studied in the R θ Z cylindrical frame. The results are not comparable to the 2D ones because of the influence of the tie rods. In the θ Z shear stress results, visible stress concentrations occur exactly under the tie rods (Figure 5.26).

Even these peak stresses are below the acceptance criteria of the coil shear strength at 4.5 K (< 24 MPa).

5.4.3 Energization

5.4.3.1 2D Energization Model

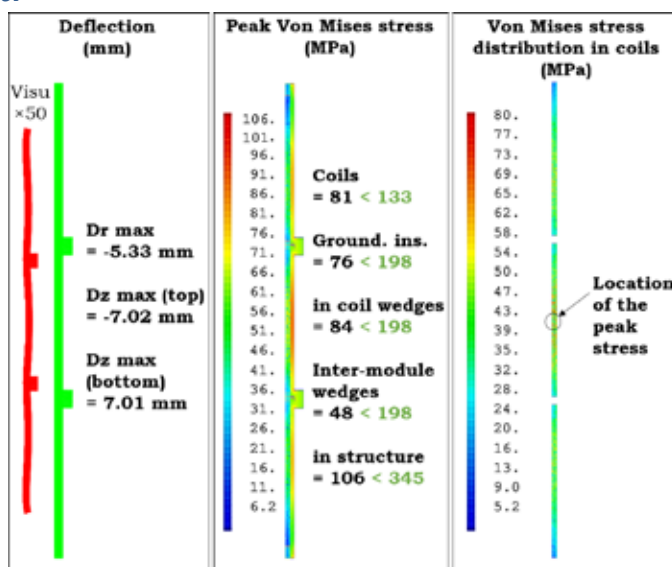


Figure 5.27 Results from 2D energization model. On the left, the deflection; in the middle, the peak von-Mises equivalent stresses; on the right, the distribution of von-Mises equivalent stress in the coils

The only official copy of this document is the one online in the SharePoint Document Center. Before using a printed copy, verify that it is current by checking the printed document's Revision History log with that of the online version.

Electron-Ion Collider, Brookhaven National Laboratory and Thomas Jefferson National Accelerator Facility			
Doc No. EIC-SHC-TN-24-005	Author: Sandesh Gopinath	Effective Date: 12/05/2024	Review Frequency: NA
Process Description: EIC Design Report MARCO Magnet			Revision: 00

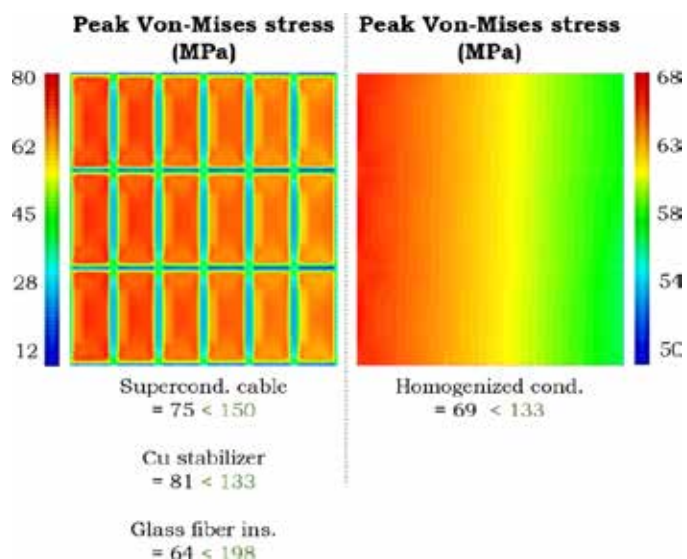


Figure 5.28 Zoom-I view of the conductor insulation area where the Von-Mises equivalent peak stress occurs, using the properties of the detailed insulated conductor (left), and of the homogenized conductor (right)

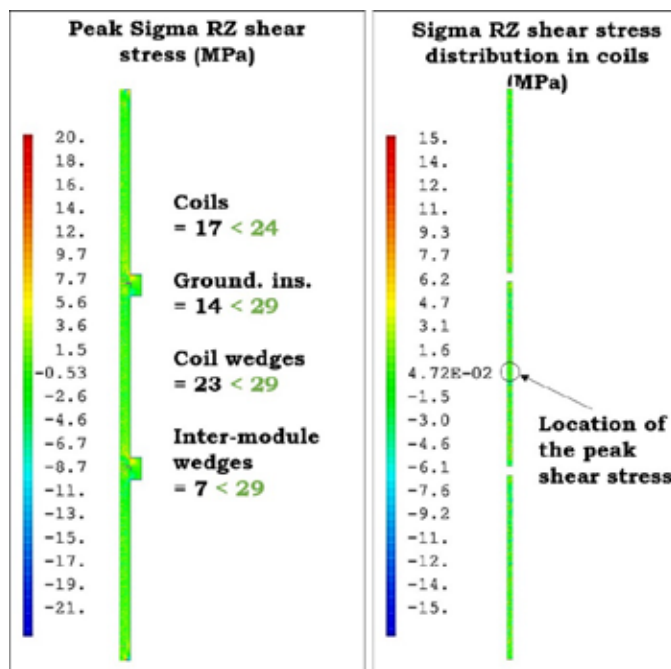


Figure 5.29 2Shear stress results from the 2D energization model. On the left, the deflection; in the middle, the von-Mises equivalent stresses; on the right, the distribution of von-Mises equivalent stress in the coils

Electron-Ion Collider, Brookhaven National Laboratory and Thomas Jefferson National Accelerator Facility			
Doc No. EIC-SHC-TN-24-005	Author: Sandesh Gopinath	Effective Date: 12/05/2024	Review Frequency: NA
Process Description: EIC Design Report MARCO Magnet			Revision: 00

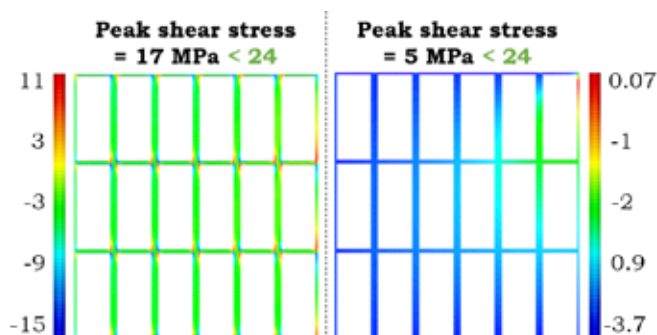


Figure 5.30 Zoom-in view of the conductor insulation area where the peak RZ shear stress occurs, using the properties of the detailed insulated conductor (left), and of the homogenized conductor (right)

At the nominal field, the coils tend to expand radially due to high radial Lorentz forces, inducing stresses in the conductor. The mandrel serves as the winding support during the fabrication and plays a crucial mechanical role in maintaining the coils and reducing the peak stress in the conductor during energization. The radial and longitudinal deflection of MARCO is shown in the Figure 5.27(left) for the energization load case. During cool-down, the von Mises equivalent peak stress is below the acceptance criteria in the coils, in the G10 components (grounding insulation, coil wedges and inter-module wedges), and in the mechanical structure, see Figure 5.27 (center). Figure 5.27 (right) shows the distribution of von Mises equivalent stress in the coils and the location of the peak stress. The peak stress occurs in the center of the central coil, where the longitudinal magnetic forces are concentrated.

Figure 5.28 shows a zoom-in view of the coil area where the von Mises peak stress occurs; the left is the detailed insulated conductor and the right is the homogenized conductor.

At energization, the RZ shear peak stress is below the acceptance criteria in the coils and in the G10 components (grounding insulation, coil wedges and inter- module wedges), see Figure 5.29(left). The distribution of RZ shear stress in the coils is illustrated in Figure 5.29 (right). The peak shear stress occurs near the interface of the middle coil with its mandrel.

Figure 5.30 shows a zoom-in view of the coil area where the peak shear stress occurs; the left is the detailed insulated conductor and the right is the homogenized conductor. All shear stresses are below the criterion of 24 MPa. During energization, the peak shear stress in the conductor insulation is only slightly higher than the peak shear stress observed during cool-down.

The 2D axisymmetric mechanical calculations features a very detailed insulated conductor, the cool-down to 4K and the energization via Lorentz forces calculated at each node of the

Electron-Ion Collider, Brookhaven National Laboratory and Thomas Jefferson National Accelerator Facility			
Doc No. EIC-SHC-TN-24-005	Author: Sandesh Gopinath	Effective Date: 12/05/2024	Review Frequency: NA
Process Description: EIC Design Report MARCO Magnet			Revision: 00

superconducting cable. The mechanical simulations for the cool-down and the energization demonstrate that the peak von-Mises stress is below the corresponding acceptance criteria in the coils, in the G10 components such as ground insulation, coil wedges and inter-module wedges, and in the brass support structure. The RZ shear peak stress is also below the corresponding acceptance criteria both in the coils and in the G10 components.

5.4.3.2 3D Energization Model

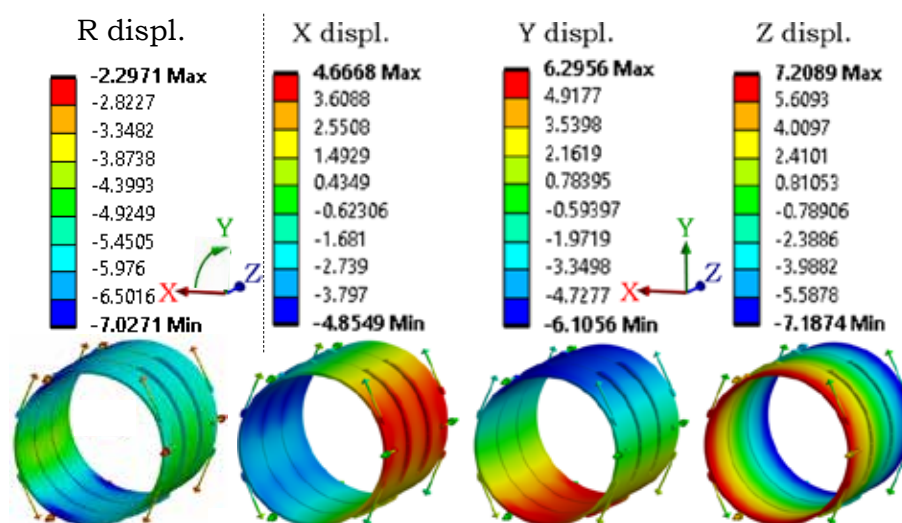


Figure 5.31 displacements of cold mass in cylindrical coordinates and Cartesian frame, during energization

Electron-Ion Collider, Brookhaven National Laboratory and Thomas Jefferson National Accelerator Facility			
Doc No. EIC-SHC-TN-24-005	Author: Sandesh Gopinath	Effective Date: 12/05/2024	Review Frequency: NA
Process Description: EIC Design Report MARCO Magnet			Revision: 00

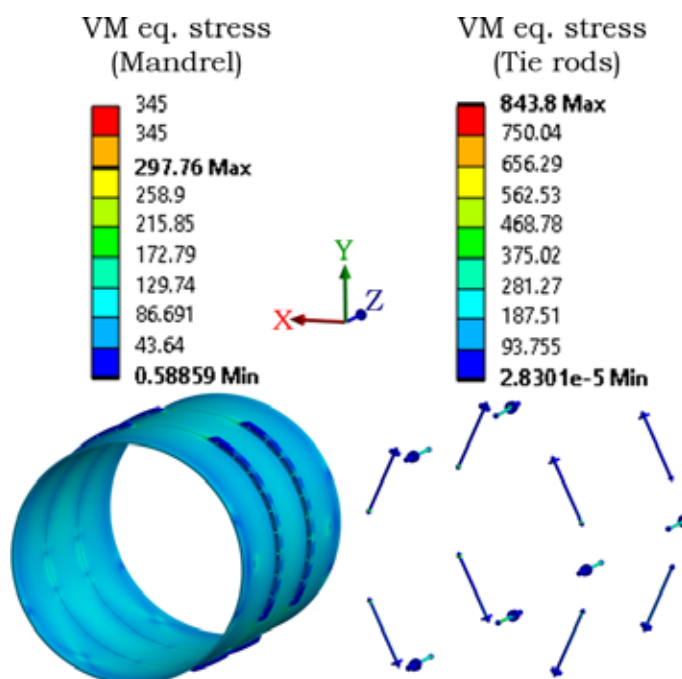


Figure 5.32 Von-Mises equivalent stress in the mandrel (left) and the tie rods (right), during energization

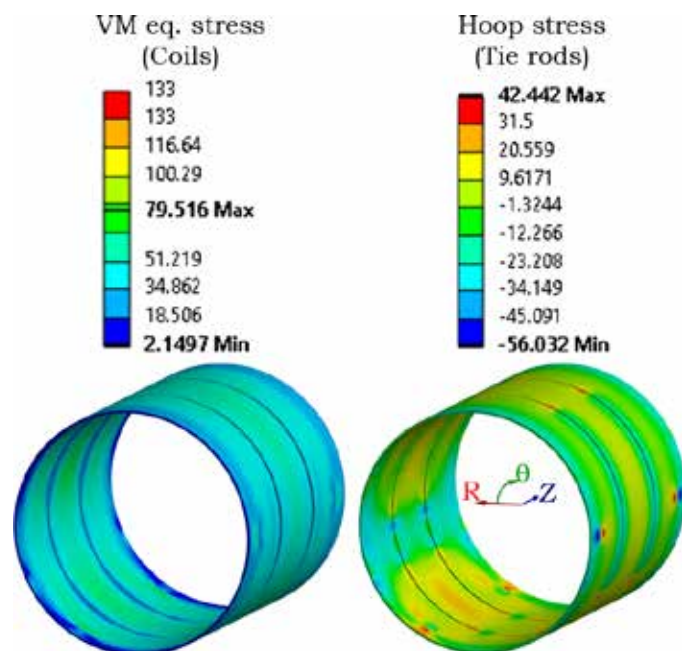


Figure 5.33 Von-Mises equivalent stress (left) and hoop stress (right) in the coils, during energization

Electron-Ion Collider, Brookhaven National Laboratory and Thomas Jefferson National Accelerator Facility			
Doc No. EIC-SHC-TN-24-005	Author: Sandesh Gopinath	Effective Date: 12/05/2024	Review Frequency: NA
Process Description: EIC Design Report MARCO Magnet			Revision: 00

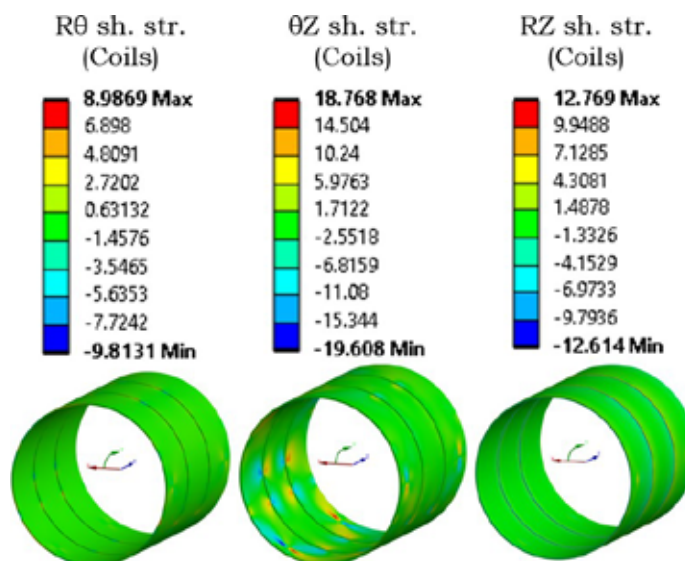


Figure 5.34 Coil shear stress in $R\theta$ (left) θZ (center) and RZ (left), during energization

Due to the shrinkage during cool-down, the diameter and length of the cold mass decrease. The maximum radial displacement R displacement is about 12 mm after cool-down (see Figure 5.23) and about 7 mm during energization (Figure 5.31). The Z displacements is about 6.8 mm after cool-down and about 7.2 mm during energization.

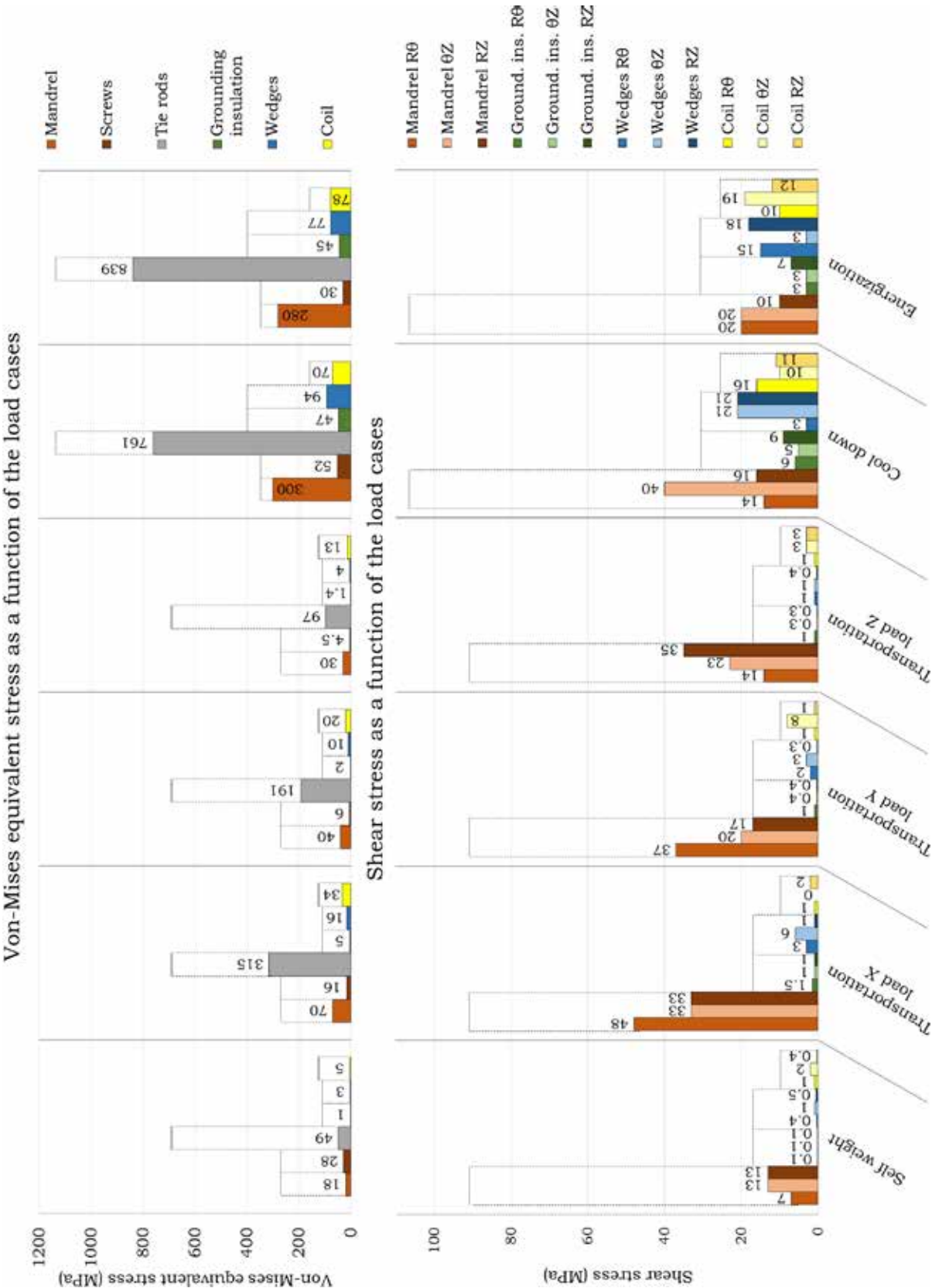
However, the stresses are higher due to the additional load of energization. The peak von Mises stress is 298 MPa (instead of 156 MPa after cool-down) in the mandrel, and 844 MPa (instead of 762 MPa after cool-down) in the tie rods (Figure 5.32). They are acceptable as the acceptance criteria is 345 MPa for brass and 1129 MPa for Ti6Al4V.

The peak von Mises stress of inter-module screws is 30 MPa . The peak von Mises stresses of the grounding insulation and the wedges are respectively 45 MPa and 77 MPa . The acceptance criterion of the coil stress is 133 MPa, which is greater than the von-Mises and hoop stress results in Figure 5.33. As explained in the introduction, the mandrel keeps the coil under constraint after cool-down. The magnetic forces are directed towards the outer side (+R in the cylindrical frame), and they pull the coil inward. This is why the coil stresses are lower during energization than after cool-down.

As shown in Figure 5.34, the shear stress in the coils is slightly higher during energization than after cool-down due to the magnetic loads, but they are still acceptable (20 MPa < 24 MPa).

The only official copy of this document is the one online in the SharePoint Document Center. Before using a printed copy, verify that it is current by checking the printed document’s Revision History log with that of the online version.

Electron-Ion Collider, Brookhaven National Laboratory and Thomas Jefferson National Accelerator Facility			
Doc No. EIC-SHC-TN-24-005	Author: Sandesh Gopinath	Effective Date: 12/05/2024	Review Frequency: NA
Process Description: EIC Design Report MARCO Magnet			Revision: 00



The only official copy of this document is the one online in the SharePoint Document Center. Before using a printed copy, verify that it is current by checking the printed document's Revision History log with that of the online version.

Electron-Ion Collider, Brookhaven National Laboratory and Thomas Jefferson National Accelerator Facility			
Doc No. EIC-SHC-TN-24-005	Author: Sandesh Gopinath	Effective Date: 12/05/2024	Review Frequency: NA
Process Description: EIC Design Report MARCO Magnet			Revision: 00

Figure 5.35 Summary of von-Mises equivalent stress for each load case with the acceptance criteria shown in dotted lines

The 3D model simulates a more accurate behavior because it takes the tie rods into account. All the stress results, even the localized peak stresses, are acceptable. The graph in Figure 5.35 summarizes all the 3D results in terms of von-Mises equivalent stresses and shear stress for all the component and presents an overview of the behavior of the magnet for each load cases. The load cases in the X-coordinate of the graph are in the chronological order in the life of the magnet: the self-weight, the transportation loads, the cool-down and the energization.

For each component, and for each batch of temperature (room temperature and cryogenic temperature), the dotted blue rectangles illustrates the relevant acceptance criteria. The margins between the critical limits and the computed results are clearly visible.

The tie rods experience significant von Mises stresses once the transportation loads, particularly in the X direction. This is expected given the orientation of the tie rods. They are more optimized in the vertical direction. Along the Z direction, the axial tie rods are perfectly co-axial to the Z axis before cool-down and this helps withstand the forces. During cool-down and energization, the tie rods experience tension and their stress increases, pulling the mandrel brackets. The temperature differential and the magnetic forces constrain the mandrel to the coil. These effects are clearly visible in the two last load cases.

Electron-Ion Collider, Brookhaven National Laboratory and Thomas Jefferson National Accelerator Facility			
Doc No. EIC-SHC-TN-24-005	Author: Sandesh Gopinath	Effective Date: 12/05/2024	Review Frequency: NA
Process Description: EIC Design Report MARCO Magnet			Revision: 00

6 Magnet Structure and Materials

This section describes the magnet structure and all the material used in the magnet system. Due to its role in the central detector, the magnet's design is constrained by strict limitations on the types of materials that can be used.

6.1 Materials Used

The materials in the EIC detector, including those in the solenoid, must be consistent with the overall material budget that allows detection of relevant particles for EIC science, with their specific energies. At the EIC, the barrel Hadron Calorimeter (bHCal) needs to act as tail catcher following the barrel Electromagnetic Calorimeter (bECal) that is approximately $1.0 \lambda_I$ (nuclear interaction length). This implies that the solenoid material needs to be “light” (approximately $1.3 \lambda_I$) to contain 95% of the hadrons with energy of science interest in the EIC. This leads to the need for all the material thickness to be less than “one” interaction length—the lower, the better. The current material budget for Marco 2T design is well within this limit.

The only official copy of this document is the one online in the SharePoint Document Center. Before using a printed copy, verify that it is current by checking the printed document's Revision History log with that of the online version.

Electron-Ion Collider, Brookhaven National Laboratory and Thomas Jefferson National Accelerator Facility			
Doc No. EIC-SHC-TN-24-005	Author: Sandesh Gopinath	Effective Date: 12/05/2024	Review Frequency: NA
Process Description: EIC Design Report MARCO Magnet			Revision: 00

Table [6.1](#) lists the materials in the magnet. Table 6.2 summarizes the thicknesses of all these materials, their nuclear interaction lengths, and the total interaction length.

The only official copy of this document is the one online in the SharePoint Document Center. Before using a printed copy, verify that it is current by checking the printed document's Revision History log with that of the online version.

Electron-Ion Collider, Brookhaven National Laboratory and Thomas Jefferson National Accelerator Facility			
Doc No. EIC-SHC-TN-24-005	Author: Sandesh Gopinath	Effective Date: 12/05/2024	Review Frequency: NA
Process Description: EIC Design Report MARCO Magnet			Revision: 00

Table 6.1 Materials in the magnet

	Component	Length along z (m)	Number of component	i.d. (m)	o.d. (m)	Thickness in radial direction (mm)	Volume (m ³)	Material	Starting position from magnet center (mm)	End position from magnet center (mm)	Starting position from magnet center (mm)	End position from magnet center (mm)	Inner radius (mm)	Outer radius (mm)
Radial	Inner vacuum vessel	3.79	1	2.8400	2.8600	10	0.339	Al	-1895	1895			1420	1430
	MLI	3.7	1	2.8600	2.9000	20	0.670	MLI	-1850	1850			1430	1450
	Inner thermal shield	3.7	1	2.9450	2.9550	5	0.171	Al	-1850	1850			1472.5	1477.5
	MLI	3.7	1	2.9550	3.0190	32	1.111	MLI	-1850	1850			1477.5	1509.5
	Inner G10	3.492	1	3.0130	3.0190	3	0.099	G10	-1746	1746			1506.5	1509.5
	Coil	3.492	1	3.0190	3.0862	33.6	1.125	Coil	-1746	1746			1509.5	1543.1
	Outer G10	3.492	1	3.0862	3.0922	3	0.102	G10	-1746	1746			1543.1	1546.1
	Coil Former	3.492	1	3.0922	3.1522	30	1.028	Brass	-1746	1746			1546.1	1576.1
	MLI	3.7	1	3.1522	3.1522	0	0.000	MLI	-1850	1850			1576.1	1576.1
	Outer Thermal shield	3.7	1	3.3550	3.3650	5	0.195	Al	-1850	1850			1677.5	1682.5
	MLI	3.7	1	3.3650	3.4900	62.5	2.490	MLI	-1850	1850			1682.5	1745
	Outer Vacuum vessel	3.79	1	3.4900	3.5400	25	1.046	Al	-1895	1895			1745	1770
Axial	Coil end support	0.0452	2	3.0190	3.0862	33.6	0.015	Brass	-1746	-1791.2	1746	1791.2	1509.5	1543.1
	G10 ends	0.003	2	3.0130	3.0922	39.6	0.001	G10	-1746	-1749	1746	1749	1506.5	1546.1
	MLI	0.015	2	2.9450	3.3650	210	0.031	MLI	-1746	-1761	1746	1761	1472.5	1682.5
	Thermal shield end 1	0.003	1	2.9450	3.3650	210	0.006	Al	-1850	-1853	1850	1853	1472.5	1682.5
	Thermal shield 2	0.005	1	2.9450	3.3650	210	0.010	Al	-1850	-1855	1850	1855	1472.5	1682.5
	MLI	0.02	2	2.8400	3.5400	350	0.070	MLI	-1850	-1870	1850	1870	1420	1770
	Vacuum vessel end	0.04	2	2.8400	3.5400	350	0.140	Al	-1895	-1935	1895	1935	1420	1770
Miscellaneous	Axial and radial coil support	size and locations of these will be decided after full mechanical analysis						Tungsten / carbon fiber						
	Instrumentation (sensors etc.)	number and locations of these will be decided later						Cu/magainin/constantan						

The only official copy of this document is the one online in the SharePoint Document Center. Before using a printed copy, verify that it is current by checking the printed document's Revision History log with that of the online version.

Electron-Ion Collider, Brookhaven National Laboratory and Thomas Jefferson National Accelerator Facility			
Doc No. EIC-SHC-TN-24-005	Author: Sandesh Gopinath	Effective Date: 12/05/2024	Review Frequency: NA
Process Description: EIC Design Report MARCO Magnet			Revision: 00

Table 6.2 Material thickness and interaction length

Material	Material Thickness (mm)	Nuclear interaction length (mm)	Thickness/Nuclear interaction length
Total Al	45.00	397.04	0.113
Total Cu	25.39	153.24	0.166
Total SS/Brass	30.00	165.50	0.181
Total NbTi	1.76	232.07	0.008
Total G10	12.00	435.56	0.028
Total Interaction Length			0.495

Figure 6.1 illustrates the cross-sectional view of the magnet system showing the coil, thermal shields and vacuum vessels. Figure 6.2 shows the internal components of the magnet showing the tie rods and cooling tubes of the magnet.

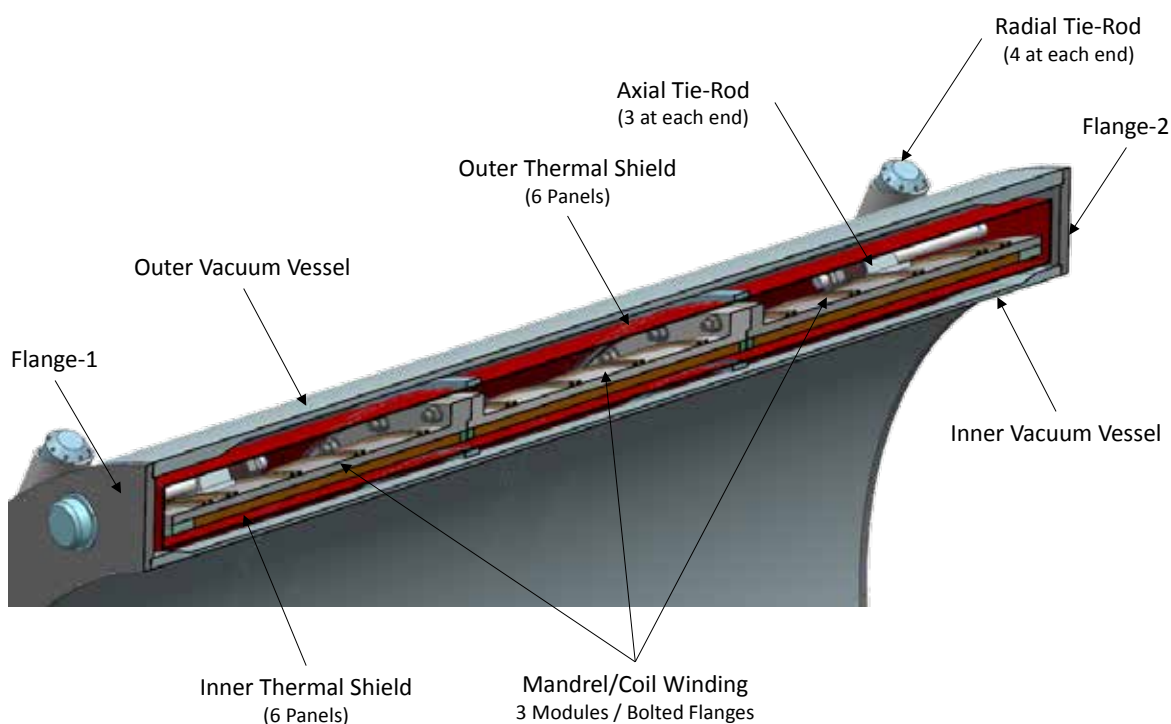


Figure 6.1 Magnet Assembly

The only official copy of this document is the one online in the SharePoint Document Center. Before using a printed copy, verify that it is current by checking the printed document's Revision History log with that of the online version.

Electron-Ion Collider, Brookhaven National Laboratory and Thomas Jefferson National Accelerator Facility			
Doc No. EIC-SHC-TN-24-005	Author: Sandesh Gopinath	Effective Date: 12/05/2024	Review Frequency: NA
Process Description: EIC Design Report MARCO Magnet			Revision: 00

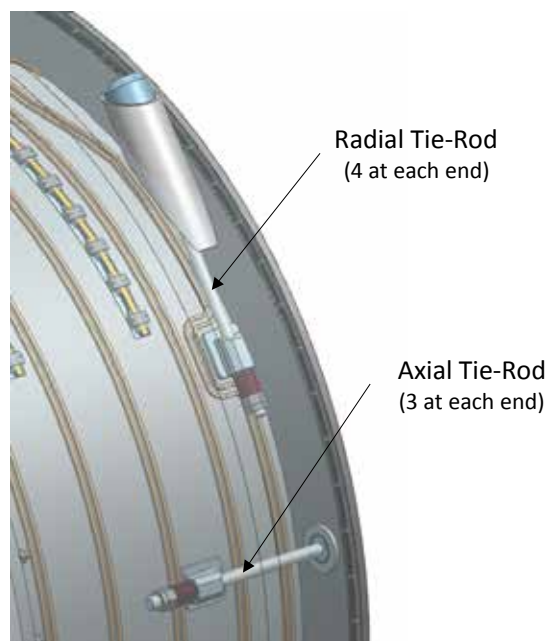


Figure 6.2 Tie rods

The reference drawings of all the sub-components are given in Appendix 5. Please note these are not the manufacturing drawings.

6.2 Magnet Structure

Magnet structure, especially all the vessels and piping, is designed in accordance with the ASME codes.

6.3 Code Requirements

EIC detector magnet shall meet the requirements of Jefferson Lab's ES&H manual, which dictates that pressure system design and construction shall comply with the ASME BPV Code and/or B31 Code for Pressure Piping as applicable. The vacuum system of the EIC detector magnet (Figure 6.3) is a Category 2 system per Jefferson Lab's ES&H Manual, not a pressure vessel system; however, ASME BPV Code shall be used to design and construct the vessels to guarantee safety. The inner vessel of phase separator shall be designed per ASME BPV Code as well. The piping system shall be governed by ASME B31.3.

The governing codes of the magnet are ASME VIII Division 1 and B31.3; the record year of the code is 2023 for Division 1 and 2022 for B31.3. It should be noted that Division 1 uses formulas and material property graphs while Division 2 is formula-based or finite element analysis based. Since Division 2 can be used to design Division 1 vessels, to avoid manually

Electron-Ion Collider, Brookhaven National Laboratory and Thomas Jefferson National Accelerator Facility			
Doc No. EIC-SHC-TN-24-005	Author: Sandesh Gopinath	Effective Date: 12/05/2024	Review Frequency: NA
Process Description: EIC Design Report MARCO Magnet			Revision: 00

reading the graphs of material properties, Division 2 was chosen to design the helium inner vessel, vacuum vessels, but the with the design factors of Division 1.

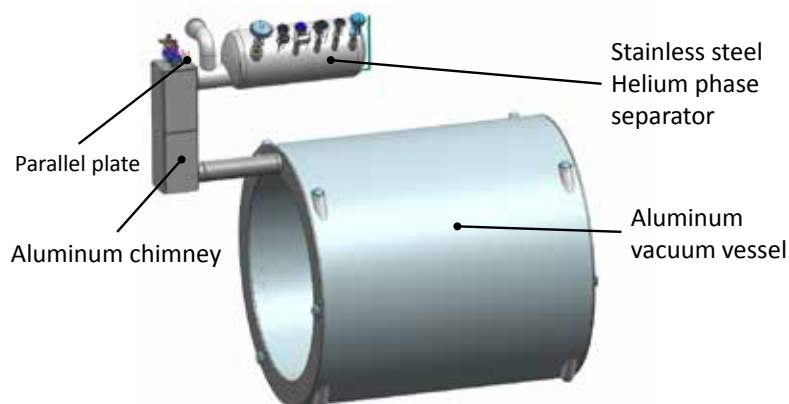


Figure 6.3 Overview of EIC detector magnet

6.3.1 Specifications

The specifications are determined by the cryogenic analysis of the EIC detector magnet. The vacuum system of the magnet has a relief valve—a parallel plate (Figure 6.3) to ensure its internal pressure is less than 0.5 atm (gauge). The set pressure is 3.5 atm (gauge) for the relief valve of the helium circuit and 5 atm (gauge) for the burst disc. In the event of loss of vacuum, the liquid helium may vaporize instantaneously; as a result, the maximum internal pressure of the helium circuit could be larger than 5 atm (gauge). The design pressure of the 4.5 K helium circuit is therefore set at 150 psig ($1.034 \cdot 10^6$, approximately 10 atm gauge). The design temperature of the vacuum system is 295 K and its operating temperature is 295 K also. The design temperature of the 4.5 K helium circuit is 295 K and its operating temperature is 4.5 K.

The design pressure of the thermal shield cooling circuit is 300 psi. The design temperature is 295 K and the operating temperature is 40 K.

6.4 Helium Phase Separator

6.4.1 Inner Vessel

The material is 314L; the nominal thickness of the head and the shell of the inner vessel is 4.0 mm; the minimum thickness is 3.0 mm for the head and 3.5 mm for the shell. Paragraph 4.4.5 of Division 2 was used to compute the maximum allowable external pressure. Paragraph 4.3.6.1 of Division 2 was used computed the internal pressure of the torispherical head; paragraph 4.4.8, the external pressure. Figure 6.4 illustrates that the code is satisfied.

Electron-Ion Collider, Brookhaven National Laboratory and Thomas Jefferson National Accelerator Facility			
Doc No. EIC-SHC-TN-24-005	Author: Sandesh Gopinath	Effective Date: 12/05/2024	Review Frequency: NA
Process Description: EIC Design Report MARCO Magnet			Revision: 00

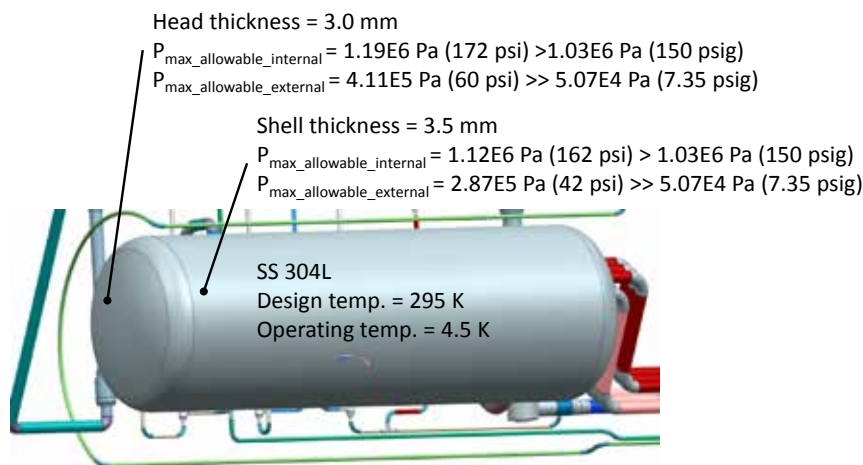


Figure 6.4 Inner vessel of helium phase separator

6.4.2 Outer Vessel

The material is 314L; the nominal thickness of the head and the shell of the inner vessel is 4.0 mm; the minimum thickness is 3.0 mm for the head and 3.5 mm for the shell. Similarly, Paragraphs 4.3.6.1, 4.4.5 and 4.4.8 of Division 2 were employed to corresponding allowable pressures (Figure 6.5). The code is satisfied.

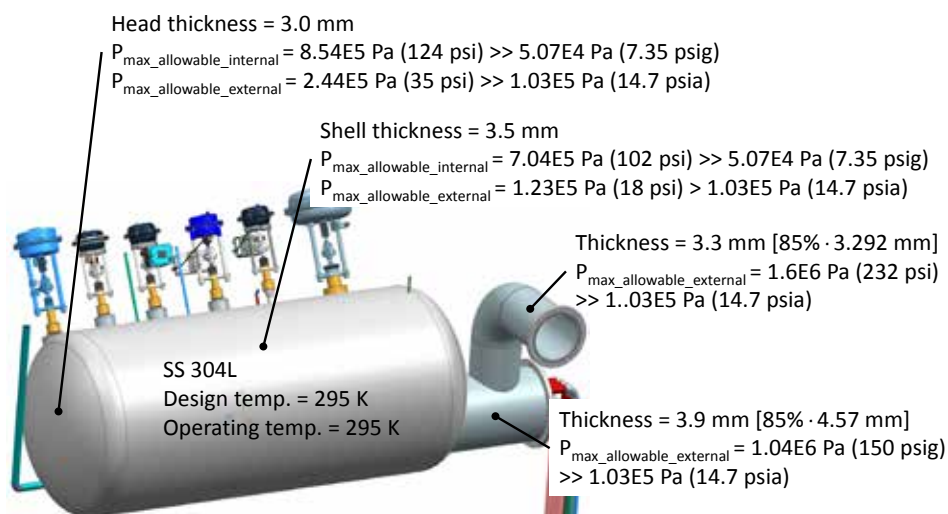


Figure 6.5 Outer vessel of helium phase separator

Electron-Ion Collider, Brookhaven National Laboratory and Thomas Jefferson National Accelerator Facility			
Doc No. EIC-SHC-TN-24-005	Author: Sandesh Gopinath	Effective Date: 12/05/2024	Review Frequency: NA
Process Description: EIC Design Report MARCO Magnet			Revision: 00

6.5 Vacuum Vessel

6.5.1 Overview

The vacuum vessel of the EIC detector magnet is made of Al 6061-T6. The thickness of the inner shell is 14 mm; the outer shell, 25 mm; the end plates, 40 mm. Its maximum allowable internal pressure is 0.5 atm (gauge) (Figure 6.6). The length of the vessel is 3850 mm; the diameter of its outer shell, 3540 mm; the diameter of its inner shell, 2840 mm. The vessel has eight radial supports and six axial supports for the cold mass. The weight of the vessel itself is supported by four pads.

Thickness = 25 mm

$P_{\text{max_allowable_internal}} = 4.67\text{E}5 \text{ Pa (68 psi)} > 5.07\text{E}4 \text{ Pa (7.35 psig)}$

$P_{\text{max_allowable_external}} = 2.74\text{E}5 \text{ Pa (40 psi)} > 1.03\text{E}5 \text{ Pa (14.7 psia)}$

Thickness = 40 mm

Al 6061-T6

Design temp. = 295 K

Operating temp. = 295 K

Thickness = 14 mm

$P_{\text{max_allowable_internal}} = 1.0\text{E}5 \text{ Pa (14.7 psi)} > 5.07\text{E}4 \text{ Pa (7.35 psig)}$

$P_{\text{max_allowable_external}} = 3.2\text{E}5 \text{ Pa (47.0 psi)} > 1.03\text{E}5 \text{ Pa (14.7 psia)}$

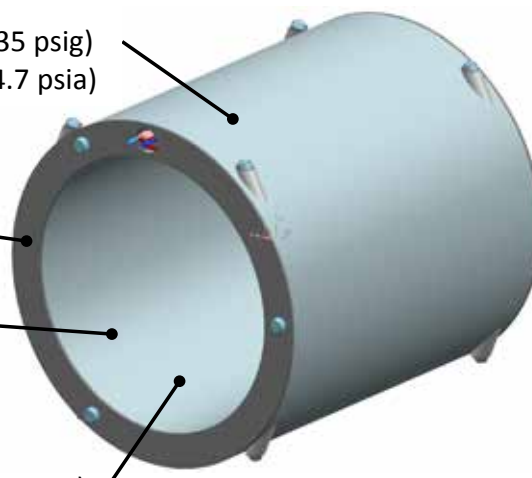


Figure 6.6 Design-by-Rules of vacuum vessel

6.5.2 Design-by-Rules

A parallel plate relief valve on the chimney (Figure 6.3) is used to prevent the vacuum vessel from pressurization exceeding 0.5 atm (7.35 psig). Thus, the maximum allowable internal pressure is 7.35 psig. The maximum external pressure is 14.7 psia. Without considering the gravity, magnetic force, and seismic load, the vacuum vessel can be sized according to atmospheric pressure and design-by-rules of Division 2. Figure 6.6 shows the code is satisfied.

6.5.3 Design-by-Analysis

Since the vacuum vessel has to support the weight of the cold mass of the magnet, load due to cool-down, unbalanced magnetic force, and seismic loads, design-by-rules is inadequate to qualify that the vessel meets the requirements of the code. Therefore, design-by-analysis of Division 2 shall be followed. The governing codes of the magnet is ASME VIII Division 1. Division

Electron-Ion Collider, Brookhaven National Laboratory and Thomas Jefferson National Accelerator Facility			
Doc No. EIC-SHC-TN-24-005	Author: Sandesh Gopinath	Effective Date: 12/05/2024	Review Frequency: NA
Process Description: EIC Design Report MARCO Magnet			Revision: 00

1 can invoke Division 2 to design Division 1 vessels; however, a design factor of 3.5—the design factor of Division 1—must be applied. The design factor of Division 2 is 2.4.

Four rigorous code-prescribed analyses must be conducted: protection against of plastic collapse; protection against local failure; protection against collapse from buckling; protection against failure from cyclic loading.

6.5.4 Protection Against Plastic Collapse

Elastic-Plastic Stress Analysis Method was chosen to evaluate protection against plastic collapse. Paragraph 5.2.4 of Division 2 prescribes the acceptance criteria and lists the assessment procedure. The key characteristics of this method are nonlinear material properties, nonlinear geometric effects, five global load case combinations, one local load case combination, one global load case combination of test, and convergence of nonlinear analysis.

Although seven load case combinations are prescribed according to Table 5.5 of Division 2, only three shall be checked because other four are less severe for the case of the EIC detector magnet. Three required load case combinations are:

- (1) $3.5(P + D)$;
- (2) $3.08(P + D + T) + 3.955L$;
- (3) $3.08(P + D) + 2.485E + 2.485L$

where P = atmospheric pressure (14.7 psi),
 D = dead weight of the vessel and cold mass,
 T = Thermal load due to cool-down of cold mass,
 E = earthquake load,
 L = live magnetic load.

The earthquake load (E) is 0.25g in X, Y, Z directions; $2.485E = 0.621g$ while $g = 9.81 \text{ m/s}^2$.

The elastic-plastic analysis converged for all three load case combinations, which means that the code is satisfied. Figure 6.9 shows the converged solution history and total deformation of the vessel under $3.08(P + D) + 3.955L$.

B: Division 2 Table 5.4 Global 2 $3.08(P+D+T)+3.955L$

global case2 $3.08(P+D+T) + 3.955L$ (B5)

Time: 0.4133 s

Items: 10 of 20 indicated

8/12/2024 11:05 AM

A 3.08P: 45.281 psi

B Pad1 Z=0

C Pad2 Z=0

D Pad3 Z=0

E Pad4 Z=0

F Z1=0

G Z2=0

H Z3=0

I 3.08g: 1189.6 in/s²

J 3.08(D+T) top1: 1.0406e+005 lbf

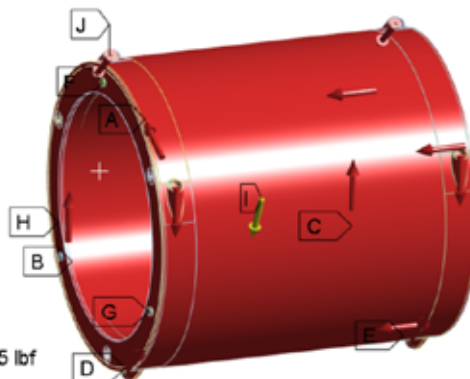


Figure 6.7 Boundary conditions for load case 2

The only official copy of this document is the one online in the SharePoint Document Center. Before using a printed copy, verify that it is current by checking the printed document's Revision History log with that of the online version.

Electron-Ion Collider, Brookhaven National Laboratory and Thomas Jefferson National Accelerator Facility			
Doc No. EIC-SHC-TN-24-005	Author: Sandesh Gopinath	Effective Date: 12/05/2024	Review Frequency: NA
Process Description: EIC Design Report MARCO Magnet			Revision: 00

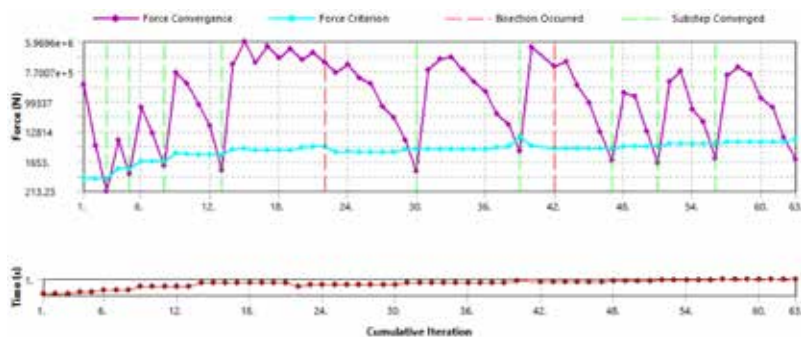


Figure 6.8 Convergence history for combination 2 load case

B: Division 2 Table 5.4 Global 2 3.08(P+D+T)+3.955L

Total Deformation

Type: Total Deformation

Unit: mm

Time: 1 s

Max: 154.29

Min: 0.89336

9/13/2023 8:49 AM

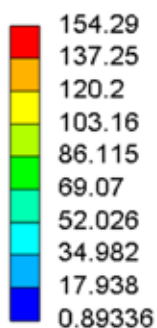


Figure 6.9 Converged solution of load case combination 2

Electron-Ion Collider, Brookhaven National Laboratory and Thomas Jefferson National Accelerator Facility			
Doc No. EIC-SHC-TN-24-005	Author: Sandesh Gopinath	Effective Date: 12/05/2024	Review Frequency: NA
Process Description: EIC Design Report MARCO Magnet			Revision: 00

6.5.5 Protection against Local Failure

Paragraph 5.3.3 of Division 2 was chosen to verify whether the vessel can pass the test of protection against local failure. The forming strain is computed as follows.

$$t := 25 \text{ mm}$$

$$R_f := 1770 \text{ mm} - 0.5 \cdot t = 1757.5 \text{ mm}$$

Table 6.1, 2023 Division 2

$$\varepsilon_{cf} := \frac{50 \cdot t}{100 \cdot R_f} = 0.0071$$

Per Table 5.7 of Division 2, $\theta_{Lu} = 0.271$, $m_2 = 0.271$, $a_{sl} = 2.2$.

$$\frac{\alpha_{sl}}{1 + m_2} = 1.7306$$

θ_L is defined as follows.

$$\varepsilon_L = \varepsilon_{Lu} \cdot \exp \left[- \left(\frac{\alpha_{sl}}{1 + m_2} \right) \left(\left\{ \frac{(\sigma_1 + \sigma_2 + \sigma_3)}{3\sigma_e} \right\} - \frac{1}{3} \right) \right] \quad (5.6)$$

$$\frac{\varepsilon_{peq} + \varepsilon_{cf}}{\varepsilon_L} < 1.0$$

The acceptance criteria are at every point.

F: local strain
local case 1.7(P+D)
Time: 0.4133 s
Items: 10 of 17 indicated
8/12/2024 11:06 AM

- A** 1.7P: 24.99 psi
- B** Pad1 Z=0
- C** Pad2 Z=0
- D** Pad3 Z=0
- E** Pad4 Z=0
- F** Z1=0
- G** Z2=0
- H** Z3=0
- I** 1.7D top1: 19376 lbf
- J** 1.7D top2: 19376 lbf

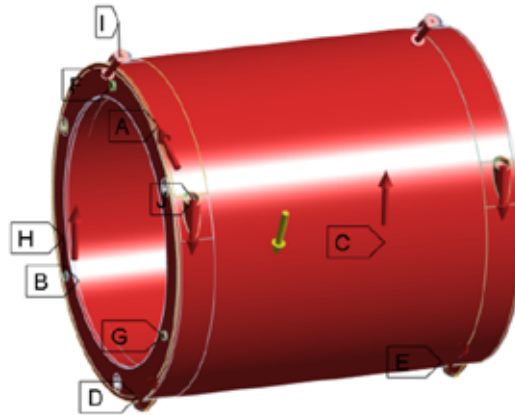


Figure 6.10 Boundary condition for the local failure analysis

Electron-Ion Collider, Brookhaven National Laboratory and Thomas Jefferson National Accelerator Facility			
Doc No. EIC-SHC-TN-24-005	Author: Sandesh Gopinath	Effective Date: 12/05/2024	Review Frequency: NA
Process Description: EIC Design Report MARCO Magnet			Revision: 00

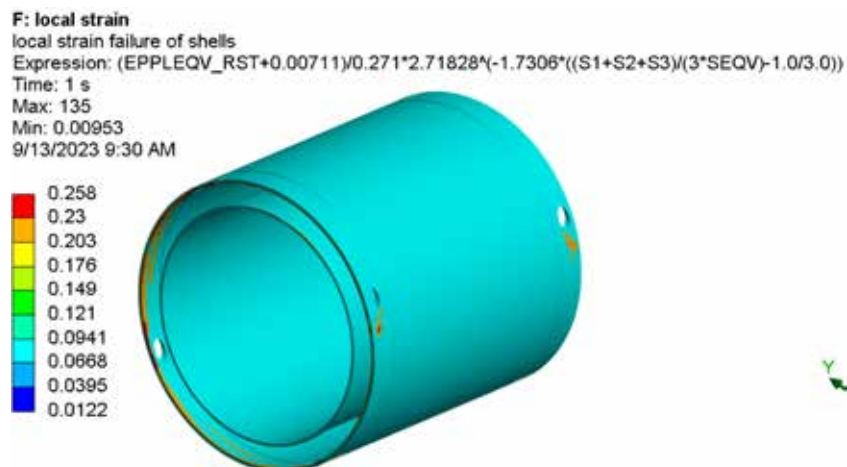


Figure 6.11 FEA local failure analysis of vacuum vessel

Figure 6.11 demonstrate that the maximum value of $(\epsilon_{peq} + \epsilon_{cf})/\epsilon_L$ is 0.258, which is less than 1.0. Therefore, the code requirement of protection against local failure is satisfied.

6.5.6 Protection against Collapse from Buckling

Paragraph 5.4.3 of Division 2 was followed to check buckling. The first step is to perform an eigenvalue buckling analysis (Figure 6.12). The second step is to introduce geometric imperfections to the model by factoring the eigenmode shape from Step 1. The factor was computed based on the tolerance (11.0 mm) defined in Paragraph 4.4.4. The third step is to perform an elastic-plastic analysis with each load combination in Table 5.14 ($\beta_b = 1.67$) and the imperfections from Step 2. If convergence is achieved, the component is stable under the applied loads for this load case.

Five design load cases in Table 5.14 of Division 2 were scrutinized. Among them, only Load Case (1), (2), and (5) are the worst and they would automatically cover other cases. For the Load Case (5), since earthquake could happen in X, Y, and Z direction, three subcases of Load

The only official copy of this document is the one online in the SharePoint Document Center. Before using a printed copy, verify that it is current by checking the printed document's Revision History log with that of the online version.

Electron-Ion Collider, Brookhaven National Laboratory and Thomas Jefferson National Accelerator Facility			
Doc No. EIC-SHC-TN-24-005	Author: Sandesh Gopinath	Effective Date: 12/05/2024	Review Frequency: NA
Process Description: EIC Design Report MARCO Magnet			Revision: 00

Case (5) were analyzed. Convergence was achieved for all of the load cases (Figure 6.14), which means that the code is satisfied.

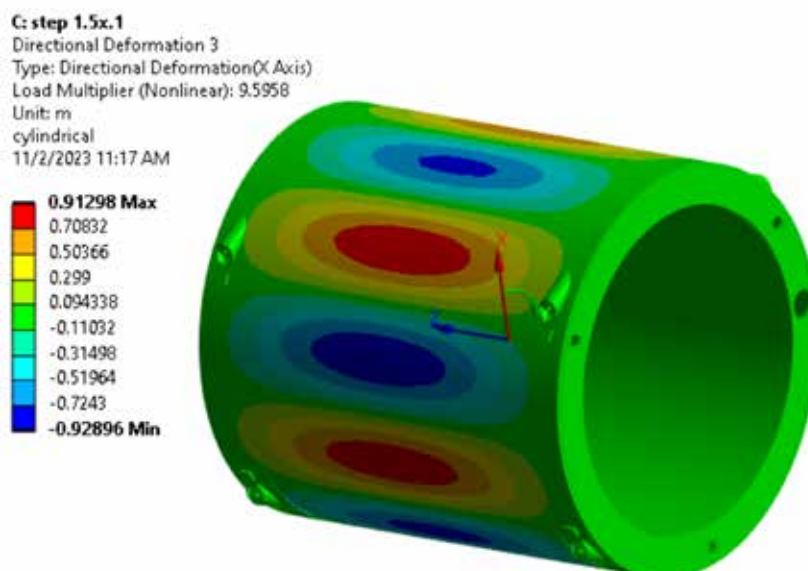


Figure 6.12 Eigenvalue buckling analysis with Load Case (5) $[0.88(P + D) + 0.71Ex + 0.71L]$. The earthquake occurs in the X direction. A factor of 0.0118 is applied to ensure the maximum imperfection is 11 mm



Figure 6.13 Boundary condition for Step 3.5x

Electron-Ion Collider, Brookhaven National Laboratory and Thomas Jefferson National Accelerator Facility			
Doc No. EIC-SHC-TN-24-005	Author: Sandesh Gopinath	Effective Date: 12/05/2024	Review Frequency: NA
Process Description: EIC Design Report MARCO Magnet			Revision: 00

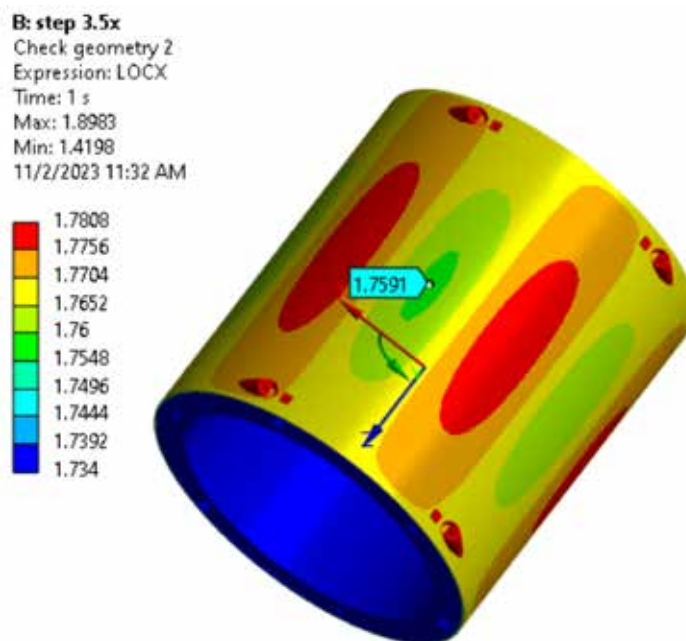


Figure 6.14 Radius (X) of the model in the converged solution in the cylindrical coordinate system. The radius of the outer shell is 1.78 m. Without any loads, the radius should be within 1.759 m to 1.781 m. Since loads were applied, the deformed radius is slightly away from 1.759 m and 1.781 m.

6.5.7 Protection against Failure from cyclic loading

Paragraph 5.5.2.3 of Division 2 is used to screen the magnet. The design life of the EIC detector magnet is 30 years. Each year it is expected to experience 4 times of warming up and cooling down. The expected full-range pressure cycles are $N_{DFP} = 120$; the expected number of operating pressure cycles are $N_{\Delta PO} = 5$; the effective number of changes in metal temperature are $N_{\Delta TE} = 5$; the number of temperature cycles for components involving welds between materials having different coefficients of thermal expansion are $N_{\Delta T\alpha} = 5$. $N_{DFP} + N_{\Delta PO} + N_{\Delta TE} + N_{\Delta T\alpha} = 135 < 350$. According to Table 5.9 of Division 2, a fatigue analysis is not required as part of the vessel design because the vacuum vessel is integral construction with full-penetration welds.

6.6 Cryogenic Chimney

The chimney and its associated components are Al 6061-T6 and 304L; the design and operating temperatures are 295 K. Figure 6.15 shows the code is satisfied. The chimney also meets the requirements of design-by-analysis of Division 2 with a design factor of 3.5—the design factor of Division 1.

Electron-Ion Collider, Brookhaven National Laboratory and Thomas Jefferson National Accelerator Facility			
Doc No. EIC-SHC-TN-24-005	Author: Sandesh Gopinath	Effective Date: 12/05/2024	Review Frequency: NA
Process Description: EIC Design Report MARCO Magnet			Revision: 00

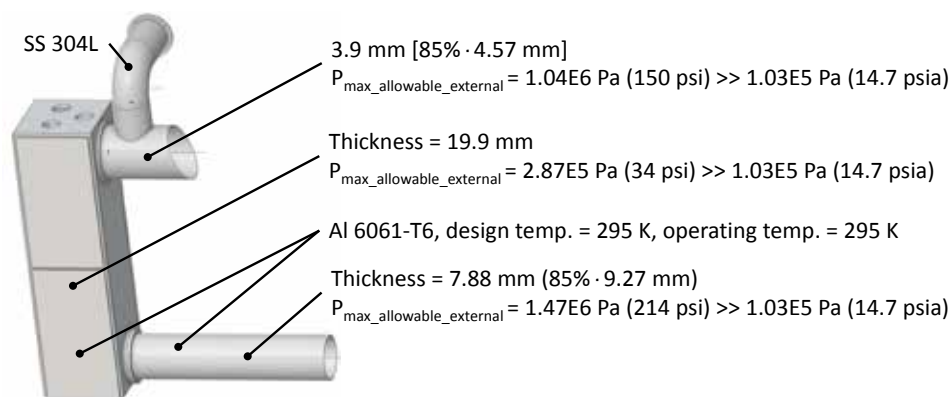


Figure 6.15 Cryogenic Chimney of EIC detector magnet

6.7 Pressure Piping

The piping is governed by ASME B31.3. Once the design is further matured, a detailed code-prescribed analysis using piping analysis software such as AutoPipe shall be performed.

6.8 Manufacturing Requirements

The vacuum system and inner vessel of the helium phase separator shall be constructed in accordance with ASME VIII Division 1. The piping shall be constructed in conformance with B31.3. A stamp is not required for the any pressure or vacuum component of the EIC detector magnet.

ASME-qualified Welding Procedure Specification (WPS) and Procedure Qualification Record (PQR) for 314L are required; the base metal, heat-affected zone and weld metal shall be impact-tested at 77 K per ASME VIII Division 1. Type 316L weld filler metal, or Type 308L filler metal shall be used; weld metal deposited from each heat of Type 316L filler metal shall have a Ferrite Number (FN) not greater than 10, and a weld metal deposited from each heat of Type 308L filler metal shall have a FN in the range of 4 to 14. ASME-qualified WPS and PQR shall be used to fabricate the 316L inner vessel and the stainless steel piping.

The base metal of the inner vessel of the helium phase separator shall be impact-tested at 77 K per ASME VIII Division 1.

ASME-qualified WPS and PQR for aluminum shall be used to fabricate the outer vacuum vessel and the cryogenic chimney.

6.9 Summary

The 4.5 K helium circuit, thermal shield cooling circuit, and vacuum system of the EIC detector magnet are designed and constructed in accordance with ASME codes. All the vessels need to be either ASME stamped or verified with the JLab Pressure Vessel Design Authority.

Electron-Ion Collider, Brookhaven National Laboratory and Thomas Jefferson National Accelerator Facility			
Doc No. EIC-SHC-TN-24-005	Author: Sandesh Gopinath	Effective Date: 12/05/2024	Review Frequency: NA
Process Description: EIC Design Report MARCO Magnet			Revision: 00

7 Cooling Scheme and Heat Loads

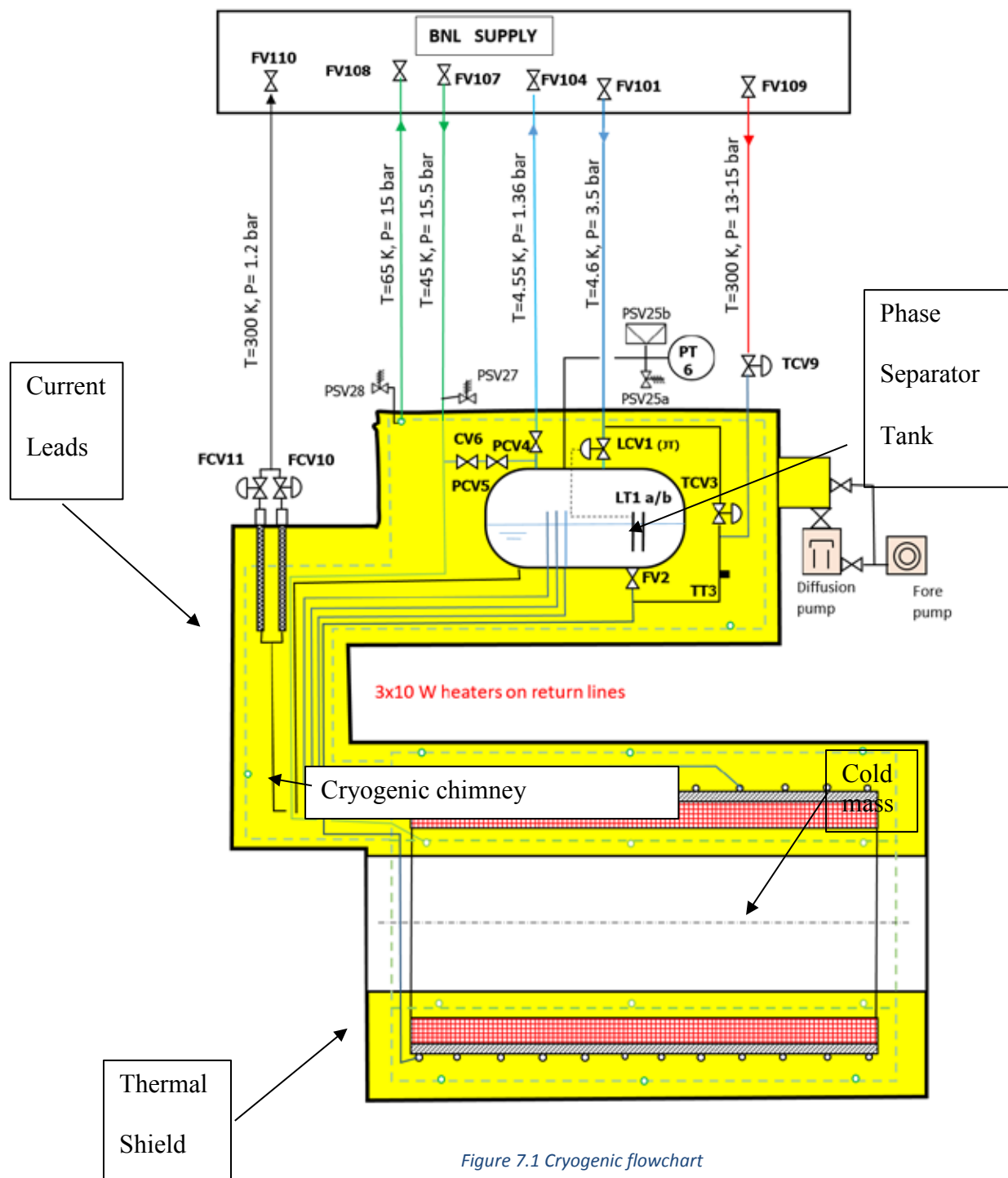


Figure 7.1 Cryogenic flowchart

Electron-Ion Collider, Brookhaven National Laboratory and Thomas Jefferson National Accelerator Facility			
Doc No. EIC-SHC-TN-24-005	Author: Sandesh Gopinath	Effective Date: 12/05/2024	Review Frequency: NA
Process Description: EIC Design Report MARCO Magnet			Revision: 00

The MARCO magnet is a conduction-cooled magnet and is indirectly cooled using the cooling tubes on the outside of the brass mandrel. Detail simulations were done to calculate the size of the tube, number of tubes, spacing of tubes. Figure 7.1 shows the cryogenic flow chart. The internal cryogenic system of the Marco solenoid for EIC experiment involves a cold mass, which consists of a mandrel and coils with two 28-tube exchangers of the thermosiphon soldered on the mandrel, a phase separator on top used also as a storage tank of liquid helium at 4.55 K, and one cryogenic chimney that holds the helium vapor cooled current leads and connect the phase separator to the cold mass. The Marco solenoid is equipped with 5 cold valves with warm actuators and 3 warm valves (Table 7.1). It also has a thermal shield to insulate the parts at 4.5 K; the thermal shield is cooled by helium gas between 45 K and 65 K.

The internal cryogenic system is connected to the BNL refrigeration supply through flexible lines.

Table 7.1 List of valves

Name	Description
FV101	BNL supercritical helium shut-off valve
FV104	BNL vapor helium shut-off valve
FV107	BNL inlet helium for thermal shield shut-off valve
FV108	BNL outlet helium for thermal shield shut-off valve
FV109	BNL inlet warm helium for cool-down shut-off valve
FCV110	BNL outlet helium for current leads shut-off valve
PSV27	Inlet helium for thermal shield safety valve
PSV28	Outlet helium for thermal shield safety valve
PSV25a	Relief valve for the phase separator tank at 4.5 bar abs. (quench)
PSV25b	Burst disc for the phase separator tank at 6 bar abs. (vacuum loss)
PT6	Pressure measurement of the phase separator tank
FCV10	Flow control valve for current lead a
FCV11	Flow control valve for current lead b
TCV9	Warm temperature control valve for cool-down
TCV3	Cold temperature control valve for cool-down
TT3	Temperature of the mixed gas coming from TCV3 and TCV9 for the cool-down
FV2	Feeding shut-off valve of the thermosiphon
PCV4	Vapor helium pressure control valve

The only official copy of this document is the one online in the SharePoint Document Center. Before using a printed copy, verify that it is current by checking the printed document's Revision History log with that of the online version.

Electron-Ion Collider, Brookhaven National Laboratory and Thomas Jefferson National Accelerator Facility			
Doc No. EIC-SHC-TN-24-005	Author: Sandesh Gopinath	Effective Date: 12/05/2024	Review Frequency: NA
Process Description: EIC Design Report MARCO Magnet			Revision: 00

PCV5	Bypass pressure control valve for vapor helium into the shield when refrigerator shut-off
LCV1	Level control valve for the liquid helium in the tank (Joule Thomson valve)
LT1a/b	Liquid helium measurement in the tank with spare

7.1 Cryogenic processes

This section describes the details of various operation scenarios.

7.1.1 Cool-down Process

The warm helium at 300 K and cold helium at 50 K from BNL supply are mixed to cool the solenoid down or warm it up. This is done by controlling the temperature difference ($T_{\text{coil}} - TT3$)— T_{coil} is the average temperature of the coils while $TT3$ is the temperature of the mixed gas from the valves TCV9 and TCV3. The total mass flow rate is 10 g/s. The mixed cold flow goes down to the thermosiphon tubes exchanger (valve FV2 is closed) and returns to phase separator tank before going back to BNL supply through valve FV4. The thermal shield is cooled at the same speed as the cold mass. Figure 7.2 shows the process flow chart.

Electron-Ion Collider, Brookhaven National Laboratory and Thomas Jefferson National Accelerator Facility			
Doc No. EIC-SHC-TN-24-005	Author: Sandesh Gopinath	Effective Date: 12/05/2024	Review Frequency: NA
Process Description: EIC Design Report MARCO Magnet			Revision: 00

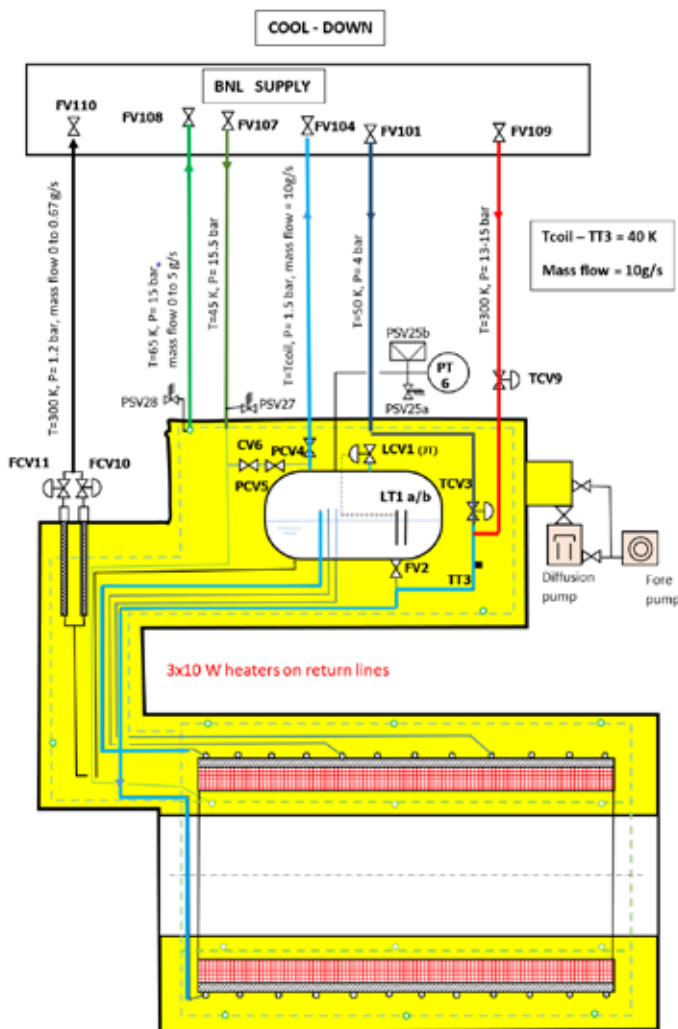


Figure 7.2 Cool-down process flowchart

7.1.2 Thermosiphon

The valve LCV1 (a JT valve) converts 3.5 bar (all pressures are absolute in the report) and 4.6 K supercritical helium into 1.36 bar and 4.55 K liquid helium. The production rate of the JT valve is 98%. The phase separator tank is the container of liquid helium, which passes through the valve FV2 and down in one supply line to the thermosiphon exchanger. The two-phase flow returns to the phase separator tank while the gas helium returns to its source at BNL through valve FV4 at a pressure of 1.36 bar. All pressures are absolute pressures in this report. Figure 7.3 illustrates the thermosiphon process.

Electron-Ion Collider, Brookhaven National Laboratory and Thomas Jefferson National Accelerator Facility			
Doc No. EIC-SHC-TN-24-005	Author: Sandesh Gopinath	Effective Date: 12/05/2024	Review Frequency: NA
Process Description: EIC Design Report MARCO Magnet			Revision: 00

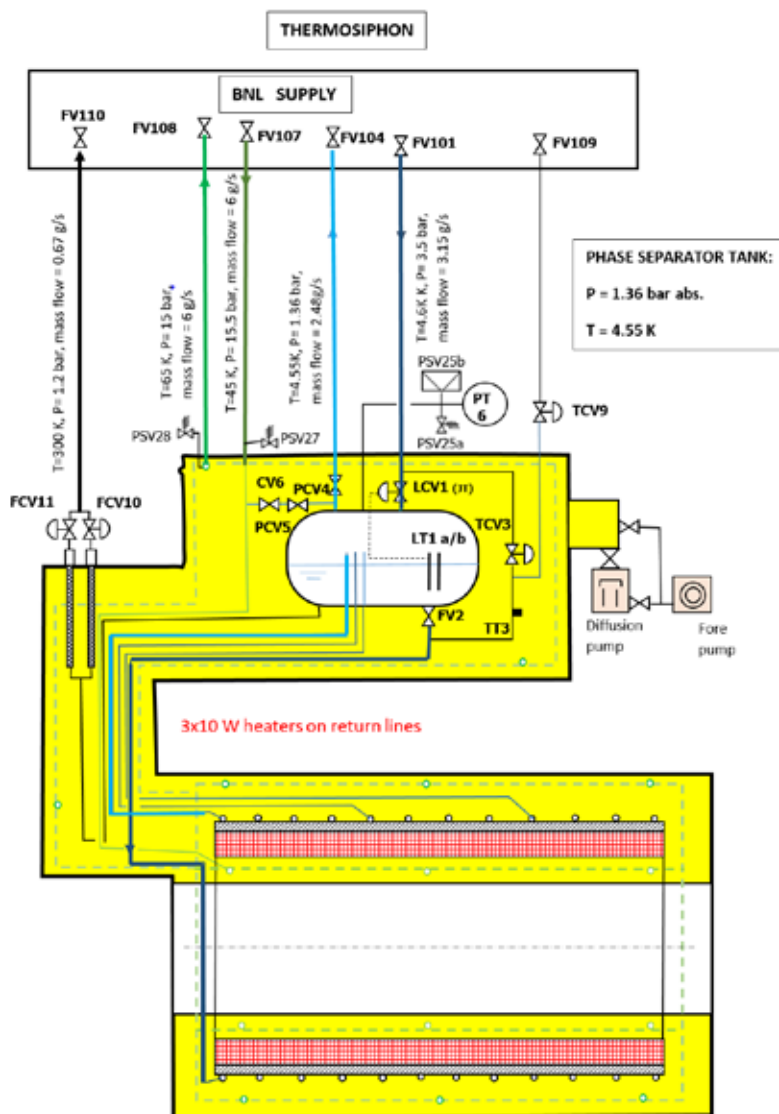


Figure 7.3 Thermosiphon process flowchart

7.1.3 Long Shut-down

There is only one helium mass flow of 5 supplied by BNL at an inlet temperature of 80 K through valve TCV3. The outlet temperature is 100 K. During long shut down, the magnet will not be warmed up to the room temperature. The intention is to maintain the coil temperature below 100K. Figure 7.4 shows the shutdown process flow chart.

Electron-Ion Collider, Brookhaven National Laboratory and Thomas Jefferson National Accelerator Facility			
Doc No. EIC-SHC-TN-24-005	Author: Sandesh Gopinath	Effective Date: 12/05/2024	Review Frequency: NA
Process Description: EIC Design Report MARCO Magnet			Revision: 00

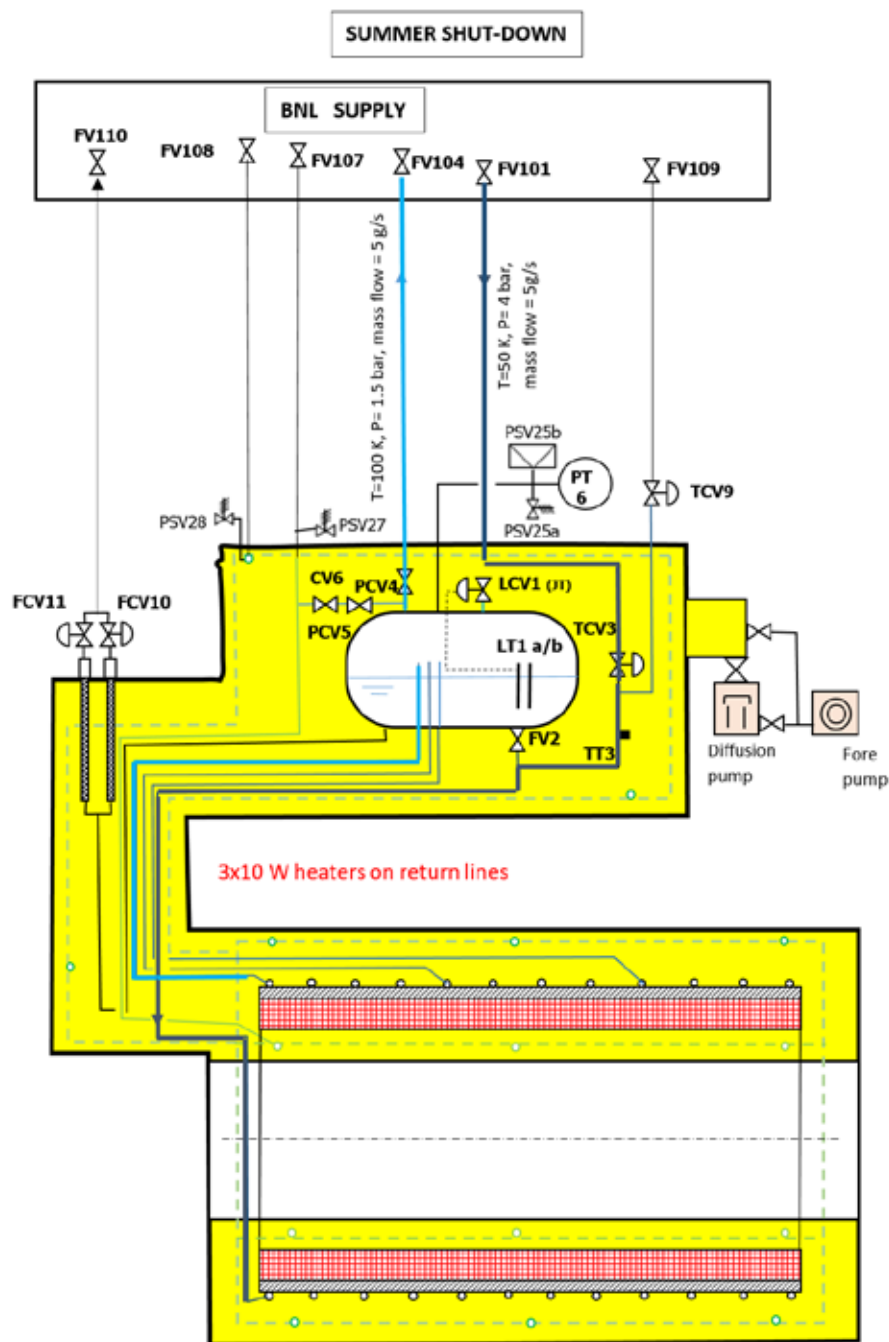


Figure 7.4 Summer (Long) shut-down process flowchart

Electron-Ion Collider, Brookhaven National Laboratory and Thomas Jefferson National Accelerator Facility			
Doc No. EIC-SHC-TN-24-005	Author: Sandesh Gopinath	Effective Date: 12/05/2024	Review Frequency: NA
Process Description: EIC Design Report MARCO Magnet			Revision: 00

7.1.4 Refrigerator Shut-down

If the BNL supply refrigerator stops working, there would be no helium supply to the shield or the phase separator tank. The magnet current must be ramped down in 1.25 hour (1 A/s) using the 110-liter volume of liquid helium stored in the phase separator tank. This quantity of liquid helium would provide the flow necessary for both the thermosiphon and the current leads. The gas helium out of the phase separator tank is used to cool the thermal shield. Two flows have to be taken into account by BNL supply of the mass flow of the current leads ($T = 300$ K, $P = 1.2$ bar, flow rate = 0.67 g/s) and the flow going out of the shield ($T = 45$ K, $P = 1.2$ bar, flow rate = 2.48 g/s). Figure 7.5 shows the flowchart during the refrigerator shutdown.

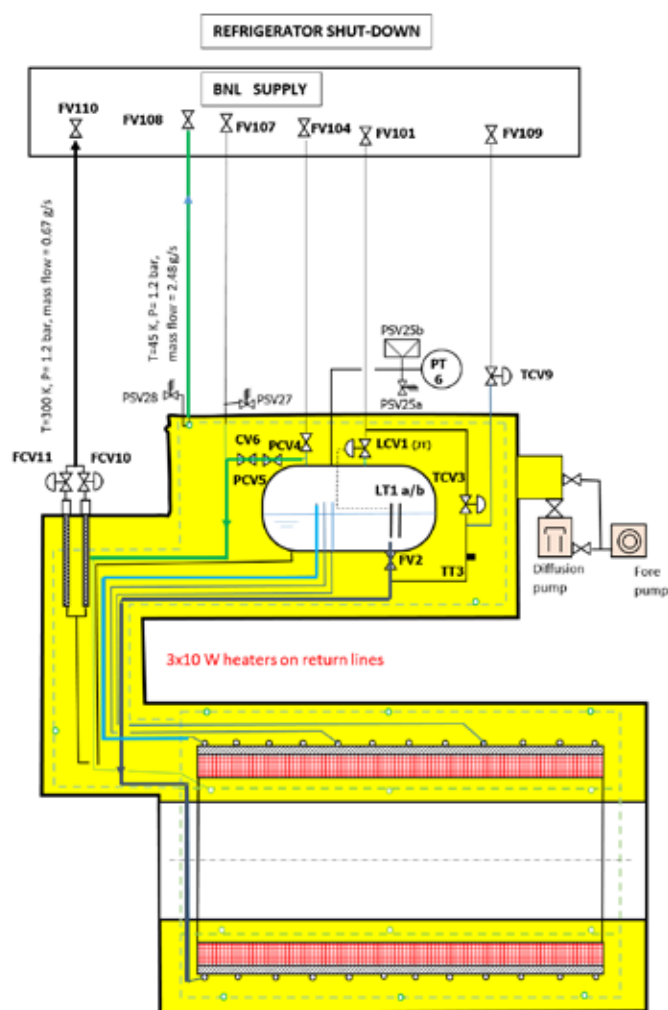


Figure 7.5 Refrigerator shut-down process flowchart

Electron-Ion Collider, Brookhaven National Laboratory and Thomas Jefferson National Accelerator Facility			
Doc No. EIC-SHC-TN-24-005	Author: Sandesh Gopinath	Effective Date: 12/05/2024	Review Frequency: NA
Process Description: EIC Design Report MARCO Magnet			Revision: 00

7.1.5 Quench

During the quench all valves are closed. The pressure rises to 4.5 bar in the phase separator tank and the relief valve PSV25a opens. The maximum mass flow rate is 2.06 kg/s of gas helium. Figure 7.6 shows the process flow chart during quench.

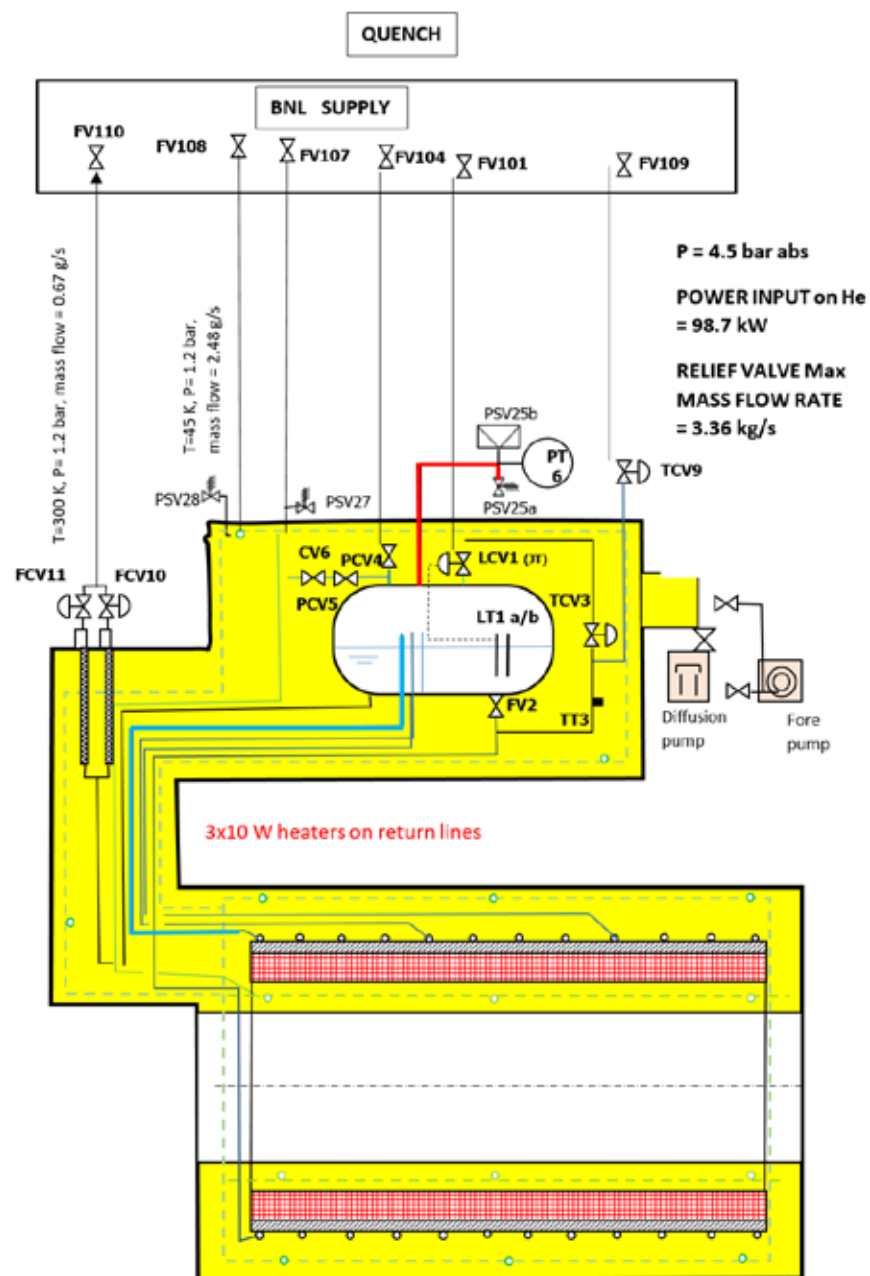


Figure 7.6 Quench process flowchart

Electron-Ion Collider, Brookhaven National Laboratory and Thomas Jefferson National Accelerator Facility			
Doc No. EIC-SHC-TN-24-005	Author: Sandesh Gopinath	Effective Date: 12/05/2024	Review Frequency: NA
Process Description: EIC Design Report MARCO Magnet			Revision: 00

7.1.6 Vacuum Loss

During a vacuum loss all valves are closed. The pressure rises to 6 bar and the burst disc PSV25b opens. The maximum mass flow rate is 3.36 kg/s of gas helium. Figure 7.7 shows the process flow chart during vacuum loss incident.

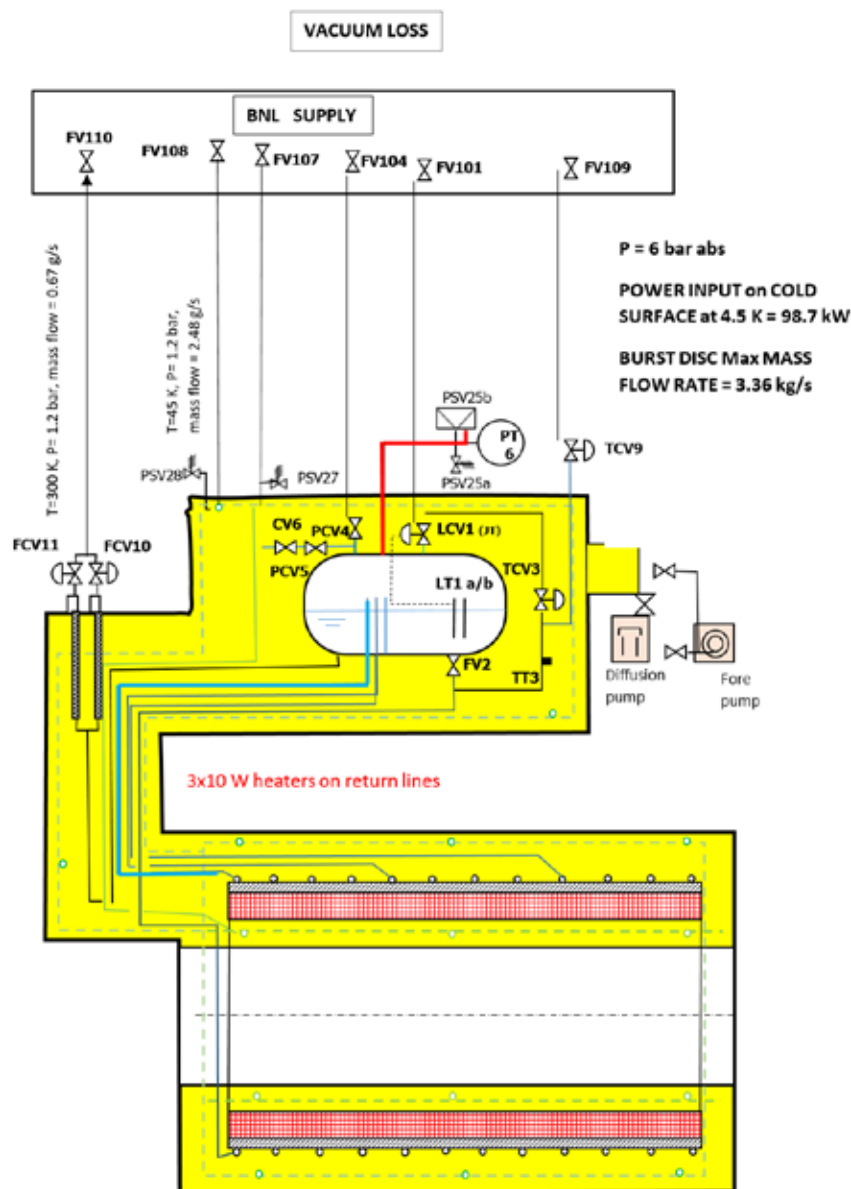


Figure 7.7 Vacuum loss process flowchart

Electron-Ion Collider, Brookhaven National Laboratory and Thomas Jefferson National Accelerator Facility			
Doc No. EIC-SHC-TN-24-005	Author: Sandesh Gopinath	Effective Date: 12/05/2024	Review Frequency: NA
Process Description: EIC Design Report MARCO Magnet			Revision: 00

7.2 Heat Loads

The cryogenic heat loads are calculated for all the components of the cryogenic system.

7.2.1 Conduction Heat Loads

The cryogenic circuit experiences conduction heat loads from a variety of components. This section provides a detailed list of those sources.

7.2.1.1 Heat Loads

Eight radial and six axial titanium tie-rods are used to support the cold mass of the magnet. Table 7.2 lists the heat load and the dimensions of the tie rods.

Table 7.2 Cold mass tie rod conduction

	Unit	Radial tie-rod	Axial tie-rod
Quantity		8	6
Diameter	mm	38	38
Cross section	m ²	$1.13 \cdot 10^{-3}$	$1.13 \cdot 10^{-3}$
Total length	mm	913.27	645.8
Length (4.5 K-65 K)	mm	608.85	430.5
Length (65 K-300 K)	mm	304.42	215.3
K _{integral} (4.5 K-65 K)	W/m	121	121
K _{integral} (65 K-300 K)	W/m	1300	1300
Heat load at 4.5 K	W	0.22	0.32
Heat load at 65 K	W	4.8	6.8

The total heat load for the tie-rods at 4.5 K is 3.68 W.

The total heat load for the tie-rods at 65 K is 79.2 W.

7.2.1.2 Heat Loads from Phase Separator Tank to Tie-rods

The phase separator tank (inner vessel) is sustained by 8 radial stainless steel tie-rods. Their thermal characteristics are listed in Table 7.3.

Table 7.3 Phase separator tie rod conduction

	Unit	Data
Quantity		8
Diameter	mm	6
Cross section	m ²	$28.26 \cdot 10^{-6}$
Length (4.5 K-65 K)	mm	100
Length (65 K-300 K)	mm	50
K _{integral} (4.5 K-65 K)	W/m	233

The only official copy of this document is the one online in the SharePoint Document Center. Before using a printed copy, verify that it is current by checking the printed document's Revision History log with that of the online version.

Electron-Ion Collider, Brookhaven National Laboratory and Thomas Jefferson National Accelerator Facility			
Doc No. EIC-SHC-TN-24-005	Author: Sandesh Gopinath	Effective Date: 12/05/2024	Review Frequency: NA
Process Description: EIC Design Report MARCO Magnet			Revision: 00

K_{integral} (65 K-300 K)	W/m	2840
Heat load at 4.5 K	W	0.06
Heat load at 65 K	W	1.6

The total heat load for the tie-rods of the phase separator tank at 4.5 K is 0.48 W.

The total heat load for the tie-rods of the phase separator tank at 65 K is 12.8 W.

7.2.1.3 Heat Load from Cold Valves

The cold valves of the phase separator have warm actuators and thus link 300 K to 4.5 K. Their heat loads are listed in the Table 7.4 according to WEKA company data.

Table 7.4 Cold valve heat conduction

Name	Size	Heat load at 65 K (W)	Heat load at 4.5 K (W)
LCV1	DN4	0	0.31
FV2	DN40	10	3
TCV3	DN8	0	0.36
PCV4	DN25	5	1.4
PCV5	DN6	0	0.31

7.2.1.4 Heat Load from Bellows

A stainless steel bellows (HYDRA from WITZENMANN with inner diameter: 42 mm, outer diameter: 60 mm, PN: 22 bar, and thickness: 0.2 mm) connects the phase separator tank to its vacuum chamber and then to the piping of the relief valve PSV25a and of the burst disc PSV25b (Figure 7.8). The heat loads are shown in Table 7.5.

Electron-Ion Collider, Brookhaven National Laboratory and Thomas Jefferson National Accelerator Facility			
Doc No. EIC-SHC-TN-24-005	Author: Sandesh Gopinath	Effective Date: 12/05/2024	Review Frequency: NA
Process Description: EIC Design Report MARCO Magnet			Revision: 00

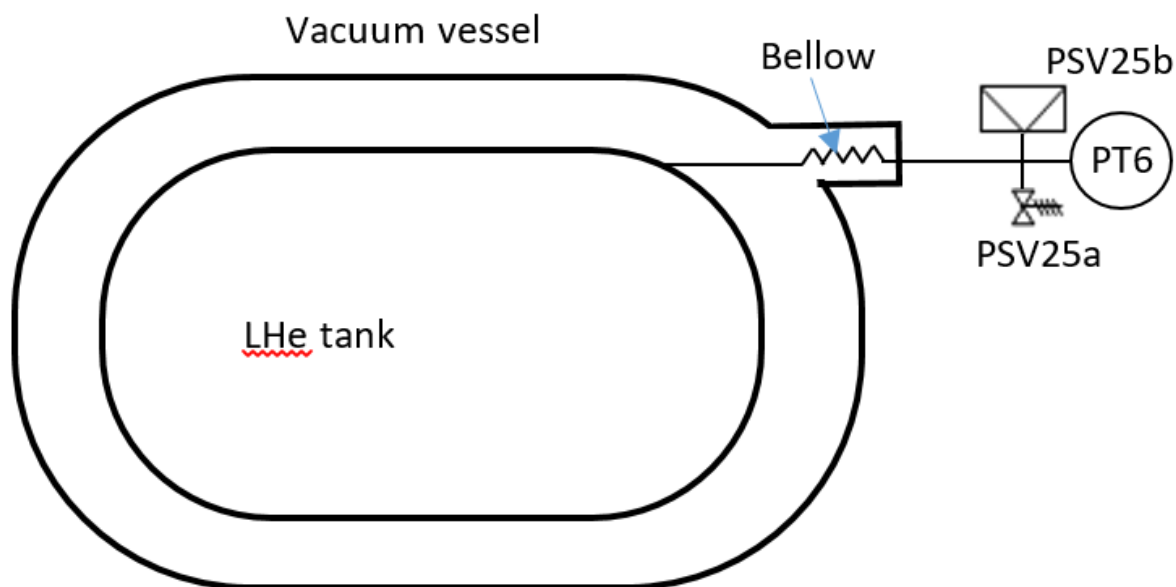


Figure 7.8 Bellow for the pressure relief valve and the burst disc

Table 7.5 Heat load from the bellows

Corrugation step (mm)	5.25
Corrugation quantity	25
Free length (mm)	131.25
Corrugation length (mm)	20
Developed length (4.5 K-300 K) [mm]	500
Cross section (m ²)	32 · 10 ⁻⁶
K _{integral} (4.5 K-300 K) [W/m]	3000
Heat load at 4.5 K (W)	0.19

7.2.1.5 Heat load from Flexible Lines

The provisional heat load budget for the flexible lines is 2 W at 4.5 K. It will be calculated once the final design is complete.

7.2.1.6 Heat load from Supports of Thermal Shield

There are 96 G10 supports for the thermal shield, 4 for each of the 24 panels. Each support has a heat load of 0.33 W at 55 K

Table 7.6). The total heat load on the thermal shield due to its supports is 32 W.

Electron-Ion Collider, Brookhaven National Laboratory and Thomas Jefferson National Accelerator Facility			
Doc No. EIC-SHC-TN-24-005	Author: Sandesh Gopinath	Effective Date: 12/05/2024	Review Frequency: NA
Process Description: EIC Design Report MARCO Magnet			Revision: 00

Table 7.6 Heat load from the thermal shield supports

Quantity	Length	Cross section	K_{integral} (55 K-300 K)	Heat load at 55 K
96	75 mm	$1.6 \cdot 10^{-4} \text{ m}^2$	156 W/m	0.33 W

7.2.2 Heat Load from Thermal Radiation

To protect the cold mass from the thermal radiation, a thermal shield is placed between the vacuum vessel and the 4.5 K surfaces. It is cooled by a gas helium flow between 45 K and 65 K. All 4.5 K surfaces are wrapped in superinsulation, also called Multi-Layer Insulation (MLI), consisting of a blanket of 10 layers. The thermal shield itself is covered by 30 layers of MLI. The thermal radiation load on the cold mass and the chimney is listed in Table 7.7.

Table 7.7 Radiation heat loads at 4.5 K

	Radiation flux	Surface area	Heat load
Thermal radiation on cold mass at 4.5 K	0.3 W/m ²	70 m ²	21 W
Thermal radiation on cryogenic chimney and phase separator tank at 4.5 K	0.3 W/m ²	7 m ²	2.1 W

The total heat load due to thermal radiation on the 4.5 K surfaces is 23.1 W. The total head load on the thermal shield is shown in Table 7.8.

Table 7.8 Radiation heat load on the thermal shield between 45 K and 65 K

	Radiation flux	Surface area	Heat load
Thermal radiation on Thermal shield	5 W/m ²	84 m ²	420 W

7.2.3 Heat Load from Electrical Junctions

Twenty electrical junctions inside the coil and to the current leads are considered. Each has an electrical resistance of 1.0 nΩ. For a current of 4000 A, the heat load is 0.32 W. This heat load is deposited in the liquid helium.

Electron-Ion Collider, Brookhaven National Laboratory and Thomas Jefferson National Accelerator Facility			
Doc No. EIC-SHC-TN-24-005	Author: Sandesh Gopinath	Effective Date: 12/05/2024	Review Frequency: NA
Process Description: EIC Design Report MARCO Magnet			Revision: 00

7.2.4 Heat Load from Eddy Current and Hysteresis of Conductor

When ramping up or down the current (1 A/s), there exist heat loads due to hysteresis in NbTi filaments and eddy current in copper. For the MARCO cable that is composed of 20 strands, each with a diameter of 0.842 mm, containing 468 filaments of $\varnothing 26 \mu\text{m}$ each, at a current of 1 A/s, the total heat load of the entire magnet due to hysteresis and eddy current is approximately 1.0 W.

- Hysteresis in the NbTi filaments: 0.8 W
- Eddy current in the strand copper: 0.2 W
- Eddy current in the channel copper and coupling between channel and cable are negligible.

7.2.5 Heat load from Eddy Current in the Mandrel

During the ramping up or down of the current at 1 A/s, eddy current occurs in the brass mandrel. The current in the mandrel and power dissipated in it are illustrated in Figure 7.9. The asymptotic power dissipated in the mandrel is 3.7 W.

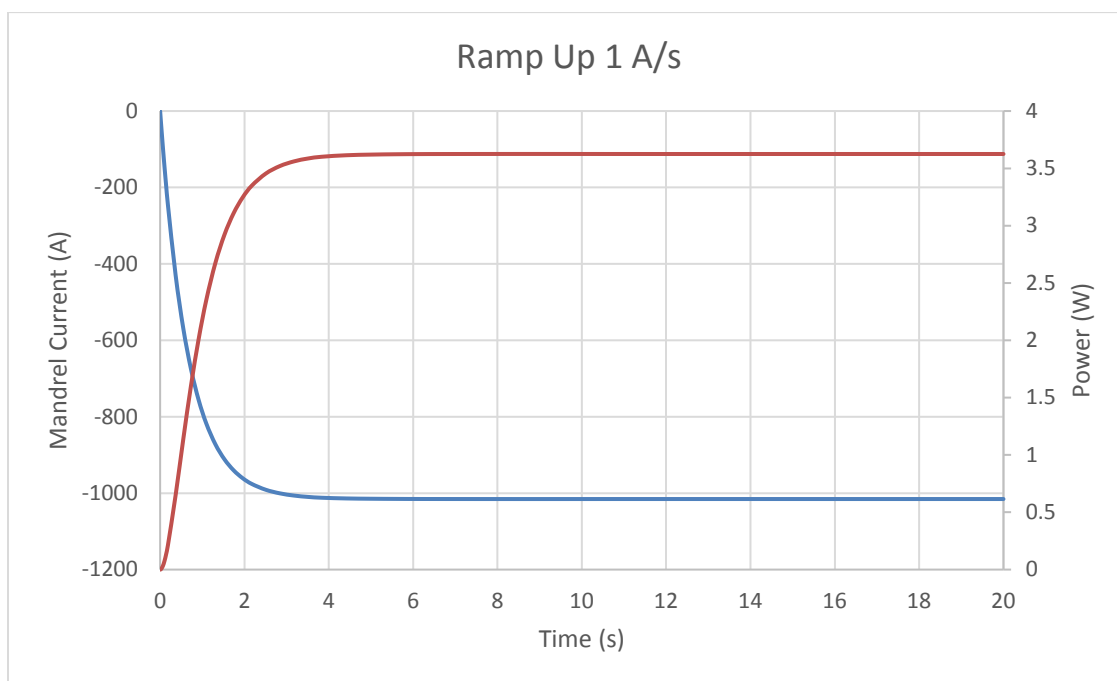


Figure 7.9 Eddy current power in the mandrel

Electron-Ion Collider, Brookhaven National Laboratory and Thomas Jefferson National Accelerator Facility			
Doc No. EIC-SHC-TN-24-005	Author: Sandesh Gopinath	Effective Date: 12/05/2024	Review Frequency: NA
Process Description: EIC Design Report MARCO Magnet			Revision: 00

7.2.6 Heat Load from Current Leads

The two current leads are helium-vapor cooled. They are assumed to be AMI (American Magnetics Inc.) type L-5000 or similar. The liquid helium consumption of a pair is 16 L/h (9.6 W) according to AMI. If a margin of 4 L/h is considered, the total liquid helium consumption is 20 L/h, equivalent to 12 W.

7.2.7 Total Heat Load Budget

The heat load budgets at 4.5 K are outlined as follows.

- Cold mass at zero current: 25 W
- Cold mass at ramping up current (1 A/s): 30 W
- Phase separator tank: 10.2 W
- Current leads: 12 W
- Margin: 5 W

The maximum heat load (when ramping up the current) at 4.5 K is 57 W.

The following are the heat load budgets on thermal shield at 45 K – 65 K.

- Thermal radiation: 420 W
- Support conduction: 32 W
- Thermal intercepts: 107 W
- Margin: 61 W

The total heat load budget on the thermal shield is 600 W.

7.3 Thermosiphon

The solenoid is cooled by two-phase flow helium thermosiphon. Twenty-eight exchanger tubes (2 · 5 tubes for module 1, 2 · 4 tubes for module 2, 2 · 5 tubes for module 3) are soldered on the brass mandrel. Liquid helium is stored in the phase separator tank and flows through valve FV2 down in the downward branch to supply 6 distributors (bottom manifolds). This flow of helium is heated up in the exchanger tubes, collected by 6 collectors (top manifolds), and goes back to the tank through 3 return lines. Three heaters (10 W maximum each) are placed on the return lines in case that there is not sufficient heat load on the cold mass. Figure 7.10 shows the piping layout of thermosiphon.

Electron-Ion Collider, Brookhaven National Laboratory and Thomas Jefferson National Accelerator Facility			
Doc No. EIC-SHC-TN-24-005	Author: Sandesh Gopinath	Effective Date: 12/05/2024	Review Frequency: NA
Process Description: EIC Design Report MARCO Magnet			Revision: 00

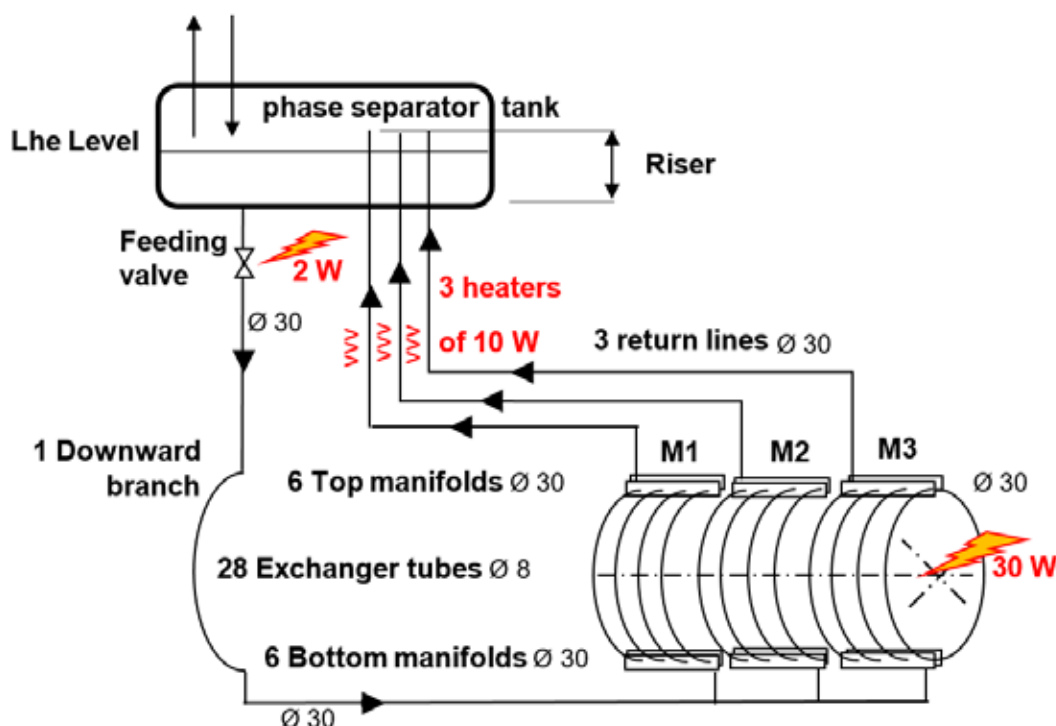


Figure 7.10 Piping for thermosiphon

The equations of the two-phase flow are for the homogeneous model [20], [21] which is relevant for a helium vapor quality less than 10 % [22], [23], [24], [25]. The two-phase mixture is considered as a single fluid, velocities of vapor and fluid are supposed to be equal.

LIST of SYMBOLS

V_v	vapor phase velocity	m/s
V_l	liquid phase velocity	m/s
ρ	Mean density of the two-phase flow	kg/m ³
ρ_l	Density of the liquid phase	kg/m ³
ρ_v	Density of the vapor phase	kg/m ³
x	Vapor quality	-
μ	Mean viscosity of the two-phase flow	Pa.s
μ_l	Viscosity of the liquid phase	Pa.s
μ_v	Viscosity of the vapor phase	Pa.s
\dot{m}	Two-phase massflow	kg/s

The only official copy of this document is the one online in the SharePoint Document Center. Before using a printed copy, verify that it is current by checking the printed document's Revision History log with that of the online version.

Electron-Ion Collider, Brookhaven National Laboratory and Thomas Jefferson National Accelerator Facility			
Doc No. EIC-SHC-TN-24-005	Author: Sandesh Gopinath	Effective Date: 12/05/2024	Review Frequency: NA
Process Description: EIC Design Report MARCO Magnet			Revision: 00

\dot{m}_v	Vapor phase massflow	kg/s
p_o	Outlet pressure of a circuit element	Pa
p_i	Inlet pressure of a circuit element	Pa
$D \text{ } r_{gz}$	Differential gravity pressure between outlet and inlet	Pa
DP_{frot}	Friction pressure drop between inlet and outlet	Pa
DP_{sing}	Singularities pressure drop (elbow, angle, valve...)	Pa
DP_{acc}	Density acceleration pressure drop	Pa
$D \text{ } r$	Density variation in a circuit element	kg/m ³
l	Friction pressure drop coefficient	-
L	Length of the circuit element	m
D	Inner diameter of the circuit element	m
A	Cross-sectional area of the circuit element	m ²
z	Singularity pressure drop coefficient	-
Sz	Sum of the coefficients of the singularities	-
$D \text{ } h_{io}$	Enthalpy variation between inlet and outlet	J/kg
h_o	Outlet enthalpy oh two phase flow	J/kg
h_i	Inlet enthalpy oh two phase flow	J/kg
Q	Heat load on the circuit element	W
C_p	Enthalpy coefficient	J/kg.K
DT_{io}	Temperature difference between outlet and inlet	K
Dx	Vapor quality variation between outlet and inlet-	
Dh_{lv}	Latent heat of vaporization in the circuit element	J/kg
Re	Reynolds number	-
p_o	Outlet pressure in a circuit element	Pa
x_o	Outlet vapor quality in a circuit element	-
h_o	Outlet enthalpy in a circuit element	J/kg
h_{lsat}	Saturation enthalpy of liquid at p_o	J/kg
Speed of vapor = speed of liquid		$V_v = V_l$
Mean density		$1/r = (1-x)/r_l + x/r_v$
Mean viscosity(Arbitrary equation)		$m = (1-x) m_l + x m_v$

The tubes in parallel are assumed to have the same heat loads and the same mass flows.

The circuit between the inlet section and the outlet section can be described as one dimensional. One can write equations in steady state.

- (0) $\dot{m} = \text{constant}$ and $\dot{m}_v / \dot{m} = x$ *Mass flow and quality*
- (1) $1/r = (1-x)/r_l + x/r_v$ **(homogeneous model)** *Mean density*
- (2) $p_o - p_i = D \text{ } r_{gz} - DP_{frot} - DP_{sing} - DP_{acc}$ *momentum*
- (3) $DP_{fr} = (l L/D) (\dot{m}^2 / (2r A^2))$ *friction*

Electron-Ion Collider, Brookhaven National Laboratory and Thomas Jefferson National Accelerator Facility			
Doc No. EIC-SHC-TN-24-005	Author: Sandesh Gopinath	Effective Date: 12/05/2024	Review Frequency: NA
Process Description: EIC Design Report MARCO Magnet			Revision: 00

- | | | |
|------|--|---|
| (4) | $DP_{\text{sing}} = (Sz) (\dot{m}^2 / (2r A^2))$ | <i>singularities: elbow, valve, etc</i> |
| (5) | $DP_{\text{acc}} = (2Dr/r) (\dot{m}^2 / (2r A^2))$ | <i>density acceleration</i> |
| (6) | $\dot{m} D h_{io} = \dot{m} (h_o - h_i) = Q$ | <i>Energy</i> |
| (7) | $D h_{io} = C_p D T_{io} + D x h_{lv}$ | <i>Enthalpy</i> |
| (8) | $f = 0.0056 + 0.5 / Re^{0.32}$ | <i>correlation of Koo, Drew, Mc Adams</i> |
| (9) | $Re = 4 \dot{m} / (\rho D m)$ | <i>Reynolds number</i> |
| (10) | $m = (1-x) m_l + x m_v$ | <i>mean viscosity</i> |

Instead of using equation (0) to calculate the vapor quality x we use the generalized definition: $x_o = (h_o - h_{\text{lsat}}) / Dh_{lv}$. Note: The generalized quality is negative when the flow is subcooled.

This system of 10 equations can be reduced to 9 as equation (5) can be neglected compared to (3) and (4): in fact in the circuit $(2Dr/r) < 2$ when $(Sz) > 20$ and $(fL/D) > 40$.

To solve the system of equations we use the pressure p and the enthalpy h as variables along the circuit in an EXCELL spreadsheet (Appendix 6).

These equations are solved in an Excel spreadsheet (Appendix 6). The outlet pressure of the return lines in the phase separator tank must be the same as the pressure inside the tank, defining thus the mass-flow rate and then the vapor quality. The case under consideration is the shut-down of the refrigerator when the liquid helium level is dropping in the phase separator tank. The limit is where the level is equal to zero. This is the limiting case for the thermosiphon because the differential height between the downward branch and the return lines (upward branch) is maximum and equal to the riser ($DH_r = 0.4$ m). The riser is needed to ensure that the two-phase flow goes back to the phase separator tank above the liquid helium surface. The diameters ($\varnothing 8$ mm) of the exchanger tubes of the supply and return lines, and the diameter ($\varnothing 30$ mm of manifolds) have been chosen to lower the frictional pressure drop. The main pressure drop is in the riser due to the gravity. In addition, the manifolds are almost isobaric as its pressure drop is less than 1 Pa.

The heat loads in the thermosiphon loop are the following:

- Constant, 3 W heat load of valve FV2
- Heat load of the cold mass
- Heaters (one on each return line with a maximum power of 10 W for each).

Several heat load scenarios on the thermosiphon were studied (Appendix 6).

Electron-Ion Collider, Brookhaven National Laboratory and Thomas Jefferson National Accelerator Facility			
Doc No. EIC-SHC-TN-24-005	Author: Sandesh Gopinath	Effective Date: 12/05/2024	Review Frequency: NA
Process Description: EIC Design Report MARCO Magnet			Revision: 00

Table 7.9 Thermosiphon calculation results at zero current

Cold mass heat load at zero current	25 W
Heaters	0 W
Total mass flow rate	25.35 g/s
Vapor quality	6.0%
Flow speed in the return lines	0.125 m/s

For the calculated heat loads under both zero current and current ramping conditions (Table 7.9 and 7.10), the vapor quality remains below 10%, and the flow speed in the return lines exceeds 0.1 m/s. This ensures proper operation of the thermosiphon.

Table 7.10 Thermosiphon calculation results for ramping up current

Cold mass heat load during ramping up current	30 W
Heaters	0 W
Total mass flow rate	29.1 g/s
Vapor quality	6.2%
Flow speed in the return lines	0.14 m/s

One limiting scenario is that the cold mass is very well insulated by its MLI blanket and thermal shield. The heat flux could be as low as 0.1 W/m^2 and the heat load could be as low as 10 W as shown in Table 7.11.

Table 7.11 Thermosiphon calculation results for low level heat load with no heaters

Cold mass low level heat load	10 W
Heaters	0 W
Total mass flow rate	11.3 g/s
Vapor quality	6.3%
Flow speed in the return lines	0.056 m/s

The flow speed is below 0.1 m/s, which could induce oscillation on the flow in the upward branch as it has been observed in the CMS solenoid at CERN. A solution is to increase the vapor quality and thus the speed in the return lines by means of electrical heaters.

Electron-Ion Collider, Brookhaven National Laboratory and Thomas Jefferson National Accelerator Facility			
Doc No. EIC-SHC-TN-24-005	Author: Sandesh Gopinath	Effective Date: 12/05/2024	Review Frequency: NA
Process Description: EIC Design Report MARCO Magnet			Revision: 00

Table 7.12 Thermosiphon calculation results for low level heat load with 20 W heaters

Cold mass low level heat load	10 W
Heaters	20 W
Total mass flow rate	18.3 g/s
Vapor quality	9.8%
Flow speed in the return lines	0.102 m/s

With an additional heat load of 20 W in the heaters, the vapor quality is below 10% and the speed in the return lines exceeds 0.1 m/s (Table 7.12). This ensures proper operation of the thermosiphon

Another limiting scenario is that the cold mass is not well insulated and has an arbitrary high heat load of 60 W.

Table 7.13 Thermosiphon calculation results for high level heat load 60 W

Cold mass low level heat load	60 W
Heaters	0 W
Total mass flow rate	45.55 g/s
Vapor quality	7.5%
Flow speed in the return lines	0.24 m/s

Even in this limiting scenario (Table 7.13), the vapor quality is less than 10% and the flow speed in the return lines is greater than 0.1 m/s. Again, this ensures proper operation of the thermosiphon.

In the case where the thermosiphon does not work for any reason, a solution is to run in the same configuration of valves as the long (summer) shut-down (TCV3 opened and LCV1 closed) with helium supply at 3.5 bar and 4.6 K.

7.3.1 Thermosiphon Piping Overview

There are two thermosiphon piping systems. One is primary and one is spare (Figure 7.11). If the primary has a leak, it is possible to use the spare one by disconnecting the primary piping in the vacuum vessel of the phase separator tank and connecting the spare piping.

The only official copy of this document is the one online in the SharePoint Document Center. Before using a printed copy, verify that it is current by checking the printed document's Revision History log with that of the online version.

Electron-Ion Collider, Brookhaven National Laboratory and Thomas Jefferson National Accelerator Facility			
Doc No. EIC-SHC-TN-24-005	Author: Sandesh Gopinath	Effective Date: 12/05/2024	Review Frequency: NA
Process Description: EIC Design Report MARCO Magnet			Revision: 00

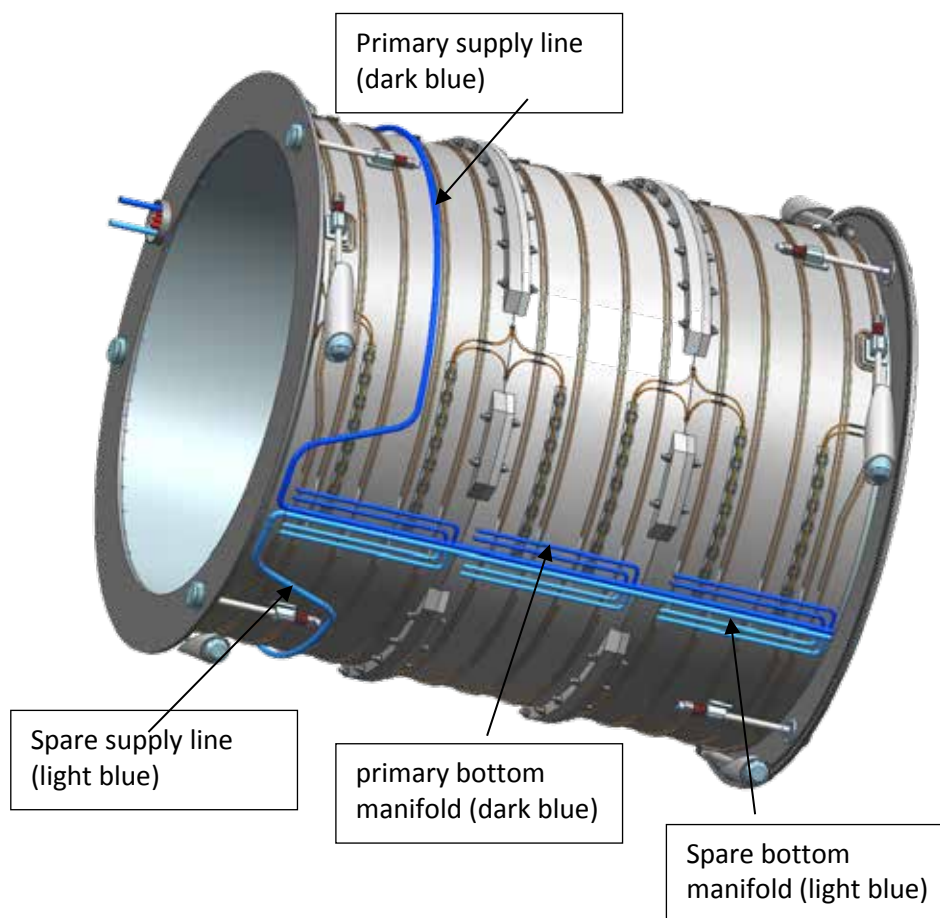


Figure 7.11 Primary and spare supply lines

The heat exchanger tubes are made of copper. They have an outer form of a square (14 mm · 14 mm) and an inner diameter of 8 mm. They are soft soldered onto the brass mandrel (Figure 7.12).

The only official copy of this document is the one online in the SharePoint Document Center. Before using a printed copy, verify that it is current by checking the printed document's Revision History log with that of the online version.

Electron-Ion Collider, Brookhaven National Laboratory and Thomas Jefferson National Accelerator Facility			
Doc No. EIC-SHC-TN-24-005	Author: Sandesh Gopinath	Effective Date: 12/05/2024	Review Frequency: NA
Process Description: EIC Design Report MARCO Magnet			Revision: 00

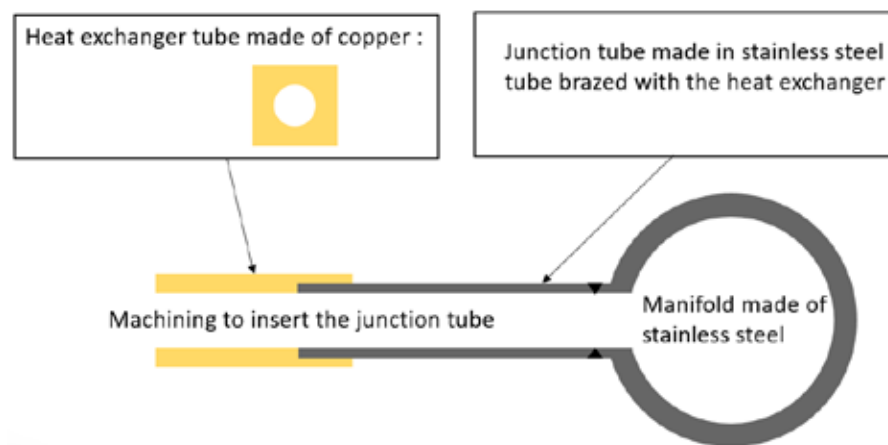


Figure 7.12 Soldering and brazing of the tubes

At their extremities, stainless steel junction tubes (jumpers) are brazed inside the copper tubes, and these junctions are welded to the stainless-steel manifolds.

There are 28 exchanger tubes: 2 · 5 tubes for the module 1, 2 · 4 tubes for the module 2, and 2 · 5 tubes for the module 3. There are more tubes on the extremity modules due to the heat loads of the tie-rods. The detailed layout is shown in Figure 7.13, Figure 7.14, and Figure 7.15.

The only official copy of this document is the one online in the SharePoint Document Center. Before using a printed copy, verify that it is current by checking the printed document's Revision History log with that of the online version.

Electron-Ion Collider, Brookhaven National Laboratory and Thomas Jefferson National Accelerator Facility			
Doc No. EIC-SHC-TN-24-005	Author: Sandesh Gopinath	Effective Date: 12/05/2024	Review Frequency: NA
Process Description: EIC Design Report MARCO Magnet			Revision: 00

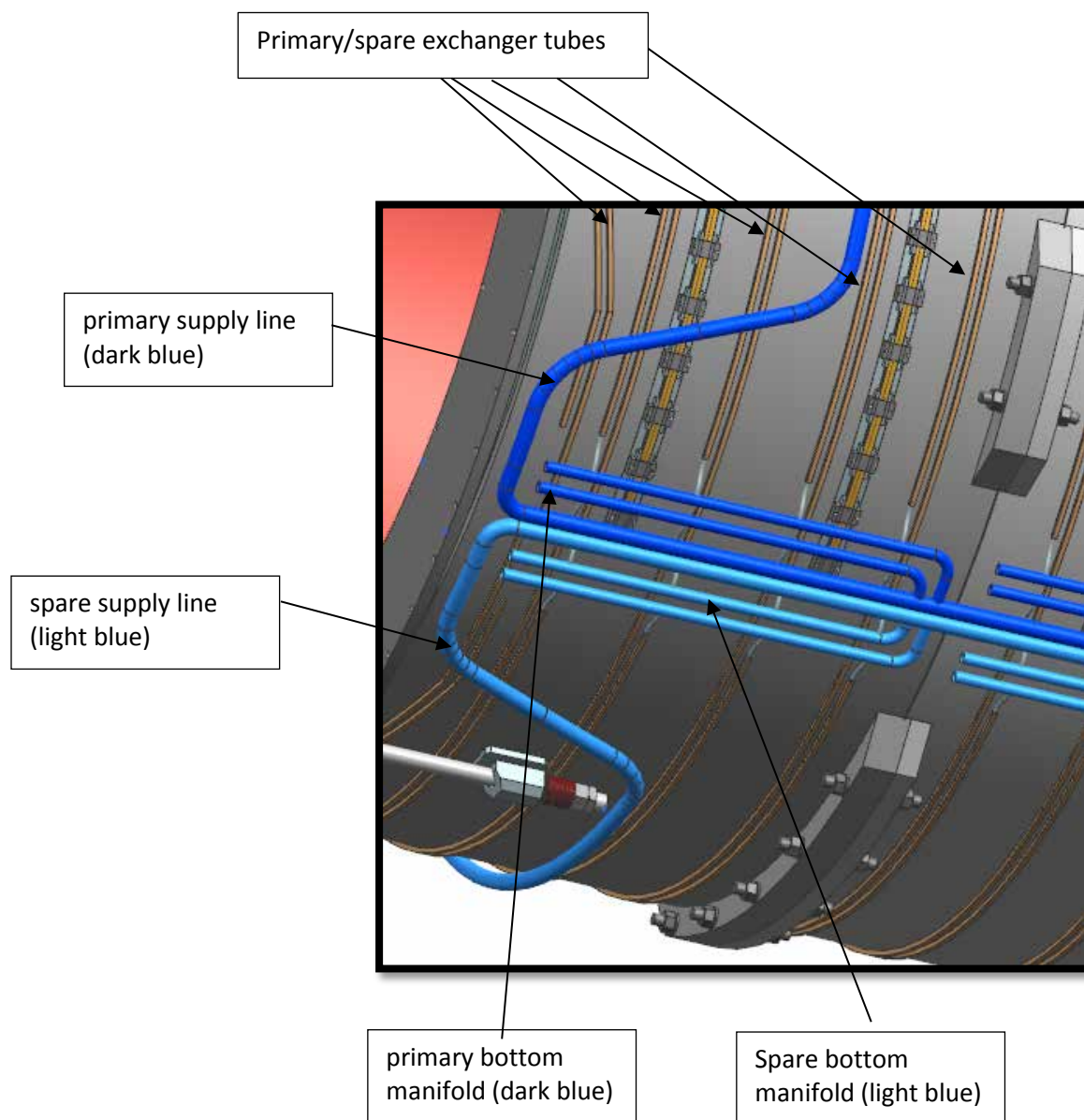


Figure 7.13 Primary and spare tubes of the heat exchanger

Electron-Ion Collider, Brookhaven National Laboratory and Thomas Jefferson National Accelerator Facility			
Doc No. EIC-SHC-TN-24-005	Author: Sandesh Gopinath	Effective Date: 12/05/2024	Review Frequency: NA
Process Description: EIC Design Report MARCO Magnet			Revision: 00

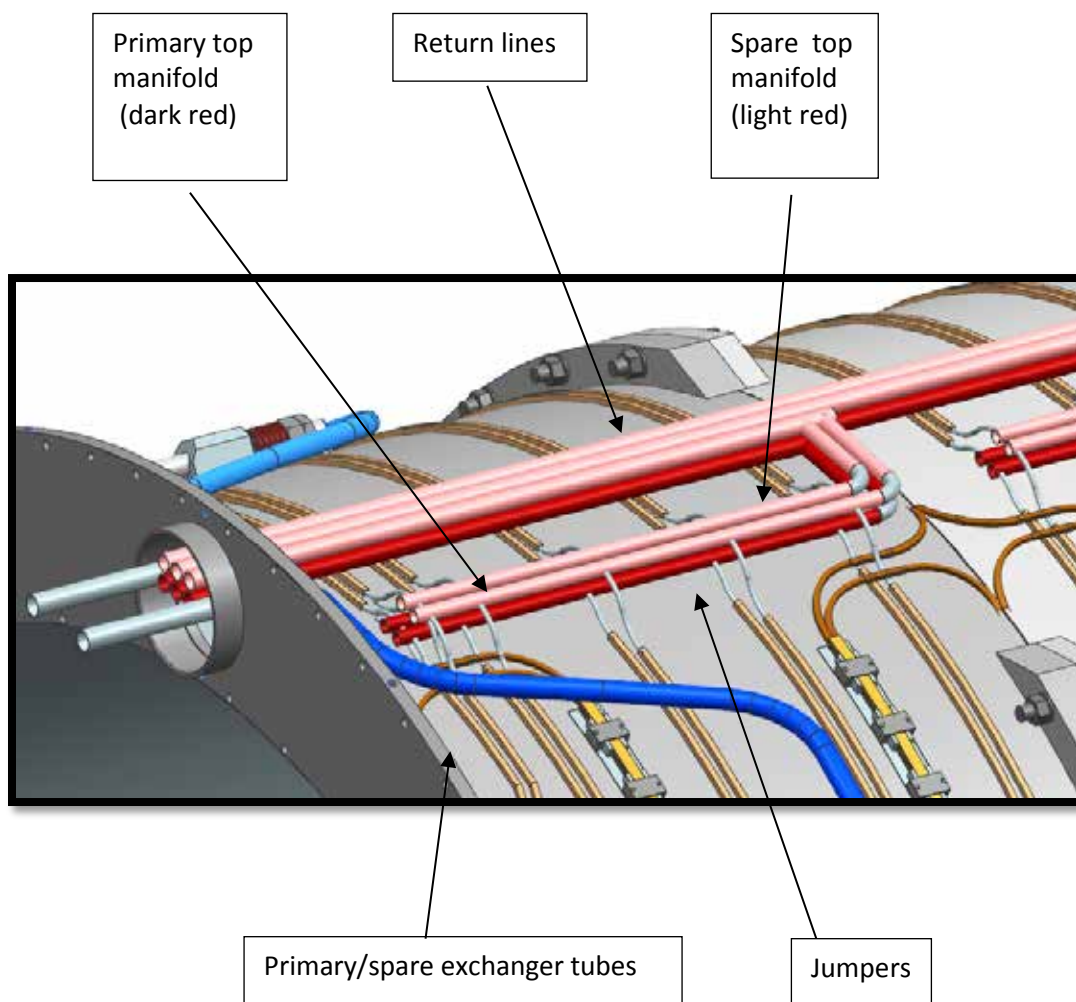


Figure 7.14 Primary and spare piping on top of the mandrel

In the vacuum vessel of the phase separator tank, the primary supply line (dark blue) is connected to valve FV2, whereas the spare supply line (light blue) is in stand-by. The three return lines have a similar configuration; the primary ones are connected to the phase separator tank and the spare ones are in stand-by.

The only official copy of this document is the one online in the SharePoint Document Center. Before using a printed copy, verify that it is current by checking the printed document's Revision History log with that of the online version.

Electron-Ion Collider, Brookhaven National Laboratory and Thomas Jefferson National Accelerator Facility			
Doc No. EIC-SHC-TN-24-005	Author: Sandesh Gopinath	Effective Date: 12/05/2024	Review Frequency: NA
Process Description: EIC Design Report MARCO Magnet			Revision: 00

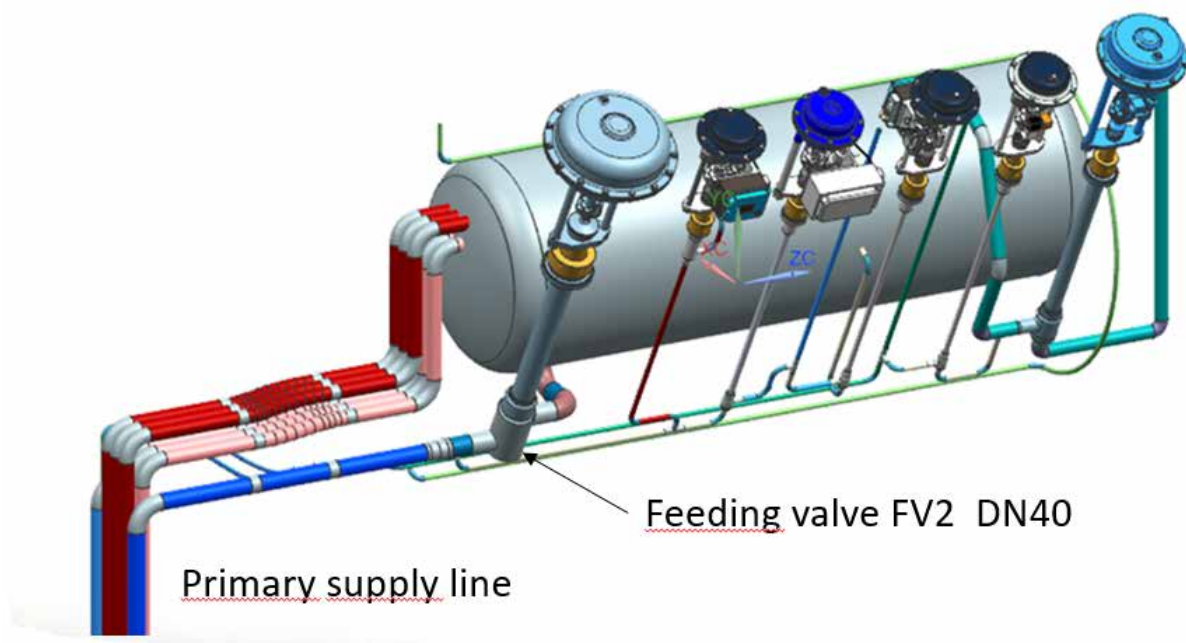


Figure 7.15 Piping in the phase separator vacuum vessel

7.4 Thermal shield

The thermal shield of the cold mass is made of 3 · 4 internal panels, 3 · 4 external panels, and end plates. It is made of Al 3003 with a thickness of 5 mm. An overview of the thermal shield is shown in Figure 7.16.

The only official copy of this document is the one online in the SharePoint Document Center. Before using a printed copy, verify that it is current by checking the printed document's Revision History log with that of the online version.

Electron-Ion Collider, Brookhaven National Laboratory and Thomas Jefferson National Accelerator Facility			
Doc No. EIC-SHC-TN-24-005	Author: Sandesh Gopinath	Effective Date: 12/05/2024	Review Frequency: NA
Process Description: EIC Design Report MARCO Magnet			Revision: 00

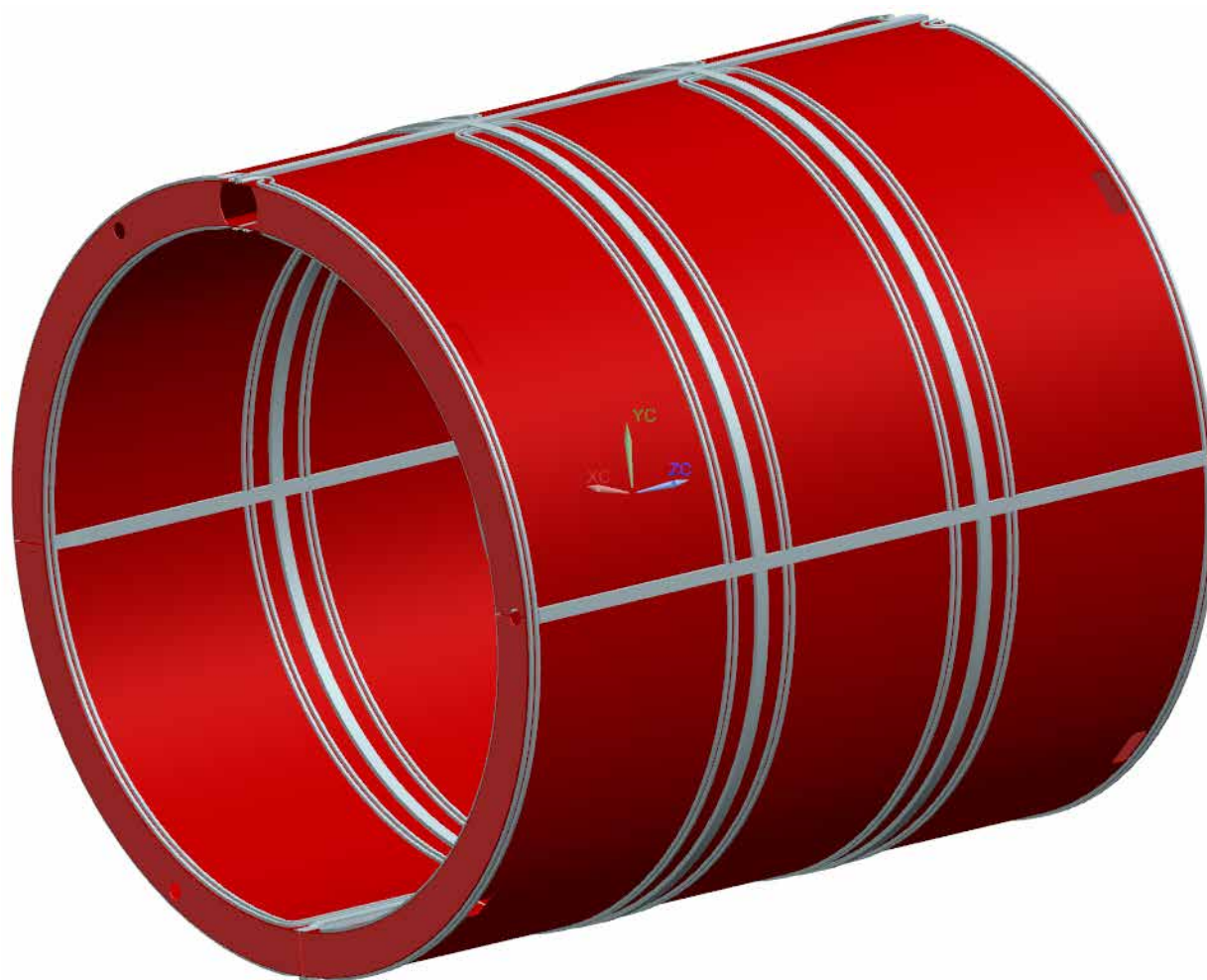


Figure 7.16 Overview of thermal shield

The surface areas of the thermal shield are illustrated in Figure 7.17. They have a heat flux of 5 W/m².

Electron-Ion Collider, Brookhaven National Laboratory and Thomas Jefferson National Accelerator Facility			
Doc No. EIC-SHC-TN-24-005	Author: Sandesh Gopinath	Effective Date: 12/05/2024	Review Frequency: NA
Process Description: EIC Design Report MARCO Magnet			Revision: 00

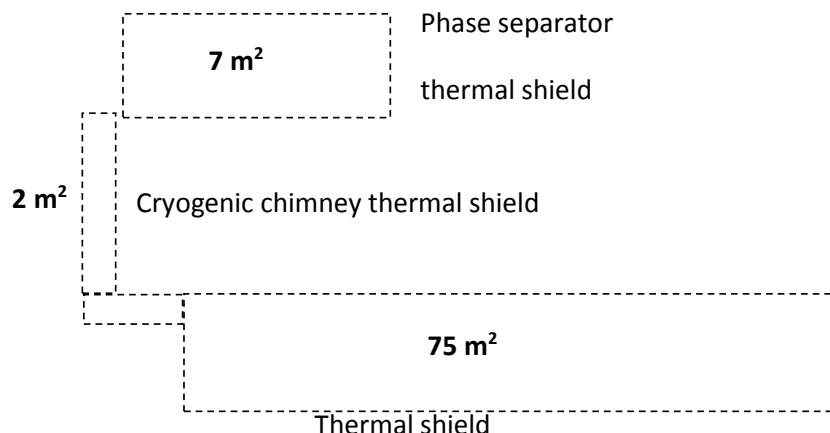


Figure 7.17 Surface areas of thermal shield

The tube, which connects the BNL flexible supply line and the thermal shield piping, has an inner diameter of 10 mm and an outer square form of 14 mm · 14 mm. This tube passes through the phase separator vacuum vessel and the cryogenic chimney without cooling any surface; it goes directly to the inner part of the cold mass thermal shield and supplies, in parallel, the left circuit and the right circuit. The left and right external shields are then cooled afterwards. The end plates are indirectly cooled by connecting with them. The two half flows are joined together at the inlet of the cryogenic chimney and then cools the thermal shield in the cryogenic chimney.

Like the thermosiphon system, there are two cooling circuits for the thermal shield. One is the primary and the other is the spare.

7.4.1 Pressure Drops and Temperature along the Circuit

The pressure drops and temperatures in the different portions of the circuit are calculated in Appendix 7.

The equations in the circuit can be written as follows.

$$DP = (fL/D + K) (\dot{m}^2 / (2 \rho A^2))$$

$$Q = \dot{m} C_p \Delta T$$

$$f = 0.0056 + 0.5/Re^{0.32}$$

Electron-Ion Collider, Brookhaven National Laboratory and Thomas Jefferson National Accelerator Facility			
Doc No. EIC-SHC-TN-24-005	Author: Sandesh Gopinath	Effective Date: 12/05/2024	Review Frequency: NA
Process Description: EIC Design Report MARCO Magnet			Revision: 00

$$Re = 4 \dot{m} / (\rho D m)$$

Sx is the sum of the pressure drop coefficients due to singularities (angle, elbow, restriction, etc) [26].

The main results are given in Table 7.14 for an inner diameter of 10 mm. The total pressure drop in the circuit is 135 mbar. The outlet temperature of helium flow is 63 K for an inlet temperature of 45 K.

LIST of SYMBOLS

DP	Pressure drop in a part of the circuit	Pa
L	Length of the part of the circuit	m
f	Friction coefficient	-
D	Inner diameter of the tube	m
Sx	Sum of Singularities coefficients [26]	-
\dot{m}	Mass flow of helium	kg/s
ρ	Density of helium	kg/m ³
A	Cross-sectional area of the tube	m ²
Cp	Enthalpy coefficient	J/kg.K
DT	Temperature variation along the part of the circuit	K
Re	Reynolds number	-
μ	Viscosity of helium	Pa.s

Table 7.14 Pressure drop in the piping of the thermal shield

Name	Qty	Mass flow	Q	L	P1	T1	P2	T2
		(g/s)	(W)	(m)	(bar)	(K)	(bar)	(K)
Phase separator supply line	1	6	0	2	15.500	45	15.488	45
Cryogenic chimney supply line	1	6	0	2.2	15.488	45	15.474	45
Internal thermal shield	2	3	88	32	15.474	45	15.439	50

Electron-Ion Collider, Brookhaven National Laboratory and Thomas Jefferson National Accelerator Facility			
Doc No. EIC-SHC-TN-24-005	Author: Sandesh Gopinath	Effective Date: 12/05/2024	Review Frequency: NA
Process Description: EIC Design Report MARCO Magnet			Revision: 00

External thermal shield	2	3	155	36	15.439	50	15.393	60
Cryogenic chimney return line	1	6	10	2.2	15.393	60	15.380	61
Phase separator Return line	1	6	68	2	15.380	61	15.365	63

7.4.2 Temperature Difference in the Panels

The temperature difference in a panel due to conduction and radiation is as follows.

$$\Delta T_p = \frac{ql^2}{2ke}$$

Here the thermal radiation heat flux $q = 5 \text{ W/m}^2$; the thermal conductivity $k = 125 \text{ W/m}^2$; the thickness $e = 5 \text{ mm}$; and $l = 0.35 \text{ m}$, which is half the axial distance between the tubes welded on the panel. The computed temperature difference (ΔT_p) is 0.5 K .

The temperature difference ΔT_w between the helium flow and the wall of the tube is maximum for the end panels and especially the end part of the tube because it has the maximum heat load, which includes thermal radiation (Q_r), supports (Q_s), thermal intercepts of the cold mass tie-rods (Q_{thInt}). The equation is the following.

$$\Delta T_w = \frac{Q_r + Q_s + Q_{thInt}}{hS}$$

Where $h = 370 \text{ W/m}^2$, which is the thermal convection coefficient; $S = 0.168 \text{ m}^2$, which is the surface area of the tube wall for half the circumference on the external right or left circuit.

$$Q_r = 5 \times (p \times 1.7 \times 0.5) = 13.3 \text{ W}$$

$$Q_s = 4 \times 0.33 = 1.32 \text{ W}$$

$$Q_{thInt} = 1.5 \times 4.8 + 2 \times 6.8 = 20.8 \text{ W}$$

$$\text{Thus, } \Delta T_w = 0.57 \text{ K}$$

The temperature difference between helium and the hot spot on a panel is 1.1 K .

7.5 Helium Phase Separator

The helium phase separator is on top of the detector, embedded in the iron and connected to the magnet assembly through the cryogenic chimney (Figure 7.18 and Figure 7.19).

Electron-Ion Collider, Brookhaven National Laboratory and Thomas Jefferson National Accelerator Facility			
Doc No. EIC-SHC-TN-24-005	Author: Sandesh Gopinath	Effective Date: 12/05/2024	Review Frequency: NA
Process Description: EIC Design Report MARCO Magnet			Revision: 00

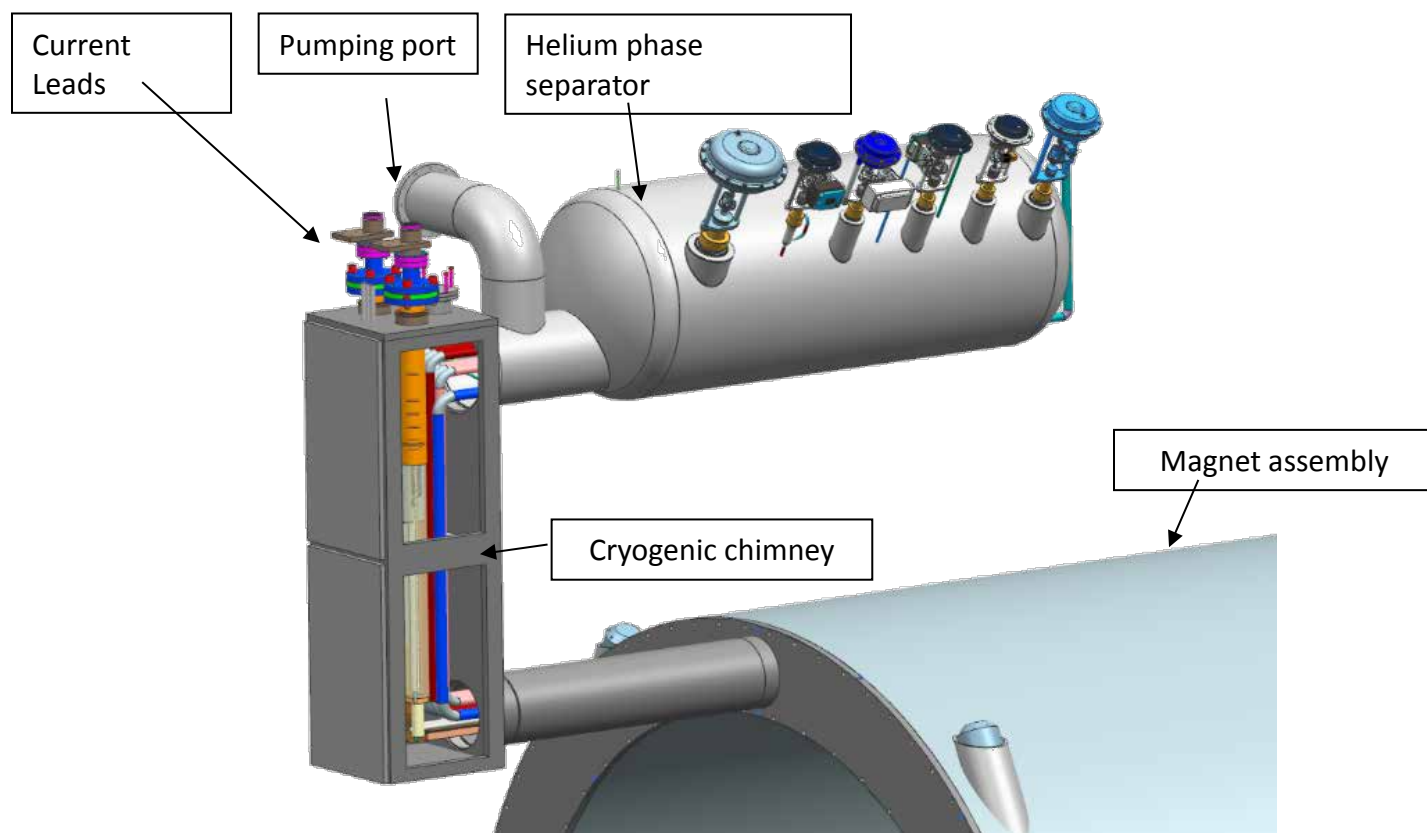


Figure 7.18 Helium phase separator and cryogenic chimney overview

In addition to the cryogenic lines, the cryogenic chimney also houses the helium vapor cooled current leads. A vacuum pumping port is located between the cryogenic chimney and the phase separator vacuum vessel.

Electron-Ion Collider, Brookhaven National Laboratory and Thomas Jefferson National Accelerator Facility			
Doc No. EIC-SHC-TN-24-005	Author: Sandesh Gopinath	Effective Date: 12/05/2024	Review Frequency: NA
Process Description: EIC Design Report MARCO Magnet			Revision: 00

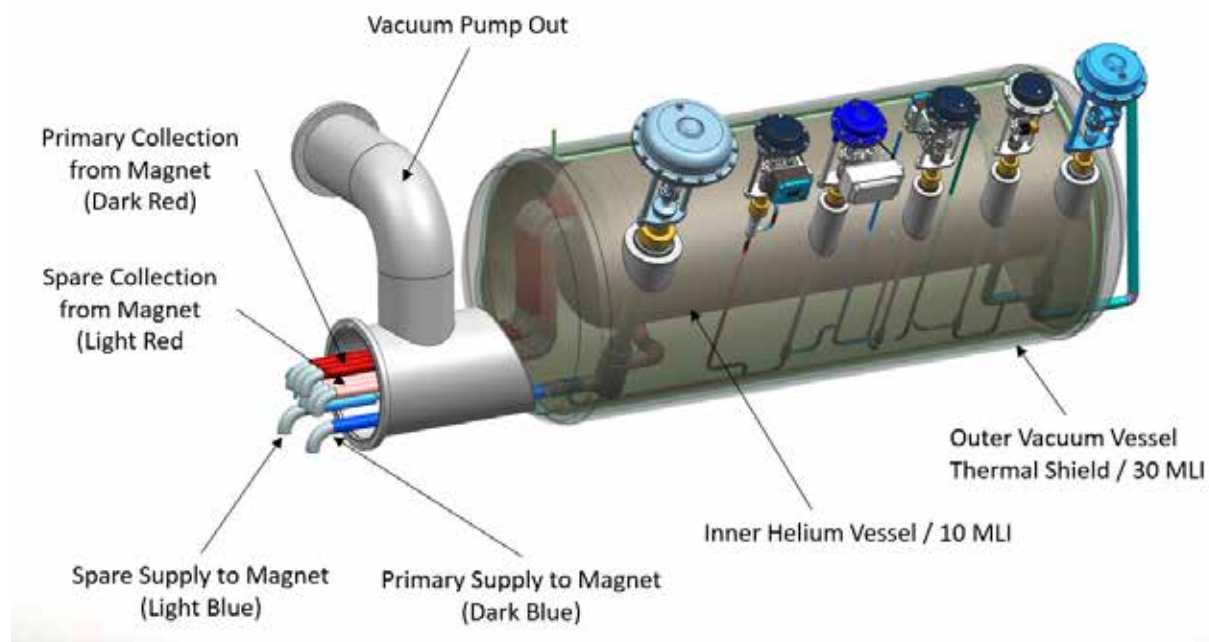


Figure 7.19 Phase separator

The phase separator vacuum vessel houses the helium phase separator, the thermal shield with 8 radial tie-rods, the 5 cryogenic valves (LCV1, FV2, TCV3, FV4, FV5) [Table 7.15] with warm actuators, and the warm valve TCV9. The calculation of the valves is in the Appendix 8.

Table 7.15 Diameters of valves

LCV1	FV2	TCV3	FV4	FV5	TCV9	FCV10	FCV11
DN4	DN40	DN8	DN25	DN6	DN6	DN6	DN6

The only official copy of this document is the one online in the SharePoint Document Center. Before using a printed copy, verify that it is current by checking the printed document's Revision History log with that of the online version.

Electron-Ion Collider, Brookhaven National Laboratory and Thomas Jefferson National Accelerator Facility			
Doc No. EIC-SHC-TN-24-005	Author: Sandesh Gopinath	Effective Date: 12/05/2024	Review Frequency: NA
Process Description: EIC Design Report MARCO Magnet			Revision: 00

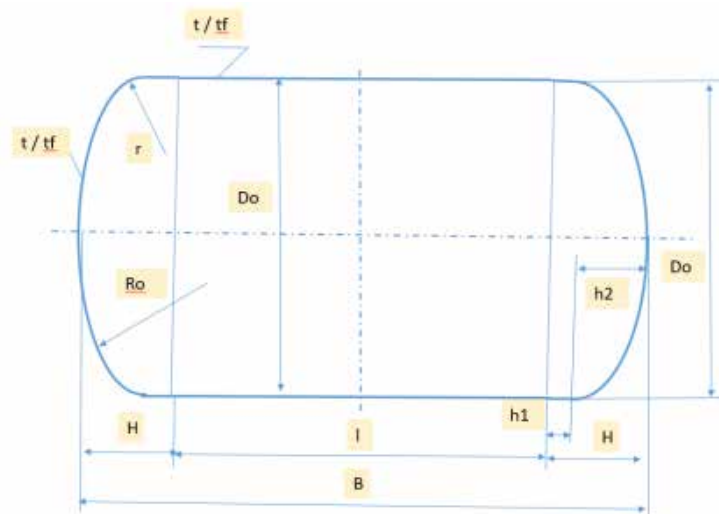


Figure 7.20 Dimensional symbols for the phase separator and its vacuum vessel

The characteristics of the vessels (vacuum vessel = outer vessel and helium phase separator = inner vessel) are illustrated in Table 7.16 and Figure 7.20.

Table 7.16 Dimensions of inner helium vessel (helium phase separator) and outer vessel (vacuum vessel)

		Dimension , in mm	
		INNER VESSEL	OUTER VESSEL
FORMED HEAD			
Type		Ellipsoidal	Ellipsoidal
Outside diameter	Do	500	700
Outside radius of crown portion of head	Ro	405	564
Inside Knuckle radius	r	77	107,8
Length of cylindrical part of head	h1	25	35
Depth of head (inner)	h2	124,3	176
Length of head (outer)	H	154,3	215,0
Thickness (Nominal / Minimum)	t / tf	5 / 3,5	4 / 3
SHELL			
Outside diameter	Do	498	700
Length of shell	l	1292	1570
Thickness (Nominal / Minimum)	t / tf	4 / 3,5	4 / 3,5
VESSEL Length	B	1600,7	2000
VESSEL volume , liters	V	284	705
EMPTY VESSEL weight, kg	M	88	148

Electron-Ion Collider, Brookhaven National Laboratory and Thomas Jefferson National Accelerator Facility			
Doc No. EIC-SHC-TN-24-005	Author: Sandesh Gopinath	Effective Date: 12/05/2024	Review Frequency: NA
Process Description: EIC Design Report MARCO Magnet			Revision: 00

The total volume of the inner helium vessel is 284 L; the liquid helium buffer used in normal operation is 110 L, which is the volume of liquid needed to ramp down the current at 1 A/s in case of a refrigerator shut-down. The set pressure of the burst disc is 6 bar.

7.6 Safety Analysis

The protection, against overpressure, of the helium circuits (European regulation: **EN21013-3**) and the vacuum vessel (European regulation **EN 13458-2**) is studied.

7.6.1 Helium Circuits

Two cases, the quench and the vacuum loss (the worst case), are considered.

Quench condition:

- $A1 = 4.57 \text{ m}^2$ surface of liquid helium piping in contact with mandrel
- $T1 = 45 \text{ K}$ mandrel and pipes temperature for calculation
- $T1h = 4.5 \text{ K}$ liquid helium temperature for calculation
- $U1 = 40 \text{ kW/m}^2[27]$ heat load rate from pipes to liquid helium (from $T1$ to $T1h$), *conservative calculation for $\Delta T > 10 \text{ K}$*
- $W1 = 40 \text{ kW/m}^2 \times 4.57 \text{ m}^2 = 182.8 \text{ kW}$ heat load from pipes to liquid helium

Vacuum loss condition:

- $A2 = 8.29 \text{ m}^2$ surface of the vessel and piping, which contains liquid helium
- $U2 = 6.4 \text{ kW/m}^2$ heat load rate from ambient temperature to liquid helium pipes/tank, covered by 10 layers of MLI [ISO 21013-3]
- $W2 = 6.4 \times 8.29 = 53 \text{ kW}$ heat load from ambient temperature to pipes and inner helium vessel with liquid helium, covered by 10 layers of MLI

When the vacuum loss occurs, it triggers the coil to quench. The capacity of the relief valve PSV25a is computed for the case of the quench; the burst disc, both the vacuum loss and quench.

The equations used to calculate the safety devices are the following according to the European regulation EN21013-3:2016:

Electron-Ion Collider, Brookhaven National Laboratory and Thomas Jefferson National Accelerator Facility			
Doc No. EIC-SHC-TN-24-005	Author: Sandesh Gopinath	Effective Date: 12/05/2024	Review Frequency: NA
Process Description: EIC Design Report MARCO Magnet			Revision: 00

For the flow we have two cases :

- Critical flow when : $\frac{P_b}{P_i} \leq \left(\frac{2}{\gamma+1}\right)^{\left(\frac{\gamma}{\gamma-1}\right)}$
- Sub critical flow when : $\frac{P_b}{P_i} > \left(\frac{2}{\gamma+1}\right)^{\left(\frac{\gamma}{\gamma-1}\right)}$

P_b is the counter pressure in Pa, P_i is the inlet pressure of the safety valve in Pa, γ is the isentropic exponent (ratio of the specific heat capacity at constant pressure to the specific heat capacity at constant volume)

For the critical flows (case of the relief valve and the burst disc) the minimum valve flow area is given by:

$$A_v = \frac{Q_m}{31.62 * P_i * C * K_{dr} * \left(\frac{M}{Z_i * T_i}\right)^{1/2}} = \frac{Q_m}{0.2883 * C * K_{dr} * \left(\frac{P_i}{\vartheta_i}\right)^{1/2}} \quad \text{with} \quad K_{dr} = 0.9 * K_d$$

List of symbols

A_v	Minimum valve flow area	mm ²
Q_m	Mass flow in the safety device	kg/h
P_i	Inlet pressure of the safety device	bar abs.
K_{dr}	Derated coefficient of discharge	-
K_d	Manufacturer coefficient of discharge	-
M	Molar mass of the gas	kg/mol
T_i	Inlet temperature of the safety device	K
Z_i	Compressibility factor at P_i and T_i	-
ϑ_i	Specific volume at safety device inlet	m ³ /kg

The coefficient C is given by : $C = \left(\gamma * \left(\frac{2}{\gamma+1} \right)^{\frac{\gamma+1}{\gamma-1}} \right)^{1/2}$

Result calculation of pressure relief valve and bursting disk of Helium circuits according to EN21013-3:2016

Relief valve PSV25a (quench condition):

1. $W_1 = 182,8 \text{ kW}$ (heat load)
2. $Q_m = 8,1 \text{ kg/s}$ (mass flow rate)

Electron-Ion Collider, Brookhaven National Laboratory and Thomas Jefferson National Accelerator Facility			
Doc No. EIC-SHC-TN-24-005	Author: Sandesh Gopinath	Effective Date: 12/05/2024	Review Frequency: NA
Process Description: EIC Design Report MARCO Magnet			Revision: 00

3. Relief valve data:

- a) $P_s = 3,5 \text{ bar g}$ (set pressure)
- b) $P = 3,5 * 1,1 + 1 = 4,85 \text{ bar a}$ (relieving pressure)
- c) $T = 6,6 \text{ K}$ (relieving temperature)
- d) $D_o = 65 \text{ mm}$ (orifice)
- e) $K_d = 0,7$ (manufacturer discharge coefficient)

Bursting disc PSV25b (quench + vacuum loss condition):

- 1. $W_3 = W_1 + W_2 = 182,8 \text{ kW} + 53,25 \text{ kW} = 236 \text{ kW}$ (total heat load)
- 2. $Q_m = 8 \text{ kg/s}$ (mass flow rate)
- 3. Bursting disc data:
 - a) $P_s = 5 \text{ bar g}$ (set pressure)
 - b) $P = 5 * 1,1 + 1 = 6,5 \text{ bar a}$ (relieving pressure)
 - c) $T = 7,8 \text{ K}$ (relieving temperature)
 - d) $D_o = 65 \text{ mm}$ (orifice)
 - e) $K_d = 0,65$ (manufacturer discharge coefficient)

7.7 Vacuum Vessel

We calculate the vacuum vessel safety device in two cases :

- Rupture of the liquid helium circuit: according to European regulation EN13458-2 Annex-I then the discharge area of the safety device shall not be less than $0.34 \text{ mm}^2/\text{l}$ capacity of the liquid helium circuits.
 - 1. $A = 0,34 \text{ mm}^2/\text{l} \times 314 \text{ l} = 107 \text{ mm}^2$ - minimum discharge area
 - 2. $D = 11,7 \text{ mm}$ - min required diameter
- Rupture of the gas thermal shield circuit: We consider here very conservative conditions that is to say an isentropic discharge of the broken tube inside the vacuum vessel with the following parameters:

	P	T	S	H	r
	(pa)	(K)	(J/kg.K)	(J/kg)	(kg/m ³)
Inlet conditions	1,55E+06	45	16011	250219	15,94
Outlet conditions	1,50E+05	17,667	16011	105988	4,10

Table 7.17 Isentropic discharge parameters in case of the rupture of gas thermal shield circuit

P is the gas pressure, T the temperature of the gas, S the entropy, H the enthalpy and r the density.

Electron-Ion Collider, Brookhaven National Laboratory and Thomas Jefferson National Accelerator Facility			
Doc No. EIC-SHC-TN-24-005	Author: Sandesh Gopinath	Effective Date: 12/05/2024	Review Frequency: NA
Process Description: EIC Design Report MARCO Magnet			Revision: 00

With the isentropic discharge the speed V of the gas at the outlet of the tube is supposed to be:

$V = (2 * (H_i - H_o))^{1/2}$ and the mass flow rate is : $Q_m = \rho * V * \pi * d^2 / 4$ with ρ the density of the gas at the outlet of the tube and d the inner diameter of the tube (10 mm). We find then $V=537$ m/s and thus a mass flow $Q_m = 0.173$ kg/s

The safety device discharge area A_v is given by : $A_v = \frac{Q_m}{1.61 * K_{dr} * \left(\frac{P_i - P_b}{\vartheta_i}\right)^{1/2}}$ with $K_{dr} = 0.9 * K_d$

LIST of SYMBOLS

A_v	Minimum valve flow area	mm^2
Q_m	Mass flow in the safety device	kg/h
P_i	Inlet pressure of the safety device	bar abs.
P_b	counter pressure of the safety device	bar abs
K_{dr}	Derated coefficient of discharge	-
K_d	Manufacturer coefficient of discharge	-
ϑ_i	Specific volume at safety device inlet	m^3/kg

To calculate the discharge area of the safety device we supposed the mass flow Q_m exhausts at 300 K which is again a conservative assumption.

- Output Helium gas : $P = 1,5$ bar a, $T = 300$ K
- Atmosphere: $P = 1,0$ bar a, $T = 300$ K
- Used mass flow rate is $Q_m = 0,173$ kg/s
- $A_v = 2376$ mm^2
- Min diameter = 55 mm

Vacuum vessel safety device conclusion : For the two cases we have studied we have found for the safety device diameter 11.7 mm and 55 mm to keep conservative we choose a 100 mm diameter.

Electron-Ion Collider, Brookhaven National Laboratory and Thomas Jefferson National Accelerator Facility			
Doc No. EIC-SHC-TN-24-005	Author: Sandesh Gopinath	Effective Date: 12/05/2024	Review Frequency: NA
Process Description: EIC Design Report MARCO Magnet			Revision: 00

8 Thermal Analysis

The cryogenic layout presented in section 7 is analyzed to further corroborate the design. The base thermosiphon system parameters in section 7 are implemented in FEA to compute the temperature gradient across the cold mass. The acceptable criteria for the temperature is based on the conductor stability analysis which showed a 2.45 K temperature margin over the assumed 4.70 K operating temperature. All pressures mentioned are absolute

8.1 Thermosiphon Overview

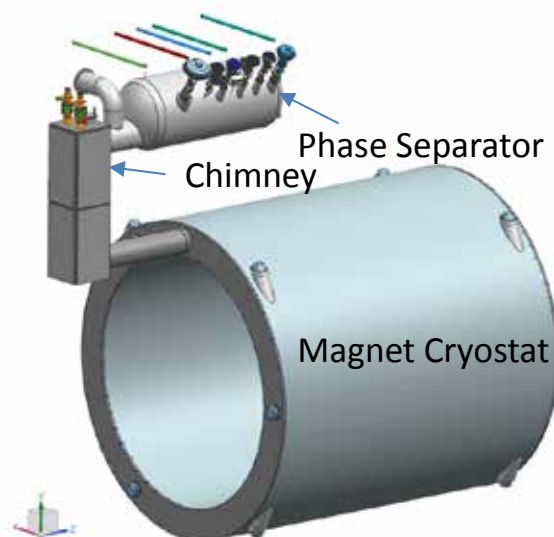


Figure 8.1 Magnet system layout

Electron-Ion Collider, Brookhaven National Laboratory and Thomas Jefferson National Accelerator Facility			
Doc No. EIC-SHC-TN-24-005	Author: Sandesh Gopinath	Effective Date: 12/05/2024	Review Frequency: NA
Process Description: EIC Design Report MARCO Magnet			Revision: 00

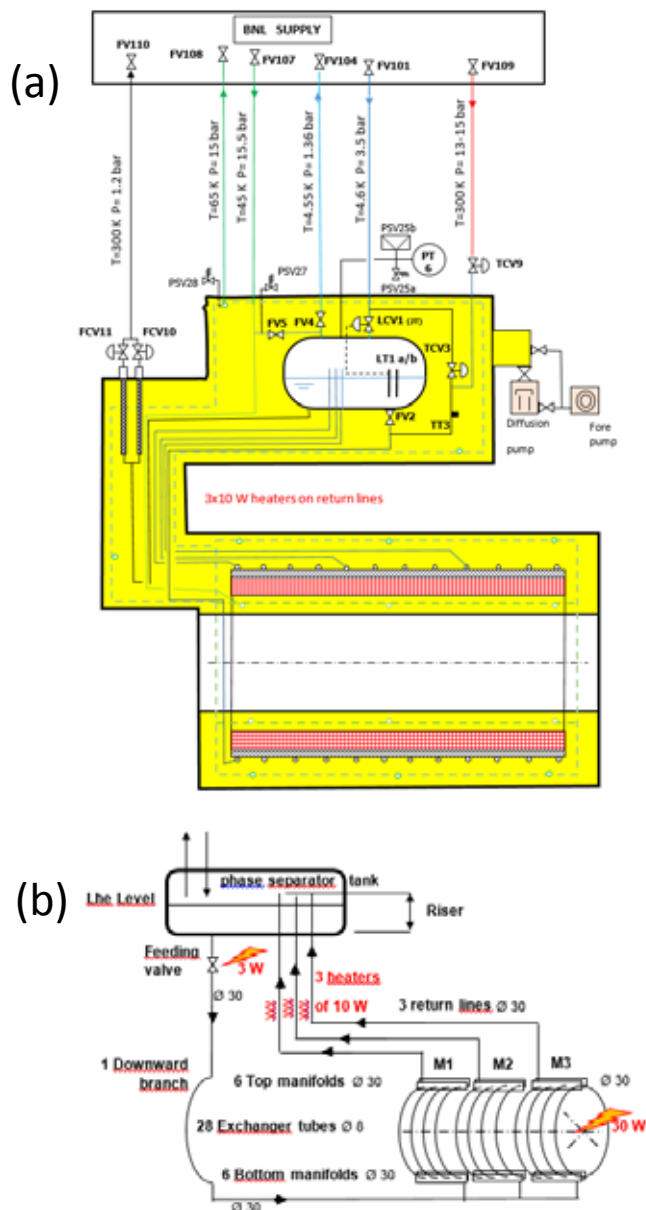


Figure 8.2 Thermosiphon Schematic, a) detailed layout , b) basic layout

MARCO solenoid is a conduction-cooled superconducting magnet at the heart of the ePIC detector. The phase separator on top of the magnet accepts this incoming helium and supplies it to the magnet coil modules at a supercritical pressure of 1.5 bar (absolute) with the help of heaters in line with the flow to maintain consistent heat load.

The only official copy of this document is the one online in the SharePoint Document Center. Before using a printed copy, verify that it is current by checking the printed document's Revision History log with that of the online version.

Electron-Ion Collider, Brookhaven National Laboratory and Thomas Jefferson National Accelerator Facility			
Doc No. EIC-SHC-TN-24-005	Author: Sandesh Gopinath	Effective Date: 12/05/2024	Review Frequency: NA
Process Description: EIC Design Report MARCO Magnet			Revision: 00

The approximate 20 metric ton cold mass is directly cooled by the helium flowing through the heat exchanger pipes that are in contact with the cold mass.

8.2 Geometry Overview

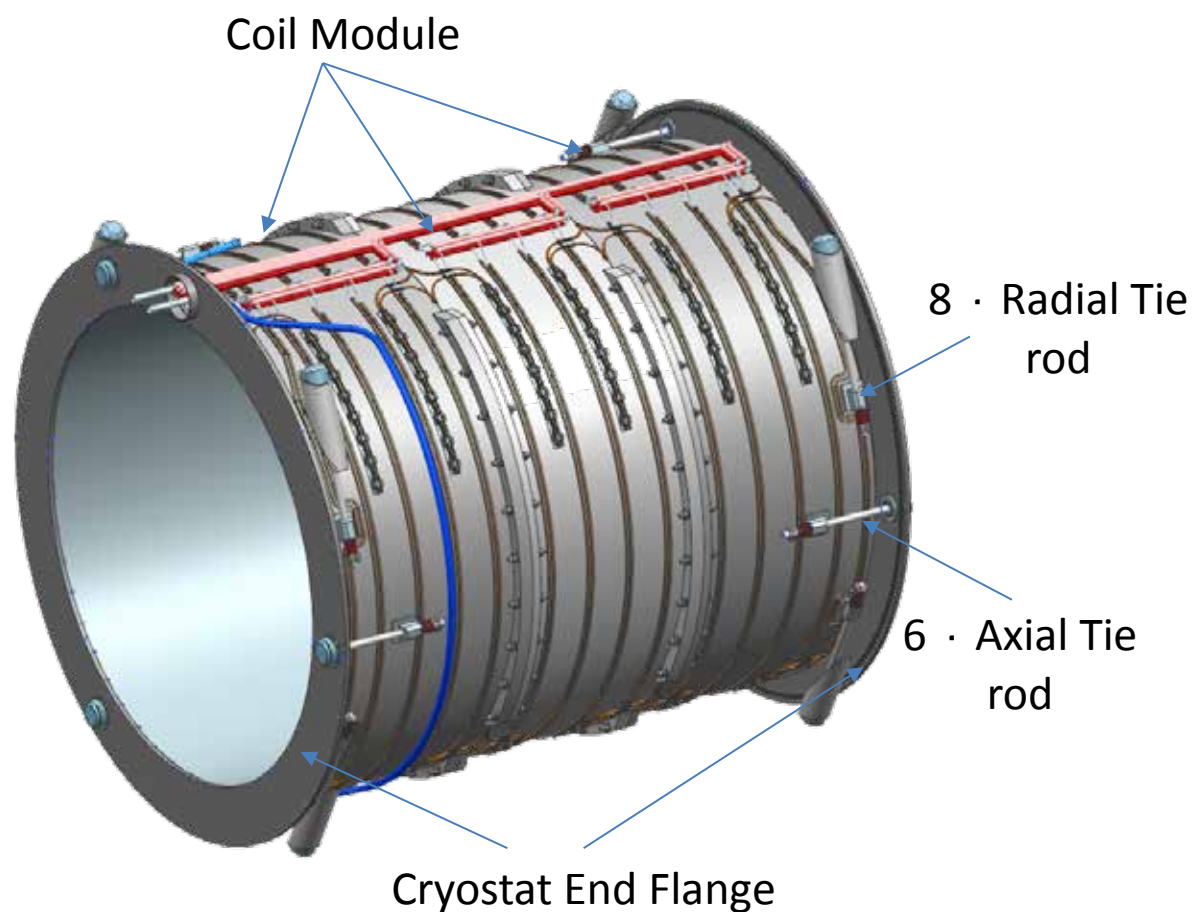


Figure 8.3 Magnet detailed model with outer cryostat cylinder hidden

The only official copy of this document is the one online in the SharePoint Document Center. Before using a printed copy, verify that it is current by checking the printed document's Revision History log with that of the online version.

Electron-Ion Collider, Brookhaven National Laboratory and Thomas Jefferson National Accelerator Facility			
Doc No. EIC-SHC-TN-24-005	Author: Sandesh Gopinath	Effective Date: 12/05/2024	Review Frequency: NA
Process Description: EIC Design Report MARCO Magnet			Revision: 00

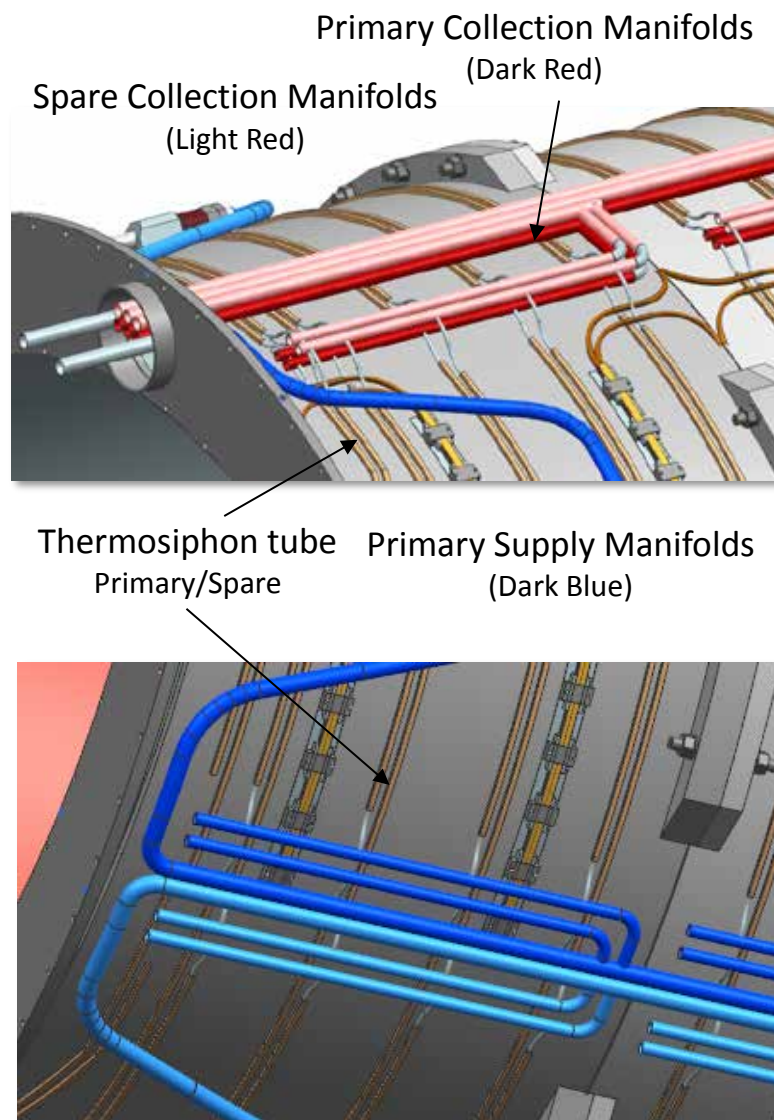


Figure 8.4 Thermosiphon piping distribution layout detail

The magnet is divided into three nearly identical modules (figure 2). Each module has a 6 layer coil that is internally wound on a brass mandrel. The coils along with the mandrel are conduction cooled using square hollow OHFC copper tubing in contact with the outer surface on the mandrel (figure 3). The detailed design contains an auxiliary flow circuit identical to the main circuit for redundancy (figure 4).

Electron-Ion Collider, Brookhaven National Laboratory and Thomas Jefferson National Accelerator Facility			
Doc No. EIC-SHC-TN-24-005	Author: Sandesh Gopinath	Effective Date: 12/05/2024	Review Frequency: NA
Process Description: EIC Design Report MARCO Magnet			Revision: 00

8.3 FEA

The detailed model of the magnet is simplified first and then analyzed using the finite element software ANSYS 2023 R1. Thermal analysis has been performed using different modules of the software to simulate the potential scenarios of concern during operation and testing of the magnet.

8.3.1 Workflow

The steady state thermal module in ANSYS is utilized to simulate the equilibrium state of the magnet during operational condition and during current ramp up (See Section 10.1)

The helium flow was simulated using ANSYS FLUENT [28] The temperature profile along with the eddy current heat generation is used as a boundary condition for steady state thermal analysis.

The worst case scenario heat load which assumes the eddy current heat load is simulated.

Transient thermal analysis was performed to predict the time taken to cool down the coils and the mandrel.

8.3.2 Geometry

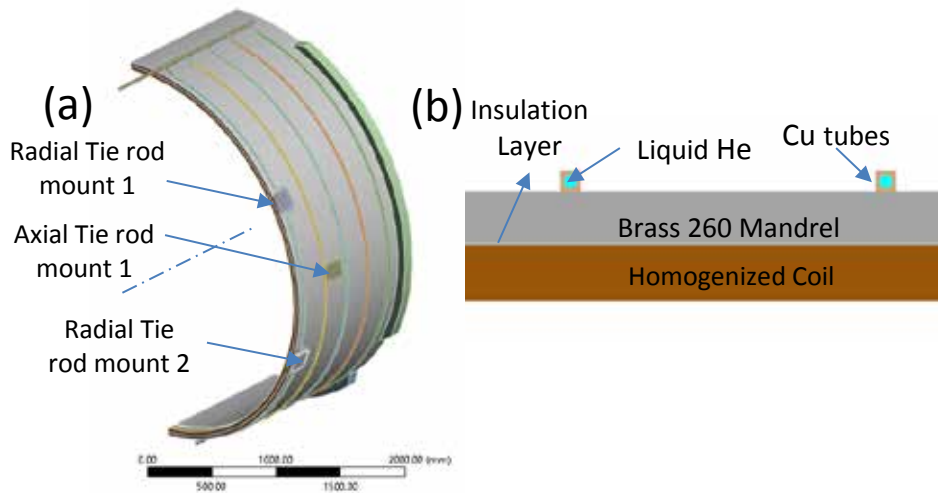


Figure 8.5 (a) FEA half module geometry with (b) cross-section view

A half module geometry (Figure 8.5) is analyzed to take advantage of the symmetry in the cold mass design including the fluid flow layout. The 3D model is simplified for reduced run time by removing small details that would not affect the simulation results significantly.

Electron-Ion Collider, Brookhaven National Laboratory and Thomas Jefferson National Accelerator Facility			
Doc No. EIC-SHC-TN-24-005	Author: Sandesh Gopinath	Effective Date: 12/05/2024	Review Frequency: NA
Process Description: EIC Design Report MARCO Magnet			Revision: 00

Module 1 (near the lepton endcap assembly) is arbitrarily chosen for simulations since each module has the same number of heat exchanger tubes cooling it. The coil is simplified as a homogenous mass.

Only the primary cooling circuit bodies are considered for FEA. The supply and return headers are further simplified to focus more on the heat exchanger tubes in contact with the cold mass.

8.4 FLUENT FEA

The half module primary circuit helium flow was analyzed to simulate the equilibrium and steady-state temperature gradient through the heat exchanger pipes during operation. Assumptions are: (1) forced flow, (2) two-phase flow.

Only the fluid volume is analyzed— without the heat exchanger pipes and the complete cold mass.

8.4.1 Fluid Geometry

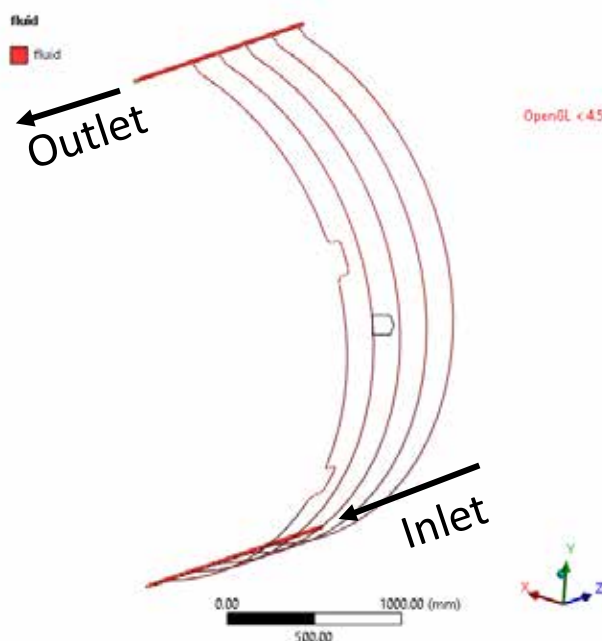


Figure 8.6 FLUENT flow volume with mesh view in the inset

The flow circuit (Figure 8.6) was further simplified compared to Figure 8.5 to add extra length of pipe to simulate a developed and steady flow into the system for better results.

Electron-Ion Collider, Brookhaven National Laboratory and Thomas Jefferson National Accelerator Facility			
Doc No. EIC-SHC-TN-24-005	Author: Sandesh Gopinath	Effective Date: 12/05/2024	Review Frequency: NA
Process Description: EIC Design Report MARCO Magnet			Revision: 00

8.4.2 Fluid Mesh

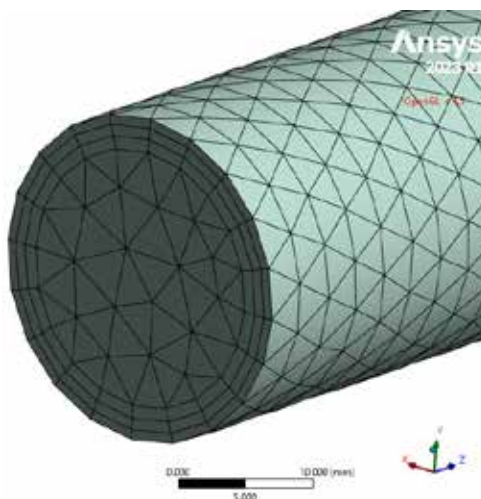


Figure 8.7 Sample mesh through pipe

The geometry is completely comprised of pipes with a maximum of three inflation layers along the pipe boundary for characterization of the heat transfer across the boundaries and for more discrete flow.

8.4.3 Fluid Properties

Table 8.1 Helium Properties considered for simulations

	He 4.5 K Liquid	He 4.55 K Gas
Density (kg/m ³)	119.09	23
Cp (J/(kg K))	6608.3	12880
Therm. Cond. (W/(m K))	0.018803	0.010344
Viscosity (Pa s)	3.02e-06	1.40E-06
Molecular Weight (kg/(kmol))	4	4
Standard state Enthalpy (J/kgmole)	6338.4	80334

Electron-Ion Collider, Brookhaven National Laboratory and Thomas Jefferson National Accelerator Facility			
Doc No. EIC-SHC-TN-24-005	Author: Sandesh Gopinath	Effective Date: 12/05/2024	Review Frequency: NA
Process Description: EIC Design Report MARCO Magnet			Revision: 00

8.4.4 Fluent Boundary Conditions

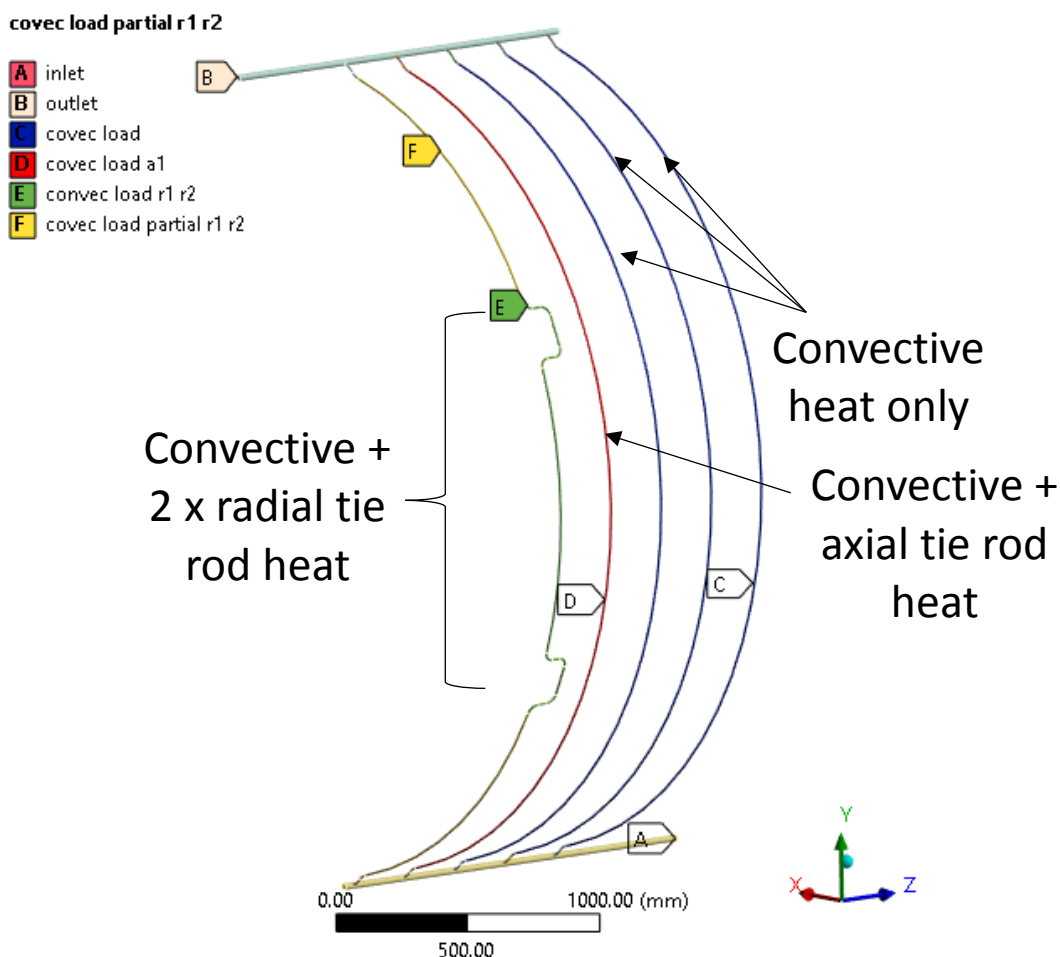


Figure 8.8 FLUENT boundary conditions

The heat load from the tie rods along with the convective head load between the thermal heat shield and the cold mass was applied as a surface flux on selective areas as shown in Figure 8.8.

A Mixture Model with evaporation-condensation phase interaction was utilized; the model homogenized the multiphase flow based on the phase transformation temperature specified. The inlet velocity is set at 0.086 m/s (4.94 g/s liquid helium flow rate) based on analytical flow calculations required to carry the input heat load away from the system with minimal temperature increase. The inlet temperature of the fluid is set at 4.5 K with the phase transformation temperature at 4.55 K and 1.36 bar.

Electron-Ion Collider, Brookhaven National Laboratory and Thomas Jefferson National Accelerator Facility			
Doc No. EIC-SHC-TN-24-005	Author: Sandesh Gopinath	Effective Date: 12/05/2024	Review Frequency: NA
Process Description: EIC Design Report MARCO Magnet			Revision: 00

A worst case convection of 0.3 W/m^2 (compared to 0.1 W/m^2) between the thermal shield and the cold mass was assumed to account for possible leakage, thermal shorts, or multi-layer insulation failure. The total heat load is summarized in Table 8.2.

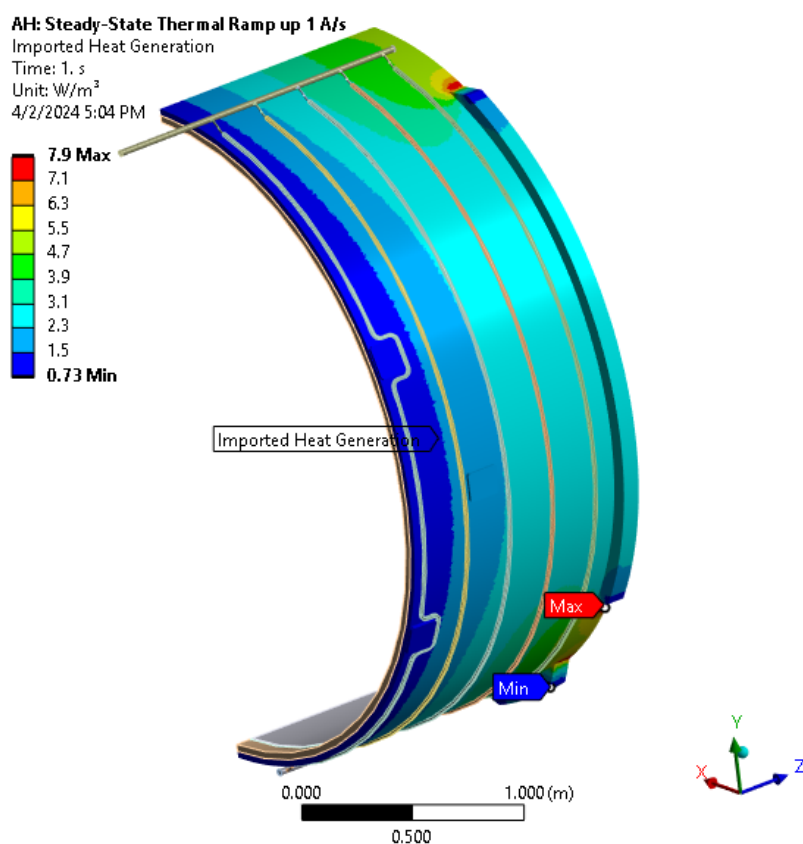


Figure 8.9 Eddy current load during 1.0 A/s ramp up as imported in ANSYS

The eddy current induced heat load during ramp up of the magnet is imported from TOSCA [2]

	Heat input
Radiant heat <i>flux</i>	0.3
total surface	12.67
radiant heat	3.801
radial <i>tr</i>	0.2
axial <i>tr</i>	0.32

The only official copy of this document is the one online in the SharePoint Document Center. Before using a printed copy, verify that it is current by checking the printed document's Revision History log with that of the online version.

Electron-Ion Collider, Brookhaven National Laboratory and Thomas Jefferson National Accelerator Facility			
Doc No. EIC-SHC-TN-24-005	Author: Sandesh Gopinath	Effective Date: 12/05/2024	Review Frequency: NA
Process Description: EIC Design Report MARCO Magnet			Revision: 00

	4.521
--	-------

8.4.5 Results and Discussion

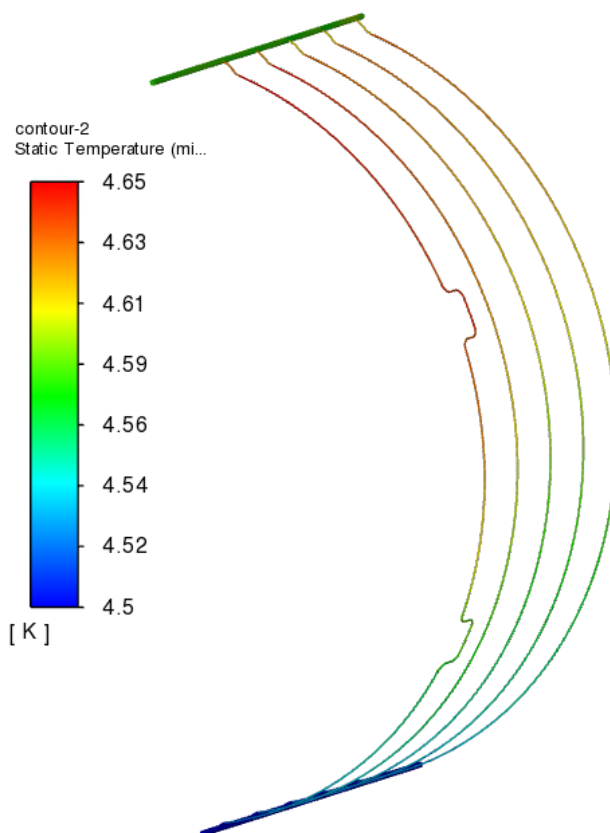


Figure 8.10 Thermosiphon pipe wall temperature distribution

The only official copy of this document is the one online in the SharePoint Document Center. Before using a printed copy, verify that it is current by checking the printed document's Revision History log with that of the online version.

Electron-Ion Collider, Brookhaven National Laboratory and Thomas Jefferson National Accelerator Facility			
Doc No. EIC-SHC-TN-24-005	Author: Sandesh Gopinath	Effective Date: 12/05/2024	Review Frequency: NA
Process Description: EIC Design Report MARCO Magnet			Revision: 00

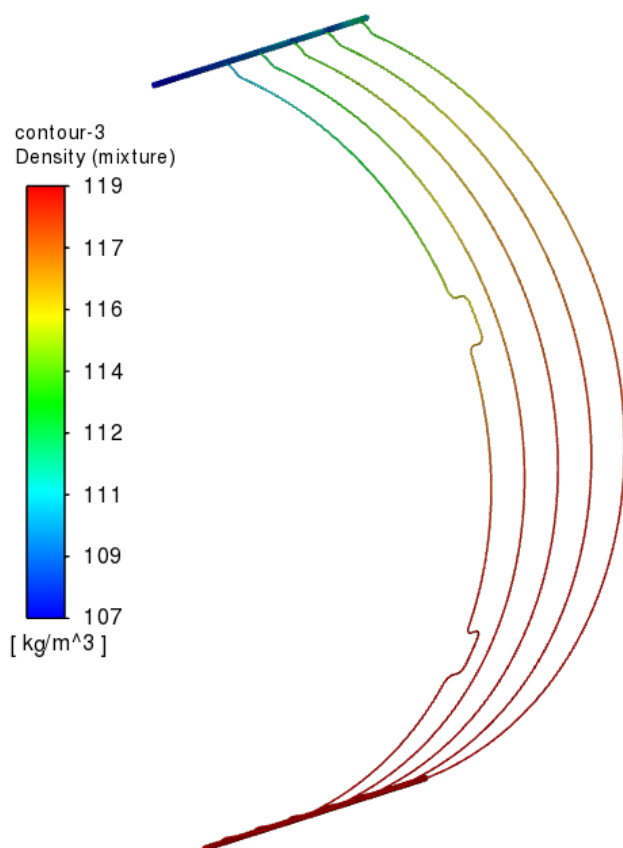


Figure 8.11 Fluid mixture density distribution along the pipe wall. The mixture is single phase at the supply header and gets lighter as it heats up

Electron-Ion Collider, Brookhaven National Laboratory and Thomas Jefferson National Accelerator Facility			
Doc No. EIC-SHC-TN-24-005	Author: Sandesh Gopinath	Effective Date: 12/05/2024	Review Frequency: NA
Process Description: EIC Design Report MARCO Magnet			Revision: 00

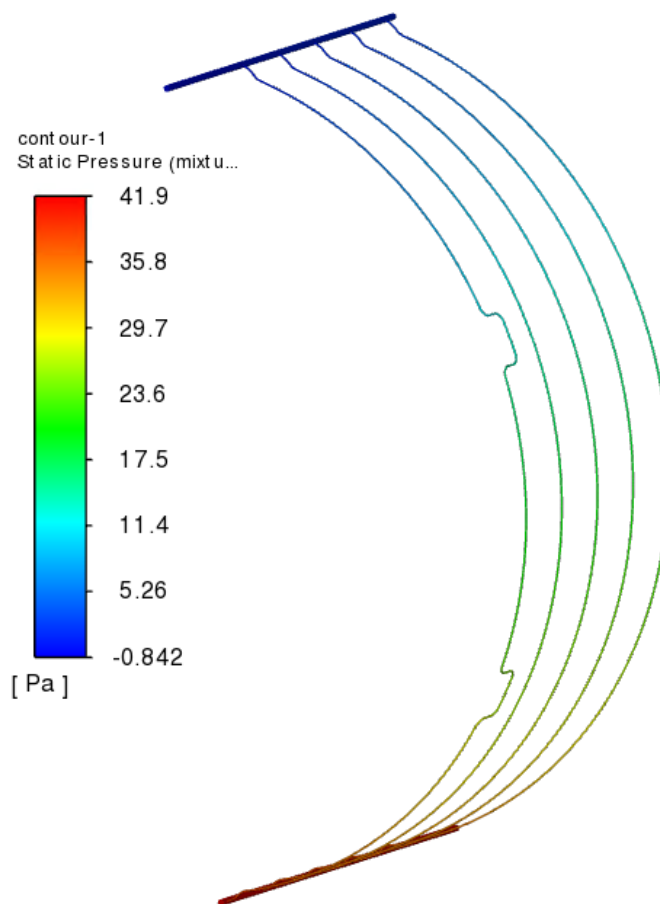


Figure 8.12 Pressure drop across flow path

The peak fluid temperature is 4.65 K near radial tie rod pad (Figure 8.10). The density of the fluid near the pipe wall reduces as the fluid sees more heat and especially after phase change (Figure 8.11).

The vapor quality of helium at the outlet is 2.6% by mass with FEA compared to 3.8% by analytical calculations. The analytical calculation approximates the heat load needed by the 4.5K liquid helium to reach the saturation temperature of 4.55 K. The pressure drop across the flow path is 41 Pa (Figure 8.12).

8.5 Steady State Thermal Analysis

The steady state thermal module in ANSYS workbench is used calculate the temperature gradient across the coil. It utilizes the temperature gradient of the fluid flow from the FLUENT analysis in conjunction with the other thermal boundary conditions.

The only official copy of this document is the one online in the SharePoint Document Center. Before using a printed copy, verify that it is current by checking the printed document's Revision History log with that of the online version.

Electron-Ion Collider, Brookhaven National Laboratory and Thomas Jefferson National Accelerator Facility			
Doc No. EIC-SHC-TN-24-005	Author: Sandesh Gopinath	Effective Date: 12/05/2024	Review Frequency: NA
Process Description: EIC Design Report MARCO Magnet			Revision: 00

8.5.1 Mesh

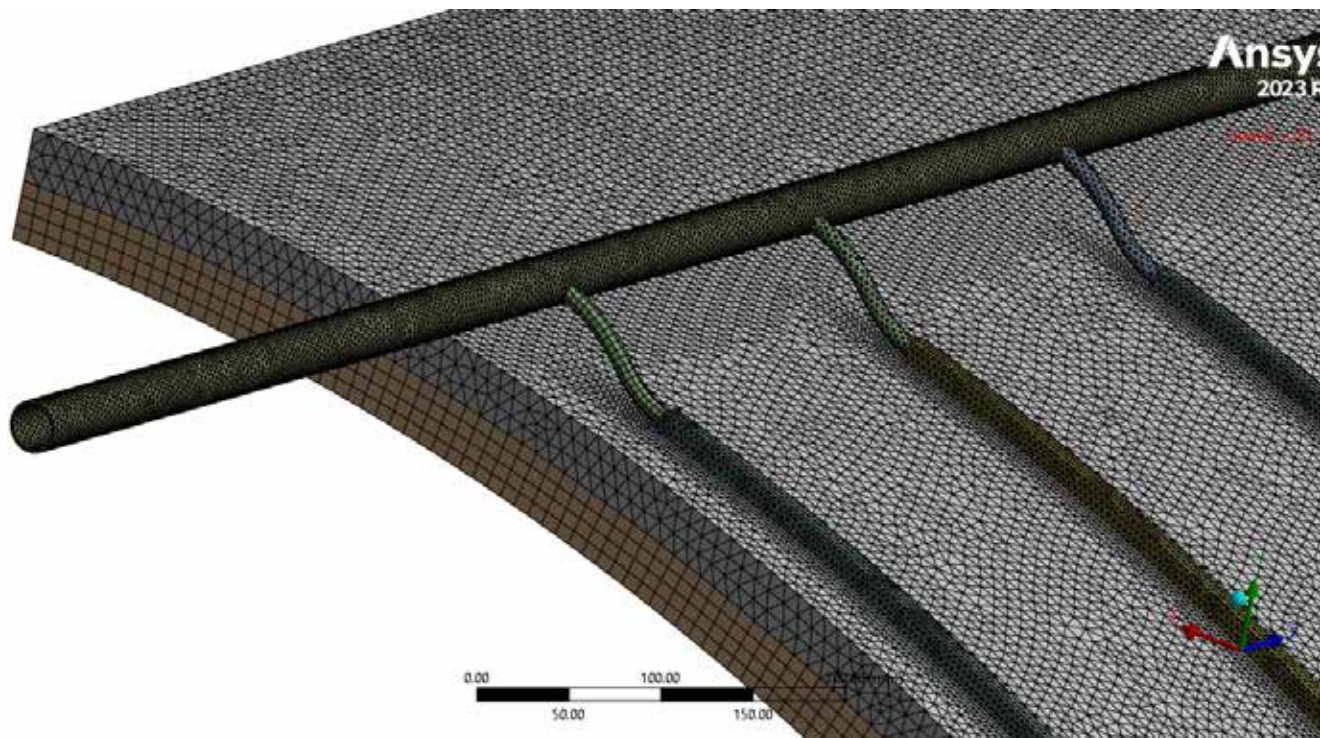


Figure 8.13 Mesh Overview

The model was meshed as in Figure 8.13 with an average mesh quality of 0.82. The coil and the spacers were primarily comprised of Hex8 (Brick) meshes while the mandrel comprised of Tet4(tetrahedral) mesh with all bodies having a minimum of 3 elements through the thickness.

8.5.2 Material Properties

The only official copy of this document is the one online in the SharePoint Document Center. Before using a printed copy, verify that it is current by checking the printed document's Revision History log with that of the online version.

Electron-Ion Collider, Brookhaven National Laboratory and Thomas Jefferson National Accelerator Facility			
Doc No. EIC-SHC-TN-24-005	Author: Sandesh Gopinath	Effective Date: 12/05/2024	Review Frequency: NA
Process Description: EIC Design Report MARCO Magnet			Revision: 00

Table 8.2 Material Properties

		Fiber glass		G10		AgSn 3.5% 96,5%		Copper		NbTi		Brass		Ti6Al4V	
Properties	Unit	293 K	4 K	293 K	4 K	293 K	4 K	293 K	4 K	293 K	4 K	293 K	4 K	293 K	4 K
Density	Kg/m ³	1948		1948		9510		8960		6550		8525		4540	
CTE 293 K to 4 K (X)	%	0.246		0.246		0.43		0.32		0.15		0.38		0.18	
CTE 293 K to 4 K (Y)	%	0.246		0.246											
CTE 293 K to 4 K (Z)	%	0.717		0.717											
Thermal Conductivity (X)	W/(m K)	0.814	0.063	0.814	0.063	76.69	250.74	398	628	9.44	0.176	115	3.59	7.7	0.403
Thermal Conductivity (Y)	W/(m K)	0.814	0.063	0.814	0.063										
Thermal Conductivity (Z)	W/(m K)	0.626	0.052	0.626	0.052										
Yield strength	MPa					48		69	86			413	517	1030	1693
Tensile strength	MPa	257	496	257	496			200	455						

Table 8.3 Homogenized conductor properties

Name	Unit	Values 293 K	Values 4 K
Density	Kg/m ³	7965.8	7965.8
Thermal expansion coef 1	K ⁻¹	1.360E-05	9.228E-06
Thermal expansion coef 2	K ⁻¹	1.361E-05	9.190E-06
Thermal expansion coef 3	K ⁻¹	1.408E-05	9.104E-06
Thermal Conductivity 1	W/(m K)	155.59	296.01

The only official copy of this document is the one online in the SharePoint Document Center. Before using a printed copy, verify that it is current by checking the printed document's Revision History log with that of the online version.

Electron-Ion Collider, Brookhaven National Laboratory and Thomas Jefferson National Accelerator Facility			
Doc No. EIC-SHC-TN-24-005	Author: Sandesh Gopinath	Effective Date: 12/05/2024	Review Frequency: NA
Process Description: EIC Design Report MARCO Magnet			Revision: 00

Thermal Conductivity 2	W/(m K)	164.23	324.88
Thermal Conductivity 3	W/(m K)	221.91	501.01

Electron-Ion Collider, Brookhaven National Laboratory and Thomas Jefferson National Accelerator Facility			
Doc No. EIC-SHC-TN-24-005	Author: Sandesh Gopinath	Effective Date: 12/05/2024	Review Frequency: NA
Process Description: EIC Design Report MARCO Magnet			Revision: 00

Temperature dependent properties are used for all components.

8.5.3 Boundary Condition

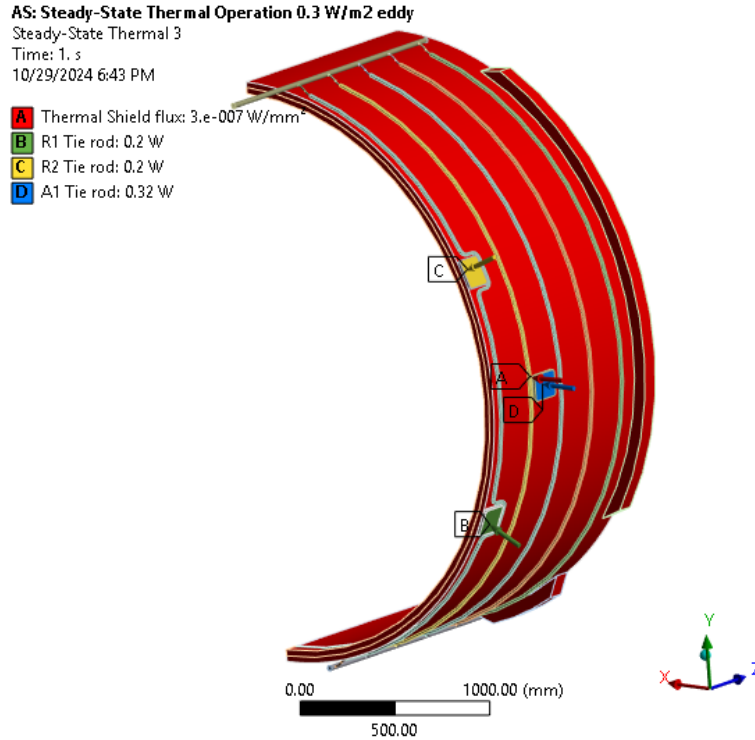


Figure 8.14 Steady State FEA boundary conditions

Latent heat of vaporization (18.13 W per 1.0 g/s of 4.55 K Helium flow) is the main source of cooling of the cold mass. The fluid temperature result from FLUENT is imported as a boundary condition on the pipe wall in steady state thermal.

Table 8.4 Summary of boundary conditions

Convection heat flux	0.30 W/m ²
Axial Tie rod heat load	0.32 W
Radial Tie rod heat load	0.20 W
Ramp up heat load	0.535 W (half module)
Total operational heat load	5.0 W per half-module

8.5.4 Results and Discussion

The peak temperature (5.25 K) on the cold mass and the coil are localized on the radial tie rod cold end location (figure 9) . The average temperature of the cold mass is 4.66 K.

The only official copy of this document is the one online in the SharePoint Document Center. Before using a printed copy, verify that it is current by checking the printed document's Revision History log with that of the online version.

Electron-Ion Collider, Brookhaven National Laboratory and Thomas Jefferson National Accelerator Facility			
Doc No. EIC-SHC-TN-24-005	Author: Sandesh Gopinath	Effective Date: 12/05/2024	Review Frequency: NA
Process Description: EIC Design Report MARCO Magnet			Revision: 00

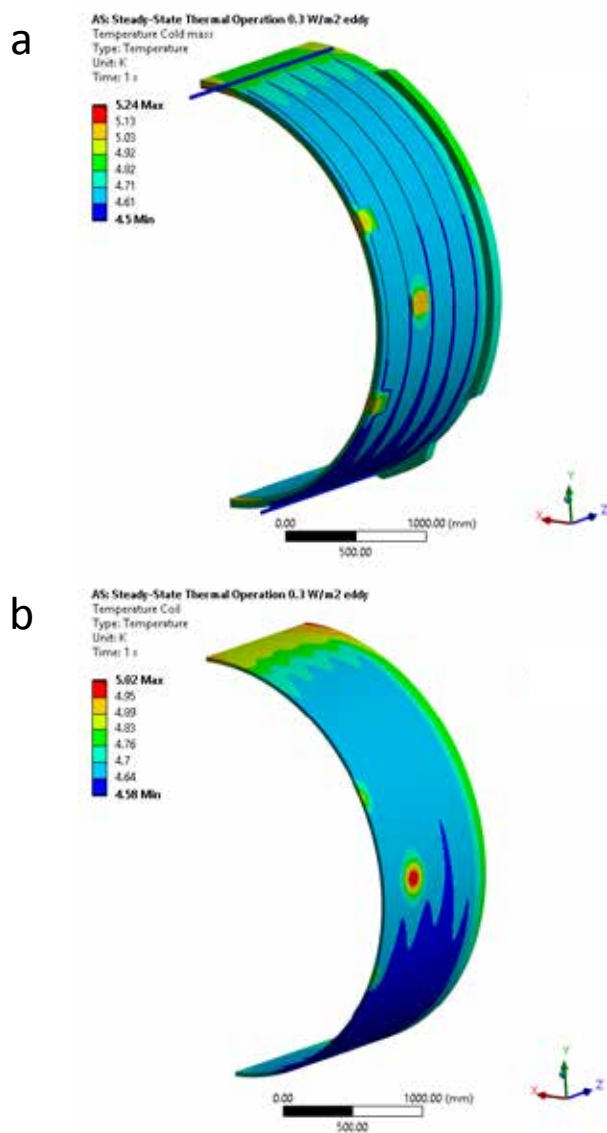


Figure 8.15 Steady state FEA temperature distribution with 1 A/s ramp up eddy current in the (a) cold mass and (b) coil

Electron-Ion Collider, Brookhaven National Laboratory and Thomas Jefferson National Accelerator Facility			
Doc No. EIC-SHC-TN-24-005	Author: Sandesh Gopinath	Effective Date: 12/05/2024	Review Frequency: NA
Process Description: EIC Design Report MARCO Magnet			Revision: 00

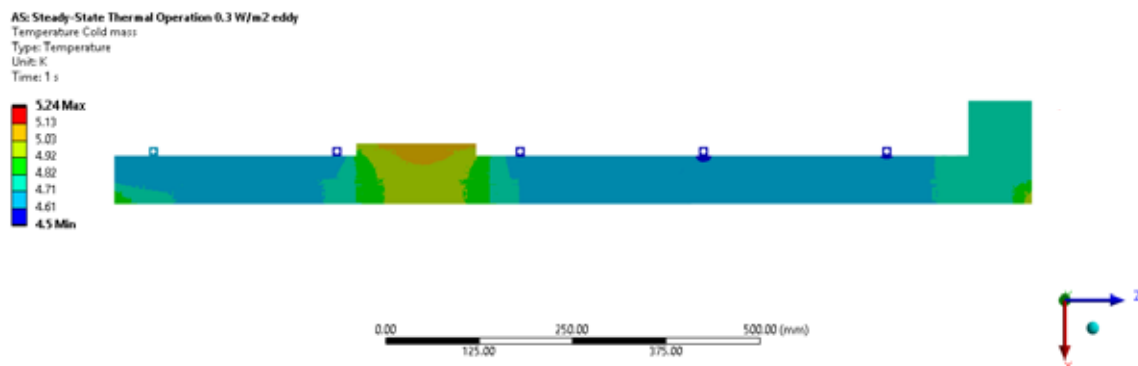


Figure 8.16 Steady state FEA temperature distribution within the cold mass thickness section

The peak temperature of the coil is 5.02 K near the axial tie rod pad. The average temperature of the coil is 4.68 K. Figure 8.17 shows the temperature gradient through the cold mass and the coil is very minimal (less than 0.01 K).

8.6 Cool-down Transient

The cold mass cool-down time is estimated using the transient thermal module in ANSYS workbench. The complete cold mass is simulated from temperatures of 300 K to 50 K.

Assumptions are:

1. Maximum allowable coil temperature gradient is 50 K
2. Thermal shield is conservatively assumed to be 10 K above cold mass up to 60 K.

Ideally thermal shield has the same cool-down temperature as the cold mass – approx. 10 days cool-down time

3. There is only one-way heat transfer between thermal shield and cold mass
4. Initial cold mass temperature is 300 K.

8.6.1 Geometry

The geometry is the same as that in the steady state analysis. It also includes the additional fluid volume.

8.6.2 Mesh

The fluid is meshed using ANSYS Element 116 which is a 1D fluid element and allows for quicker thermal analysis; the element incorporates fluid properties to calculate temperature gradient across the flow path without having to solve fluid flow equations.

The only official copy of this document is the one online in the SharePoint Document Center. Before using a printed copy, verify that it is current by checking the printed document's Revision History log with that of the online version.

Electron-Ion Collider, Brookhaven National Laboratory and Thomas Jefferson National Accelerator Facility			
Doc No. EIC-SHC-TN-24-005	Author: Sandesh Gopinath	Effective Date: 12/05/2024	Review Frequency: NA
Process Description: EIC Design Report MARCO Magnet			Revision: 00



Figure 8.17 1D fluid mesh element 116

8.6.3 Material Properties

Helium gas properties at 10 bar are used for the fluid volume. The rest of the material properties are carried over from the steady state analysis.

8.6.4 Boundary Conditions

Table 8.5 Transient FEA cool-down parameters, highlighted in red are FEA inputs

Time (Days)	helium inlet (K)	Cold mass temp (K)	Thermal shield temp (K)	Radiant flux (W/m ²)	Flow rate (kg/s)	Heat transfer coefficient (W/(m ² K))	Axial Tie rod load (W)	radial Tie rod load (W)
0	300	300	300	0.0	0.01	3189.9	0.00	0.00
1	250	250	260	2.6	0.01	3108.6	0.04	0.02
2	200	200	210	1.4	0.01	3011.7	0.04	0.02
3	150	150	160	0.6	0.01	2892.2	0.04	0.02
4	100	100	110	0.2	0.01	2714.4	0.04	0.02

The only official copy of this document is the one online in the SharePoint Document Center. Before using a printed copy, verify that it is current by checking the printed document's Revision History log with that of the online version.

Electron-Ion Collider, Brookhaven National Laboratory and Thomas Jefferson National Accelerator Facility			
Doc No. EIC-SHC-TN-24-005	Author: Sandesh Gopinath	Effective Date: 12/05/2024	Review Frequency: NA
Process Description: EIC Design Report MARCO Magnet			Revision: 00

5	50	50	60	0.0	0.01	2485.6	0.04	0.02
---	----	----	----	-----	------	--------	------	------

Time dependent inputs based on analytical calculations are applied to the geometry. An analytically calculated heat transfer co-efficient is applied to the heat exchanger tube wall that is in contact with the fluid. The tie rod heat loads are also analytically calculated based on the thermal shield and cold mass temperature.

AK: Transient Thermal 300 K - 50 K

Transient Thermal 2

Time: 1.728e+005 s

4/8/2024 3:43 PM

- A** Thermal Shield flux: 2.633e-006 W/mm²
- B** R1 Tie rod: 2.4789e-002 W
- C** R2 Tie rod: 2.4789e-002 W
- D** A1 Tie rod: 4.1316e-002 W
- E** Mass Flow Rate: 1.e-002 kg/s
- F** Temperature: 250. K
- G** Convection: 250. K, 3.1086e-003 W/mm².K
- G** Edge

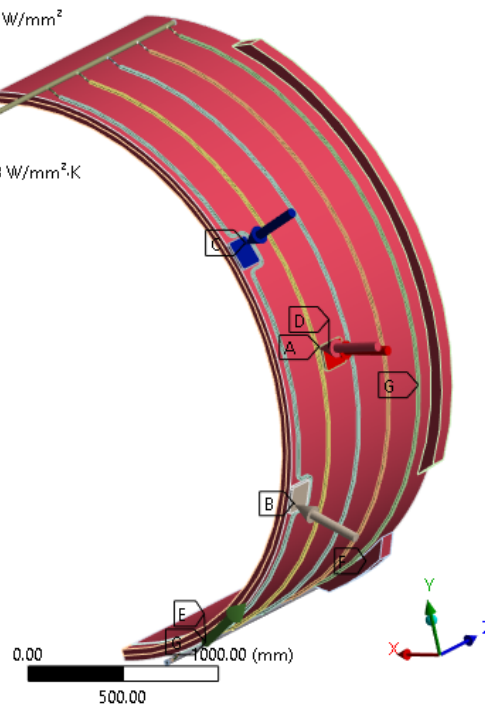


Figure 8.18 Transient FEA - boundary conditions after 2 days

The only official copy of this document is the one online in the SharePoint Document Center. Before using a printed copy, verify that it is current by checking the printed document's Revision History log with that of the online version.

Electron-Ion Collider, Brookhaven National Laboratory and Thomas Jefferson National Accelerator Facility			
Doc No. EIC-SHC-TN-24-005	Author: Sandesh Gopinath	Effective Date: 12/05/2024	Review Frequency: NA
Process Description: EIC Design Report MARCO Magnet			Revision: 00

8.6.5 Results and Discussion

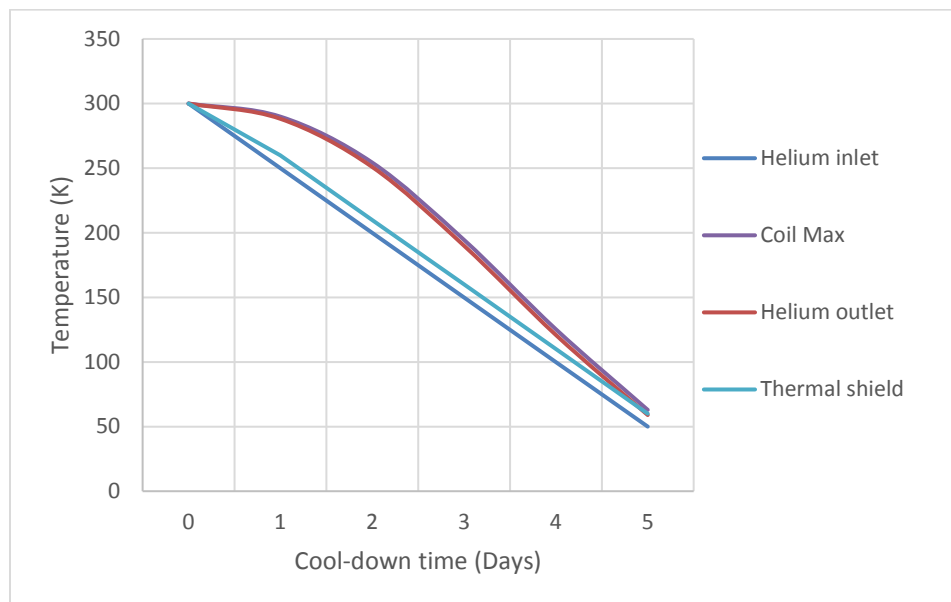


Figure 8.19 Transient FEA results showing duration needed to cool down cold mass from 300 K-50 K

Electron-Ion Collider, Brookhaven National Laboratory and Thomas Jefferson National Accelerator Facility			
Doc No. EIC-SHC-TN-24-005	Author: Sandesh Gopinath	Effective Date: 12/05/2024	Review Frequency: NA
Process Description: EIC Design Report MARCO Magnet			Revision: 00

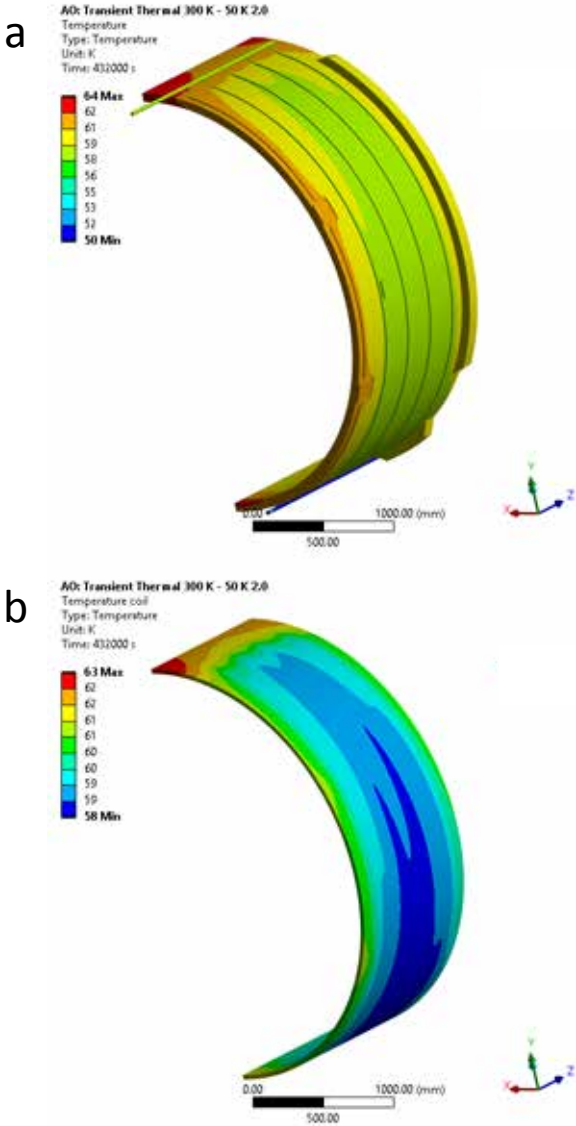


Figure 8.20 Transient FEA temperature distribution in the a. cold mass and b. coil after 5 days of cool down

With a 10 g/s helium gas flow, the coil maximum temperature is shown in figure 19. The peak temperature gradient on the cold mass is 31 K and on the coil is 3 K. The analysis shows a total of 5 days is needed to cool the cold mass while considering the aforementioned conservative assumptions. This duration can be increased by throttling the flow if required. Once the cold mass reaches 50 K, 4.5 K liquid helium is introduced in to the heat exchanger tubes which utilizes the latent heat of vaporization to reduce the temperature of the cold mass. This is not simulated due to the complex nature of film boiling but is analytically estimated.

The only official copy of this document is the one online in the SharePoint Document Center. Before using a printed copy, verify that it is current by checking the printed document's Revision History log with that of the online version.

Electron-Ion Collider, Brookhaven National Laboratory and Thomas Jefferson National Accelerator Facility			
Doc No. EIC-SHC-TN-24-005	Author: Sandesh Gopinath	Effective Date: 12/05/2024	Review Frequency: NA
Process Description: EIC Design Report MARCO Magnet			Revision: 00

8.7 Summary

Detailed analyses were performed; the results show the temperature gradients across coil and helium flow path is acceptable during Operation, Ramp up, and Cool-down. Steady State and Transient analyses were conducted. Fluid density variation during operation was validated. Analysis are developed to quickly incorporate future manufacturing design iterations as and when suggested by the vendor.

Electron-Ion Collider, Brookhaven National Laboratory and Thomas Jefferson National Accelerator Facility			
Doc No. EIC-SHC-TN-24-005	Author: Sandesh Gopinath	Effective Date: 12/05/2024	Review Frequency: NA
Process Description: EIC Design Report MARCO Magnet			Revision: 00

9 Quench Protection and Analysis

This section gives the details of quench analysis and the quench protection circuit design.

9.1 Transient Analysis

The transient analysis is performed for the magnet during different ramp-up and ramp-down scenarios. Since the mandrel is made from Brass 70/30, it plays a noticeable role during the transients of the magnet—in particular, during ramp-up / ramp-down, fast discharge, and quench. Its magnetic behavior has been simulated using OPERA.

9.1.1 Ramp-up and Ramp-down

The ramping rate (up and down) of the magnet is 1.0 A/s, which is a compromise found between ramping the magnet in approximately one hour and not overheating it at the same time due to the mandrel dissipated power. This case has been used to define the main magnetic specifications of the mandrel. Results are reported in Table 9.1; the current density distribution, in Figure 9.1. The impact of the flanges is significant, showing that the current tends to pass through them between the adjacent modules.

Table 9.1 – Ramp-up / ramp-down results and main magnetic parameters of the mandrel

Parameter	Values	Unit
Initial Current	0	A
Ramping Rate	1.0	A/s
Power	3.642	W
Eddy Current at $t = +\infty$	-1015.	A
R [mandrel (P/I^2)]	3.516	$\mu\Omega$
M (mandrel)	3.570	mH
L (mandrel)	2.346	μH
K (coupling coefficient between the mandrel and the coils)	0.964	

Electron-Ion Collider, Brookhaven National Laboratory and Thomas Jefferson National Accelerator Facility			
Doc No. EIC-SHC-TN-24-005	Author: Sandesh Gopinath	Effective Date: 12/05/2024	Review Frequency: NA
Process Description: EIC Design Report MARCO Magnet			Revision: 00

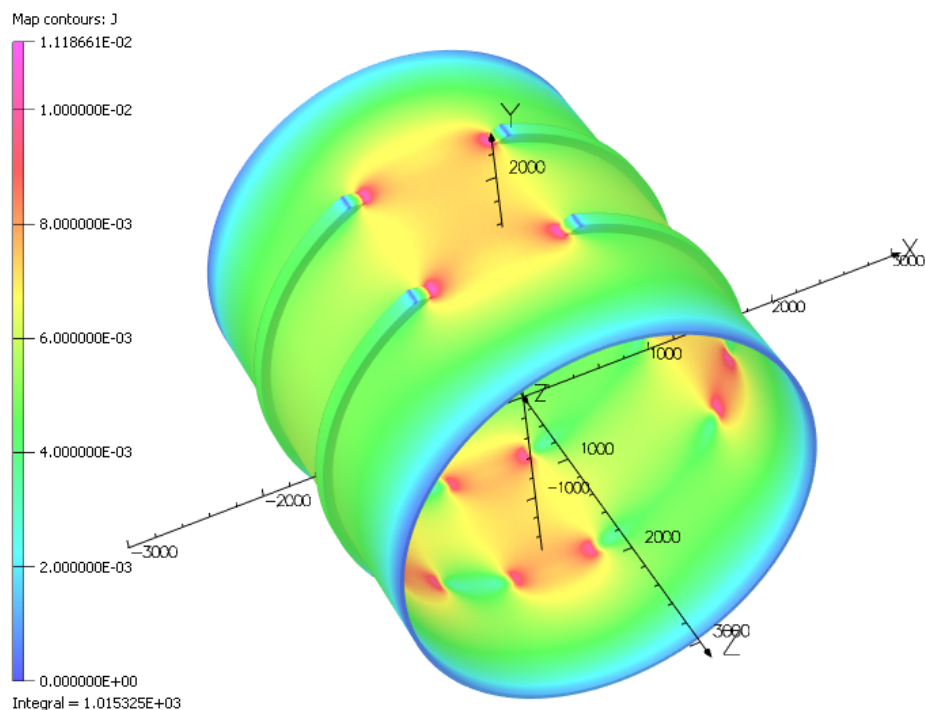


Figure 9.1 Current density distribution in the mandrel during ramp-up

9.1.2 Fast Discharge

Fast discharge is the worst case for induced eddy currents in the mandrel due to the dump resistor of the circuit, since the di/dt is the highest at the beginning of the discharge. In this case, the mandrel behaves as shown in Figure 9.2 and Figure 9.3

The current in the mandrel can increase up to 165 kA in 0.3 s; a vertical force of F_y of -22 kN acts on the mandrel, due to the asymmetric distribution of the eddy currents around the flanges.

The only official copy of this document is the one online in the SharePoint Document Center. Before using a printed copy, verify that it is current by checking the printed document's Revision History log with that of the online version.

Electron-Ion Collider, Brookhaven National Laboratory and Thomas Jefferson National Accelerator Facility			
Doc No. EIC-SHC-TN-24-005	Author: Sandesh Gopinath	Effective Date: 12/05/2024	Review Frequency: NA
Process Description: EIC Design Report MARCO Magnet			Revision: 00

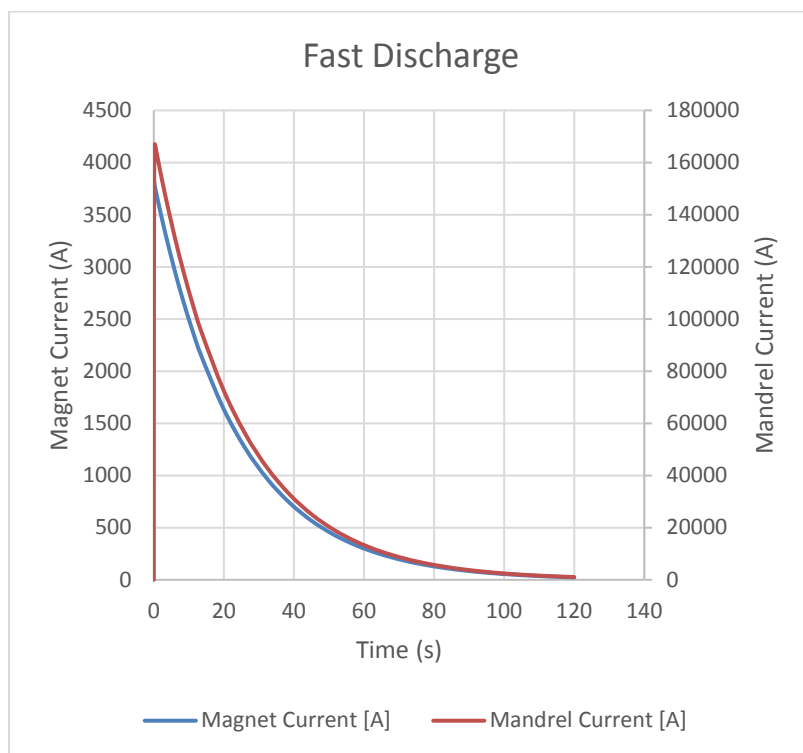


Figure 9.2 Current decay of the mandrel and the magnet during a fast discharge

Electron-Ion Collider, Brookhaven National Laboratory and Thomas Jefferson National Accelerator Facility			
Doc No. EIC-SHC-TN-24-005	Author: Sandesh Gopinath	Effective Date: 12/05/2024	Review Frequency: NA
Process Description: EIC Design Report MARCO Magnet			Revision: 00

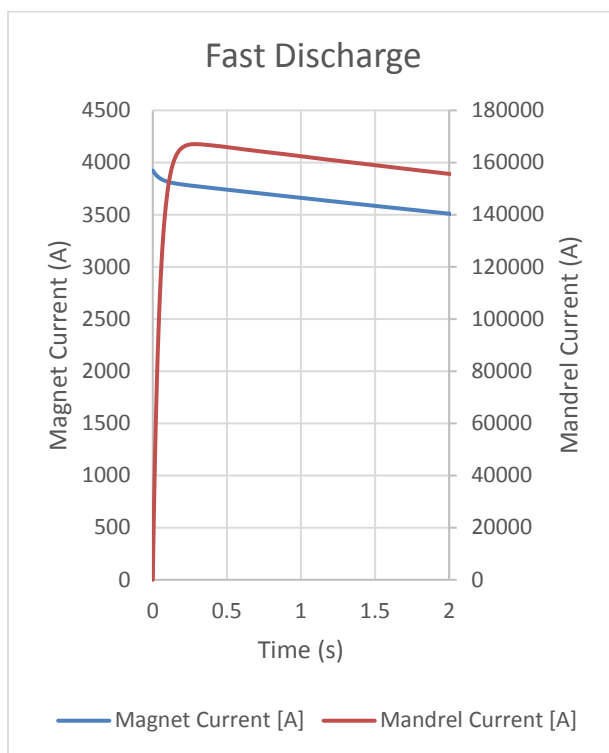


Figure 9.3 A zoom-in view on the first seconds of the fast discharge. Current decays of the mandrel and of the magnet are shown.

9.2 Quench Analysis

A detailed quench analysis is performed to protect the magnet. The quench protection is designed based on the quench analysis. Analytical calculations of a single coil quench calculation is performed and a detailed quench analysis is performed in COMSOL.

9.2.1 Single coil quench analysis

The analysis of MARCO magnet design carried out to evaluate primarily the “Hot spot temperature” and other quench parameters in case of the magnet/coil quenches or becomes normal under any operating conditions.

The following are the steps taken to perform the analysis-

A. Coil/magnet design - Conductor design and basic magnet parameters

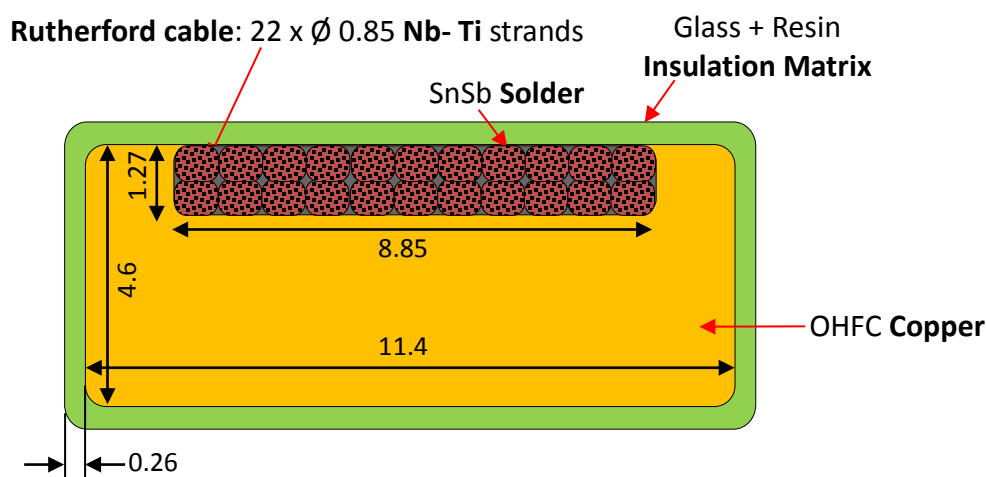
Table 9.2 : Conductor design parameters

Description	Unit	Value(s)
Copper Fraction Cu:Sc ratio (Strand)	[]	1.31
Cu:Sc ratio (overall)	[]	8.6
Strand Wire diameter	mm	0.847

The only official copy of this document is the one online in the SharePoint Document Center. Before using a printed copy, verify that it is current by checking the printed document's Revision History log with that of the online version.

Electron-Ion Collider, Brookhaven National Laboratory and Thomas Jefferson National Accelerator Facility			
Doc No. EIC-SHC-TN-24-005	Author: Sandesh Gopinath	Effective Date: 12/05/2024	Review Frequency: NA
Process Description: EIC Design Report MARCO Magnet			Revision: 00

Strand wire, RRR	[]	100
Number of wire strand	[]	22
Bare conductor	mm x mm	11.4 x 4.6
Channel dimension	mm x mm	8.85 x 1.41
Copper stabilizer, RRR	[]	100 (for Magnet design purpose only)
Total Copper Cross section Area	mm ²	46.99
Total NbTi	mm ²	5.366
Insulation thickness (around)	mm	0.26
Unit cell (Overall insulated conductor)	mm ²	61.03
A _{cu}	mm ²	46.991
A _{solder}	mm ²	0.08
A _{ins}	mm ²	8.59
I _c (cable) at 4.22K -	-	2T, 15.61kA; 4.5T, 10.94kA
Number of filaments	[]	468



Dimensions in mm

Figure 9.4 MARCO Conductor cross section showing copper stabilizer and superconducting strands

Table 9.3 Magnet design parameters

Description	Unit	Value(s)
Total number of turns per layer	[]	278
Total number of layers	[]	6
Number of coils in the magnet configuration	[]	3
Average perimeter length/turn (Lp)	m	9.6
AT required (designed)	MA	6.589
I _{op} (Operating current)	A	3950
B(0) / Bmax	T	2.0 / 2.6
T _{op} (Operating temperature)	K	4.7
L (Total Inductance)	H	5.94

Electron-Ion Collider, Brookhaven National Laboratory and Thomas Jefferson National Accelerator Facility			
Doc No. EIC-SHC-TN-24-005	Author: Sandesh Gopinath	Effective Date: 12/05/2024	Review Frequency: NA
Process Description: EIC Design Report MARCO Magnet			Revision: 00

E (Magnet stored Energy)	MJ	46.34
--------------------------	----	-------

B. The assumptions made long with the results of the single coil quench analysis carried out are presented below.

1. Assumptions
 - a) Average density of the winding (proportional to the cross-section area fraction)
 - b) Average specific heat (proportional to the cross-section area fraction)
 - c) Coil resistivity with an assumption that Solder and NbTi is 100 times of copper (magneto resistance considered)
 - d) Bottura's Model is used for $J_c/B_c/T_c$ calculations

Coil model –

- e) H_L = Coil thickness = 32.73 mm
- f) W_T = Coil length = 3317 mm
- g) L_p = Average perimeter length = 9587 mm
- h) γ_{av} = Average winding density = 7787 kg/m³

$$\text{Coil mass: } M_1 = H_L \cdot \frac{W_T}{3} \cdot L_p \cdot \gamma_{av} \quad M_1 = 2.702 \times 10^3 \text{ kg}$$

$$C_{av}(\theta_0) = 0.178 \cdot \text{J} \cdot \text{kg}^{-1} \cdot \text{K}^{-1} \quad C_{av}(295\text{K}) = 3.913 \times 10^6 \cdot \text{J} \cdot \text{kg}^{-1} \cdot \text{K}^{-1}$$

2. Results
 - a) $T_c = 8.29 \text{ K}$, $T_g = 7.30 \text{ K}$, $T_s = 7.79 \text{ K}$, dT (margin) = 2.6 K (wrt T_g)
 - b) Wilson model – $v(z) = 3.1 \text{ m/s}$, $v(tt) = 0.0.123 \text{ m/s}$, $v(II) = 0.187 \text{ m/s}$
 - c) $L_{MPZ} = 14.7 \text{ mm}$, Minimum Quench Energy (MQE) = 102 mJ, Movement of wire by 0.22 mm can initiate the quench
 - d) Hot Spot temperature = 92.7 K in 7.97 s, $V_{max} = 980 \text{ V}$
 - e) This is considering all 46 MJ dumped in 1/3 coil magnet configuration (one coil)
 - f) With the coil only weight and heat capacity (approximated at varying temperature) the maximum temperature is expected to be about 84K
 - g) Along with the single coil quench calculation, MIITs calculations were carried out with worst case scenario and the results are as follows-
 - i. MIITs (with copper only) and limited to 150 K temp = 201.7 MA².s (Max)
 - ii. MIITs without Dump Resistor, 4634 MA².s
 - iii. MIITs with Dump resistor, $R_D = 0.25 \text{ Ohms}$ = 178.3 MA².s
 - iv. Quench detection time with $R_D = 1.5 \text{ seconds}$

The only official copy of this document is the one online in the SharePoint Document Center. Before using a printed copy, verify that it is current by checking the printed document's Revision History log with that of the online version.

Electron-Ion Collider, Brookhaven National Laboratory and Thomas Jefferson National Accelerator Facility			
Doc No. EIC-SHC-TN-24-005	Author: Sandesh Gopinath	Effective Date: 12/05/2024	Review Frequency: NA
Process Description: EIC Design Report MARCO Magnet			Revision: 00

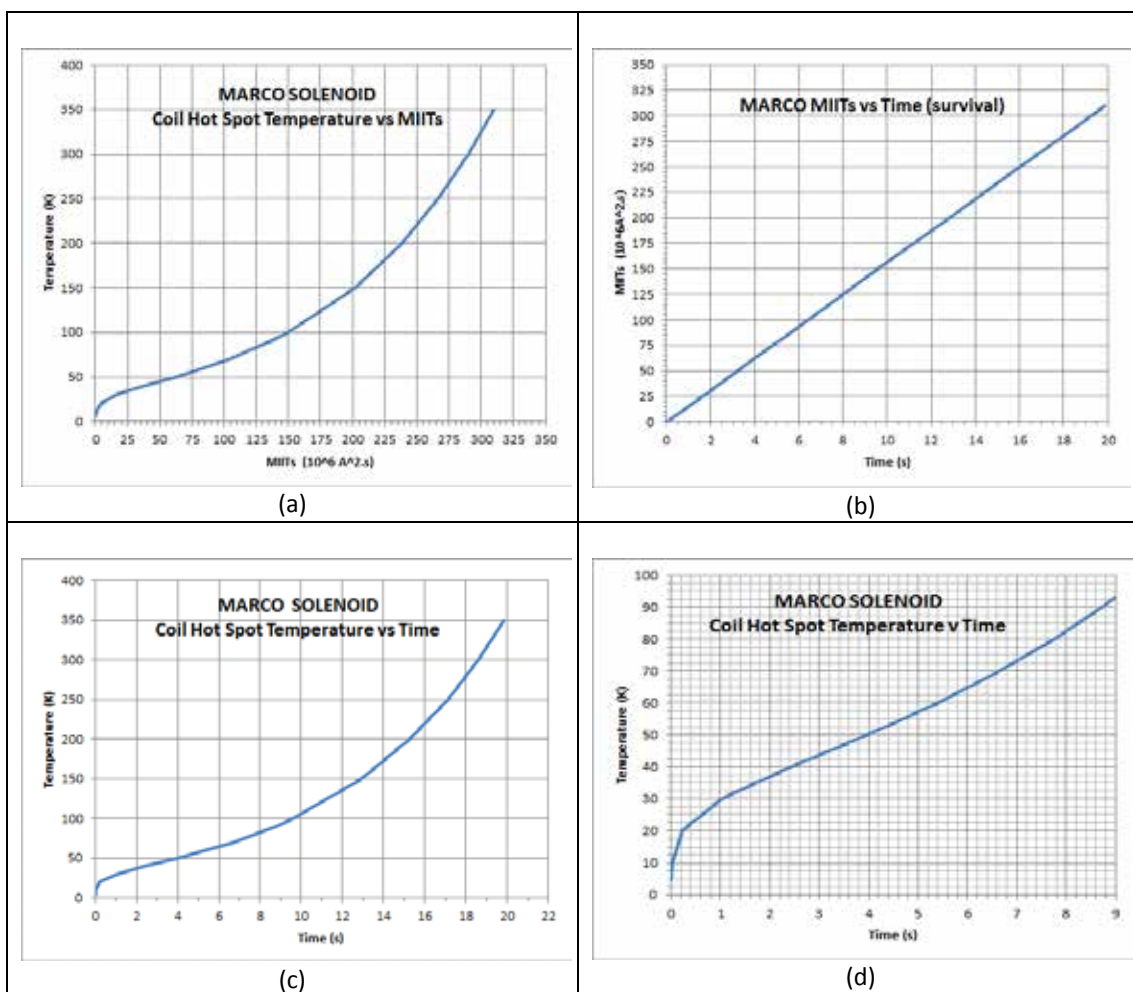


Figure 9.5 MIITs plots for the magnet evaluation - (a) Plot showing the Coil Hot spot temperature vs MIITs (b) The plot showing the magnet/coil survival time wrt to MIITs, and (c) The Coil hot spot temperature with time evaluated based on MIITs, (d) the coil hot spot temperature in first few seconds (MIITs estimate)

Electron-Ion Collider, Brookhaven National Laboratory and Thomas Jefferson National Accelerator Facility			
Doc No. EIC-SHC-TN-24-005	Author: Sandesh Gopinath	Effective Date: 12/05/2024	Review Frequency: NA
Process Description: EIC Design Report MARCO Magnet			Revision: 00

9.2.2 Quench analysis in COMSOL

The quench analysis has been conducted using COMSOL, with a coupled 2D axisymmetric FE model and 1D model to consider the heat propagation—both for transverse propagation and axial propagation. The logic structure of the model is shown in Figure 9.6.

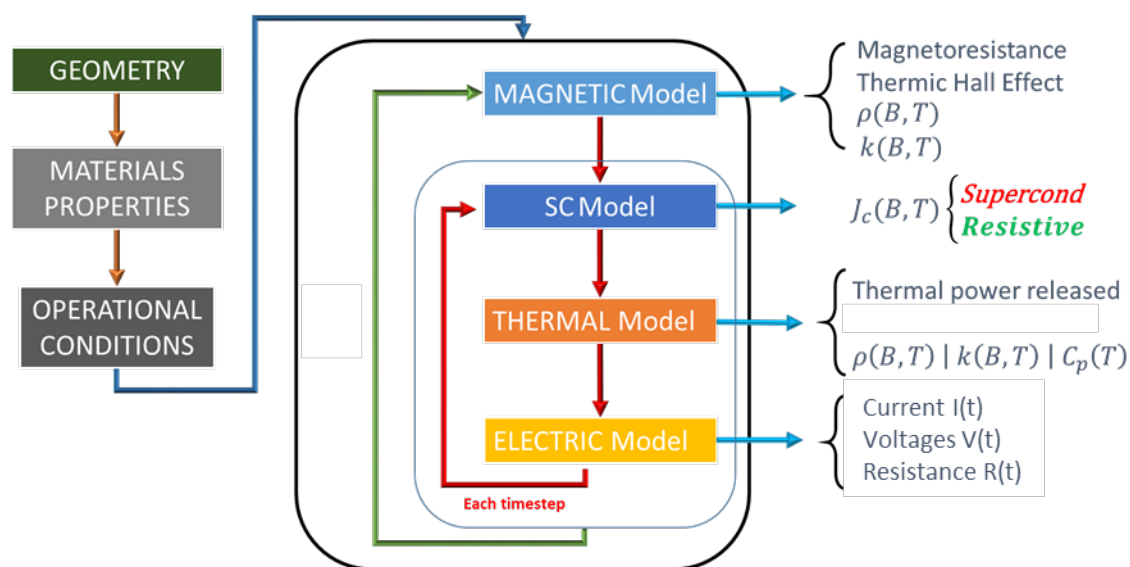


Figure 9.6 Logic structure of the COMSOL quench model

Once the geometry, material properties and operational conditions are defined, the magnetic model is solved to determine the resistivity (ρ) of each element with respect to the magnetic field and thermal conductivity (k). Once the magnetic field and materials properties are defined over the domain, the model calculates the critical current density J_c and solves the coupled thermal and electric model associated to the geometry.

The model considers the full geometry of the magnet, and it defines every turn with details of the conductor. The conductor is represented by a homogenized material (homogenized cable and copper stabilizer). The insulation is modelled separately to consider its own material

The only official copy of this document is the one online in the SharePoint Document Center. Before using a printed copy, verify that it is current by checking the printed document's Revision History log with that of the online version.

Electron-Ion Collider, Brookhaven National Laboratory and Thomas Jefferson National Accelerator Facility			
Doc No. EIC-SHC-TN-24-005	Author: Sandesh Gopinath	Effective Date: 12/05/2024	Review Frequency: NA
Process Description: EIC Design Report MARCO Magnet			Revision: 00

properties. A representation of the geometry is shown in Figure 9.7.

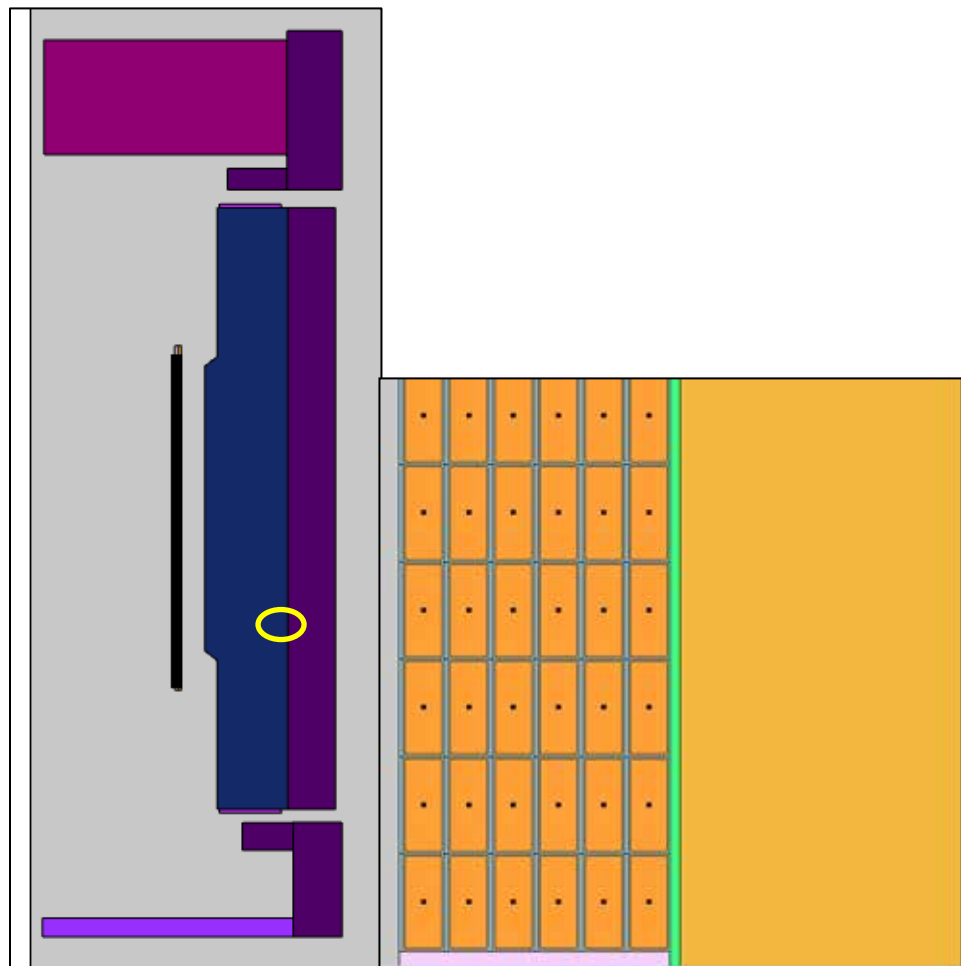


Figure 9.7 Model used in COMSOL. The overall geometry includes the yoke. A zoom-in view on the area marked with the yellow circle is shown, which illustrates the turns, interlayer insulation, ground insulation, and mandrel.

The only official copy of this document is the one online in the SharePoint Document Center. Before using a printed copy, verify that it is current by checking the printed document's Revision History log with that of the online version.

Electron-Ion Collider, Brookhaven National Laboratory and Thomas Jefferson National Accelerator Facility			
Doc No. EIC-SHC-TN-24-005	Author: Sandesh Gopinath	Effective Date: 12/05/2024	Review Frequency: NA
Process Description: EIC Design Report MARCO Magnet			Revision: 00

The material properties are from Cryocomp (P. Eckels, 1993). The thermal hall effect (Figure 9.8) and magnetoresistivity (Figure 9.9) in copper are considered.

Conductor Thermal Conductivity (W/mK)

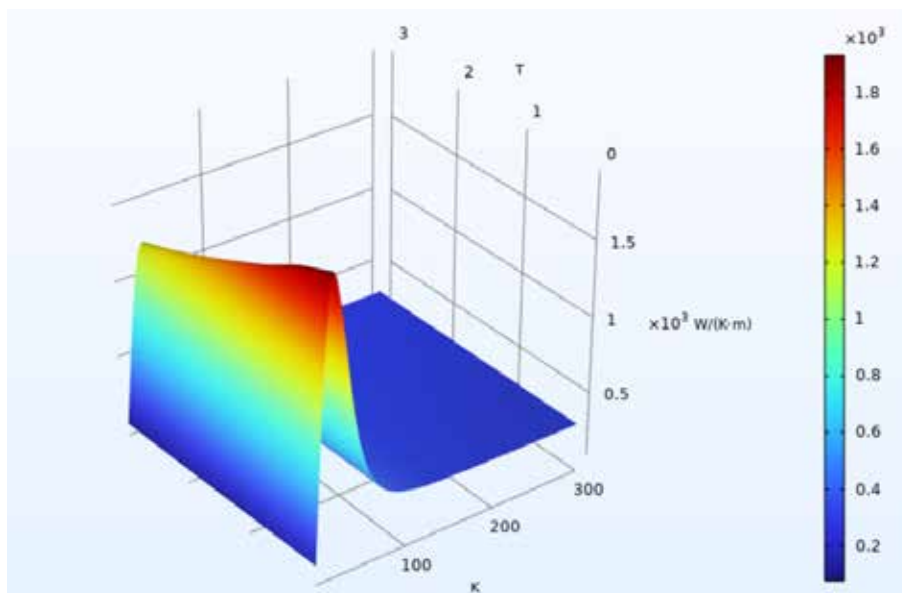


Figure 9.8 Conductor thermal conductivity.

The only official copy of this document is the one online in the SharePoint Document Center. Before using a printed copy, verify that it is current by checking the printed document's Revision History log with that of the online version.

Electron-Ion Collider, Brookhaven National Laboratory and Thomas Jefferson National Accelerator Facility			
Doc No. EIC-SHC-TN-24-005	Author: Sandesh Gopinath	Effective Date: 12/05/2024	Review Frequency: NA
Process Description: EIC Design Report MARCO Magnet			Revision: 00

Conductor Electrical Resistivity ($\Omega \text{ m}$)

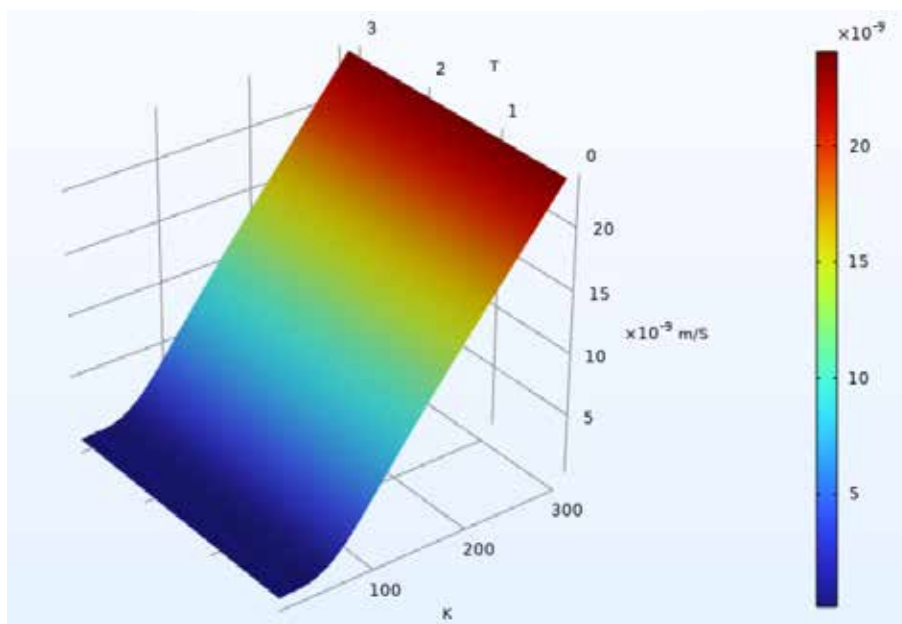


Figure 9.9 Conductor electrical resistivity

Electron-Ion Collider, Brookhaven National Laboratory and Thomas Jefferson National Accelerator Facility			
Doc No. EIC-SHC-TN-24-005	Author: Sandesh Gopinath	Effective Date: 12/05/2024	Review Frequency: NA
Process Description: EIC Design Report MARCO Magnet			Revision: 00

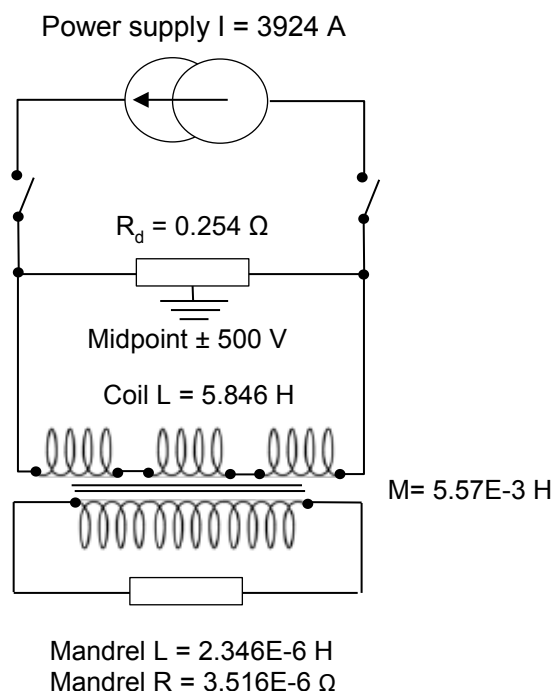


Figure 9.10 MARCO electrical circuit

The quench starts at the bottom angle of MOD1, where the peak magnetic field is located. The case studied is the one at the nominal current (3924 A) and nominal temperature (4.7 K). Once the quench starts and after that the resistive tension reaches 1 V, a validation time of 1 s is needed to validate the quench and open the breakers to activate the dump resistance. The electrical circuit is shown in Figure 9.10. A dump resistance of 0.254Ω is used to limit the maximum voltage to 1000 V.

The magnetic model is solved by COMSOL with the same geometry and material properties used in the OPERA model as described in section 3.4.

The results of two models agree with each other. Figure 9.11 and Figure 9.12 respectively show the magnetic field and the resistivity of each turn of MOD1, presented here as an example.

The only official copy of this document is the one online in the SharePoint Document Center. Before using a printed copy, verify that it is current by checking the printed document’s Revision History log with that of the online version.

Electron-Ion Collider, Brookhaven National Laboratory and Thomas Jefferson National Accelerator Facility			
Doc No. EIC-SHC-TN-24-005	Author: Sandesh Gopinath	Effective Date: 12/05/2024	Review Frequency: NA
Process Description: EIC Design Report MARCO Magnet			Revision: 00

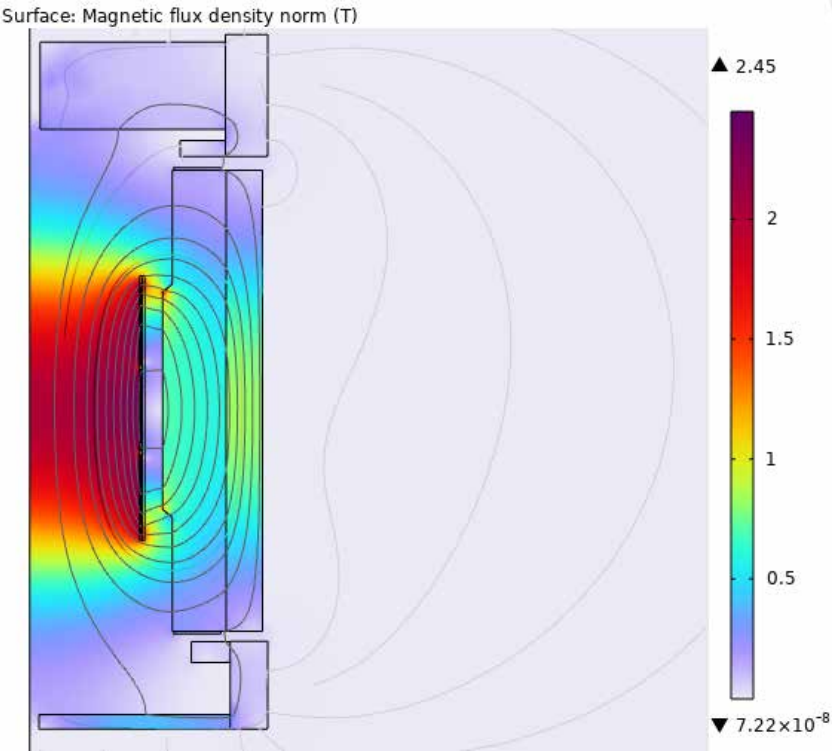


Figure 9.11 Magnetic field computed by COMSOL

Electron-Ion Collider, Brookhaven National Laboratory and Thomas Jefferson National Accelerator Facility			
Doc No. EIC-SHC-TN-24-005	Author: Sandesh Gopinath	Effective Date: 12/05/2024	Review Frequency: NA
Process Description: EIC Design Report MARCO Magnet			Revision: 00

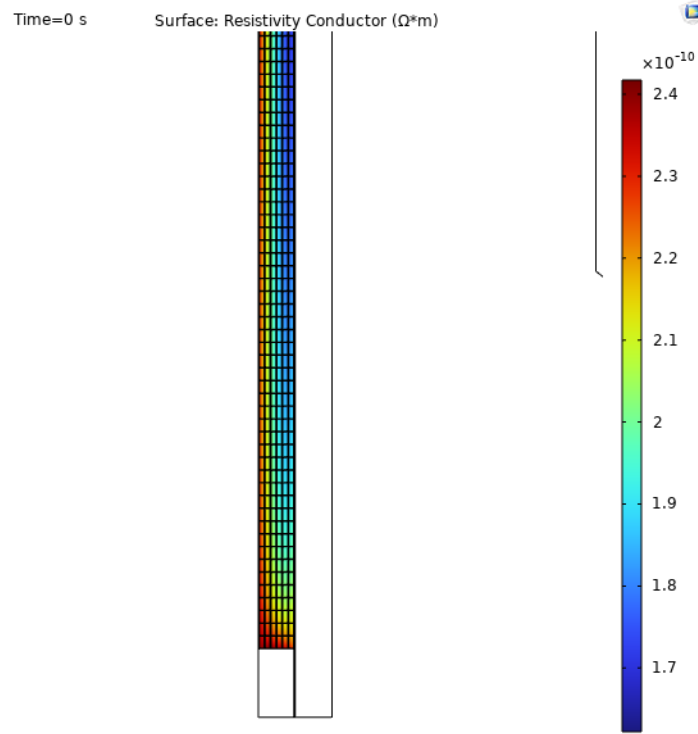


Figure 9.12 Conductor resistivity for MOD

The superconducting model calculates at every turn to determine if the conductor is in the superconductive state, in the resistive state, or in the current sharing state. It uses the Bottura fit parameters to calculate the critical current density in the cable. A simple model of current redistribution is considered—if the critical current $I_c \geq 0$ and $I_c < I(t)$, where $I(t)$ is the current flowing through the cable, the ohmic power dissipated is smoothed by an inverse sigmoid $Q_{step}(I, I_c)$ (Figure 9.13).

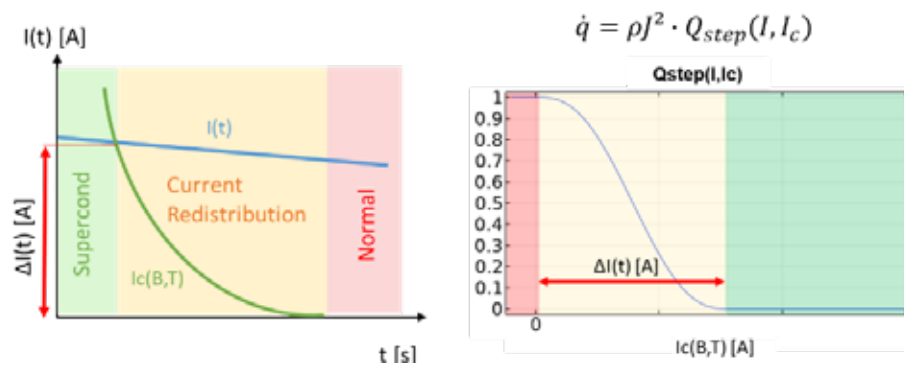


Figure 9.13 Current redistribution model

Electron-Ion Collider, Brookhaven National Laboratory and Thomas Jefferson National Accelerator Facility			
Doc No. EIC-SHC-TN-24-005	Author: Sandesh Gopinath	Effective Date: 12/05/2024	Review Frequency: NA
Process Description: EIC Design Report MARCO Magnet			Revision: 00

The thermal model solves the heat transfer equations in 2D associated with every node of the model and the 1D propagation along the length of the conductor according to the computed axial quench velocity. The ohmic power releases at every turn when quenched is considered starting at the node in the center of the conductor geometry.

The electrical model calculates the resistivity and voltage associated with every turn and the eddy currents induced in the mandrel during the quench current decay.

9.2.2.1 RESULTS FOR NOMINAL CASE SCENARIO

In the nominal case, due to the high inductance, the current decay is very slow and it takes 65 s to reach less than 1% of the original current in the magnet. The time constant of the quench circuit is 20.31 s.

Figure 9.14 shows the current decay in the coils and the eddy current in the mandrel. Thanks to the good magnetic coupling between the coils and the mandrel, the mandrel is subjected to the high eddy current, which generates the quench-back in the coil.

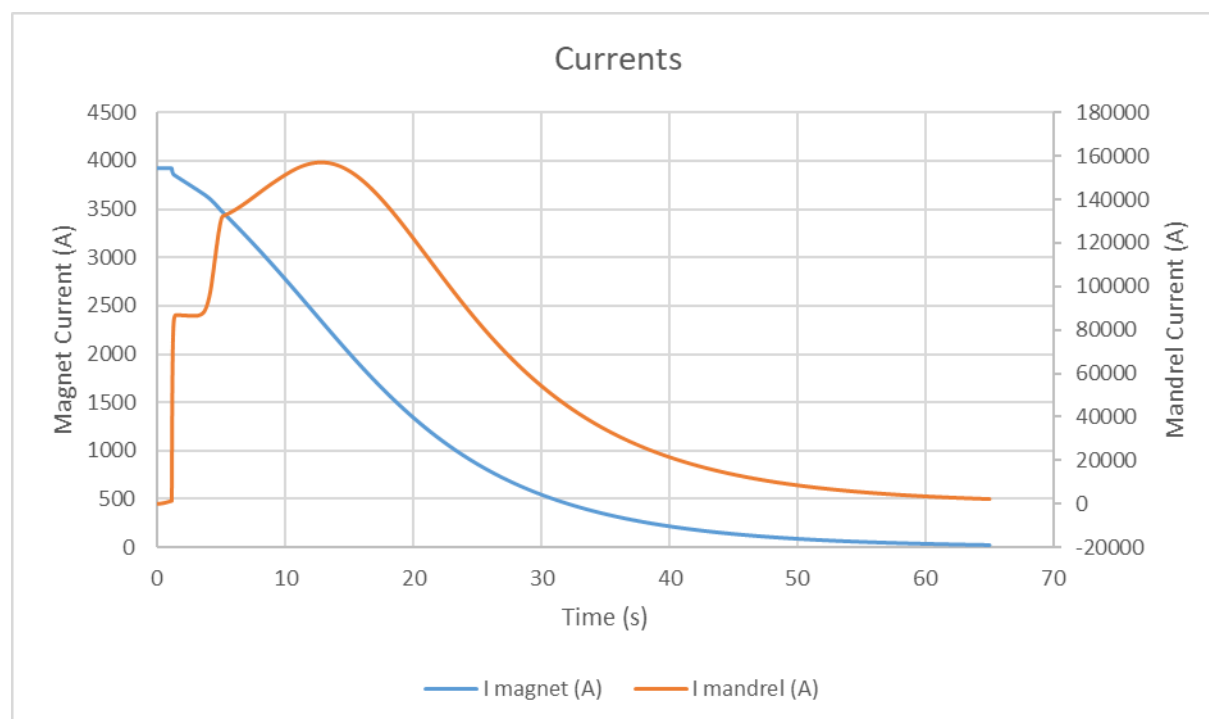


Figure 9.14 Current decay in the coils (blue) and in the mandrel (orange)

Electron-Ion Collider, Brookhaven National Laboratory and Thomas Jefferson National Accelerator Facility			
Doc No. EIC-SHC-TN-24-005	Author: Sandesh Gopinath	Effective Date: 12/05/2024	Review Frequency: NA
Process Description: EIC Design Report MARCO Magnet			Revision: 00

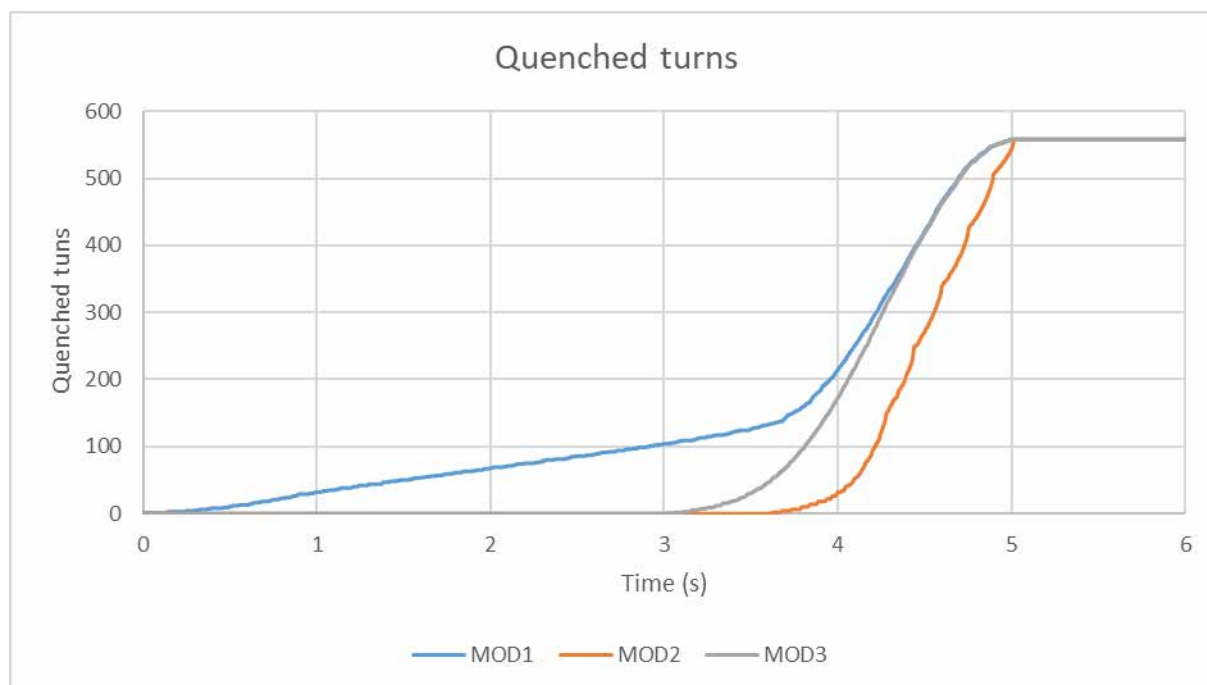


Figure 9.15 Quenched turns as a function of the time

Figure 9.15 shows the number of quenched turns as a function of the time. The quench velocity is constant for the first three seconds in MOD1, and it increases after that due to the quench-back induced by the mandrel.

The coil voltage profile during quench (Figure 9.16) shows no issue; the coil voltages are well below 1000 V—the acceptable criterion defined for the magnet. The coil resistance is shown in Figure 9.17.

The only official copy of this document is the one online in the SharePoint Document Center. Before using a printed copy, verify that it is current by checking the printed document's Revision History log with that of the online version.

Electron-Ion Collider, Brookhaven National Laboratory and Thomas Jefferson National Accelerator Facility			
Doc No. EIC-SHC-TN-24-005	Author: Sandesh Gopinath	Effective Date: 12/05/2024	Review Frequency: NA
Process Description: EIC Design Report MARCO Magnet			Revision: 00

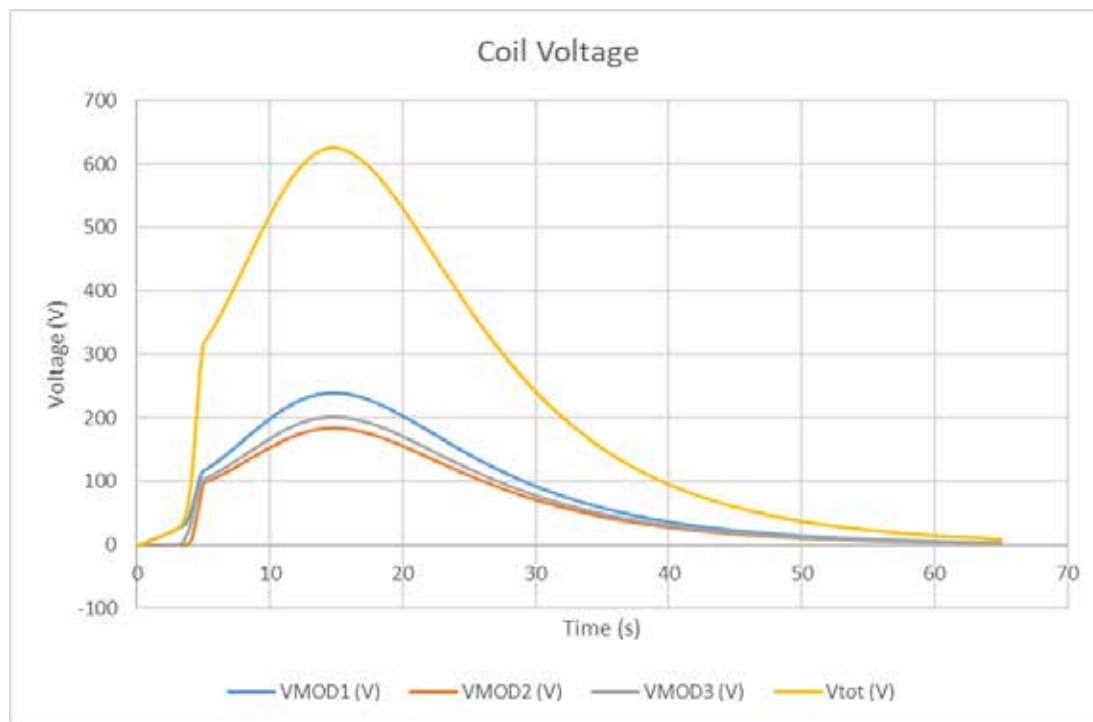


Figure 9.16 Coil voltage for each module and total resistive voltage at the extremities of the magnet

The only official copy of this document is the one online in the SharePoint Document Center. Before using a printed copy, verify that it is current by checking the printed document's Revision History log with that of the online version.

Electron-Ion Collider, Brookhaven National Laboratory and Thomas Jefferson National Accelerator Facility			
Doc No. EIC-SHC-TN-24-005	Author: Sandesh Gopinath	Effective Date: 12/05/2024	Review Frequency: NA
Process Description: EIC Design Report MARCO Magnet			Revision: 00

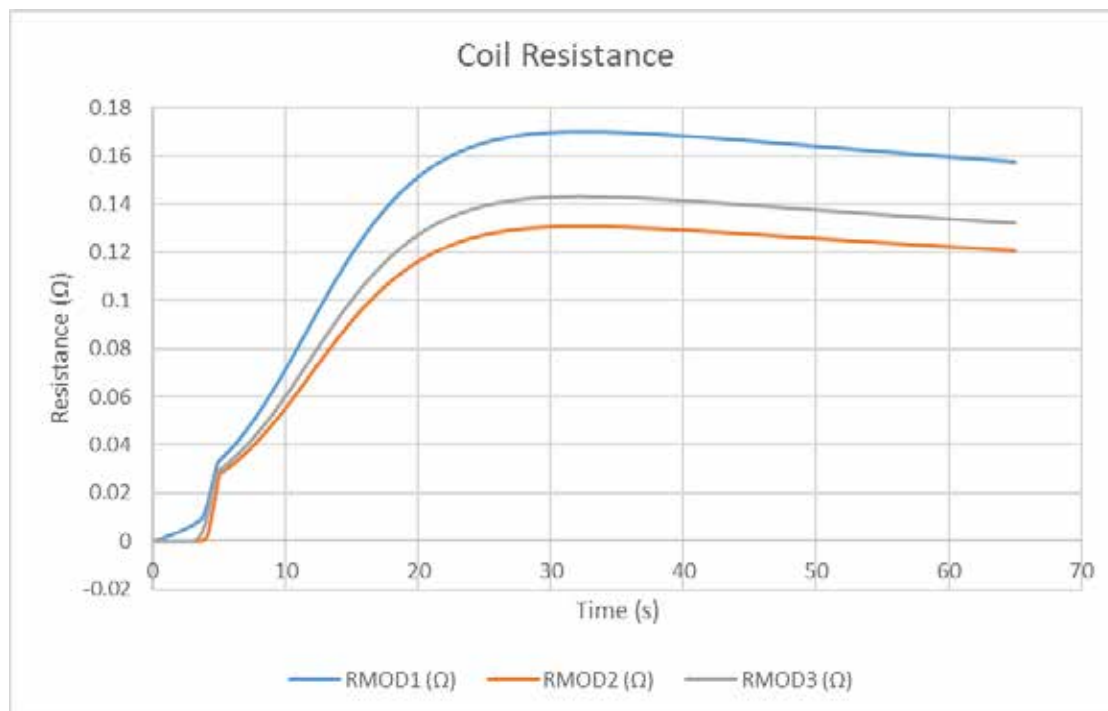


Figure 9.17 Coils resistance as a function of time

The total power dissipated in the circuit is shown in Figure 9.18. The dump resistance has a peak power of 3.8 MW; the coils, 1.5 MW; the mandrel, 86 kW.

The only official copy of this document is the one online in the SharePoint Document Center. Before using a printed copy, verify that it is current by checking the printed document's Revision History log with that of the online version.

Electron-Ion Collider, Brookhaven National Laboratory and Thomas Jefferson National Accelerator Facility			
Doc No. EIC-SHC-TN-24-005	Author: Sandesh Gopinath	Effective Date: 12/05/2024	Review Frequency: NA
Process Description: EIC Design Report MARCO Magnet			Revision: 00

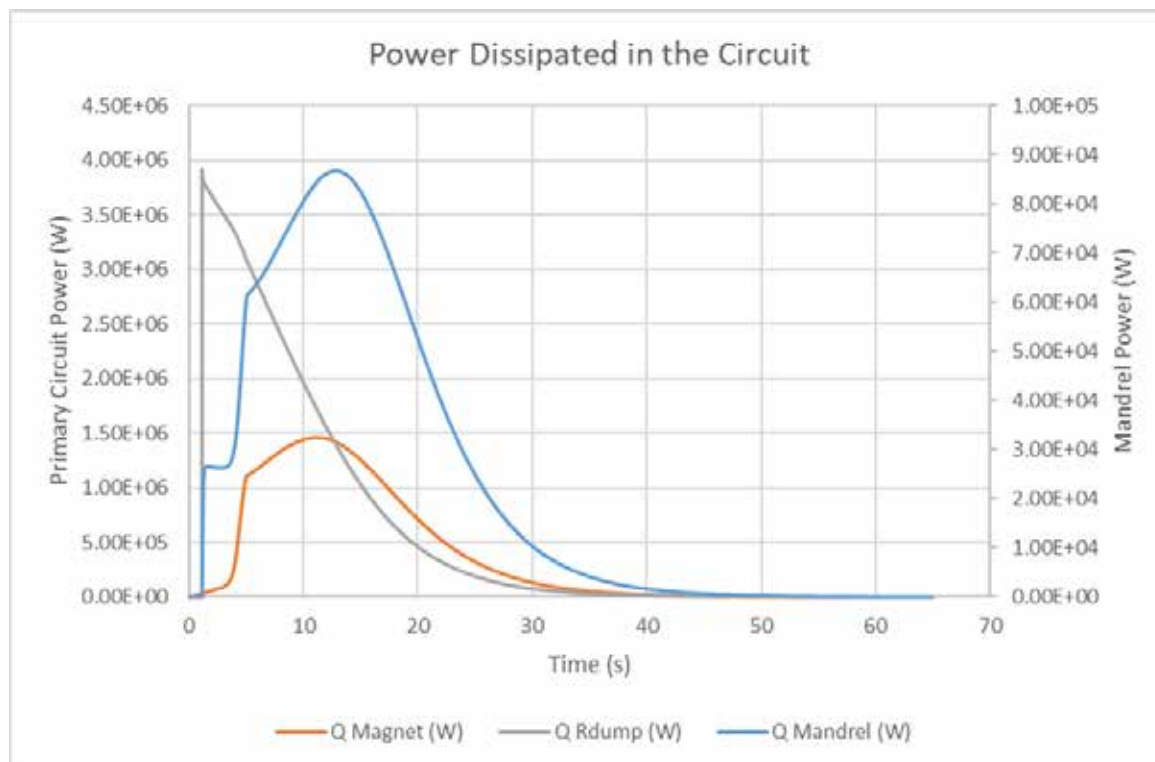


Figure 9.18 Power dissipated in the circuit. The primary circuit consists in the magnet plus the dump resistance

The maximum temperature (hotspot) reaches during quench is 96 K, showing no issue for the structural integrity of the magnet. The hotspot is located at the quench starting point (Figure 9.19).

The only official copy of this document is the one online in the SharePoint Document Center. Before using a printed copy, verify that it is current by checking the printed document's Revision History log with that of the online version.

Electron-Ion Collider, Brookhaven National Laboratory and Thomas Jefferson National Accelerator Facility			
Doc No. EIC-SHC-TN-24-005	Author: Sandesh Gopinath	Effective Date: 12/05/2024	Review Frequency: NA
Process Description: EIC Design Report MARCO Magnet			Revision: 00

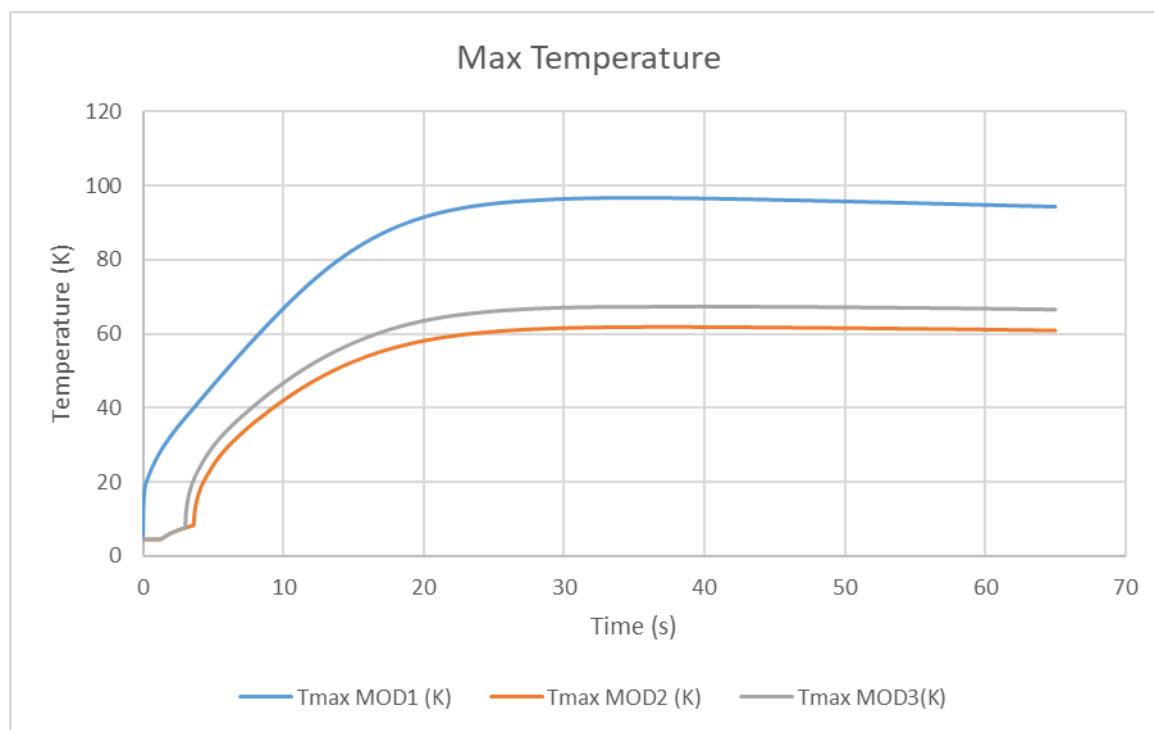


Figure 9.19 Maximum temperature of each module during quench.

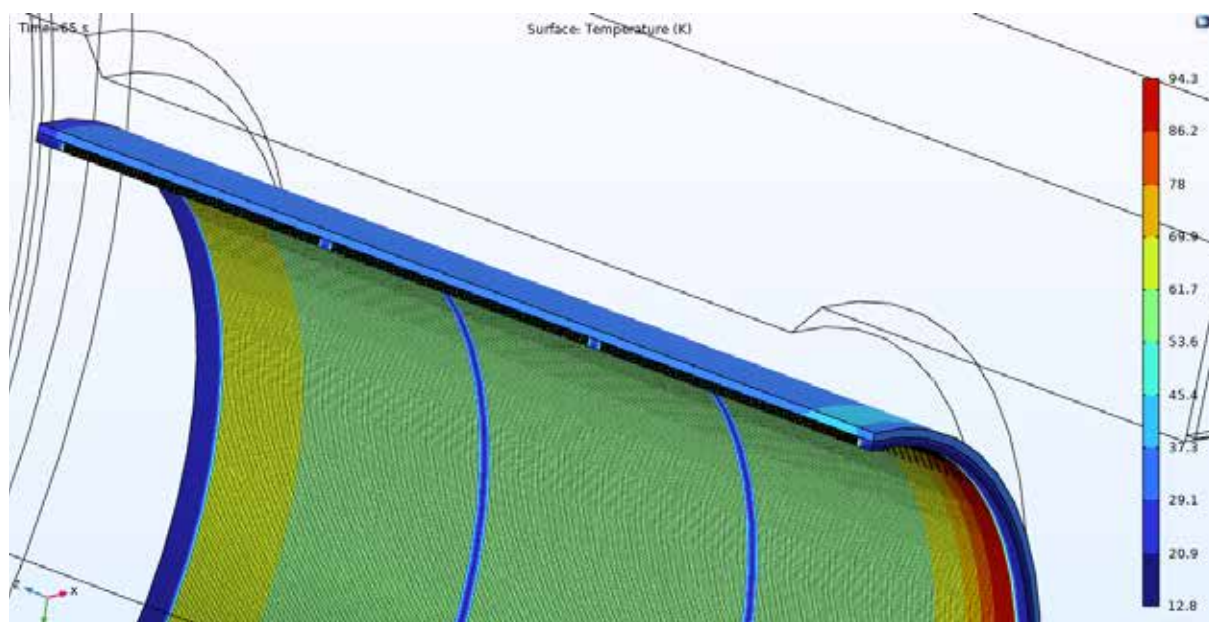


Figure 9.20 Temperature profile on the three modules after 65 s. The hotspot is localized in MOD1, where the quench started.

Electron-Ion Collider, Brookhaven National Laboratory and Thomas Jefferson National Accelerator Facility			
Doc No. EIC-SHC-TN-24-005	Author: Sandesh Gopinath	Effective Date: 12/05/2024	Review Frequency: NA
Process Description: EIC Design Report MARCO Magnet			Revision: 00

9.2.2.2 Fault Case

The fault case scenario is represented by not opening breakers. In this scenario, all the magnetic energy is dissipated within the coils. Even in this scenario, the magnet is relatively safe—the maximum hotspot temperature is 115 K (Figure 9.21) while the maximum resistive voltage is 1165 V (Figure 9.22).

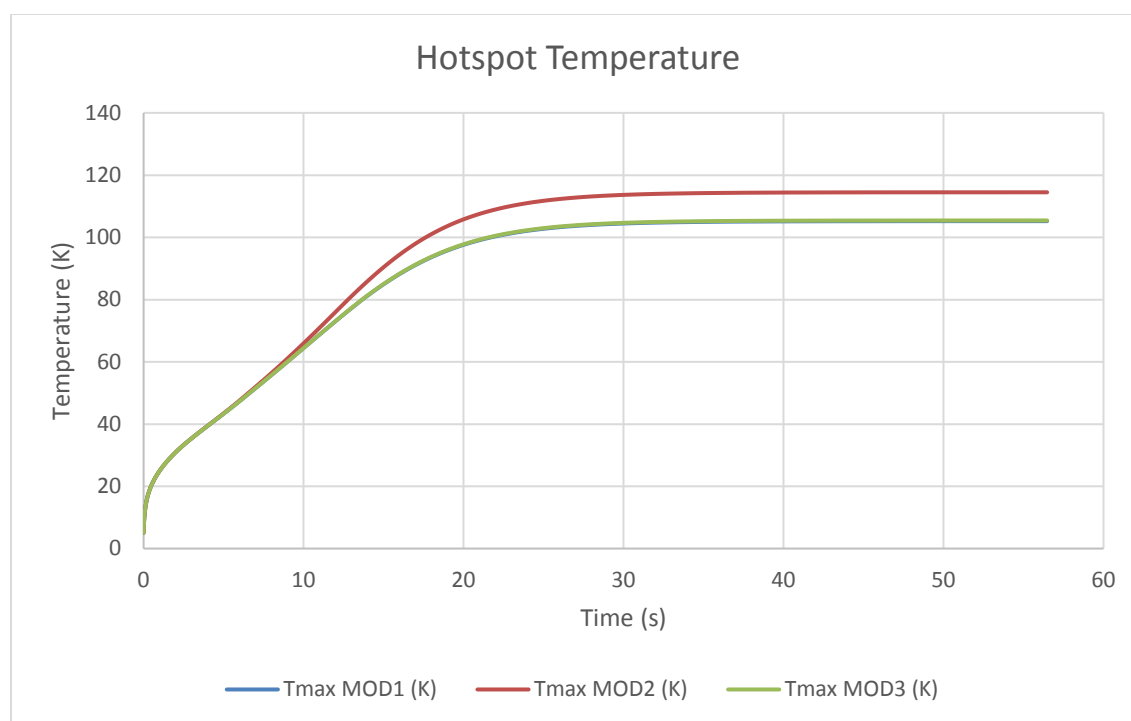


Figure 9.21 Hotspot temperature for the fault case scenario

Electron-Ion Collider, Brookhaven National Laboratory and Thomas Jefferson National Accelerator Facility			
Doc No. EIC-SHC-TN-24-005	Author: Sandesh Gopinath	Effective Date: 12/05/2024	Review Frequency: NA
Process Description: EIC Design Report MARCO Magnet			Revision: 00

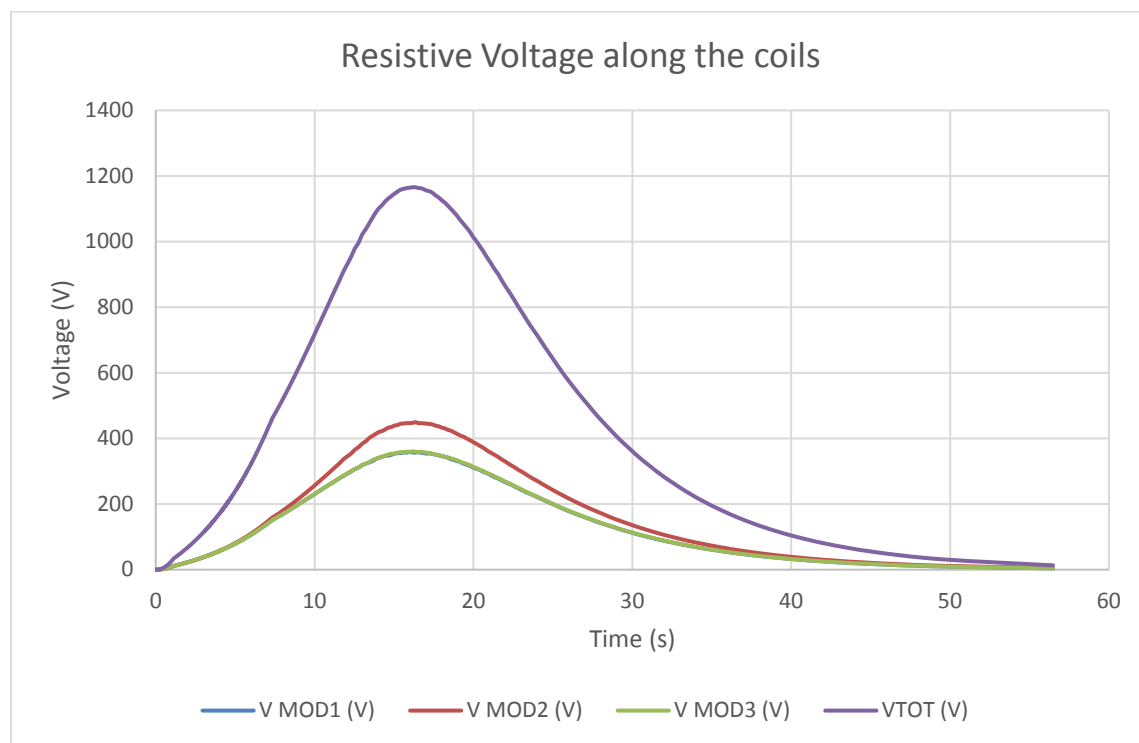


Figure 9.22 Resistive voltage in case of fault scenario

9.3 Quench Protection circuit

The magnet protection and I&C layout for process and system interlocks, shown in Figure 9.23 and Figure 9.24

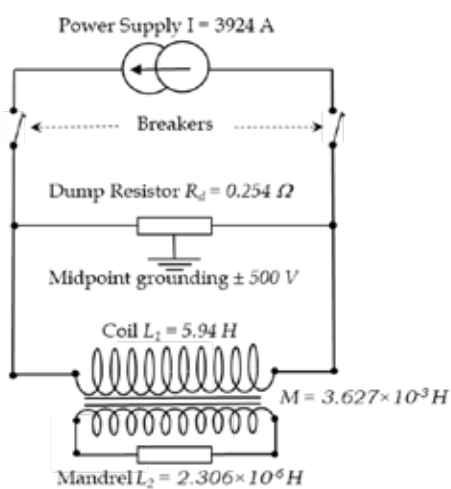


Figure 9.23 Magnet protection schematic with dump resistor and two breakers

The only official copy of this document is the one online in the SharePoint Document Center. Before using a printed copy, verify that it is current by checking the printed document's Revision History log with that of the online version.

Electron-Ion Collider, Brookhaven National Laboratory and Thomas Jefferson National Accelerator Facility			
Doc No. EIC-SHC-TN-24-005	Author: Sandesh Gopinath	Effective Date: 12/05/2024	Review Frequency: NA
Process Description: EIC Design Report MARCO Magnet			Revision: 00

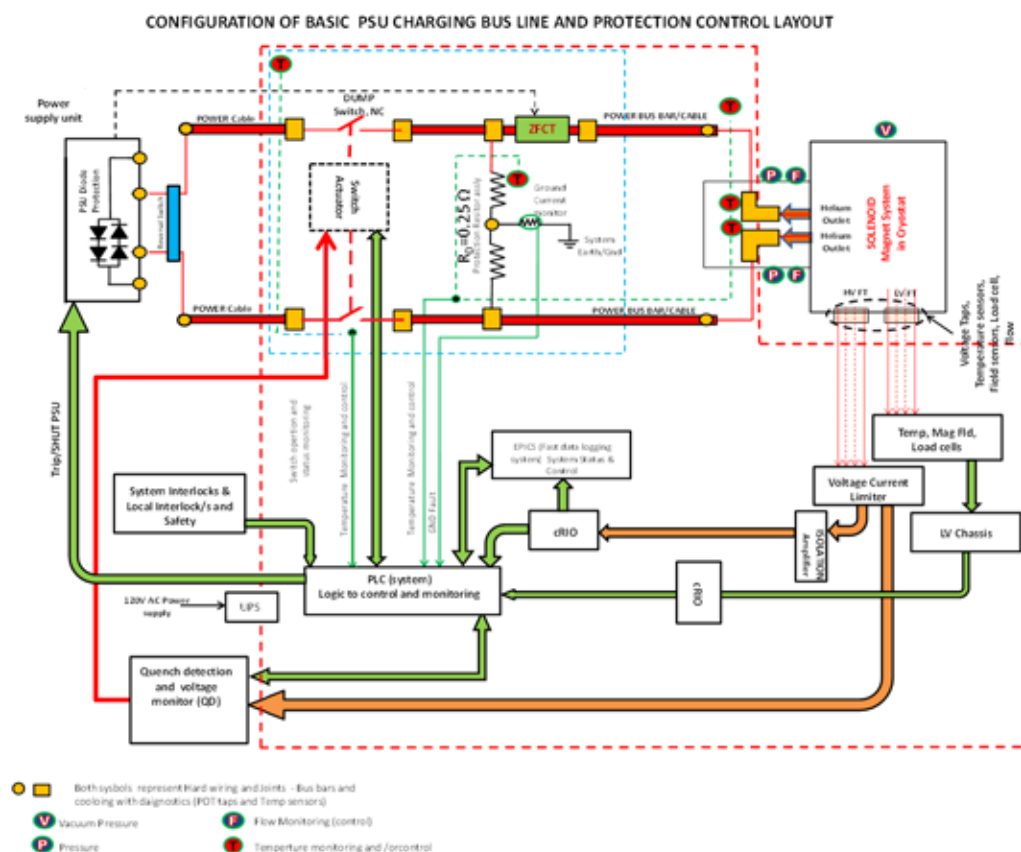


Figure 9.24 Schematic arrangement of magnet protection and I&C layout for interlocks identified

Electron-Ion Collider, Brookhaven National Laboratory and Thomas Jefferson National Accelerator Facility			
Doc No. EIC-SHC-TN-24-005	Author: Sandesh Gopinath	Effective Date: 12/05/2024	Review Frequency: NA
Process Description: EIC Design Report MARCO Magnet			Revision: 00

10 Instrumentations

In order to operate and monitor the MARCO solenoid an extensive instrumentation plan has been defined. The instrumentation covers the electrical measurements, the cryogenics data measurements as well as the mechanical ones. The electrical measurements gather the voltage measurements and the current measurements. The cryogenics ones collect the temperature data, the pressure, the liquid helium level, the he mass flows and the vacuum level. Finally, the mechanical measurements concern especially the tie-rods whose stress is monitored during all the magnet life. This section will present the MARCO instrumentation plan in details.

10.1 Voltage Taps

The electrical instrumentation scheme has been done based on the magnet protection analysis and choices. As the magnet will be protected by a magnet safety system (MSS) the voltage will be monitored for each coil segment with a redundancy. The quench detector will be made by making the difference between two segments of the coil having the same inductance. Allowing to remove the inductive voltage and read only the resistive voltage. This will allow the MSS to detect the transition time and to protect the magnet by opening the contactor to discharge the magnet on the dump resistor. Figure 10.1 shows the protection scheme with the contactor and the dump resistor.

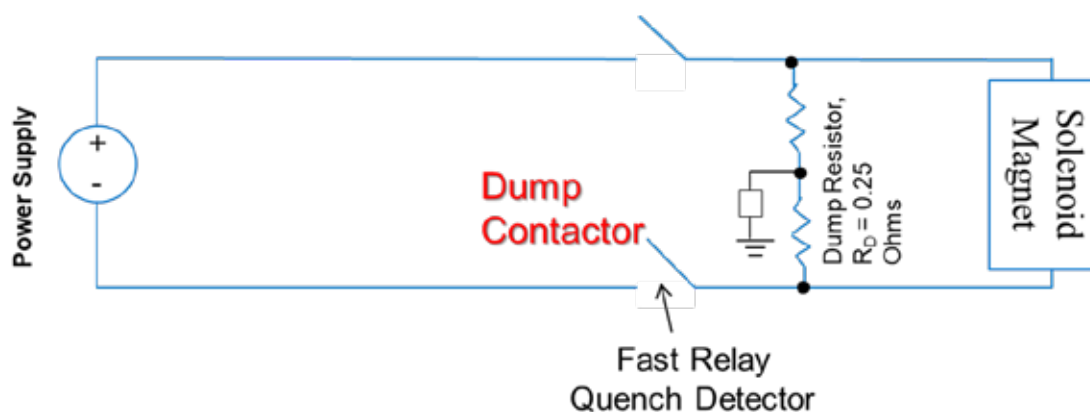


Figure 10.1 MARCO Solenoids layout

Figure 10.2 shows the voltage taps distribution all along the MARCO magnet while Figure 10.3, Figure 10.4, and Figure 10.5 shows respectively the voltage taps on one module of the solenoid, the voltage taps redundancy on the magnet and the voltage taps for the current leads. With the redundancy, 50 voltage taps shall be positioned in the magnet giving 25 differences of potential to measure and send to the MSS and acquisition system. These measured values can be

Electron-Ion Collider, Brookhaven National Laboratory and Thomas Jefferson National Accelerator Facility			
Doc No. EIC-SHC-TN-24-005	Author: Sandesh Gopinath	Effective Date: 12/05/2024	Review Frequency: NA
Process Description: EIC Design Report MARCO Magnet			Revision: 00

combined in 16 quench detectors with 12 for the coils, 2 for the current leads and 2 for the busbars (one per current lead and one per busbar). For the coils the voltage threshold has been set to 0.1 V to 1 V in the simulation with at least one second of validation time. For the busbars, the voltage threshold is smaller and have been set to 10 mV with a validation time of 10 ms. Finally, the voltage threshold of the current leads shall be smaller than the maximum operating voltage in the current leads. Figure 10.6 shows the DCCTs positions in the MARCO circuits. Two DCCTs shall be position to monitor and regulate the current. The first one between the power supply and the contactor shall be used for the power supply regulation while the second one between the coil and the dump resistor will be used to monitor the current in case of quench or contactor opening.

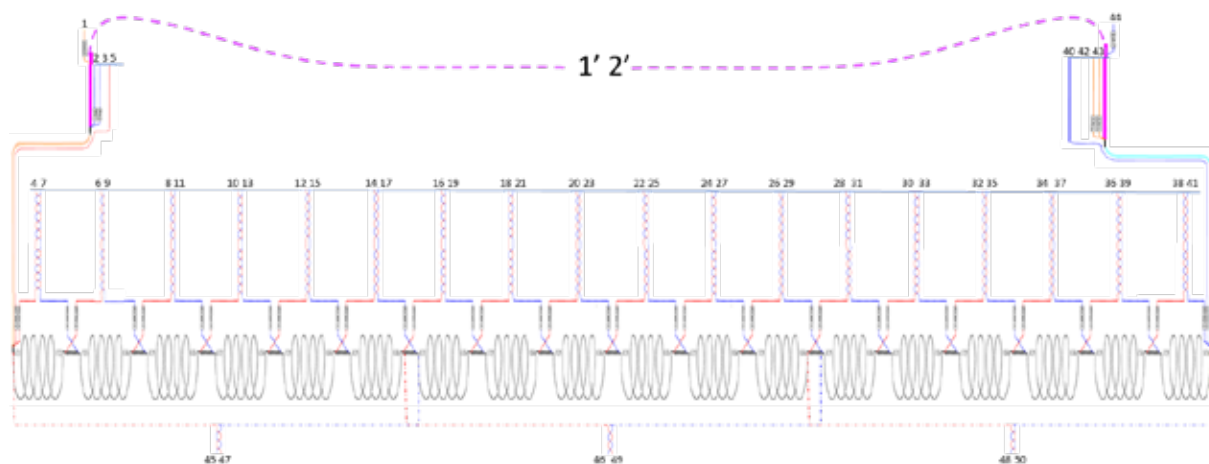


Figure 10.2 Distribution of voltage taps for the MARCO solenoid and its current leads and busbars. The redundant voltage taps are in dashed line.

The only official copy of this document is the one online in the SharePoint Document Center. Before using a printed copy, verify that it is current by checking the printed document's Revision History log with that of the online version.

Electron-Ion Collider, Brookhaven National Laboratory and Thomas Jefferson National Accelerator Facility			
Doc No. EIC-SHC-TN-24-005	Author: Sandesh Gopinath	Effective Date: 12/05/2024	Review Frequency: NA
Process Description: EIC Design Report MARCO Magnet			Revision: 00

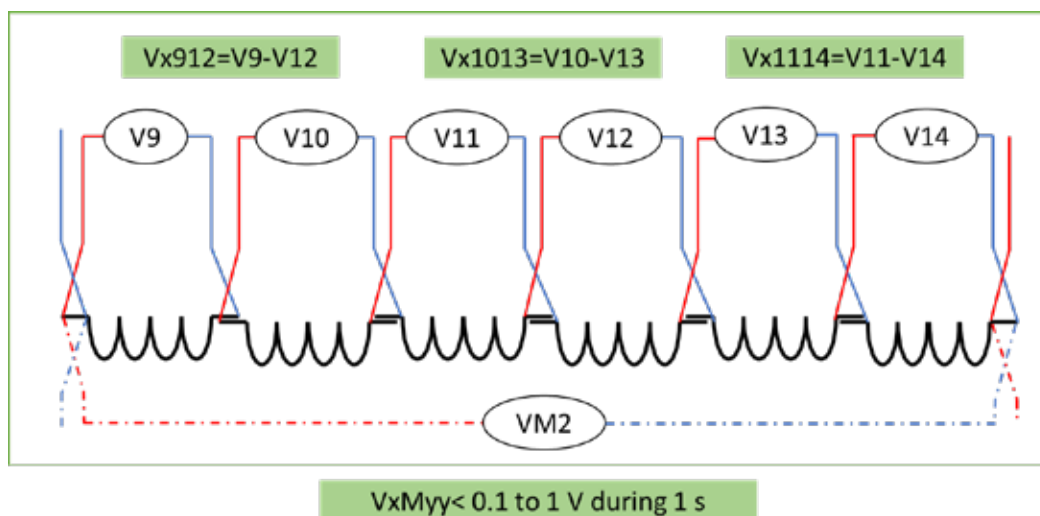


Figure 10.3 Voltage taps distribution on one module. The redundant voltage taps are in dashed line.

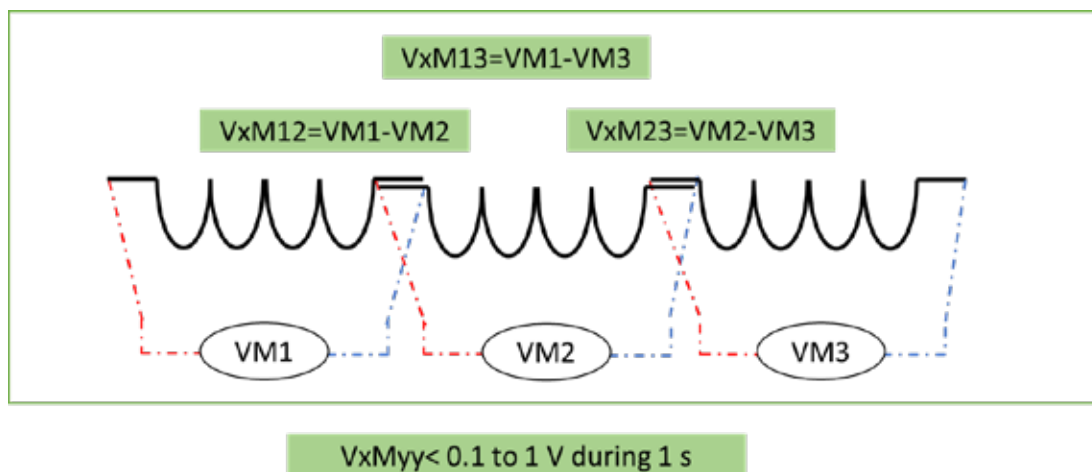


Figure 10.4 Redundant voltage taps distribution for the full Marco coil

Electron-Ion Collider, Brookhaven National Laboratory and Thomas Jefferson National Accelerator Facility			
Doc No. EIC-SHC-TN-24-005	Author: Sandesh Gopinath	Effective Date: 12/05/2024	Review Frequency: NA
Process Description: EIC Design Report MARCO Magnet			Revision: 00

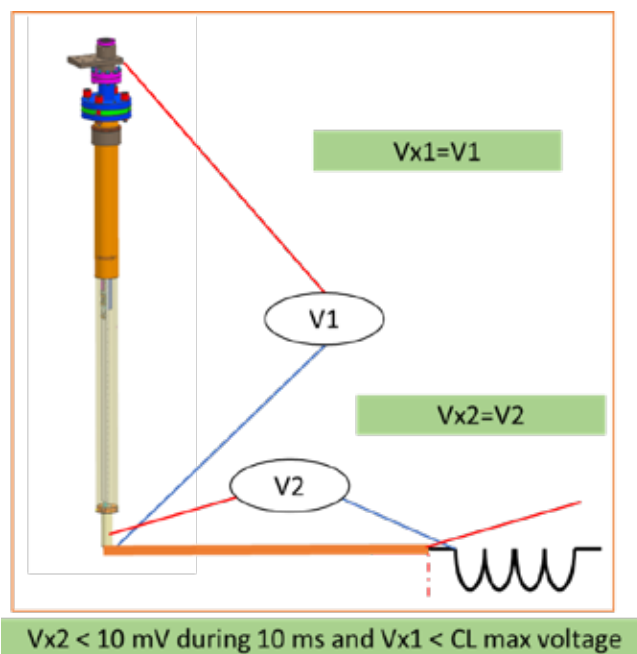


Figure 10.5 Distribution of voltage taps on one module for the current leads

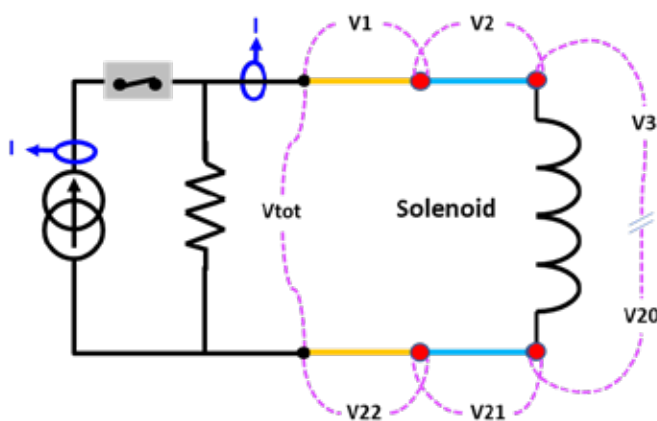


Figure 10.6 DCCTs positions in the MARCO solenoid lay out

10.2 Cryogenic Instrumentation Plan

For the cryogenic instrumentation plan, different type of sensors will be used. The first ones are the temperature sensors whose are divided in two types, the PT100 for all the temperature above 50 K i.e. for the thermal screen and the CERNOX® sensors used for all the 4.5 K measurements. Figure 10.7 shows the distribution of the thermal sensors. For the PT100, 10 will be placed on the thermal screen while 6 will be placed on the current leads. Concerning the CERNOX, 12 will be

Electron-Ion Collider, Brookhaven National Laboratory and Thomas Jefferson National Accelerator Facility			
Doc No. EIC-SHC-TN-24-005	Author: Sandesh Gopinath	Effective Date: 12/05/2024	Review Frequency: NA
Process Description: EIC Design Report MARCO Magnet			Revision: 00

distributed all over the magnet and shell and 6 distributed between the busbars, the phase separator, the thermosiphon inlet and outlet. Completing the thermal sensors flow meters (2 for the current leads, 2 to 4 for the thermosiphons inlet and outlet and 2 for the 50 K shield inlet and outlet) will be used to monitor the cryogenic operation as well as 2 liquid helium level gauges, 2 manometers and 2 vacuum gages (Figure 10.8).

For the cryogenic operation some heaters will be placed at different location of the cryogenic circuits. In order to initiate the helium mass flow, if needed, three heaters of 10 W are planned to be used on the rising branch of the thermosiphon.

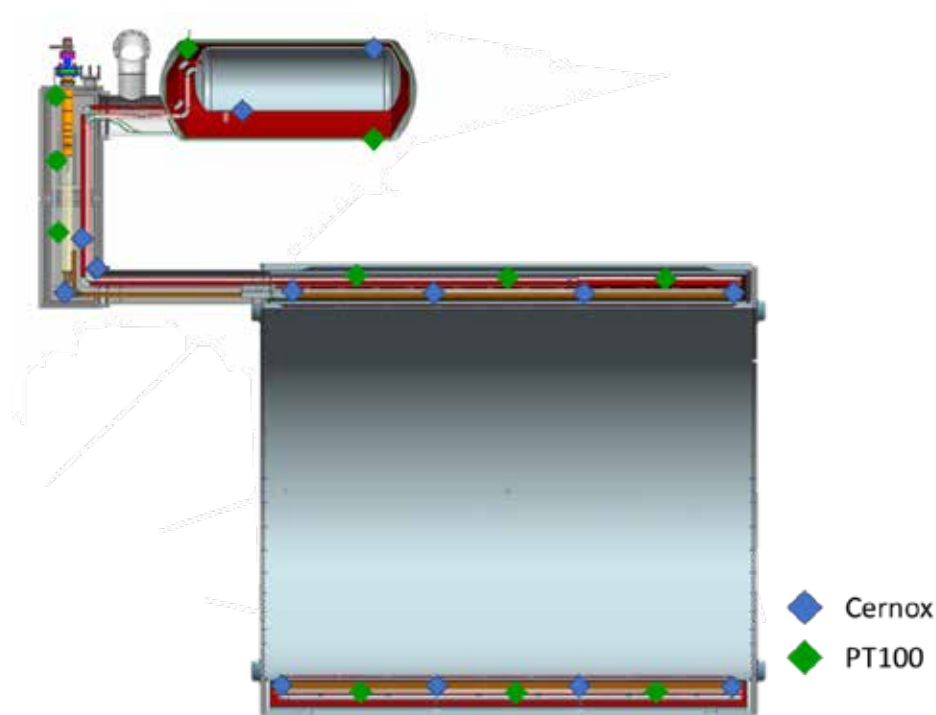


Figure 10.7 Thermal sensors distribution

Electron-Ion Collider, Brookhaven National Laboratory and Thomas Jefferson National Accelerator Facility			
Doc No. EIC-SHC-TN-24-005	Author: Sandesh Gopinath	Effective Date: 12/05/2024	Review Frequency: NA
Process Description: EIC Design Report MARCO Magnet			Revision: 00

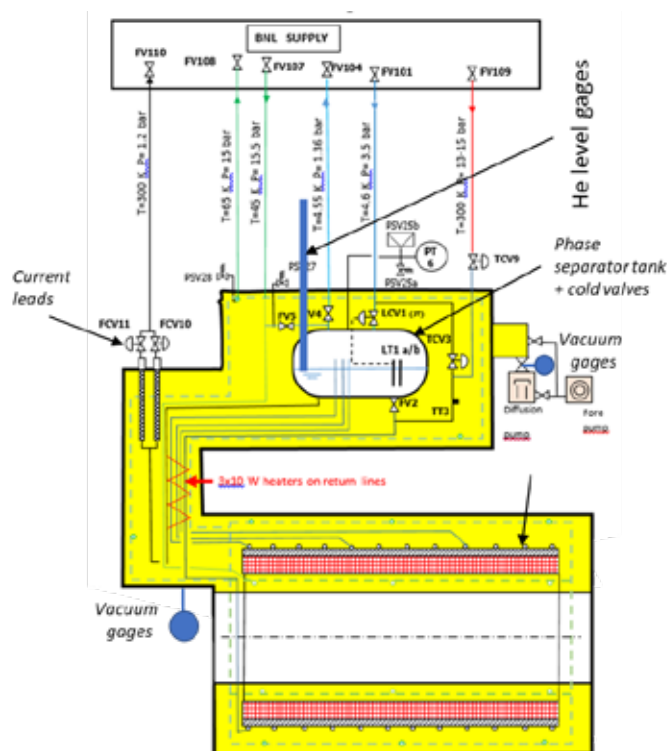


Figure 10.8 Cryogenic scheme with the vacuum gauges and the helium level and flow meters localization

10.3 Mechanical sensors

In order to monitor the tie-rods preload during the magnet assembly in its cryostat, the transportation, the magnet cool down and energization, it is planned to use load cells placed at the end of each tie-rods (Figure 10.9). These load cells shall be dimensioned adequately pending the stress analyses made during the design phase in discussion with the magnet vendor.

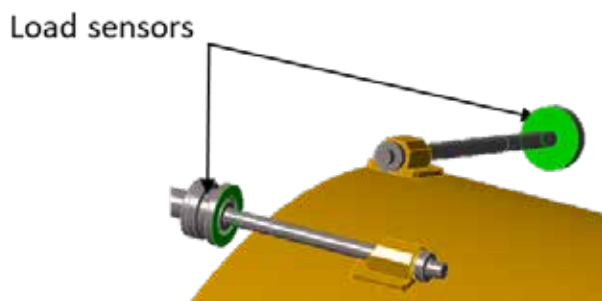


Figure 10.9 Load cells localization on the tie-rods

Electron-Ion Collider, Brookhaven National Laboratory and Thomas Jefferson National Accelerator Facility			
Doc No. EIC-SHC-TN-24-005	Author: Sandesh Gopinath	Effective Date: 12/05/2024	Review Frequency: NA
Process Description: EIC Design Report MARCO Magnet			Revision: 00

11 Shipping

The goal of this document is to define a design criteria that accounts for the shipping and transportation loads for the MARCO magnet system which includes the cryostat and the cold mass.

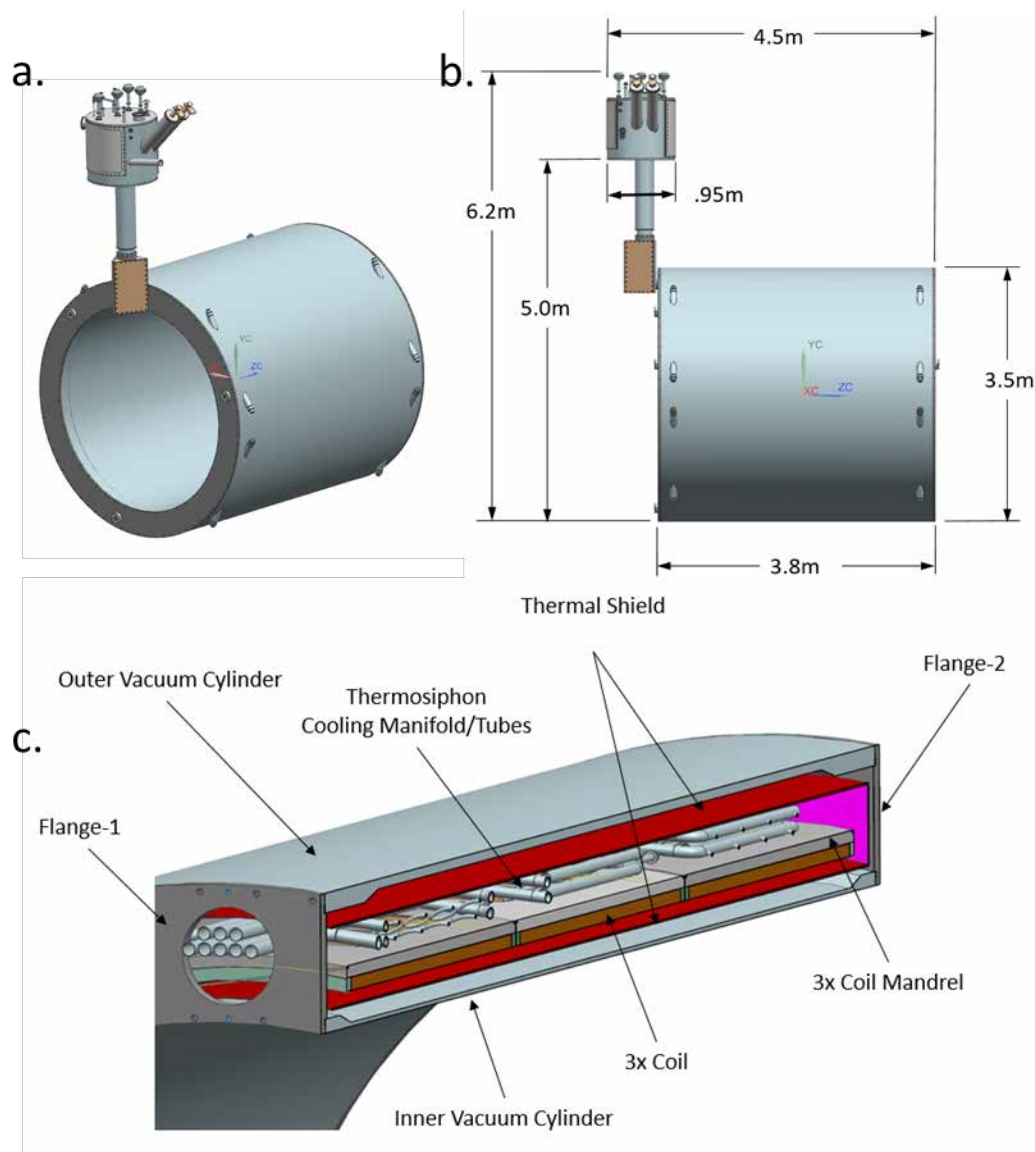


Figure 11.1 MARCO Magnet Overview a. 3D view, b. Overall dimensions, c. Assembly cross-section

The solenoid is 3.5 m in diameter and 3.8 m long, will use a niobium-titanium conductor cooled at 4.5 K. It will be made in 3 modules of 6 conductor layers. The stored energy is approx. 46 MJ

Electron-Ion Collider, Brookhaven National Laboratory and Thomas Jefferson National Accelerator Facility			
Doc No. EIC-SHC-TN-24-005	Author: Sandesh Gopinath	Effective Date: 12/05/2024	Review Frequency: NA
Process Description: EIC Design Report MARCO Magnet			Revision: 00

with a nominal current of about 4000 A. The conductor will be wound with an outer mandrel and no inner mandrel. The approximate mass of the EIC detector solenoid MARCO magnet system is 30 tonnes and the expected journey of the shipment includes road as well as air travel from a prospective vendor to BNL.

Based on the review of references that studied loads during transport of superconducting magnets and cryomodules, we reach a recommendation of a minimum shipping load design criteria of **3g** in all directions for the MARCO magnet along with a properly designed shipping fixture with isolators. This acceleration value is driven by the peak loads seen by the MQXFA magnet [29] shipment incident during its transport [30]. During the incident the magnet sustained loads of **Y 6g, Z 2g (approx.), and X 3g (approx.)** which is higher than the specification of **5g** in the **Y** direction. The magnet was designed with higher safety margins and hence did not see any damages. This is a good example where having a high safety factor (up to 4 [29]) was beneficial. It is relevant to note that MQXFA shipping fixture **did not** have any isolators to dampen the loads. Isolators like helicoils may provide up to 90% isolation of input vibration [31].

This shipping load design criteria could be driven by the stress and/or strain limitations on the coil and/or any other components of the system being transported. The alignment requirement of components after shipping may also contribute to this requirement. The design criteria may also consider the thermal design margin to allow for stronger suspension link system design. Having a low or a high magnet design acceleration load criteria can have its advantages and disadvantages. For e.g. a low load design criteria might have a stringent requirement on the shipping frame design consequently have a low safety factor against mishaps before the magnet is placed on the shipping frame. At the same time a high load design criteria might require bulkier tie rods which will increase the thermal loads during operation.

The only official copy of this document is the one online in the SharePoint Document Center. Before using a printed copy, verify that it is current by checking the printed document's Revision History log with that of the online version.

Electron-Ion Collider, Brookhaven National Laboratory and Thomas Jefferson National Accelerator Facility			
Doc No. EIC-SHC-TN-24-005	Author: Sandesh Gopinath	Effective Date: 12/05/2024	Review Frequency: NA
Process Description: EIC Design Report MARCO Magnet			Revision: 00

12 Quality Assurance Plan

The Detector Solenoid Magnet is to be procured as a Vendor-Design-build contract from an International Partner. The vendor completes the manufacturing design, produces their own manufacturing drawings, fabricate and test the system, and furnishes related documents and records.

The strategy places responsibility on the vendor for design, manufacturing and transportation.

This Quality Control Plan describes in general terms how JLAB plans to ensure conformance of the provided designs, manufacturing and shipping preparation to requirements until transfer of ownership upon delivery to BNL. JLAB requirements convey through all vendors and subcontractors.

The EIC equipment owner (JLab and BNL) ensures selected vendors manufacturer under a Quality System certified or equivalent to ISO 9001.

12.1 Requirements Traceability

Project requirements for this and other systems within the EIC Detector are maintained in a project database and are published on the EIC BNL SharePoint page.

Requirements for partners and vendors will be defined in the Purchase Order Package and are generally described in sections below.

Brookhaven National Lab (BNL) uses VISURE, a Requirements Register, to record and manage EIC requirements. Management of requirements are described in:

- EIC Systems Engineering Management Plan (EIC-SEG-PLN-022)*
- EIC [General] Requirements Management Plan (EIC-SEG-PLN-016)*
- Requirements Management for Detector Systems Plan EIC-SEG-PLN-017*

and other documents, per the table below.

The only official copy of this document is the one online in the SharePoint Document Center. Before using a printed copy, verify that it is current by checking the printed document's Revision History log with that of the online version.

Electron-Ion Collider, Brookhaven National Laboratory and Thomas Jefferson National Accelerator Facility			
Doc No. EIC-SHC-TN-24-005	Author: Sandesh Gopinath	Effective Date: 12/05/2024	Review Frequency: NA
Process Description: EIC Design Report MARCO Magnet			Revision: 00

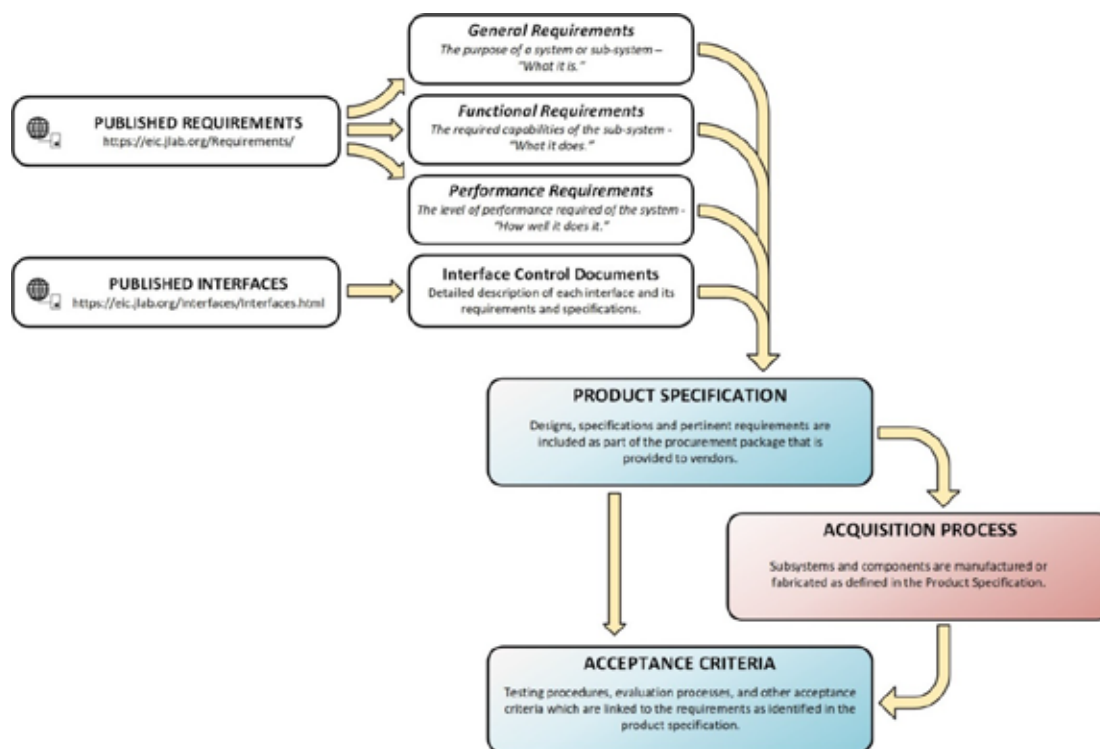


Figure 12.1 requirements to product specifications and acceptance criteria

The traceability of the EIC Project requirements can be found in table 12.1:

Table 12.1 The traceability of the EIC Project requirements

Document Number	Document Title	Storage Location
EIC-SEG-PLN-016	General Requirements Management Plan	Requirements Management Plan.pdf
EIC-SEG-RSI-007	General, Functional, and Performance Requirements for the EIC Detector Systems	General, Functional, and Performance Requirements for the EIC Detector Systems.pdf
EIC-SEG-PLN-022	EIC Systems Engineering Management Plan	
	General Requirements Document (GRD)	
EIC-ESH-PLN-007	Integrated Safety Management Plan (ISM)	
	Functional Requirements Document (FRD)	
	Performance Requirement Document (PRD)	

The only official copy of this document is the one online in the SharePoint Document Center. Before using a printed copy, verify that it is current by checking the printed document's Revision History log with that of the online version.

Electron-Ion Collider, Brookhaven National Laboratory and Thomas Jefferson National Accelerator Facility			
Doc No. EIC-SHC-TN-24-005	Author: Sandesh Gopinath	Effective Date: 12/05/2024	Review Frequency: NA
Process Description: EIC Design Report MARCO Magnet			Revision: 00

Document Number	Document Title	Storage Location
	Interface Control Documents (ICD)	
EIC-ORG-RSI-026	EIC Code of Record	https://brookhavenlab.sharepoint.com/sites/eic-document-center/_layouts/15/Doc.aspx?sourcedoc=%7B6BA958EC-BE5B-40F4-AAD6-96CCDCEF3682%7D&file=EIC%20Code%20of%20Record.docx&action=default&mobileredirect=true&DefaultItemOpen=1
EIC-ESH-PLN-007	Integrated Safety Management Plan (ISM)	
JLAB ES&H Manual 6151	Pressure Systems, Design Authority	PSSPart1 General Program Info; (jlab.org)
	Central Detector Solenoid Acceptance Plan	
ENG-AD-01-001	Conduct of Engineering Manual	ENG-AD-01-001 - Conduct of Engineering Manual - rev A reverified 2015.docx.pdf (jlab.org)

12.2 In-Process Inspection and Test

Manufacturing tests, inspections, and acceptance parameters are described in table 12.2 :

Table 12.2 Manufacturing tests, inspections, and acceptance parameters

Document Title	Document Number	Storage Location
Acceptance Criteria Template for Detector Solenoid		
Solenoid Magnet Acceptance Plan		
EIC 6.10.07 (ITP) Inspection and Test Plan Note: To be expanded after manufacturing schedule becomes available.		

12.3 Vendor/Partner In-Process Monitoring and Measurement Activities

JLAB TR conducts periodic design and manufacturing status meetings with the International Partner to review:

1. Requirements lists

The only official copy of this document is the one online in the SharePoint Document Center. Before using a printed copy, verify that it is current by checking the printed document's Revision History log with that of the online version.

Electron-Ion Collider, Brookhaven National Laboratory and Thomas Jefferson National Accelerator Facility			
Doc No. EIC-SHC-TN-24-005	Author: Sandesh Gopinath	Effective Date: 12/05/2024	Review Frequency: NA
Process Description: EIC Design Report MARCO Magnet			Revision: 00

2. Designs
3. JLAB Inspection and Test Plans status and activities
4. Deliverables Register, Change Logs, Nonconformance
5. Manufacturing schedules and Vendor's Manufacturing Inspection Plan
6. Operational, Functional, Performance and Commissioning Test plans vs. actual

After review of the Partner's manufacturing plans (MIP) JLAB updates the inspection and test plan, and may expand the witness and hold points, or required additional submittals for review or approval.

Additional monitoring needs of the Partner or Manufacturer(s) may be identified during the manufacturing phase based on risk identification and graded approach.

12.4 Incoming Inspection and Acceptance Tests

Acceptance test plans are referenced in Section 3.

Installation and commissioning of the detector magnet will be performed at BNL; however, the JLab TR and other SMEs will oversee the vendor's installation and commissioning activities, including verification of all final acceptance tests.

The vendor must specify in the Quality plan all tests to be carried out during the installation and commissioning of the magnet to comply with the specification of the SM operation: All acceptance tests must be successfully performed, in particular the final acceptance test of the magnet at low temperature and nominal current; and records are to be provided for JLAB review.

12.5 Travelers, Procedures, and Checklists

The Vendor (Partner and their manufacturers) will provide the complete list of travelers and procedures which are to be submitted to JLAB.

JLAB TRs review submittal registers and the register/lists of all travelers, procedures and checklists created by the Vendor and identify and track gaps, or changes, to closure.

An example of registers is provided above by the document owners. Expected due dates versus status of receipt are to be part of the JLAB/ Vendor (Partner) status meetings. Digital registers may be submitted for JLAB review and approval as an alternative.

12.6 Verification Plans: Methods and Activities

JLab/BNL describes how verification of requirements is to be documented in the Requirements Management Plan.

The Vendor is to create a master tracking spreadsheet which lists all vendor-performed activities and, required deliverables, which includes documents and records.

The only official copy of this document is the one online in the SharePoint Document Center. Before using a printed copy, verify that it is current by checking the printed document's Revision History log with that of the online version.

Electron-Ion Collider, Brookhaven National Laboratory and Thomas Jefferson National Accelerator Facility			
Doc No. EIC-SHC-TN-24-005	Author: Sandesh Gopinath	Effective Date: 12/05/2024	Review Frequency: NA
Process Description: EIC Design Report MARCO Magnet			Revision: 00

JLAB and the Vendor review the tracking spreadsheet versus status of submittal at the periodic design review and manufacturing status meetings. For this meeting, JLAB TR creates and follows a meeting agenda to ensure all requirements and scheduled activities are reviewed, and gaps and changes are identified and tracked to closure.

- Inputs should include: Status of submittals, schedules, design or document/record reviews and pending approvals, ITPs and MIP activities, Travelers, Tool Lists, Procedures and Checklists can be reviewed to ensure schedule and delivery/submittal in accordance with plans.
- Locations of stored or submitted documents should be clear.
- Outputs should include identification of gaps, problems or missed deliverables, next actions and their owners, addition of review items as needed to ensure conformance and schedule, any gap identification, risk identification, or escalation items which need to be presented to JLAB or EIC project teams for containment planning; and notes indicating actual checks, in meetings, of submittal register reviews.

12.7 Deliverable Documentation and Records

JLAB defines in a Documents/Records Register(s) the minimum documents and records which the vendor (partner and their manufacturers) shall deliver during the project.

- Content of the Register must be sufficiently
 - a. facilitate quality and conformance reviews of designs, manufacturing, shipping preparation, long term storage, etc. to requirements.
 - b. include any applicable documented information JLAB is required to submit to BNL.
 - c. reference ITP and MIPs and their requirements
 - d. reference registers for submittal, traveler, procedure, tools, checklists
 - e. design, manufacturing code and standard, and technician qualification records (example, ASME certificate, WPS/WPQ/PQRs, ISO 9001 certificate, ASME certificate, etc).

These requirements may be listed as part of the Technical Specification provided with the Scope of Work (per BNL Records and Document Requirements and JLAB Procurement Plan).

The Vendor will provide a list of all end-item documentation and records and their expected availability date (or stage of manufacturing), for use in manufacturing meetings. JLAB submittal and ITP requirements shall be included. Typical items include the following: Inspection/test reports, NCRs with

The only official copy of this document is the one online in the SharePoint Document Center. Before using a printed copy, verify that it is current by checking the printed document's Revision History log with that of the online version.

Electron-Ion Collider, Brookhaven National Laboratory and Thomas Jefferson National Accelerator Facility			
Doc No. EIC-SHC-TN-24-005	Author: Sandesh Gopinath	Effective Date: 12/05/2024	Review Frequency: NA
Process Description: EIC Design Report MARCO Magnet			Revision: 00

Use-As-Is disposition, As-built drawings, design specifications, etc. Digital or other tracking systems are likely to be accepted in lieu of a list, pending JLAB review and approval.

JLAB TR review the register(s) at regular intervals internal to ensure:

- Records and Documents are received and are in a defined storage location;
- Project required reviews, their outcomes/next actions of reviews, and sign-offs are executed per plans
- JLAB transmittals to BNL are successfully delivered to BNL per requirements per Project requirements and schedule expectations.

JLAB reviews the registers (or In-Kind Contributor, or International Partner) at periodic (per section 4) vendor design/manufacturing meetings to confirm receipt per schedule, identify gaps, or implement change control when applicable.

12.8 Associated Equipment

The vendor specifies all measuring and test equipment in their Manufacturing Plan, Inspection Plan, or similar documents. Typical devices include the following: CMM, calipers, gages, sensors, PMI equipment, etc.

12.9 Calibration Plans

The vendor will include calibration in their overall Quality Program.

The vendor will include traceability to specific calibrated instruments in their inspection reports. Calibration records are to be made available to JLAB upon request.

12.10 Serialization and Material Traceability Requirements

JLAB to define any serialization and traceability required by the Project in the Technical Specifications.

Vendor will include serialization and traceability methods in their design. At a minimum serialization and traceability will include the completed magnet, coils, and yokes. They must be traceable to their respective heat lot(s).

In addition to code and design standard requirements, manufacturer markings and traceability are required for the following when furnished with or for the equipment:

1. Piping and Piping Components (these include mechanical and metal products)

The only official copy of this document is the one online in the SharePoint Document Center. Before using a printed copy, verify that it is current by checking the printed document's Revision History log with that of the online version.

Electron-Ion Collider, Brookhaven National Laboratory and Thomas Jefferson National Accelerator Facility			
Doc No. EIC-SHC-TN-24-005	Author: Sandesh Gopinath	Effective Date: 12/05/2024	Review Frequency: NA
Process Description: EIC Design Report MARCO Magnet			Revision: 00

2. Electrical and Electronic Components
3. Fasteners (e.g. Bolts Grade 5 and Grade 8)
4. Hoisting and Rigging Components (material handling)
5. Documentation and Certification

12.11 Planned Partner and Vendor Communication & Visits

- JLAB will hold regular, periodic meetings with the vendor during design phase.
- JLAB will hold regular, periodic meetings with the vendor during manufacturing phase.
- Vendor will provide a manufacturing, inspection and test schedule.
- JLAB plans to witness much of the manufacturing process and most or all of the testing.
- Witness/hold point visits will typically be attended by JLAB TR and QA and may include additional subject matter experts and EIC Project representatives. Schedule or nonconformance issues may result in JLAB increasing surveillance.

12.12 Control of Nonconformances

Vendor (partner) will control nonconformances in accordance with their quality program. Vendor will present to JLAB, and track to closure, design or manufacturing related nonconformances which:

- have a use-as-is disposition, or which
- are likely to impact schedule or quality

Review of new and previously reported open nonconformances are to be part of the periodic meetings.

JLAB reports nonconformances which

- are likely to delay the EIC project or
- increase project costs

to the EIC Project managers responsible for risk identification and containment planning.

Electron-Ion Collider, Brookhaven National Laboratory and Thomas Jefferson National Accelerator Facility			
Doc No. EIC-SHC-TN-24-005	Author: Sandesh Gopinath	Effective Date: 12/05/2024	Review Frequency: NA
Process Description: EIC Design Report MARCO Magnet			Revision: 00

13 References

- [1] R. A. Khalek *et al.*, "Science Requirements and Detector Concepts for the Electron-Ion Collider: EIC Yellow Report," *Nucl. Phys. A*, vol. 1026, p. 122447, Oct. 2022, doi: 10.1016/j.nuclphysa.2022.122447.
- [2] Dassault Systèmes UK Ltd.: Kidlington, U, "Opera-3D 18R2 Reference Manual." 2018.
- [3] L. Bottura, "A practical fit for the critical surface of NbTi," *IEEE Trans. Appl. Supercond.*, vol. 10, no. 1, pp. 1054–1057, Mar. 2000, doi: 10.1109/77.828413.
- [4] H. Kanithi, D. Blasiak, J. Lajewski, C. Berriaud, P. Vedrine, and G. Gilgrass, "Production Results of 11.75 Tesla Iseult/INUMAC MRI Conductor at Luvata," *IEEE Trans. Appl. Supercond.*, vol. 24, no. 3, pp. 1–4, Jun. 2014, doi: 10.1109/TASC.2013.2281417.
- [5] *CryoComp 5.2*. (2012). Eckels Engineering, Florence, SC, USA.
- [6] T. G. O'Connor *et al.*, "Design and testing of the 1.5 T superconducting solenoid for the BaBar detector at PEP-II in SLAC," *IEEE Trans. Appl. Supercond.*, vol. 9, no. 2, pp. 847–851, Jun. 1999, doi: 10.1109/77.783429.
- [7] P. Fabbriatore *et al.*, "The Manufacture of Modules for CMS Coil," *IEEE Trans. Appl. Supercond.*, vol. 16, no. 2, pp. 512–516, Jun. 2006, doi: 10.1109/TASC.2005.869550.
- [8] T. M. Flynn, *Cryogenic engineering*, 2nd ed., rev.Expanded., 1 online resource (xi, 895 pages) : illustrations vols. New York: Marcel Dekker, 2005. doi: 10.1201/9780203026991.
- [9] "Copper and copper alloys - plate, sheet, strip and circles for general purposes." National standards and national normative documents, NF EN 1652, Jun. 2004.
- [10] C. L. Goodzeit, "Superconducting accelerator magnets," *USPAS*, Jan. 2001.
- [11] W. H. Gray and C. T. Sun, "Theoretical and experimental determination of mechanical properties of superconducting composite wire," United States, 1976.
- [12] M. Guan, X. Wang, and Y. Zhou, "Cryogenic Temperature Dependence of Tensile Response of NbTi/Cu Superconducting Composite Wires," *IEEE Trans. Appl. Supercond.*, vol. 22, no. 6, pp. 8401106–8401106, Dec. 2012, doi: 10.1109/TASC.2012.2215857.
- [13] M. B. Kasen, G. R. MacDonald, D. H. Beekman, and R. E. Schramm, "Mechanical, Electrical, and Thermal Characterization of G-10Cr and G-11Cr Glass-Cloth/Epoxy Laminates Between Room Temperature and 4 K," in *Advances in Cryogenic Engineering Materials: Volume 26*, A. F. Clark and R. P. Reed, Eds., Boston, MA: Springer US, 1980, pp. 235–244. doi: 10.1007/978-1-4613-9859-2_24.
- [14] A. W. Chao, M. Tigner, H. Weise, and F. Zimmermann, *Handbook Of Accelerator Physics And Engineering (Third Edition)*. World Scientific, 2023.
- [15] "National Institute of Standards and Technology," NIST. Accessed: Aug. 07, 2024. [Online]. Available: <https://www.nist.gov/>
- [16] "Structural Material Database, Article 3 Non-Metallic Materials Database & Specifications." ITER.
- [17] "The CMS magnet project: Technical Design Report." in Technical design report. CMS. CERN, Geneva, 1997. doi: 10.17181/CERN.6ZU0.V4T9.

Electron-Ion Collider, Brookhaven National Laboratory and Thomas Jefferson National Accelerator Facility			
Doc No. EIC-SHC-TN-24-005	Author: Sandesh Gopinath	Effective Date: 12/05/2024	Review Frequency: NA
Process Description: EIC Design Report MARCO Magnet			Revision: 00

- [18] J. E. Campbell, E. A. Eldridge, and J. K. Thompson, "Handbook on Materials for Superconducting Machinery,," Battelle Columbus Labs Ohio Metals and Ceramics Information Center; Army Materials And Mechanics Research Center, Watertown, Mass., ADA002698, 1974. Accessed: Aug. 08, 2024. [Online]. Available: <https://ntrl.ntis.gov/NTRL/dashboard/searchResults/titleDetail/ADA002698.xhtml>
- [19] *Cast3m is a trademark of cea/saclay france*. [Online]. Available: <https://www-cast3m.cea.fr/>
- [20] R. M. Nedderman, "One-Dimensional Two-Phase Flow. BY G. B. WALLIS. McGraw Hill, 1969. 408pp. £7. 18s. Cocurrent Gas-Liquid Flow. Edited by E. RHODES AND D. S. SCOTT. Plenum Press, 1969. 698 pp. \$27.50.,," *J. Fluid Mech.*, vol. 42, no. 2, pp. 428–430, Jun. 1970, doi: 10.1017/S0022112070211362.
- [21] P. Bredy, F. P. Juster, B. Baudouy, L. Benkheira, and M. Cazanou, "Experimental and theoretical study of a two phase helium high circulation loop," *AIP Conf Proc*, vol. 823, no. 1, pp. 496–503, 2006, doi: 10.1063/1.2202453.
- [22] S. W. Sciver, *Helium cryogenics: Second edition*. 2012, p. 470. doi: 10.1007/978-1-4419-9979-5.
- [23] R. Boom, "Experimental Investigation of the Helium Two Phase Flow Pressure Drop Characteristics in Vertical Tubes," *Proc ICEC*, vol. 7, pp. 468–473, 1978.
- [24] Yu. P. Filippov, "Characteristics of horizontal two-phase helium flows: Part II: pressure drop and transient heat transfer," *Cryogenics*, vol. 39, no. 1, pp. 69–75, Jan. 1999, doi: 10.1016/S0011-2275(98)00115-5.
- [25] X. Huang and S. W. Van Sciver, "Pressure drop and void fraction of two-phase helium flowing in horizontal tubes," *Cryogenics*, vol. 35, pp. 467–474, Jan. 1995, doi: 10.1016/0011-2275(95)93582-K.
- [26] R. Comolet, "Mécanique expérimentale des fluides," *No Title*, Accessed: Aug. 08, 2024. [Online]. Available: <https://cir.nii.ac.jp/crid/1130282271922915072>
- [27] E. G. Brentari, "Boiling heat transfer for oxygen, nitrogen, hydrogen, and helium," National Bureau of Standards, Gaithersburg, MD, NBS TN 317, 1965. doi: 10.6028/NBS.TN.317.
- [28] "Ansys Fluent User's Guide, Release 2023 R1." Ansys, Inc, Jan. 2023.
- [29] M. Baldini *et al.*, "MQXFA Magnet Handling & Shipping Requirements," Fermi National Accelerator Laboratory (FNAL), Batavia, IL (United States); Brookhaven National Laboratory (BNL), Upton, NY (United States); Lawrence Berkeley National Laboratory (LBNL), Berkeley, CA (United States), FERMILAB-TM-2790-TD, Oct. 2022. doi: 10.2172/1969681.
- [30] M. Baldini, G. Ambrosio, J. Blower, J. Cozzolino, T. Strauss, and G. Vallone, "US HL-LHC Accelerator Upgrade Project: MQXFA11 shipping incident report," Brookhaven National Laboratory (BNL), Upton, NY (United States); Lawrence Berkeley National Laboratory (LBNL), Berkeley, CA (United States); Fermi National Accelerator Laboratory (FNAL), Batavia, IL (United States), FERMILAB-FN-1224-TD; US-HiLumi-doc-4341, Aug. 2022. doi: 10.2172/1958786.
- [31] M. Kane, J. Holzbauer, T. Jones, and E. Jordan, "Design of a Transport System for the PIP-II HB650 Cryomodule," *JACoW*, vol. LINAC2022, Art. no. FERMILAB-CONF-22-819-PIP2, Oct. 2022, doi: 10.18429/JACoW-LINAC2022-TUPOGE08.

The only official copy of this document is the one online in the SharePoint Document Center. Before using a printed copy, verify that it is current by checking the printed document's Revision History log with that of the online version.

Electron-Ion Collider, Brookhaven National Laboratory and Thomas Jefferson National Accelerator Facility			
Doc No. EIC-SHC-TN-24-005	Author: Sandesh Gopinath	Effective Date: 12/05/2024	Review Frequency: NA
Process Description: EIC Design Report MARCO Magnet			Revision: 00

14 Appendix

- Appendix 1- ICD
- Appendix 2- Power Supply Specifications
- Appendix 3- RCS stray field minimization
- Appendix 4- FMEA Document
- Appendix 5- Reference Drawings
- Appendix 6- Cryogenic flow pressure drop –
Thermosiphon and other circuits
- Appendix 7- Heat load Scenarios
- Appendix 8- Cold and Warm Cryogenic Valves